THE JOURNAL
OF
CHEMICAL PHYSICS

VOLUME 16, NUMBER 5 MAY, 1948

The Low Temperature Heat Capacities, Enthalpies, and Entropies of UF_4 and UF_6*

FERDINAND G. BRICKWEDDE, HAROLD J. HOGE, AND RUSSELL B. SCOTT
National Bureau of Standards, Washington, D. C.

(Received December 2, 1947)

The heat capacity of UF_4 has been measured from 20° to 350°K and that of UF_6 from 14° to 370°K. Molar heat capacities have been tabulated at 5-degree intervals and extrapolated to 0°K. From them the entropies and enthalpies of the compounds have been found by integration and tabulated. The triple point temperature of UF_6 was found to be 337.212°K (64.052°C) and the heat of fusion was found to be 19,193 j $mole^{-1}$.

THE heat capacities of UF_4 and UF_6 were measured in the Low Temperature Laboratory of the National Bureau of Standards between April and October 1942.[1] The work has been the subject of reports A-201 and A-607 to the OSRD.

MATERIALS

The materials were prepared at Columbia University shortly before our measurements were made. The UF_4, a green powder, was received in a glass bottle sealed with wax. It was stated to contain about two percent of UO_2F_2. As this impurity may be expected to have a heat capacity not greatly different from that of UF_4, it should not introduce serious error.

The UF_6 was brought to us in a glass trap, as a colorless or slightly yellowish crystalline solid. It was handled entirely in apparatus from which air and moisture had been evacuated. The method of transfer from the trap to the calorimeter involved distillation, and would tend to eliminate impurities of higher or lower vapor pressure than UF_6. Graphs of the melting range of UF_6 are shown in Fig. 1. They indicate, with the usual assumptions regarding freezing-point depression, that the mole fraction of impurity was 2×10^{-4}. Considering the corrosive nature of the substance, this is quite gratifying. There may, of course, have been some gaseous and liquid-insoluble impurities which the melting curve would not show up.

EXPERIMENTAL

The UF_4 was measured in a platinum calorimeter previously used in measurements on a synthetic rubber.[2] Temperatures were measured

* This document is based on work performed for the Atomic Energy Project, and the information covered therein will appear in Division VIII of the National Nuclear Energy Series (Manhattan Project Technical Section) as part of the contribution of the National Bureau of Standards.

[1] The heat capacity of UF_5 also was subsequently measured by Robert D. Rands, Jr. Although this material (a gray powder) was protected from water vapor, analyses made by Homer F. Priest at Columbia University, both before and after our measurements, showed a substantial change in the sample. For this and other reasons we have decided not to publish the results, but take this opportunity of calling them to the attention of anyone who might wish to make use of them in a subsequent investigation.

[2] Norman Bekkedahl and Russell B. Scott, "Specific heat of the synthetic rubber hycar-O.R.," J. Research Nat. Bur. Stand. **29**, 87 (1942), RP1487.

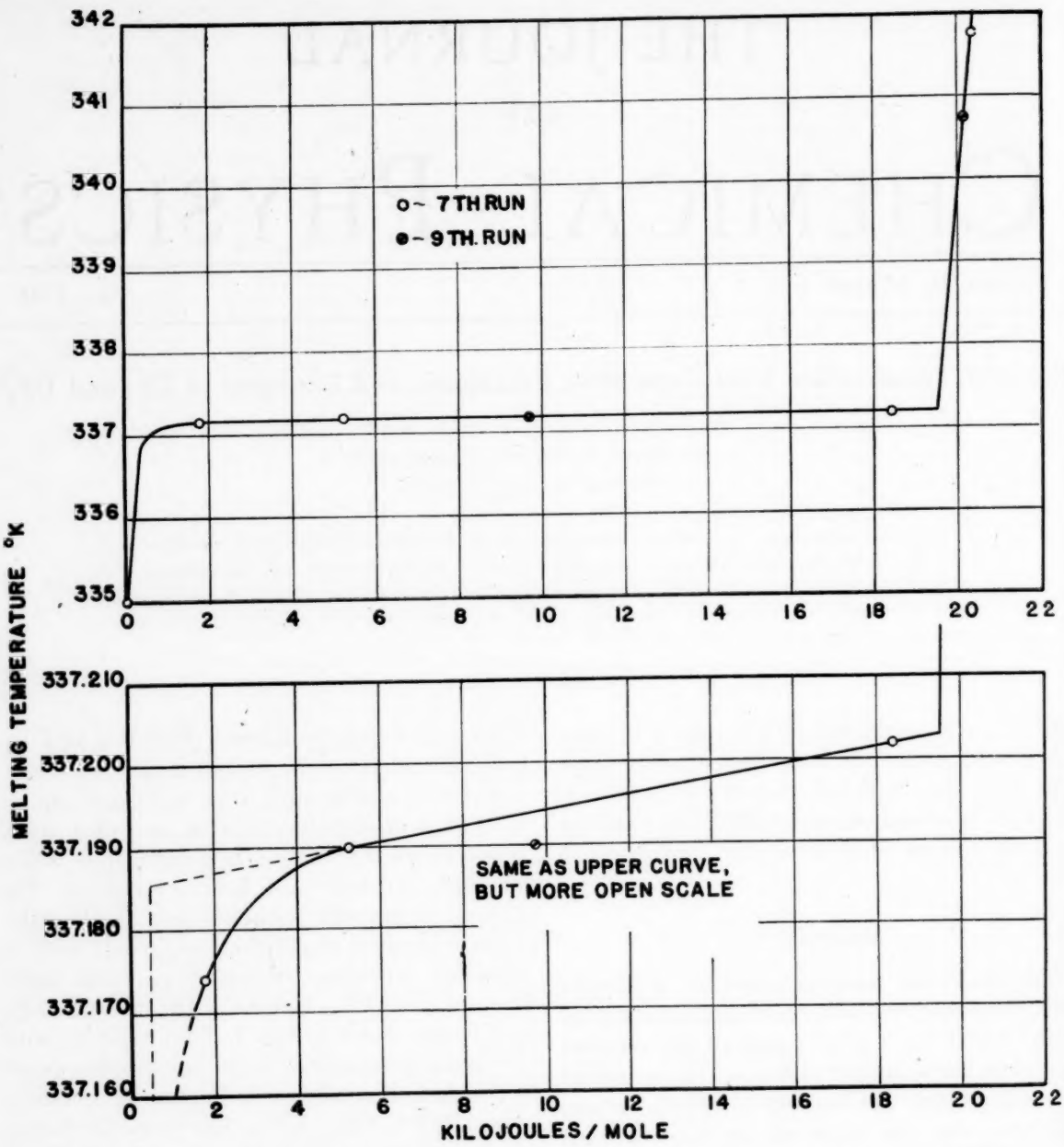

FIG. 1. Melting data for the UF_6 sample; the energy supplied is measured from an arbitrary zero (335°K).

with the 90 Pt:10 Rh resistance thermometer M4, which served also as a heater. The calorimeter was filled with UF_4 and soldered shut. When proved vacuum tight, a small protruding tube was opened, the calorimeter placed in a glass container and evacuated for about 48 hours. It was then filled with helium to a pressure of one atmosphere and quickly soldered shut in an atmosphere of helium. The calorimeter was weighed, installed in the cryostat, and measurements made. After removal the weight was checked and the calorimeter opened by unsoldering with a flame. After thoroughly brushing out the UF_4, the empty calorimeter, lid, and solder were weighed. The net weight was taken to be the difference between this value and the

gross weight of the unopened calorimeter. The values, after correction to vacuum, are

UF_4	123.849 g
He (calculated)	0.005 g
Tare weight	188.060 g.

Taking the molecular weight to be 314.07, the calorimeter contained 0.39433 mole of UF_4.

To check the weighings, the removed UF_4 was weighed. It weighed somewhat more than expected and proved to be gaining weight at a rate of more than 1 mg $min.^{-1}$. The weight was observed at intervals for several days. After an initial rise of about 450 mg, the change was found to be erratic. It is attributed to absorption of water vapor from the air. It is thought that any water in the sample in the calorimeter would have been substantially removed by the initial two-day evacuation, so that the results are not in error from this source. The tare heat capacity had been determined previous to the present measurements, but a correction was made for a small difference in the weight of solder used to close the calorimeter.

The UF_6 was measured in a special fluted copper calorimeter. The corrugations in this calorimeter (see Fig. 2) permitted it to be deformed by the material, which undergoes a very large expansion at or just below the melting point. The corrugated design proved to be very necessary. After the measurements the calorimeter showed marked distortion, and immersion in water showed a volume increase of about ten percent. A 95 Sn:5 Sb solder was used for all joints that came in contact with UF_6. Temperatures were measured with a pure platinum resistance thermometer (thermometer *P*). The heater consisted of a resistance of about 50 ohms of AWG 34 double glass insulated constantan wire wound bifilarly on the outside of the platinum case of the thermometer. It was imbedded directly in solder, where it worked satisfactorily without developing grounds.

The short filling tube was connected to a glass train consisting of a trap containing the supply of UF_6, an empty bulb, and a bulb full of helium. By opening glass break seals and suitably changing temperatures the charge was transferred first to the empty bulb and then collected in the calorimeter as a liquid. After cooling below the triple point, helium was admitted above the UF_6, the small copper tube was pinched off and immediately soldered shut. On completion of the measurements the gross weight of calorimeter and charge was determined. Then the calorimeter was drilled open in an atmosphere of dry CO_2, transferred to a helium atmosphere, and attached to a vacuum system. The UF_6 was vaporized into a dry-ice trap, after which the emptied calorimeter was filled with helium and closed with a weighed amount of solder. The tare weight was then determined. Making due allowance for the small amounts of solder, drill chips, and helium fillings, the weights (reduced to vacuum) are as follows:

UF_6	128.565 g
Tare weight	71.211 g.

Taking the molecular weight to be 352.07, the calorimeter contained 0.36517 mole of UF_6. The material is known to attack copper, but a protective coating is formed which slows down the rate of attack. Most of the reaction probably took place as the result of the first filling, which was unsuccessful. Even attack by the sample whose heat capacity was measured would not necessarily cause error, because the tare heat capacity was measured after the UF_6 was removed. If as a result of attack some of the UF_6 was reduced to UF_4 and copper fluoride was formed, these products, being non-volatile, would have remained in the calorimeter during the tare measurements, so that their heat capacities would have been eliminated from the net heat capacity.

The electrical measurements, control circuits, and procedures for both UF_4 and UF_6 were

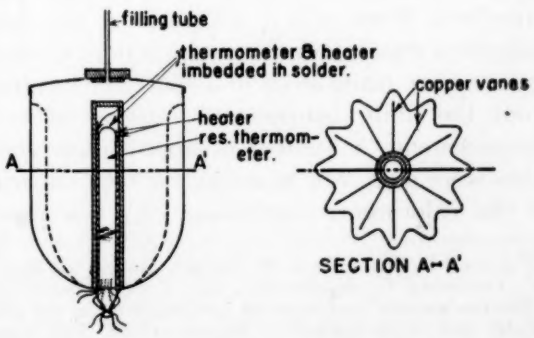

FIG. 2. Diagram of the sample container used for UF_6.

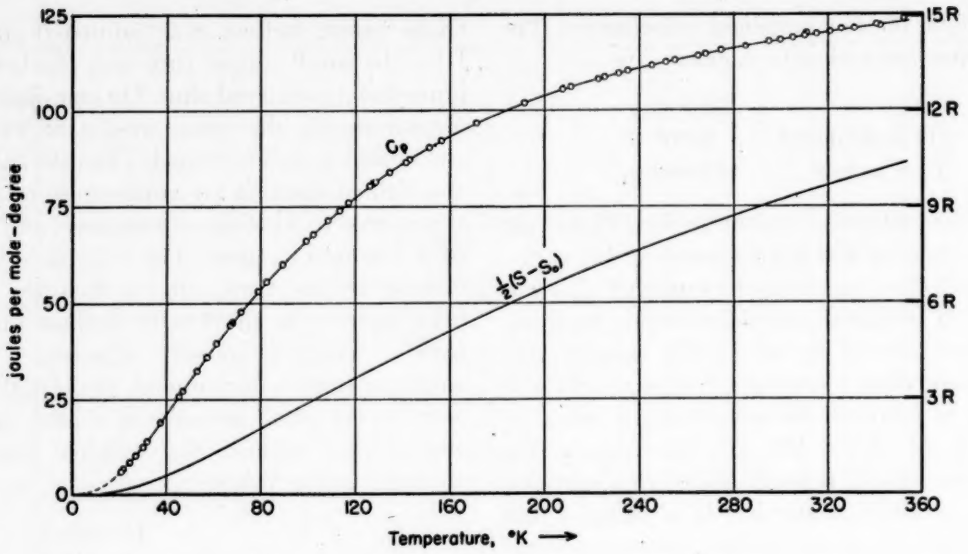

FIG. 3. Molar heat capacity and entropy of UF_6.

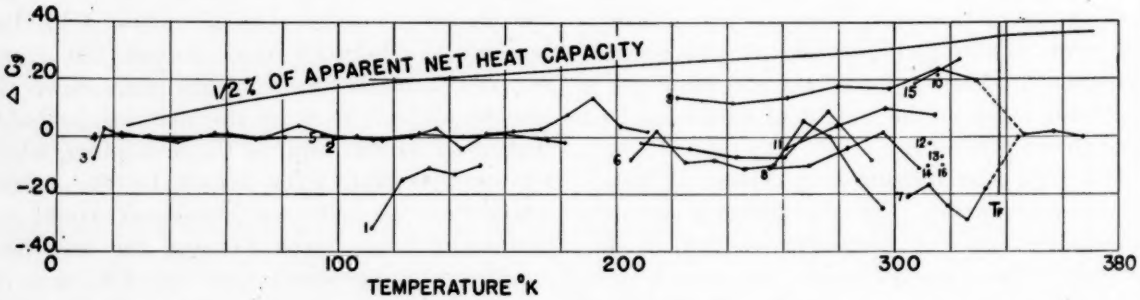

FIG. 4. Deviations of observed gross heat capacity of UF_6 from the smooth tabular values of heat capacity. The runs are numbered to indicate the order in which they were taken.

similar to those described in a recent publication.[3]

The observed heat capacities were plotted as deviations from approximate functions. Smooth curves were drawn through the points, from which values were read at five-degree intervals. These were added to the approximate functions to give tables of both gross and tare heat capacities, from which a table of net heat capacities was obtained by subtraction. Computations were made so as to avoid error resulting from the finite temperature interval of each measurement. A number of approximate functions were used. For example, the heat capacity of the calorimeter containing UF_6 was represented below 165°K, by C (approximate, j deg.$^{-1}$) $=80D(x)$, with x, the argument of the Debye function, set equal to $350/(T+16)$. After removal of the UF_6 the tare heat capacity was represented throughout the entire temperature range by C (approximate, j deg.$^{-1}$) $=27D(x)$, with $x=315/T$.

The scattering of the data for UF_4 was found by reading the distance of each point from the smooth curve of a deviation plot of the gross heat capacity. These values were divided by the number of moles of UF_4 in the calorimeter, and gave a mean deviation from the smooth curve of $0.06-$j mole^{-1} deg.$^{-1}$. Figure 3 is a graph of the molar heat capacity showing the sixty experimental points.

For UF_6 the deviations were found by a different procedure, somewhat preferable to that

[3] Russell B. Scott, Cyril H. Meyers, Robert D. Rands, Jr., Ferdinand G. Brickwedde, and Norman Bekkedahl, "Thermodynamic properties of 1,3-butadiene in the solid, liquid, and vapor states," J. Research Nat. Bur. Stand. **35**, 39 (1945), RP1661.

used for UF_4. The gross heat capacity table was integrated over the interval of each individual measurement, the result subtracted from the actual energy input, and the difference divided by ΔT. This gives the deviation of each experimental point from the table. The deviations of the ninety-six experimental points are shown in Fig. 4. They refer to the actual gross heat capacity rather than the molar heat capacity. The mean deviation is $0.08-j$ deg.$^{-1}$.

In the case of UF_6 it was necessary to apply a vapor correction both to the heat capacity and to the heat of fusion. This was done according to the procedure outlined in reference 4. The vapor-pressure data of Crist and Weinstock and those of Haworth and Simon were represented by two equations intersecting at 337.212°K (64.052°C) which is the triple-point temperature found in the present investigation. The equations are: $\log_{10}P$ (solid, mm Hg) $=(-2559.5/T)+10.648$ and $\log_{10}P$ (liquid, mm Hg) $=(-1511.3/T)+7.5396$. These equations give a triple point pressure of 1142-mm Hg. The vapor correction reaches about five percent of the net heat capacity just below the triple point, but drops again when the material melts because of the great reduction in vapor volume. The volume of the calorimeter after measurements were completed was determined from the mass of water required to fill it. The value found, 56.27 cm^3, was used in all the corrections. The specific volume of the liquid was computed from the equation

$$v/v_f=\rho_f/\rho=1+1.727\times10^{-3}(T-T_f)+3.59\times10^{-6}(T-T_f)^2,$$

taken from the work of Wechsler and Hoge,[5]

TABLE I. Vapor correction to the heat capacity of UF_6, and contribution of $\int VdP$ to the enthalpy. C is the uncorrected heat capacity and C_{sat} the desired heat capacity of saturated condensed phase. Vapor pressures were computed from the equations given in the text.

T °K	p mm Hg	$C-C_{sat}$ j mole^{-1} deg.$^{-1}$	$\int VdP$ j mole^{-1}
230	0	0	
235	1	0	
240	1	0.03	
245	2	0.03	
250	3	0.06	
255	4	0.08	
260	6	0.14	
265	10	0.19	
270	15	0.25	
275	22	0.36	
280	32	0.52	
285	47	0.68	0
290	66	0.96	1
295	94	1.26	1
300	131	1.67	1
305	180	2.19	2
310	246	2.85	2
315	333	3.64	3
320	446	4.66	4
325	592	5.89	6
330	780	7.39	7
335	1018	9.20	10
337.212	1142	—	11
340	1243	2.08	12
345	1442	2.27	15
350	1666	2.41	18
355	1916	2.60	21
360	2195	2.77	24
365	2507	2.90	28
370	2851	3.09	33

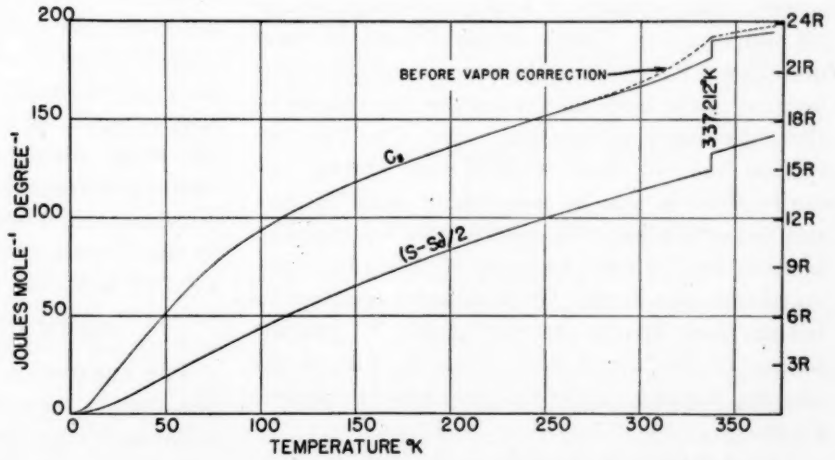

FIG. 5. Molar heat capacity and entropy of UF_6.

[4] Harold J. Hoge, "Heat capacity of a two-phase system, with applications to vapor corrections in calorimetry," J. Research Nat. Bur. Stand. **36**, 111 (1946), RP1693.

[5] Martin T. Wechsler and Harold J. Hoge, Report A-456; see also the later report A-1591.

TABLE II. Thermodynamic properties of UF_4; $S-S_0=\int(C_p/T)dT$; $H-H_0=\int C_p dT$; the energy unit is the international joule (=1/4.1833 cal.).

T °K	C_p j mole^{-1} deg.$^{-1}$	$S-S_0$ j mole^{-1} deg.$^{-1}$	$H-H_0$ j mole^{-1}
0	0	0	0
5	0.08	0.03	0.1
10	0.68	0.22	1.7
15	2.24	0.76	8.5
20	5.13	1.7	26.1
25	7.93	3.2	58.1
30	11.80	4.9	107.3
35	16.15	7.1	177.2
40	20.49	9.5	268.8
45	24.84		
50	29.22	15.0	517.2
55	33.51		
60	37.72	21.1	852
65	41.84		
70	45.81	27.6	1270
75	49.55		
80	53.14	34.2	1766
85	56.59		
90	59.88	40.8	2331
95	63.00		
100	65.96	47.4	2961
105	68.84		
110	71.60	54.0	3649
115	74.26		
120	76.76	60.5	4391
125	79.19		
130	81.50	66.8	5183
135	83.66		
140	85.66	73.0	6020
145	87.57		
150	89.39	79.0	6895
155	91.14		
160	92.83	84.9	7806
165	94.42		
170	95.92	90.6	8750
175	97.33		
180	98.66	96.2	9724

TABLE II.—*Continued.*

T °K	C_p j mole^{-1} deg.$^{-1}$	$S-S_0$ j mole^{-1} deg.$^{-1}$	$H-H_0$ j mole^{-1}
185	99.93		
190	101.12	101.6	10,723
195	102.24		
200	103.32	106.8	11,745
205	104.36		
210	105.35	111.9	12,789
215	106.32		
220	107.24	116.9	13,852
225	108.10		
230	108.92	121.7	14,933
235	109.71		
240	110.47	126.3	16,030
245	111.20		
250	111.89	130.9	17,142
255	112.56		
260	113.20	135.3	18,267
265	113.81		
270	114.41	139.6	19,405
273.16	114.80	140.9	19,767
275	115.03		
280	115.63	143.8	20,556
285	116.20		
290	116.75	147.8	21,717
295	117.28		
298.16	117.62	151.1	22,674
300	117.81	151.8	22,890
305	118.33		
310	118.84	155.7	24,074
315	119.35		
320	119.85	159.5	25,267
325	120.33		
330	120.81	163.2	26,470
335	121.28		
340	121.74	166.8	27,683
345	122.20		
350	122.64	170.4	28,905

with a triple-point density $\rho_f=3.674$ g cm^{-3} taken from Priest.[6] For the solid the data were scanty, and a density of 4.93-g cm^{-3} was used at all temperatures. Better values of some of these quantities have since become available, but because of the large uncertainty in the volume of the calorimeter at any particular time the correction has not been recalculated. During the entire time it was in use, which included one unsuccessful filling, the calorimeter increased in volume by 5.4 cm^3. In view of this the vapor correction can hardly be considered accurate to better than fifteen percent. Table I contains values of the vapor correction. In Fig. 5 the uncorrected heat capacity is shown by the dashed curve.

Two determinations of the triple-point temperature and heat of fusion of UF_6 were made. The results are plotted in Fig. 1. The second gave a somewhat lower temperature and a heat of fusion lower by 1.6 per mille. Possibly the material had become less pure. The mean of the two runs gave a value of 19,193 j mole^{-1} for the heat of fusion after making the vapor correction discussed above. Corrections were made for the heat capacity of the material below and above the triple point. From Fig. 1 the change in melting temperature as the last half of the material melts in 9 millidegrees. Adding this amount to the highest point in the melting range gives 337.212°K for the triple point of pure UF_6.

THERMODYNAMIC PROPERTIES

The calculation of the heat-capacity tables has already been outlined. Extrapolation of the molar heat capacity of UF_4 from 20° to 0°K was performed with the equation $C=3R[D(150/T)+0.0041T^3]$. Extrapolation of the molar heat capacity of UF_6 from 14° to 0°K was performed

[6] Homer F. Priest, Report A-139.

TABLE III. Thermodynamic properties of UF_6; C_{sat} is the heat capacity of 1 mole of condensed phase in equilibrium with saturated vapor; $H-H_0=\int C_{sat}dT+\int VdP$; $S-S_0=\int(C_{sat}/T)dT$; for vapor corrections and $\int VdP$, see Table I; the energy unit is the international joule (=1/4.1833 cal.).

T °K	C_{sat} j mole^{-1} deg.$^{-1}$	$H-H_0$ j mole^{-1}	$S-S_0$ j mole^{-1} deg.$^{-1}$	$T(S-S_0)$ j mole^{-1}
0	0	0	0	0
20	17.00	117.1	8.2	164
25	23.14	217.6	12.7	318
30	28.95	347.9	17.4	522
35	34.59	506.8	22.3	780
40	40.31	694.0	27.3	1092
45	46.01	909.8	32.3	1454
50	51.62	1154	37.5	1875
55	57.13	1426	42.7	2348
60	62.33	1725	47.9	2874
65	67.23	2049	53.1	3452
70	71.80	2396	58.2	4074
75	76.24	2767	63.3	4748
80	80.32	3158	68.4	5472
85	84.24	3570	73.4	6239
90	87.80	4000	78.3	7047
95	91.03	4447	83.1	7894
100	94.07	4910	87.8	8780
105	96.92	5388	92.5	9712
110	99.65	5879	97.1	10,681
115	102.34	6384	101.6	11,684
120	104.91	6902	106.0	12,720
125	107.35	7433	110.3	13,788
130	109.73	7976	114.6	14,898
135	112.00	8530	118.8	16,038
140	114.20	9096	122.9	17,206
145	116.28	9672	126.9	18,400
150	118.39	10,258	130.9	19,635
155	120.38	10,855	134.8	20,894
160	122.33	11,462	138.7	22,192
165	124.27	12,079	142.4	23,496
170	126.14	12,705	146.2	24,854
175	128.00	13,340	149.9	26,232
180	129.80	13,985	153.5	27,630
185	131.45	14,638	157.1	29,064
190	133.31	15,299	160.6	30,514
195	134.98	15,970	164.1	32,000

TABLE III.—*Continued.*

T °K	C_{sat} j mole^{-1} deg.$^{-1}$	$H-H_0$ j mole^{-1}	$S-S_0$ j mole^{-1} deg.$^{-1}$	$T(S-S_0)$ j mole^{-1}
200	136.60	16,649	167.5	33,500
205	138.24	17,336	170.9	35,034
210	139.96	18,032	174.3	36,603
215	141.31	18,735	177.6	38,184
220	143.17	19,446	180.9	39,798
225	144.73	20,165	184.1	41,422
230	146.26	20,893	187.3	43,079
235	147.82	21,628	190.4	44,744
240	149.36	22,371	193.6	46,464
245	150.89	23,122	196.7	48,192
250	152.40	23,880	199.7	49,925
255	153.88	24,646	202.8	51,714
260	155.38	25,419	205.8	53,508
265	156.86	26,199	208.7	55,306
270	158.37	26,987	211.7	57,159
273.16	*159.32*	*27,490*	*213.5*	*58,320*
275	159.87	27,783	214.6	59,015
280	161.30	28,586	217.5	60,900
285	162.72	29,396	220.4	62,814
290	164.15	30,214	223.2	64,728
295	165.71	31,039	226.0	66,670
298.16	*166.75*	*31,565*	*227.8*	*67,921*
300	167.35	31,871	228.8	68,640
305	169.10	32,714	231.6	70,638
310	170.96	33,564	234.4	72,664
315	172.88	34,424	237.1	74,686
320	174.85	35,295	239.9	76,768
325	176.82	36,176	242.6	78,845
330	178.93	37,066	245.3	80,949
335	181.01	37,969	248.0	83,080
337.212	181.92	38,371	249.2	84,033
melts	(L=19,193,	L/T_f=56.9)		
337.212	190.73	57,564	306.1	103,221
340	191.09	58,098	307.7	104,618
345	191.78	59,058	310.5	107,122
350	192.52	60,022	313.3	109,655
355	193.26	60,989	316.0	112,180
360	193.83	61,960	318.7	114,732
365	194.46	62,935	321.4	117,311
370	195.04	63,914	324.0	119,880

with the equation $C=3R[D(73/T)+E(110/T)]$. The symbols D and E represent the Debye and Einstein specific heat functions. The heat capacity given for UF_6 is C_{sat}, which refers to the condensed phase in equilibrium with saturated vapor. Since UF_4 has no appreciable vapor pressure in the range of our measurements, C_{sat} and C_p are not significantly different for it, and the curve in the graph has been labeled C_p.

Table II gives the heat capacity, enthalpy, and entropy of UF_4 at uniform temperature intervals. Table III gives the same quantities for UF_6, and also $T(S-S_0)$. Enthalpies were computed by integrating $dH=C_{sat}dT+VdP$ along the saturation curve, using Simpson's rule and the values of C in the tables. The contribution of the last term was nearly negligible, as may be seen from Table I. Entropies were obtained along the same path by a similar integration of $dS=(C/T)dT$. The heat capacities and entropies are plotted in Figs. 3 and 5.

DISCUSSION OF RESULTS

The measurements on UF_4 gave no particular difficulty. Those made on UF_6 were complicated by the deformation of the calorimeter which made the vapor corrections uncertain. There was some lack of reproducibility in the heat capacity of UF_6. This may be seen in Fig. 4, where the initial points of the various runs are numbered in chronological order. Between about 300°K and the triple point there was a tendency for the calorimeter to drift down after it would normally have come to temperature equilibrium. Above

the triple point the tendency was to drift upward. The upward drift may have been due to chemical reaction. For this reason the calorimeter was kept at high temperatures no longer than absolutely necessary, and it is thought that change in chemical composition produced by reaction was not serious. Some tests were made to relate the irregularities in heat capacity with past thermal history, but these were inconclusive.

Considering errors arising from the experimental measurements as well as those resulting from possible impurities, the data for UF_6 are not considered reliable to much better than one percent. This is about equal to the extreme spread of the points in Fig. 4. The errors in the UF_4 data are probably only about half as large, but the uncertainty resulting from impurity is larger, so that the over-all accuracy for the two compounds is probably about the same. The errors in the other quantities in the tables are probably about the same as those in the heat capacities from which they are derived.

THE JOURNAL OF CHEMICAL PHYSICS VOLUME 16, NUMBER 5 MAY, 1948

The Vapor Pressure of Uranium Hexafluoride*

B. WEINSTOCK[1] AND R. H. CRIST[2]
S. A. M. Laboratories, Columbia University, New York, New York

(Received December 17, 1947)

The vapor pressure of uranium hexafluoride, UF_6, has been measured from 273°K to 358°K. The measurements were made by a null method in an all metal apparatus with a brass sylphon bellows. The data are represented by the equations:

$$\text{Solid}-\text{vapor } \log_{10}P(\text{mm Hg}) = -3.77962 \log_{10}T - (3123.479/T) + 21.87103,$$
$$\text{Liquid}-\text{vapor } \log_{10}P(\text{mm Hg}) = -3.72662 \log_{10}T - (2065.679/T) + 18.60033.$$

The constants in the equations were adjusted so that the equations would give the same heat of fusion and triple-point temperature as was determined by Brickwedde, Hoge, and Scott. The vapor pressure at the triple point is 1133 ± 7 mm. The sublimation point at which the vapor pressure is 1 atmosphere is 56.5°C. The heat of vaporization has been calculated using the Berthelot equation to obtain the vapor volume. From this and the entropies measured by Brickwedde, the absolute entropy of the gas has been calculated.

INTRODUCTION

THE vapor pressure of uranium hexafluoride had been previously measured by Ruff and Heinzelmann[3] over the temperature range 37–56.2°C. Their results are not precise showing large deviations from linearity in a $\log P$ against $1/T$ plot. The vapor pressures obtained by them are always higher than those obtained in the present work, the percentage differences being very much greater at lower pressure. This situation could be explained by the presence of a volatile impurity in their sample, e.g., HF. The purpose of the present work was to improve the accuracy of these measurements as well as to extend the range of measurement.

EXPERIMENTAL

The experimental arrangement is shown in Fig. 1. This consists of a reservoir in a thermostat and a brass sylphon bellows for the measurement of pressure by a null method. At the time the experiments were made, it was thought that only a limited number of metals were safe materials for use with UF_6. Accordingly, the vessels and connecting tubes were of copper, the pack-

* This work was performed under the auspices of the O. S. R. D. under Contract OEM sr 412 with Columbia University.
[1] Now at Argonne National Laboratory, Chicago, Illinois.
[2] Now at Carbide and Carbon Chemical Corporation, South Charleston, West Virginia.
[3] Ruff and Heinzelmann, Zeits. anorg. Chemie **72**, 63 (1911).

less valves were brass with a silver gasket ring, the sylphon bellows was brass and the whole was joined with silver solder or "Phoscopper." To maintain the characteristics of the sylphon, its vertical motion was restricted to about a millimeter by guards on both sides. The inner one served the additional purpose of decreasing the working volume of the system. The lower end of the sylphon was soldered to a copper plate and the flange at the upper end was attached to the top plate of the pressure can. Butyl rubber served as a gasket. A pointer was attached to the outer sylphon guard and this was moved by a pin soldered to the sylphon. The pointer and reference were damped by dipping into transformer oil as indicated. The pointer was illuminated and viewed by appropriately located windows.

The manometer for reading pressures above an atmosphere was of the multiple type and contained mercury and dibutylphthalate. The latter served as a piston liquid providing a very satisfactory meniscus. It was not possible to fill the manometer with the two liquids in proper amounts and at the same time keep the dibutylphthalate free from dissolved air. To avoid release of this gas on evacuating the completed unit for use, a permanent head greater than an atmosphere was furnished by having mercury in the limbs standing to appropriate heights. For measurements up to an atmosphere an ordinary wide tube precision manometer was

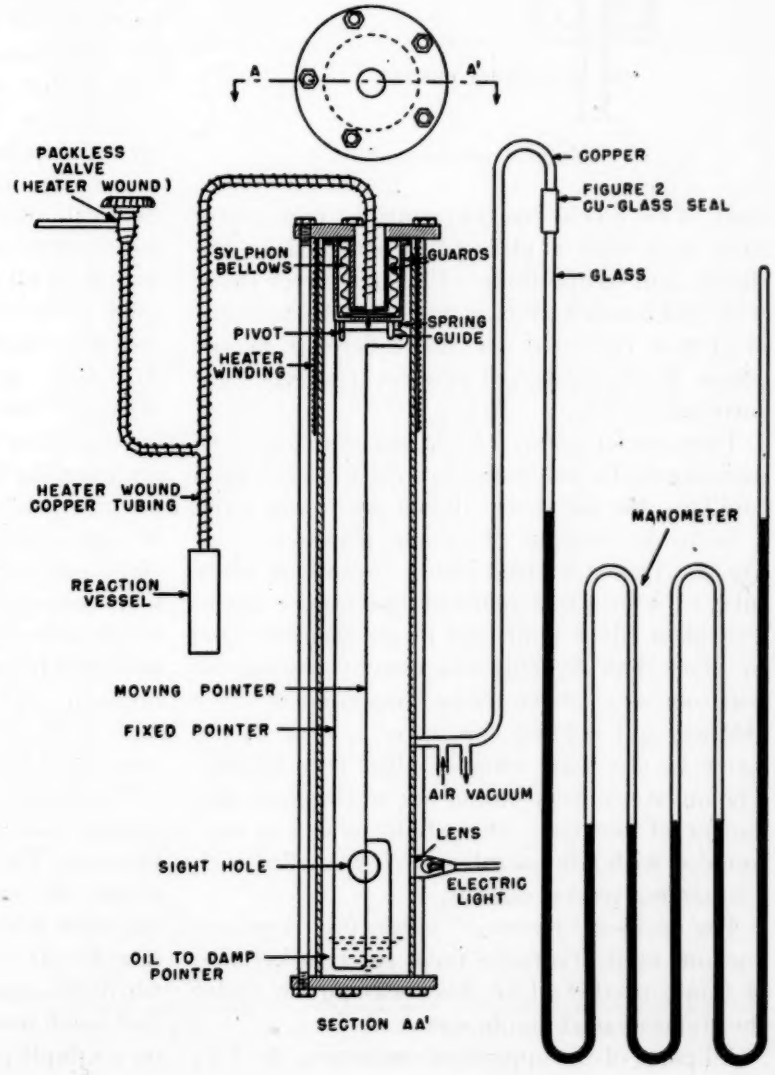

FIG. 1. Vapor pressure apparatus. $\frac{1}{4}$ actual size.

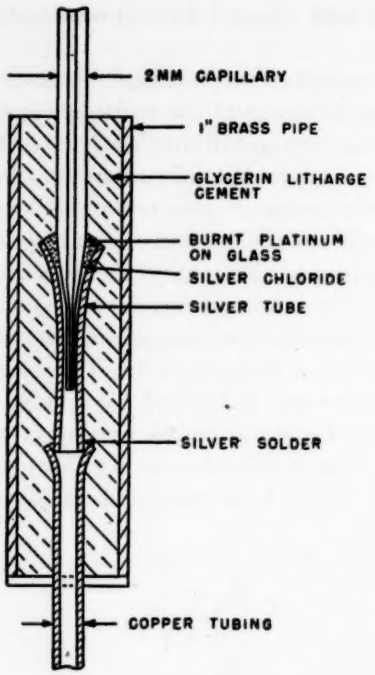

FIG. 2. Metal glass seal.

used. The levels on the multiple manometer were read with a glass plate attached to the sliding arm on the frame of a three-meter Invar scale. All levels were read and the total mercury head was corrected for the difference in the piston liquid levels. All pressure readings were corrected to 0°C.

Two special points in construction might be mentioned. To join copper to thick-walled glass capillary, the latter was drawn down and given a burnt in coating of bright platinum. (See Fig. 2.) This was fitted into a 2-mm wall silver tube to which was soldered the copper stock. The glass silver joint was made vacuum tight by silver chloride. This was done by heating the unit somewhat above the melting point of silver chloride and holding the tip of a stick of the latter to the joint when it filled immediately. The union was very strong but to eliminate any danger of breaking, the whole joint was surrounded with a brass tube which was filled with a litharge-glycerine cement.

The packless "Kerotest" valves used were not vacuum tight. To make them so, a gasket ring of thin annealed silver sheet was put in under the stainless steel diaphragm.

All parts of the apparatus containing the UF_6 to be measured were heated to around 100°C to prevent any condensation of vapor. This included the upper part of the pressure can.

The samples of UF_6 used for the measurements were supplied by Mr. Homer Priest and were resublimed over solid KF several times before using. The first portion was put into the apparatus and left standing for several days to condition the inside surfaces which had baked out as well as possible. An appropriate amount was then sublimed into the reservoir for measurement.

The equilibrium was approached, as indicated in Table I, both by heating and cooling to the desired temperature. Considerable difficulty was experienced in achieving equilibrium for the solid-vapor system at the lower temperatures, in particular at 0°C. Care was taken to maintain the null indicator around the rest point to prevent undue strain on the sylphon and pointer system. For a final setting, the null point was always approached from the same direction.

The data are given in Table I and shown on a two-scale plot in Fig. 3. The first measurements indicated by the numeral (I) were made with a sample of UF_6 sublimed a number of times over solid potassium fluoride. On making measurements at higher temperatures and then cooling to −79°C, a non-condensible gas (2–6 mm) remained. This non-condensible gas was removed by repeating heating above room temperature, then cooling to 0°C and pumping. The measurements on the sample from then on are indicated by the numeral (II). A second sample of specially purified UF_6 used for the measurements at high temperature is denoted by (III). The asterisk indicates that the equilibrium was approached from high temperature side. The measurement marked (IV) was made at a later date with a third sample of UF_6 and an equimolar amount of solid potassium fluoride present.

For obtaining number (II) and (III) data, the sample was at equilibrium pressure for 30–60 minutes. The 0°C point was measured many times, the most satisfactory data being those obtained with number (III) sample. The first sample (I) came to equilibrium very slowly when the approach was from room temperature, and much more rapidly when from below 0°C or on a sample pumped around 0°C or lower.

The temperatures were measured to about 0.05°C, but are reported to the nearest 0.1°C. An error of ±0.1°C introduces an error in the pressure of about 3 mm at 60°C and 5 mm at 85°C. The error in reading the manometer was about 2 mm in the higher pressures and less than 0.5 mm at the lower ones.

CALCULATIONS

The data were fitted to equations of the form:

$$\ln P = A/T + B + C \ln T, \qquad (1)$$

where A, B, and C are arbitrary constants to be determined from the data, P is the pressure in mm Hg, and T is the absolute temperature. Since it is desirable to have the equations consistent with the measured value of the triple-point temperature and the heat of fusion, it was decided to adjust the constants accordingly. This means that the following two relationships among the constants must be satisfied:

$$A_s/T_t + B_s + C_s \ln T_t = A_l/T_t + B_l + C_l \ln T_t, \qquad (2)$$

$$\Delta H_f = P_t V_t \left[\frac{A_l - A_s}{T_t} + (C_s - C_l) \right], \qquad (3)$$

where the subscript t refers to the triple point, s to the solid, and l to the liquid, and ΔH_f is the measured heat of fusion. It is convenient to have a third relation among the constants in order to put the equations into a form easily adaptable to a least-square determination. This was chosen so that the difference in specific heats between the solid and liquid agree with the measured

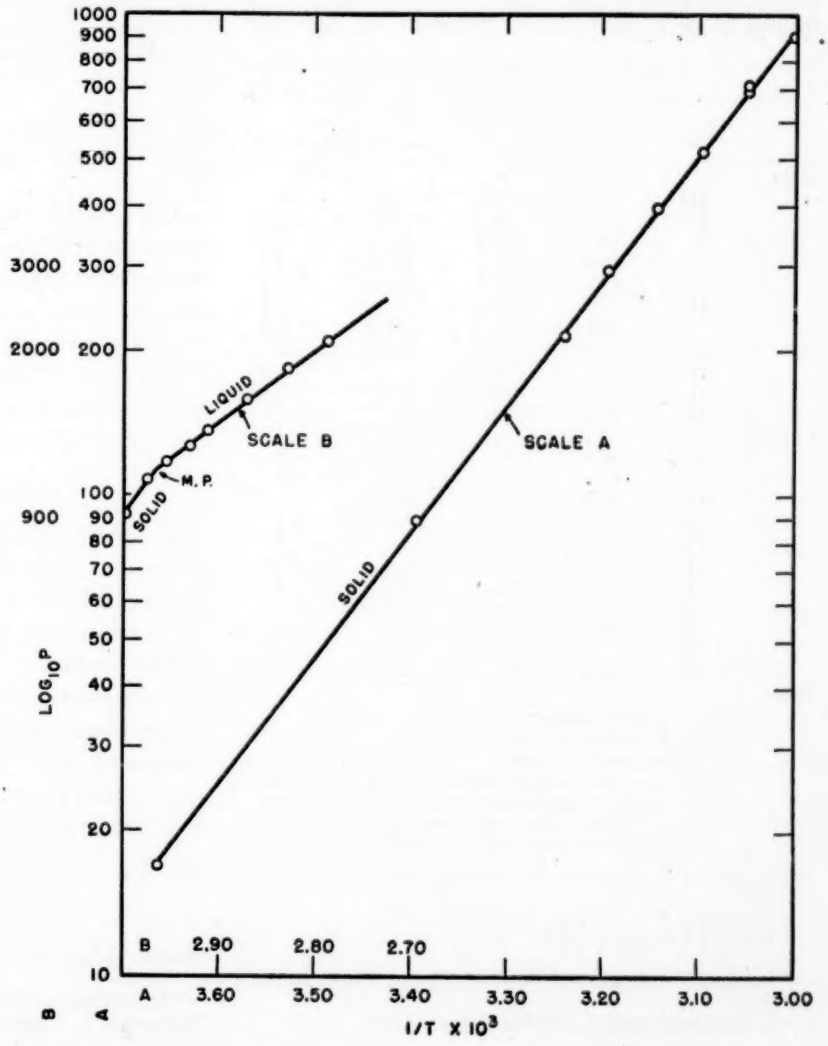

FIG. 3. Vapor pressure of UF_6 $\log_{10}P$ (mm Hg) *vs.* $1/T$ (°K).

value at the triple point. Using the Berthelot equation of state[4] this can be shown to be:

$$C_s - C_l = \frac{\Delta C_P^{(t)} + (9/128)(P_t/P_c)(T_c/T_t)[1-(18T_c^2/T_t^2)][\Delta H_f/(1+\alpha)_t T_t]}{R(1+\alpha)_t}, \quad (4)$$

where the subscript c refers to the critical point, $\Delta C_P^{(t)}$ is the measured difference in specific heats at the triple point, and $(1+\alpha)$ is the ratio of the actual volume to the ideal volume, as calculated by the Berthelot equation.

The values of T_t, ΔH_f, and $\Delta C_P^{(t)}$ used were those determined by Brickwedde, Hoge, and Scott,[5] namely, $T_t = 337.213°K$, $\Delta H_f = 4588$ cal./mole, and $\Delta C_P^{(t)} = -2.10$ cal./mole/°C. The values of the critical constants used were those given by Kirshenbaum,[6] namely, $T_c = 518°K$, and $P_c = 36{,}000$ mm. The value of the triple-point pressure P_t used was 1130 mm and was determined from a preliminary solution for the constants. Substituting these values, the vapor pressure equations become:

$$\ln P_s = (A_s/T) + B_s + C_s \ln T, \quad (5)$$

$$\ln P_l - (2435.7/T) - 0.053 \ln T + 7.53108 = (A_s/T) + B_s + C_s \ln T.$$

By substituting the observed values of P and T into these equations, a set of equations involving the constants A_s, B_s, and C_s is obtained. The constants are readily obtained from these equations by the method of least squares, both solid and liquid points being taken together. The solution then yields the equations:

$$\log_{10} P_s = -(3123.479/T) + 21.87103 - 3.77962 \log_{10} T,$$

$$\log_{10} P_l = -(2065.679/T) + 18.60033 - 3.72662 \log_{10} T. \quad (6)$$

The average deviation of the log of the vapor pressures over the whole range is ± 0.00276. The triple-point pressure is calculated to be 1133 ± 7 mm, the error being estimated from the average deviation over the whole range.

The heat of vaporization at the vapor pressure can be calculated from the relationship (the volume of the condensed phase being negligible):

$$\Delta H_{vap} = VT(dP/dT)_V, \quad (7)$$

where $(dP/dT)_V$ is obtained from the vapor pressure equations and V from the Berthelot equation. Four values have been calculated and are tabulated in Table II.

The absolute entropy of the ideal gas at 1-atmosphere pressure, $S°$, was calculated. The values obtained are listed in Table II and will be compared with those calculated from spectroscopic data in another paper.[7] The calculation of $S°$ was made from the well known relationship

$$S° = \Delta S_{vap} + S_s + (S_{ideal} - S_{actual}) + R \ln(P_{mm}/760), \quad (8)$$

where ΔS_{vap} is the entropy change upon va-

TABLE I. Vapor pressure of UF_6.

	Sample No.	Temp. °C	P_{exp} mm Hg	P_{cal} mm Hg	$P_{cal} - P_{exp}$
Solid					
	III	0.	16.9	16.9	0
	I	21.6	88.3	87.5	−0.8
	I	35.5	216.8	220.5	3.7
	I	40.0	295.4	291.7	−3.7
	I	45.0	397.8	294.2	−3.6
	II		395.8		−1.6
	I	50.0	522.1	527.2	5.1
	I	55.0	711.1	698.2	−12.9
	II		697.2		1.0
	II	60.0	910.0	916.2	6.2
	III	63.1	1072.	1079.	7.0
Liquid					
	II	65.0	1169.	1167.	−2.
	II	67.9	1273.	1274.	1.
	II	70.1	1360.	1361.	1.
	IV	70.2	1366.	1365.	−1
	III		1370.		5.
	III*		1376.		11.
	III	75.2	1582.	1577.	−5.
	III*	75.3	1568.	1582.	14.
	III*	80.3	1830.	1820.	−10.
	III		1838.		−18.
	III	85.4	2087.	2089.	2.

Note:
I is first sample
II is first sample purified
III is second sample
IV is a new sample measured one month later with an equimolar amount of KF present
* indicates that the equilibrium was approached from higher temperatures.

[4] $V = \frac{RT}{P}\left[1 + \frac{9}{128}\frac{P}{P_c}\frac{T_c}{T}\left(1 - \frac{6T_c^2}{T^2}\right)\right]$.

[5] Brickwedde, Hoge, and Scott, J. Chem. Phys. **16**, 429 (1948).

[6] I. Kirschenbaum, Columbia Report A753.

[7] J. Bigeleisen, M. G. Mayer, P. C. Stevenson, and J. Turkevich, J. Chem. Phys. **16**, 442 (1948).

porization at the vapor pressure of the actual gas and is equal to $V(dP/dT)_v$; S_s is the entropy of the condensed phase under its own vapor pressure and is taken from Brickwedde's[5] measurements; $S_{ideal}-S_{actual}$ is the entropy change in converting the actual gas to the ideal gas which by the Berthelot equation is given by $(27R/32)\times(P/P_c)(T_c/T)^3$; $R\ln(P_{mm}/760)$ is the entropy change on taking the ideal gas from its saturation pressure to 1 atmosphere.

The values of these quantities are tabulated in Table II. In Table II, column 1 gives the absolute temperature, column 2, the gas imperfection $1+\alpha$, column 3, the heat of vaporization of the actual gas, column 4, the values of S_s determined by Brickwedde,[5] column 5, ΔS_{vap}, column 6, $R\ln P/760$, column 7, $(27R/32)(P/P_c)\times(T_c/T)^3$, and column 8, S°. The heat of vaporization is given in cal./mole and the entropy terms in cal./mole/°C.

TABLE II.

°K T	$1+\alpha$	ΔH_{vap}	S_s	ΔS_{vap}	$R\ln P/760$	$\frac{27R}{32}\frac{P}{P_c}\left(\frac{T_c}{T}\right)^3$	S°
273	.9987	12,220	51.02	44.77	−7.59	0.01	88.21
298	.9936	11,970	54.42	40.18	−3.87	0.03	90.76
323	.9764	11,580	57.73	35.86	−0.75	0.12	92.96
*348	.9441	6,487	74.62	18.64	1.42	0.29	94.97

* Liquid.

The absolute entropy values have a probable error of 0.6 e.u. This arises from a probable error of 0.5 e.u. in S_s reported by Brickwedde[5] and a probable error of 0.3 e.u. in ΔS_{vap}. The error assigned to ΔS_{vap} is much higher than that calculated from the deviations in ΔH_{vap}. It is based on the usual discrepancy of the order of 100 cal. between calorimetric values of ΔH_{vap} and those obtained from vapor pressure data. The errors in the other two terms used in calculating S° are small in comparison.

Vibrational Spectrum and Thermodynamic Properties of Uranium Hexafluoride Gas*

JACOB BIGELEISEN[1] AND MARIA GOEPPERT MAYER[2]
S.A.M. Laboratories, Columbia University, New York, New York

AND

PETER C. STEVENSON AND JOHN TURKEVICH
Frick Chemical Laboratory, Princeton University, Princeton, New Jersey

(Received December 12, 1947)

The Raman spectra of liquid UF_6 and of UF_6 dissolved in C_7F_{16} have been photographed. Three Raman lines are found for UF_6 at 200, 511, and 656 cm^{-1}. The infra-red spectrum of the gas has been obtained in the region between 2 and 17μ. A vibrational assignment of all the fundamental frequencies is made on the basis of the regular octahedral model. The calculated infra-red active overtones are in good agreement with experiment. Using 2.0A as the U–F distance from electron diffraction measurements, the entropy, heat capacity and $-(F°-E_0°/T)$ are calculated from 100°K to 1000°K for the gas. The calculated and experimental entropies are in good agreement.

I. INTRODUCTION

THE most regular form that a molecule of the type XY_6 can have is that of a regular octahedron. The molecules SF_6, SeF_6, and TeF_6 have been studied by electron diffraction,[3] infra-red absorption,[4] and Raman effect[5] and have been found to be regular octahedra. The Raman effect of the ions $SbCl_6^-$, $SnCl_6^=$, seems to indicate that these ions too are octahedral.[6,7] $SnBr_6^=$ has a lower symmetry which is easily explained by steric effects.[7] The hexafluorides of molybdenum, tungsten, and uranium have previously been studied by electron diffraction only[8] and all three were found to have a lower symmetry than O_h.

Uranium hexafluoride has no dipole moment (less than 0.5 debye),[9] which rules out a number of unsymmetrical configurations. The results of the infra-red and Raman measurements discussed in this paper show that uranium hexafluoride has the structure of a regular octahedron.

II. RAMAN EXPERIMENTS

The spectrograms were obtained in collaboration with Dr. R. F. Stamm of the Stamford Research Laboratories of the American Cyanamid Company. The spectrograph and the light sources have been described by Dr. Stamm.[10] We wish to thank Dr. R. B. Barnes and Dr. R. F. Stamm for their cooperation in obtaining the Raman spectra.

Three sets of exposures under different exciting conditions were necessary before the complete spectrum could be obtained. In the first set of exposures the spectrum of liquid UF_6 was obtained using 4358A excitation; in the second set the Raman spectrum of a solution UF_6 in C_7F_{16} was photographed using 4358A excitation; finally, the spectrum of a solution of UF_6 in C_7F_{16} was photographed using 5461A excitation. The cell used for all three sets of experiments is shown in Fig. 1. Great care was taken to keep the highly purified samples protected from ultraviolet light.

* This paper is based on work performed under Contract No. W-7405-eng-50 for the Atomic Energy Project, and it will appear in Division IV of the National Nuclear Energy Series (Manhattan Project Technical Section) as part of the contribution of Columbia University.

[1] Now at the Institute for Nuclear Studies, The University of Chicago, Chicago, Illinois.

[2] Now at the Argonne National Laboratory, Chicago, Illinois, and the Institute for Nuclear Studies, The University of Chicago, Chicago, Illinois.

[3] L. O. Brockway and L. Pauling, Proc. Nat. Acad. Sci. **19**, 68 (1933).

[4] (a) A. Eucken and H. Ahrens, Zeits. physik. Chemie **B26**, 297 (1934); (b) A. Eucken and F. Sauter, *ibid.* **B26**, 463 (1934); (c) H. Sachsse and E. Bartholomé, *ibid.* **B28**, 257 (1937).

[5] D. M. Yost, C. C. Steffens, and S. T. Gross, J. Chem. Phys. **2**, 311 (1934).

[6] O. Redlich, T. Kurz, and P. Rosenfeld, Zeits. physik. Chemie **B19**, 231 (1932).

[7] O. Redlich, T. Kurz, and W. Stricks, Monatshefte f. Chemie **71**, 1 (1938).

[8] H. Braune and P. Pinnow, Zeits. physik. Chemie **B35**, 239 (1937).

[9] C. P. Smyth and N. B. Hannay, Princeton University report number A2130.

[10] R. F. Stamm, Ind. and Eng. Chem., anal. ed. **17**, 318 (1945).

In spite of the precautions taken, the exposures of liquid UF_6 at 70°C using 4358A excitation had to be stopped after fifteen minutes. A considerable amount of fine fluffy solid appeared, which was caused by the photo-chemical reaction of the UF_6 and the glass, and gave rise to excessive Raleigh scattering. The gas bubbles of the boiling liquid also gave rise to a large amount of scattered primary light. The 4358A line was highly overexposed and the Rowland ghosts were very prominent so that no Raman lines below 300 cm^{-1} could be observed. In these experiments two Raman lines were found at 656 ± 3 cm^{-1} and 511± 3 cm^{-1}. In the second set of experiments using first a sample of pure C_7F_{16} and then a 20-mole percent solution of UF_6 in C_7F_{16} to eliminate scattering by the gas bubbles, the photo-chemical reaction of UF_6 with either C_7F_{16} and/or the glass gave rise to significant amounts of fine solid. Here again no Raman lines below 300 cm^{-1} could be observed. Finally, using 5461A excitation, a two-hour exposure of UF_6 in C_7F_{16} showed three Raman lines. One line was definitely due to C_7F_{16}. The other two lines were at 666 cm^{-1} and 202 cm^{-1}. The Raman line of UF_6 at 511 cm^{-1} did not appear because of the weakness of the exposure. The results are tabulated in Table I.

The samples were prepared as follows. The UF_6 was a purified laboratory sample which was molten in the presence of fused KF in a sealed glass system which had been previously baked while connected to a high vacuum system. This process frees the UF_6 from traces of HF. The UF_6 was distilled under high vacuum into the storage bulb connected to the Raman cell. For the investigation of the Raman spectrum the solid UF_6 was heated to the melting point in the storage bulb. The liquid was poured into the connecting Raman tube which was heated to prevent freezing by means of a Nichrome wire wrapped around the tube. The C_7F_{16} was obtained from Dr. W. T. Miller formerly at the S.A.M. Laboratories. The C_7F_{16} was refluxed overnight with UF_6 in a closed dry system after which it was fractionally distilled into a glass vessel containing sodium. The sodium had been distilled in, under high vacuum. The C_7F_{16} was then distilled into another bulb containing UF_6 and KF solids. The solution of UF_6 in C_7F_{16} was then distilled from the solid KF into the Raman storage bulb. All operations were done in high vacuum systems which had been thoroughly baked and outgassed.

TABLE I. Raman lines of UF_6.

Liquid (70°C)	Solution in C_7F_{16} (20°C)
656±3	666±3
511±3	—
—	202±3

III. INFRA-RED SPECTRUM

The infra-red spectrum of UF_6 from 2 to 17μ was obtained on the Princeton rocksalt spectrometer described by W. W. McCarthey and J. Turkevich.[11] The uranium hexafluoride used was a highly purified sample obtained from the S.A.M. Laboratories through the courtesy of Professor Anthony Turkevich to whom we are highly indebted for counsel and aid. A portion of this material was distilled in high vacuo into an infra-red absorption cell. The latter was made out of glass and had at the ends rocksalt

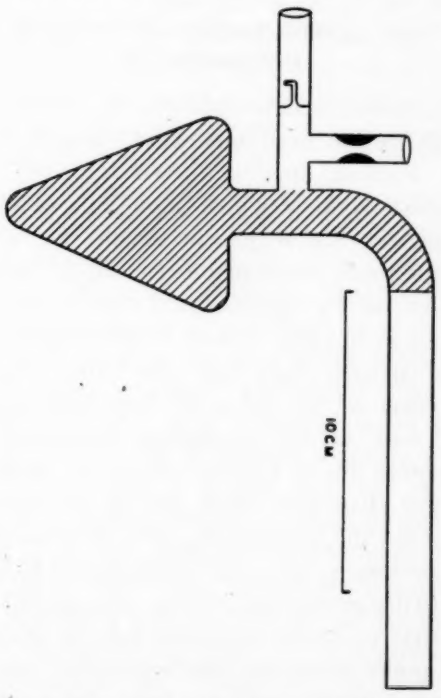

FIG. 1. Raman cell for UF_6. The shaded portion is made of "Pyrex Lifetime Red" glass.

[11] W. W. McCarthey and J. Turkevich, J. Chem. Phys. 12, 461 (1944).

TABLE II. Fundamental vibrations of UF_6.

	Frequency	Symmetry	Degeneracy	Activity	Observed
ν_1	656	A_{1g}	1	Raman	656±3
ν_2	511	E_g	2	Raman	511±3
ν_3	200	T_{2g}	3	Raman	202±3
ν_4	130	T_{2u}	3	Inactive	—
ν_5	200	T_{1u}	3	Infra-red	—
ν_6	640	T_{1u}	3	Infra-red	623 or larger

windows baked on in vacuum at 150°C with glyptal. The length of the cell was 20 cm. A side tube on the cell always contained some solid UF_6. The pressure of the UF_6 in the absorption cell was regulated by controlling the vapor pressure of the solid UF_6 in the side tube by use of appropriate temperature baths. During the course of repeated measurements a slight reaction of the UF_6 and the moisture in the rocksalt took place. This resulted in the formation of a slight film whose absorption was determined by freezing out the UF_6 from the cell into the side tube by liquid air. The infra-red spectrum of UF_6 was taken at several pressures and the results are tabulated in Table III.

IV. CONFIGURATION OF URANIUM HEXAFLUORIDE

If uranium hexafluoride has the structure of a regular octahedron, one would expect to find three Raman lines and two infra-red active vibrations, one of which should be of low frequency. In the region in which the infra-red measurements were made one would expect to find one active fundamental. Table III shows one line at 623 cm^{-1} which is about one hundred times stronger than any other line. However, inspection of the infra-red data indicates that there may be an accidental degeneracy. The absorption line at 675 cm^{-1} is two to three times stronger than any other line in the spectrum, except for the line at 623 cm^{-1}. It seems reasonable to assume that the fundamental frequency is actually somewhat higher, say at 640 cm^{-1}; and that a double overtone falls at about the same point. Thus the two lines at 623 cm^{-1} and 675 cm^{-1} would originate from the interaction of the two levels at about 640 cm^{-1}. The experimental results of the number and the positions of active lines both in the infra-red and Raman spectra are strong arguments in favor of this completely symmetrical model.

On this basis the following assignment of the fundamental frequencies is made (Table II).

The results of x-ray diffraction on single crystals of uranium hexafluoride of Hoard and Stroupe[12] are in agreement with the symmetrical model, although they can also be reconciled with a less symmetrical structure. Hoard and Stroupe propose a configuration in which there are two sets of U—F distances. Two opposite U—F distances are assumed to be equal and longer than the remaining four. This reduction in symmetry would introduce a splitting of all but the breathing vibration, A_{1g}. One component of the vibration T_{2u} would become infra-red active.

Electron diffraction measurements of the gas have been made by Braune and Pinnow[8] and more recently by Bauer.[13] Both workers do not find a completely symmetrical structure. Bauer considers a model in which there are two sets of U—F distances and the U—F bonds are at right angles. This is not in agreement with Hoard and Stroupe's results. With this model all triply degenerate frequencies in Table II split. In addition, all Raman active frequencies should be infra-red active and *vice versa*. One component of the inactive vibration, ν_4, should also be infra-red and Raman active.

It is conceivable that the deviations from regular octahedral symmetry might be small enough so that the splitting is not resolvable and the new lines are too weak to be observed. In that case, there is still one argument left in favor of complete symmetry. In Section VI the

TABLE III. Infra-red spectrum of UF_6.

	Calculated	Observed	Strength
ν_5	200 cm^{-1}	—	
$\nu_4+\nu_3$	330	—	
$\nu_5+\nu_3$	400	—	
ν_6	640	623	1000
$\nu_4+\nu_2$	641	675	10
$\nu_5+\nu_2$	711	713–719	½
$\nu_6+\nu_3$	840	825	2
$\nu_5+\nu_1$	856	850	¼
$\nu_6+\nu_2$	1151	1163	4
$\nu_6+\nu_1$	1296	1295	3
		2053	½

[12] J. L. Hoard and J. D. Stroupe, Columbia Report A 1242, March, 1944. Declassified October 7, 1946.

[13] S. H. Bauer, Columbia Report A-1209. Declassified October 14, 1946.

entropy of the gas is calculated from the frequency assignment of Table II with the use of the symmetry number 24. This is shown to be in good agreement with, although somewhat lower than the experimental value. On the basis of the Hoard and Stroupe model the calculated entropy will be raised by $R \ln 3 = 2.18$ e.u., and Bauer's model would be higher by $R \ln 8 = 4.13$ e.u. Both of these results are in poor agreement with the experimental entropy. We are therefore led to believe that the gas UF_6 has the structure of a regular octahedron.

V. ANALYSIS OF INFRA-RED DATA

With the help of the assignment of the fundamentals it is possible to calculate all the infra-red active double combination frequencies. The assignment of the inactive frequency, ν_4, was made to obtain an accidental degeneracy by combining ν_4 with ν_2 to give 641 cm^{-1}, which is accidentally degenerate with the active fundamental at 640 cm^{-1}. The calculated and observed values are compared in Table III.

VI. THERMODYNAMICS OF URANIUM HEXAFLUORIDE

The vibrational spectra together with the interatomic distances provide a basis for the calculation of the thermodynamic functions of uranium hexafluoride gas. The vibrational assignment given in Table II was used. The structure of the molecule was taken as a regular octahedron in conformity with the vibrational assignment. The six uranium to fluorine distances were taken as 2.0A. This is very close to the average of the distances given by Bauer[13] and by Braune and Pinnow.[8] In any case, there is little error introduced into the rotational contributions if the distances differ from 2.0A by as much as five percent. In accordance with the usual convention the entropies of nuclear spin and isotope mixing are neglected. The symmetry number was taken as 24. The results for the ideal gas are given in Table IV.

TABLE IV. Thermodynamic properties of UF_6 from spectroscopic data.

T°K	S° in cal. deg.$^{-1}$ mole^{-1}	Cp in cal. deg.$^{-1}$ mole^{-1}	$-(F°-E_0°)/T$ cal. deg.$^{-1}$ mole^{-1}
100	62.99	18.93	50.91
150	71.58	23.45	56.41
200	78.81	26.74	61.14
273	87.65	30.13	67.08
298	90.34	31.00	68.92
323	92.89	31.75	70.69
348	95.22	32.38	72.33
373	97.47	32.93	73.93
400	99.86	33.46	75.65
500	107.45	34.80	81.25
750	122.37	36.35	92.99
1000	132.58	36.94	101.37

TABLE V. Calculated and experimental entropy of UF_6 gas.

T°K	S° Exp.	S° Calc.	S°Exp. −S°Calc.
273	88.21	87.65	+0.56
298	90.76	90.34	+0.42
323	92.96	92.89	+0.07
348	94.97	95.22	−0.25

The calculated values may be compared in part with the best experimental data available. Brickwedde, Hoge, and Scott[14] have determined the heat capacity of solid uranium hexafluoride from 20°K to 337.2°K and of the liquid from 337.2°K to 370°K. Crist and Weinstock[15] have measured the vapor pressures of uranium hexafluoride from 273°K to 358°K. From these measurements and the critical constants of the gas, Crist and Weinstock have calculated the entropy of the gas at several temperatures. Their experimental entropies are compared with some of the entropies calculated from spectroscopic data in Table V.

It will be seen that the calculated entropies agree with the experimental ones to better than 0.7 percent. The differences are within the probable limits of error of either determination. There is a somewhat larger than usual uncertainty in the third law entropy of the condensed phases.[14] The entropy of sublimation has not been directly determined and may be in error by about 0.2 cal. deg.$^{-1}$ mole^{-1}. There are nine vibrational frequencies below 200 cm^{-1}, which have been treated as harmonic. This approximation will give a low calculated entropy. In addition if one of the triply degenerate frequencies ν_4 or ν_5 has been incorrectly assigned by about 10 cm^{-1}, the calculated entropy will be changed by about 0.5 cal. deg.$^{-1}$ mole^{-1}.

[14] F. G. Brickwedde, H. J. Hoge, and R. B. Scott, J. Chem. Phys.
[15] R. H. Crist and B. Weinstock, J. Chem. Phys.

Infra-Red Emission Spectra of Hot Liquids*

S. F. KAPFF
Research Laboratories, Distillation Products, Inc., Rochester 13, New York
(Received October 16, 1947)

When a liquid is heated as a thin film, specific infra-red emission bands are observed, most of which are of the same wave-length as the absorption bands of the material. These emission bands are rapidly obscured by the background radiation as the thickness of the film is increased. The optimum sample thickness is of the order of 0.001 inch with most of the bands being obscured at thicknesses of 0.010 inch. The intensity of any band increases with temperature in accordance with the equation $N_1 = N_0 e^{-E/RT}$. The value of E calculated from this equation has been found to agree in most cases with that calculated from the wave-length of the emission band. Certain bands have been observed which are not equivalent in emission and absorption. It has been tentatively suggested that these may be explained on the basis of overtone and combination bands.

INTRODUCTION

THE infra-red emission spectra of organic liquids can be shown to exist by the simple expedient of exposing them in a very thin, warmed layer in front of the slit of an infra-red spectrometer.[1] Failure to observe specific emission spectra previously has probably arisen from the use of the hot liquid in bulk in which circumstance it emits only blackbody radiation.

When the heated film is about 0.001 inch thick, specific infra-red emission bands are obtained which are mainly the inverse of the absorption bands observed by conventional methods. Upon increasing the temperature the intensities of all the bands are increased, those of shorter wave-length more than the longer. Since the emission at long wave-lengths is already small by reason of the blackbody laws, the increase in temperature has the effect of further emphasizing the already strong short wave-length bands.

Attempts to obtain emission spectra as close as possible to room temperature have given reliable values for the emissions at the positions of the strong bands at temperatures as low as 35–40°C. The relatively feeble response obtained at these temperatures does not indicate that the vibrational transitions involved are infrequent but rather arises from the fact that the spectrometer can only measure energy differences between the temperature of the receiver and that of the source. It seems quite likely that with a cooled instrument emission spectra could be obtained from liquids at room temperature or even lower.

TABLE I. Blackbody emission. Experimental data by null method (arbitrary units).

Wave-length μ	Temperature, °C 75	100	125	150	175
3.36	0.33	0.76	1.81	3.19	5.56
3.93	0.67	1.55	3.01	5.36	8.6
4.92	1.37	2.72	4.85	7.76	11.8
5.77	1.53	2.88	4.91	7.48	11.0
6.32	1.60	2.82	4.72	6.88	10.0
6.85	1.32	2.67	4.35	6.24	8.4
7.02	1.42	2.56	4.13	5.72	7.95
7.22	1.38	2.42	3.79	5.44	7.29
7.80	1.43	2.30	3.70	5.18	6.91
8.34	1.21	1.90	3.03	4.35	5.78
8.84	1.09	1.76	2.57	3.57	4.64
9.30	1.02	1.64	2.37	3.03	4.15
9.59	0.99	1.46	2.07	2.81	3.75
10.42	0.79	1.11	1.48	2.15	2.87
12.65*	0.94	1.38	1.81	2.49	2.95

* Slits =0.800 mm (other values 0.500 mm).

EXPERIMENTAL

The instrument used throughout this investigation was a Perkin-Elmer infra-red spectrometer 12A[2] connected to a Brown recorder through the conventional galvanometer-photo-cell system. Calibration of the wave-length drum was effected by the use of reported values[3] of the absorption bands of water vapor, carbon dioxide, and ammonia. The instrument was operated in an air-conditioned room and only slight changes in

* Communication No. 118 from the Research Laboratories of Distillation Products, Inc., Rochester, New York.
[1] S. F. Kapff, Science **104**, 274 (1946).
[2] R. B. Barnes, R. S. McDonald, V. Z. Williams, and R. F. Kinnaird, J. App. Phys. **16**, 77–86 (1945).
[3] R. A. Oetjen, Chao-Lan Kao, and H. M. Randall, Rev. Sci. Inst. **13**, 515–523 (1942).

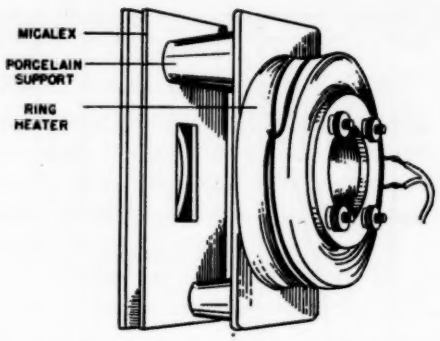

FIG. 1. Cell holder for emission spectra.

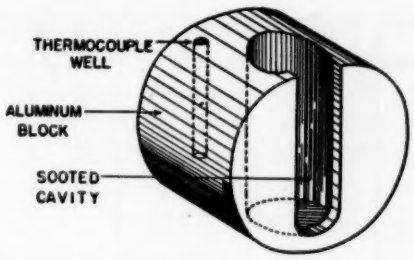

FIG. 2. Blackbody radiator.

calibration have been noticed over a period of two years. Proper calibrations were readily determined by using the carbon dioxide doublet at 4.28 and 4.225μ as a standard and checking its position periodically.

The cells used for absorption spectra were the conventional sodium chloride plates with 0.0005-inch spacers.

For emission spectra the cell holder shown in Fig. 1 was used. It consists of a ring heater for heating the cell and a heat shield to protect the spectrometer. This type of mounting was found essential because placing the heated cell directly in the cell guides of the spectrometer caused such a rapid drift in the recorder that accurate measurements were impossible.

The emission cell itself consisted of a sodium chloride plate, an aluminum spacer, and a backing plate of polished aluminum. This backing added some undesirable blackbody background to the curves, but its use was continued since it afforded a convenient place to insert a thermocouple and the polished surface reflected additional infra-red emission into the spectrometer. Cell thicknesses were adjusted from 0.001 inch to 0.010 inch by using aluminum foil spacers. No attempt was made at this time to seal the cell and hence the materials usable were limited to those of low vapor pressure. The same cell was used throughout a series of comparable measurements to eliminate possible errors from changing cells.

Temperatures were read with a copper-constantan thermocouple placed in a small hole in the aluminum backing plate. The current through the heater coil was manually controlled to hold the temperature within ± 2°C.

To determine the emission spectrum of a material, the cell was made up as described and placed in the spectrometer. It was rapidly raised to the desired temperature and maintained there by careful adjustment of the heater current. The slits were adjusted to a suitable value, 0.300 to 1.500 mm, depending on the temperature, the recorder and wave-length drives started, and the spectrum recorded through the desired interval.

For determining the quantitative intensities of emission at various individual wave-lengths, a null method was employed to eliminate possible errors from slow changes in the brightness of the galvanometer lamp. Briefly, the method consisted in adjusting the position of the photo-cells in the amplifier arrangement so that a certain zero was obtained with a shutter in the beam. After removal of the shutter, the photo-cells were

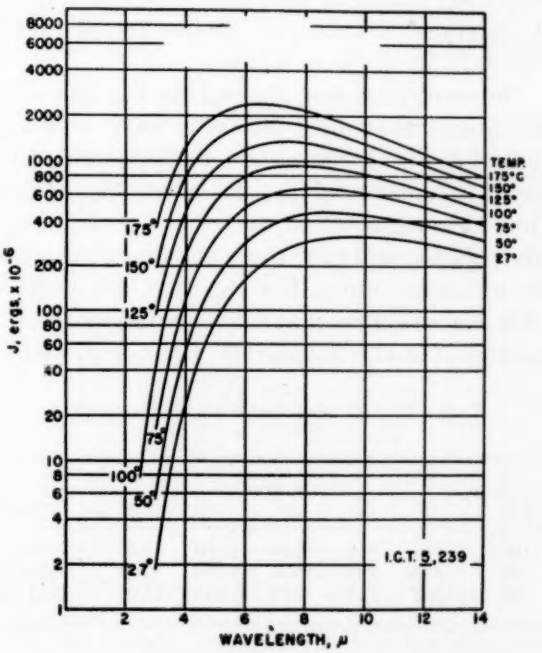

FIG. 3. Blackbody radiation.

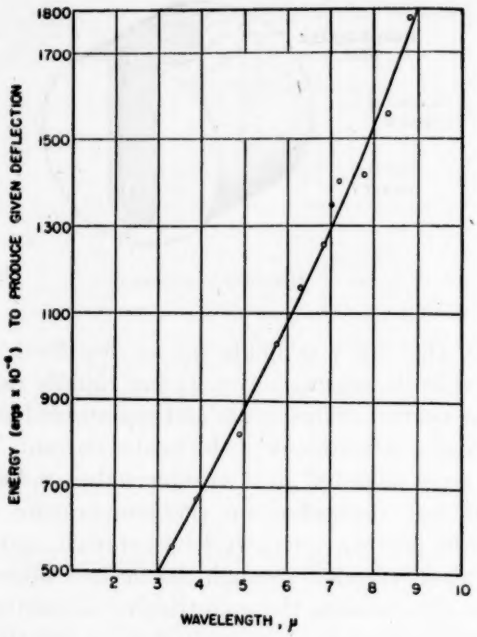

FIG. 4. Response curve of receiver.

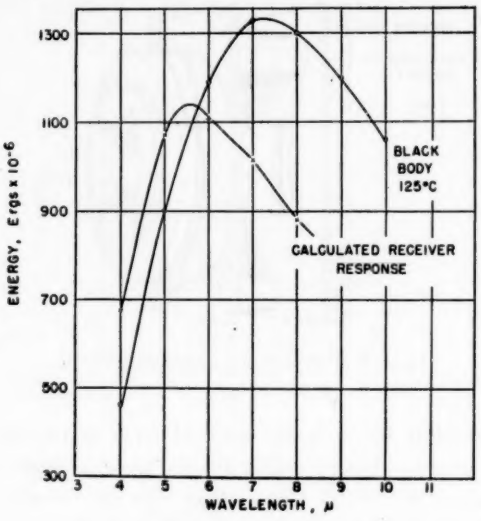

FIG. 5. Shift in emission maximum.

again positioned so that the same zero was obtained. The differences in the two readings of the adjusting mechanism are the values given in the tables of experimental results.

To furnish a standard for conversion of null method readings to absolute energy values, the blackbody shown in Fig. 2 was made and readings of its emission taken at various temperatures. The data are given in Table I.

The conversion was accomplished by the use of the literature values for blackbody emission[4] plotted in Fig. 3. Since the zero of the recorder is the 27°C curve and the blackbody readings of Table I correspond to the other curves, simple interpolation will give the value of a given reading in energy units. For example, the band at 6.85μ has an emission at 125°C, which results in a reading of 3.42 (Table III). From Fig. 4, it is found that a blackbody at this wave-length emits 2.30 and 13.30×10^8 ergs/cm^3/sec. at 27°C and 125°C, respectively. Since the reading in Table I at this wave-length for a blackbody at 125°C is 4.35, the value of the emission of the sample is given by:

$$J=[(3.42/4.35)\times11.00\times10^8]+2.30\times10^8,$$
$$J=10.95\times10^8 \text{ ergs/cm}^3\text{/sec.}^1$$

Trouble was experienced in the blackbody determinations in obtaining correspondence with the literature values for the position of the maximum of emission at various temperatures. For example, in one series of determinations this maximum occurred at 5.5μ which, according to the literature,[4] indicated a temperature of 250°C instead of the 125°C read on the thermocouple. At 125°C the maximum emission should occur at 7.26μ.

This anomaly might arise from either of two sources: non-blackbody emission from the blackbody standard, or changing response of the receiver with changing wave-length. If we assume the blackbody to be correct, then from the data of Table I and Fig. 3 we can plot the energy needed at various wave-lengths to produce a given reading. This gave the response curve of Fig. 4 which shows a regular decrease in response so that roughly three times the energy is required at 8μ as is needed at 3μ to produce a given deflection of the recorder. That the response of the receiver is at fault seems more likely in view of

TABLE II. Effect of non-blackbody standard J_λ, ergs$-$cm.^{3}/sec$^1\times10^{-6}$.

Percent of B.B.	Temperature, °C 75	100	125	150	175	E, Slope
100	564	848	1150	1510	1920	3.73 Cal.
90	536	792	1064	1390	1760	3.64 Cal.
80	507	735	975	1265	1590	3.52 Cal.

[4] *International Critical Tables* (McGraw-Hill Publishing Company, Inc., 1926–1930), Vol. V, p. 239.

the data below on the effect of a non-blackbody standard.

In Fig. 5 the blackbody curve for 125°C radiation is shown. This curve was recalculated using the response curve of Fig. 4 and the second curve obtained. This curve has its maximum emission at 5.6μ in good agreement with the observed experimental value of 5.5μ.

If the blackbody standard actually emitted only 90 percent or 80 percent of blackbody intensity at a given wave-length, then the slopes of the log$J$ *vs.* $1/T$ plots would be changed. The calculations of this possibility are shown in Table II for the emission band at 7.80μ.

It is apparent that the use of an imperfect blackbody as a standard produces considerable change in the values calculated for the absolute emission; however, the slope is much less affected, an error of 20 percent in obtaining true blackbody emission producing an error of 7 percent in the slope. Further calculations have shown that the greater the slope, the smaller is the error introduced by using a non-blackbody radiator. This effect results from corrections being less important at the shorter wave-lengths since here the 27°C radiation for a blackbody is quite small.

Several minor experimental difficulties were experienced in determining the emission spectra. The zero drift of the spectrometer, resulting from the proximity of the source to the instrument, caused some inconvenience, but it was found that the apparatus and cell reached an equilibrium after 20 to 30 min. and thereafter a fairly constant zero was obtained. This drift may be eliminated by placing the emitting cell at the globar position. However, this is inconvenient when both emission and absorption spectra are desired.

The chemicals used for obtaining these spectra were diamylphthalate (Amoil), diamyl sebecate (Amoil-S), di-(2-ethyl-hexyl) phthalate (Octoil), and di-(2-ethyl hexyl) sebecate (Octoil-S). The samples on hand were those supplied commercially for use as diffusion pump fluids and were used without further purification. The selection of materials was governed by the vapor pressures because of the previously mentioned limitations of the cell.

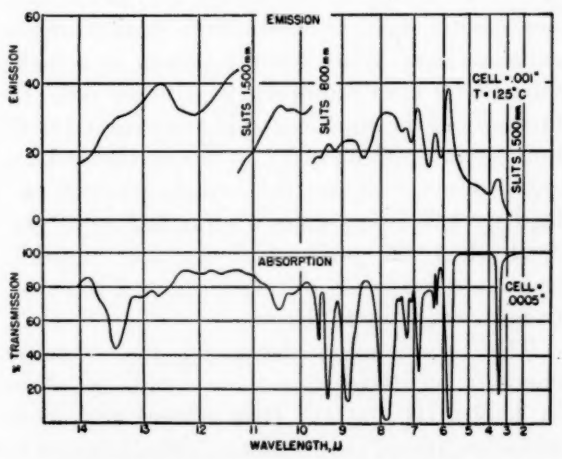

FIG. 6. Infra-red spectra of Octoil.

DISCUSSION

Representative spectra are shown in Figs. 6 to 9 where the absorption and emission bands can be compared. After making allowance for the much poorer resolution of the emission spectra, it is evident that within the experimental error no shift in wave-length is observed for emission and absorption bands.

This close agreement between the wave-lengths of the emission and absorption bands suggests that the same two pairs** of energy levels are involved. However, at low energies especially, the spacings between adjacent levels are very nearly constant and hence different transitions could easily have the same energy. When the vibrational transition is known to be a fundamental,

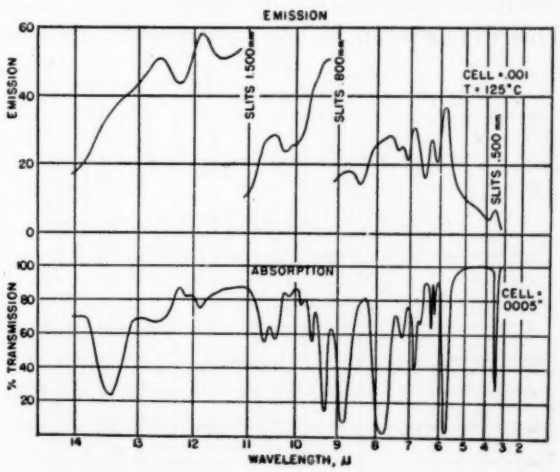

FIG. 7. Infra-red spectra of butyl phthalate.

** In the following discussion, for simplicity, the system of a vibrational level and all of its rotational levels is spoken of as though a single level.

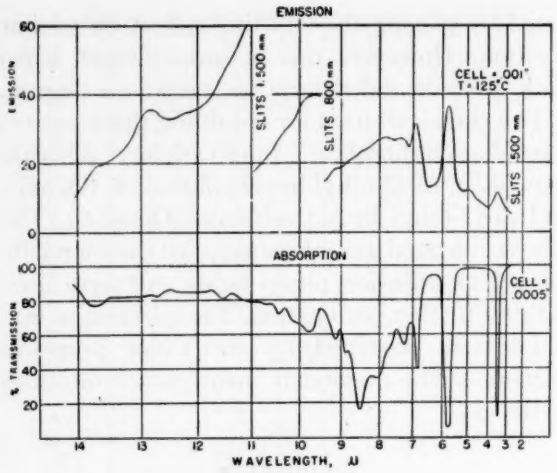

FIG. 8. Infra-red spectra of Octoil-S.

then in the absence of strong overtone absorption bands the return transition must be from the first excited state to the ground state.

In certain portions of the spectrum absorption bands occur without any corresponding specific emission bands being observed, e.g., Octoil-S and Amoil-S at 8.5μ. Since at the temperatures employed it is impossible for the particular system involved in the absorption to remain in the excited state for an appreciable time, a loss of the energy and a return to the normal state have occurred without radiation of the characteristic frequency. A transfer of the vibrational energy to other parts of the molecule and its subsequent radiation as several smaller quanta might occur. This would result in new, or stronger, emission

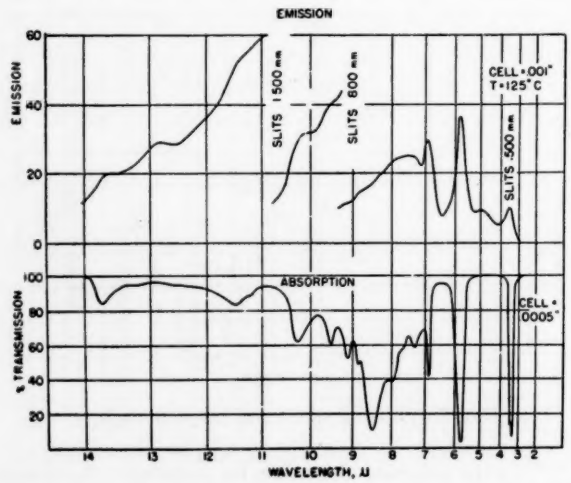

FIG. 9. Infra-red spectra of Amoil-S.

bands at longer wave-lengths. Another possibility arises if the vibration band observed is a combination frequency. Then emissions may occur as the individual quanta. This also will result in bands at longer wave-lengths. Unexpectedly strong emission bands are shown at long wave-lengths and further work on them is planned.

TEMPERATURE DEPENDENCE

The temperature dependence of the emission bands can be seen in Fig. 10 where the curves at 75°, 125°, and 175°C are given for Octoil in a 0.001-inch cell. It can be seen that the intensities are increased at all wave-lengths as the temperature is increased and that the rate of increase depends on the wave-length.

According to Wien's law for blackbody radiation, the emission at a given wave-length is given by the equation: $J_\lambda = c_1\lambda^{-5}e^{-c_2/\lambda T}$ where c_1 and c_2 are constants and T is the absolute temperature. Data following this law yield straight lines on a $\log J$ *vs.* $1/T$ plot. Figure 11 shows this for a few wave-lengths from the data of Table IV. The constants c_1 and c_2 can be determined from these graphs but they will obviously have different values depending on the wave-length since the present conditions of emission are far from the blackbody conditions for which the law was derived.

A more comprehensive explanation of the temperature effect on emission can be obtained by the use of the Boltzmann equation $N_1 = N_0e^{-E/RT}$ which gives the number of molecules in an activated state at any temperature T when the activation energy of the process is E. In the emission spectra this sort of situation obtains since an emission band arises from a system in a higher vibrational state dropping to a lower one. The intensity of the emission, J, is proportional to the number of molecules, N_1, in the excited state at any instant. Plotting the emission values on a $\log J$ *vs.* $1/T$ graph gives a straight line of slope E/R where the units of E are determined by those selected for R. In this research R was taken to be 1.99 cal/mole °K.

The experimental data and the transition energies calculated from these results are shown in Tables III and IV. It is evident that as the wave-lengths of the emission bands increase the transition energies become less. In other words,

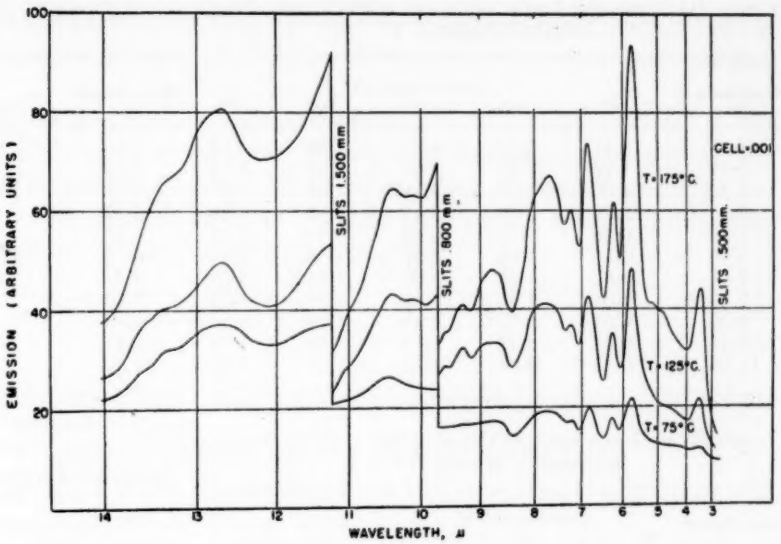

FIG. 10. Infra-red emission spectra of Octoil as a function of temperature.

the rate of increase of the emission intensity with temperature is less at longer wave-lengths.

The molal energy of the transition between two vibrational energy levels can be calculated by the equation $E = Nh\nu$, where ν is the frequency of the band observed as the result of the transition. A comparison has been made of this value with the E obtained from the slopes. The values are compared in the last two columns of Table IV where the agreement is satisfactory at most wave-lengths.

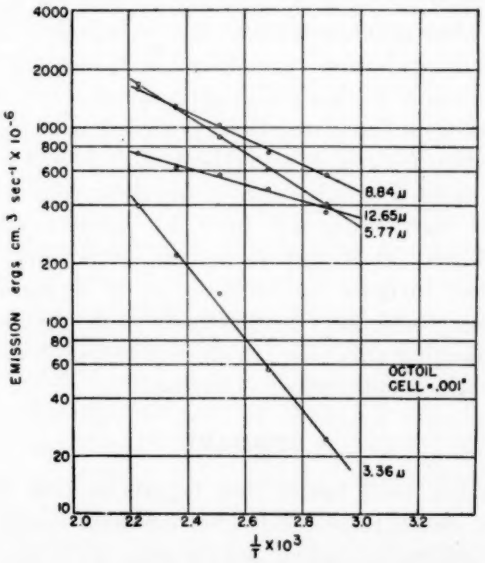

FIG. 11. Infra-red emission as a function of temperature. (The label of the ordinate should read "Emission ergs cm^{-3} $sec.^{-1} \times 10^{-6}$.)

It will be noticed that the strong bands at 5.77μ and 6.32μ show temperature dependencies that result in E values lower than that calculated from $Nh\nu$. Experimental data are lacking as to the cause of this, but the following hypothesis is suggested. It is well established that absorption of energy can raise the molecule either to the first excited state or a higher state. If an appreciable number of molecules make the transition to the second excited state, then the number in state 1 will be less than calculated on the basis of $e^{-E/RT}$ in such a manner as to make $E_{(obs.)}$ appear to be too small compared to $E_{(Nh\nu)}$. This explanation

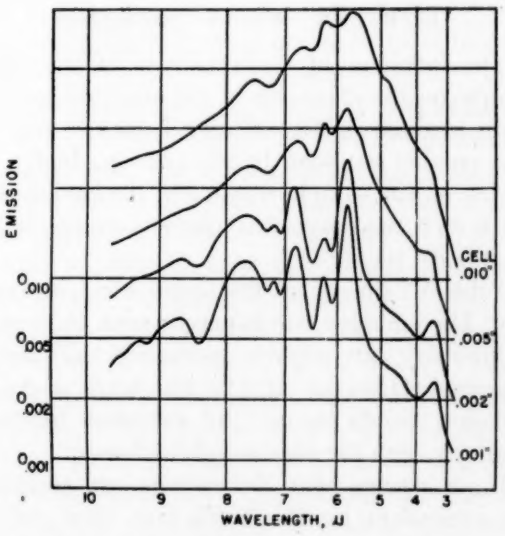

FIG. 12. Emission of Octoil at various thicknesses.

TABLE III. Emission bands of Octoil (0.001" cell). Null method readings.

Wave-length μ	Temperature, °C 75	100	125	150	175
3.36	0.21	0.45	0.89	1.90	3.44
5.77	1.26	2.19	3.65	5.44	7.73
6.32	1.00	1.68	2.78	4.06	5.57
6.85	1.27	2.16	3.42	4.74	6.72
7.22	0.96	1.75	2.68	3.93	5.42
7.80	1.10	1.98	3.07	4.32	5.91
8.84	0.82	1.28	2.00	2.81	3.70
9.30	0.64	1.06	1.76	2.29	3.00
9.59	0.51	0.92	1.49	1.90	2.47
10.42	0.41	0.72	1.16	1.49	1.81
12.65	0.53	0.95	1.25	1.51	1.90

TABLE IV. Emission bands of Octoil (0.001" cell). Corrected readings, J in ergs$\times 10^{-6}$.

Wave-length μ	Temperature, °C 75	100	125	150	175	E, Cal. (slope)	E, Cal. ($Nh\nu$)
3.36	22.4	56	137	217	391	8.46	8.46
5.77	401	614	895	1277	1680	4.41	4.92
6.32	404	588	833	1126	1426	3.90	4.49
6.85	586	772	1095	1420	1970	4.10	4.15
7.22	508	743	993	1373	1793	3.88	3.94
7.80	564	848	1150	1510	1920	3.73	3.64
8.84	566	740	1020	1285	1590	3.17	3.22
9.30	518	673	941	1173	1383	3.17	3.06
9.59	474	651	887	1035	1219	2.90	2.97
10.42	450	615	850	950	1040	2.71	2.72
12.65	369	479	565	613	738	2.08	2.25

requires the presence of a weak band at $m\nu$, where ν is the frequency of the transition to the first excited level and m is some small integer. Such emissions have been looked for but so far have not been found.

EFFECT OF SAMPLE THICKNESS

The influence of the thickness of the liquid sample on the character of the emission spectrogram is given in Fig. 12 and Tables V and VI. The specific emission bands were gradually obscured as the sample was made thicker until at 0.010 inch the curve was almost completely the blackbody type.

Table VI illustrates this same effect numerically. The emission bands can be seen to increase in intensity only slightly as the cell thickness is increased. However, at 3.93 and 4.92μ where no emission bands occur, the emission increases regularly with the increasing thickness.

If we assume that absorptions and emissions are equivalent by Kirchoff's law, then we can assume that emission will vary in a manner

TABLE V. Emission bands of Octoil at 125°C. Null method readings.

Wave-length μ	Cell thickness 0.001"	0.002"	0.005"	0.010"
3.36	1.27	1.31	1.57	1.49
3.93*	0.84	1.05	1.88	2.11
4.92*	1.32	1.54	2.83	3.27
5.77	4.26	4.39	4.53	4.49
6.32	2.78	3.47	4.06	4.05
6.85	3.55	3.97	3.92	3.80
7.22	3.13	3.60	3.51	3.50
7.80	3.41	3.52	3.51	3.51
9.30	2.14	2.19	2.19	2.11
10.42	1.37	1.48	1.57	1.48
12.65	1.42	1.61	1.80	1.70

* No emission band at this point.

TABLE VI. Percentage of blackbody radiation as a function of cell thickness. (Octoil at 125°C.)

λ, μ	Cell thickness 0.001"	0.002"	0.005"	0.010"
3.36	71	73	87	83
3.93*	31	38	64	72
4.92*	34	38	62	70
5.77	89	91	93	93
6.32	65	78	88	88
6.85	85	93	92	90
7.22	85	95	93	92
7.80	94	96	96	96
9.30	93	94	94	92
10.42	95	100	104	100
12.65	87	93	100	96

* No emission band at this point.

similar to absorption calculated by Beer's law. Consider two wave-lengths A and B in the infra-red absorption spectrum of a compound such that the radiation transmitted is 90 percent and 20 percent. If this occurred in a cell 0.001 inch thick, then the absorption coefficient μ in Beer's equation $I/I_0 = e^{-\mu z}$ would be 41.7 and 632 for the two cases. Further calculations show that a cell 0.005 inch thick will emit 41 percent like a blackbody at A and 99 percent at B. Since no further increase in emission at B is possible, further increases in thickness will result in submerging this band in the background radiation which continues to increase.

SUMMARY

It has been found that liquids in thin films show characteristic infra-red emission bands on heating, most of which are the same wave-lengths as the absorption bands of the material.

The temperature dependence of the emission

has been shown to be given by the Boltzmann equation $N_1 = N_0 e^{-E/RT}$ where E is the energy of the transition involved.

The equivalence of the E from temperature coefficients of emission and that calculated from the wave-length of emission has been confirmed.

New bands have been observed which are not equivalent in emission and absorption. It has been tentatively suggested that these may be explained on the basis of overtone and combination bands.

The thickness of the liquid film has been shown to affect the type of emission spectrum obtained, the thicker films giving more non-specific radiation of the blackbody sort, as elementary considerations suggest.

THE JOURNAL OF CHEMICAL PHYSICS VOLUME 16, NUMBER 5 MAY, 1948

The Calculation of Perturbation Energies in Vibrating Rotating Polyatomic Molecules*

ROBERT C. HERMAN
Applied Physics Laboratory, The Johns Hopkins University, Silver Spring, Maryland

AND

WAVE H. SHAFFER
Mendenhall Laboratory of Physics, The Ohio State University, Columbus, Ohio

(Received October 20, 1947)

An account is presented of the calculation of the purely vibrational contribution to the eigenvalues of the vibration-rotation Hamiltonian of a polyatomic molecule. Special attention is given to the expansion of the quantum-mechanical Hamiltonian; and to the results of the contact transformation of the Hamiltonian which simplifies the calculation of the second-order energy corrections. The results of the transformation theory have been presented in the form of tables. For each type of perturbation term which appears in the first-order Hamiltonian it is possible to obtain the second-order energy corrections by inspection. This procedure eliminates the need for applying the transformation to each specific problem. The use of these results is illustrated by working out in considerable detail the case of the X_2YZ_2 tetrahedrally symmetric molecular model.

I. INTRODUCTION

ONE of the excellent means of investigating molecular structure is the study of infra-red spectra which originate when a molecule makes transitions between different vibration-rotation energy states. It is essential, for the adequate interpretation of vibration-rotation spectra and the full utilization of the information which they afford, that the investigator know to a high order approximation the manner in which the vibrational and rotational energy states of the molecule depend upon the geometry and symmetry properties of the molecule, intramolecular forces, and other factors to be discussed below.

The interpretation of infra-red and Raman spectra can usually be carried out satisfactorily if a polyatomic molecule is considered as a system of atomic nuclei that rotate as a whole about the center of mass and in which the individual particles oscillate about equilibrium positions fixed in the molecular frame-work. Although the motions of the electrons of the molecule are independent of the motion of the atomic nuclei to a high order approximation, the electrons contribute to the force fields in which the atoms oscillate. Early investigators assumed that the total energy of such a molecule could be regarded as the sum of the energies of a set of harmonic oscillators and the energy of a rotator. However,

* A preliminary account of a portion of this paper was presented at the Symposium on Molecular Structure and Spectroscopy sponsored by the Graduate School and Department of Physics and Astronomy of The Ohio State University, Columbus, Ohio, June 9–14, 1947.

as experimental techniques were improved and more accurate observations were made, it became apparent that this assumption was only approximately correct. For the case of the comparatively simple diatomic molecule the assumption was found to be valid only to a low order approximation, while for more complex molecules there was even less agreement between theory and experiment. A more exact theory of the diatomic molecule was developed by Kratzer[1] Fues,[2] and others which showed that such factors as anharmonicity of the oscillations, effective change in the moment of inertia due to the oscillations, and centrifugal expansion effects had to be considered. A variation in the rotational line spacing from band to band in the spectra of symmetrical molecules, such as methane and the methyl halides, was considered by Teller and Tisza,[3] Teller,[4] and Dennison and Johnston,[5] who showed that it was caused by an interaction between vibration and rotation. The bands exhibiting the anomalous spacings arise from degenerate vibrations which cause an internal angular momentum of the molecule. This type of interaction has been called Coriolis interaction because of the similarity to the effect in classical mechanics. It is evident that an adequate theory of the vibration-rotation energy states of polyatomic molecules must take into account the perturbation terms which modify the zero-order energies. The perturbation terms,[6–9] other than the effects of double minima such as occur in NH_3 and internal rotations such as may occur in ethane, include the following types: (a) anharmonic potential energy terms, (b) Coriolis interactions between total angular momentum and the internal angular momentum of vibration, (c) variation of the rotational constants with the state of vibration, (d) *l*-type doubling in linear molecules,[9,10] (e) centrifugal stretching due to rotation, (f) accidental degeneracies in which perturbations of types (a), (b), and (c) may become very large.

Since the early work of Adel and Dennison[11] on the CO_2 problem, there has been an increasing number of papers[12–22] in which the vibration-rotation energies of polyatomic molecules have been derived to second-order approximation with varying degrees of completeness. The methods employed, apart from details, are essentially those developed in principle by Wilson and Howard.[23] A few years ago Nielsen[24] systematized the calculation of vibration-rotation energies in such a manner that once the normal coordinates are known for a polyatomic molecule, the vibration-rotation energies may be calculated to second-order approximation from the formulas given.

Although the calculation of vibration-rotation energies of polyatomic molecules is well known, the procedures are so complex as to deserve further attention. The purpose of the present paper is to discuss some of the details involved in the expansion of the quantum-mechanical Hamiltonian as well as to present the contact transformation theory which simplifies the calculation of perturbation effects. The results are given in such form as to be useful to those not already expert in this field. Once the Hamiltonian of a molecule is written down to second-order approximation the contributions to the vibrational energy may be obtained from tables presented in Section III. For purposes of illustration,

[1] A. Kratzer, Zeits. f. Physik **3**, 289 (1920).
[2] E. Fues, Ann. d. Physik **80**, 367 (1926).
[3] E. Teller and L. Tisza, Zeits. f. Physik **73**, 791 (1932).
[4] E. Teller, Hand- und Jahrbuch der chemischen Physik **9** (1934).
[5] D. M. Dennison and M. Johnston, Phys. Rev. **47**, 93 (1935).
[6] G. B. B. M. Sutherland, *Infra-Red and Raman Spectra* (Methuen and Company, Ltd., London, 1935).
[7] D. M. Dennison, Rev. Mod. Phys. **12**, 175 (1940).
[8] W. H. Shaffer, Rev. Mod. Phys. **16**, 245 (1944).
[9] G. Herzberg, *Infrared and Raman Spectra of Polyatomic Molecules* (D. Van Nostrand Company, Inc., New York, 1945).
[10] H. H. Nielsen and W. H. Shaffer, J. Chem. Phys. **11**, 140 (1943).
[11] A. Adel and D. M. Dennison, Phys. Rev. **43**, 716 (1933).
[12] W. H. Shaffer and H. H. Nielsen, Phys. Rev. **56**, 188 (1939).
[13] W. H. Shaffer, H. H. Nielsen, and L. H. Thomas, Phys. Rev. **56**, 895, 1052 (1939).
[14] B. T. Darling and D. M. Dennison, Phys. Rev. **57**, 128 (1940).
[15] Ta-You Wu, J. Chem. Phys. **8**, 489 (1940).
[16] S. Silver and W. H. Shaffer, J. Chem. Phys. **9**, 599 (1941).
[17] W. H. Shaffer, J. Chem. Phys. **9**, 607 (1941).
[18] W. H. Shaffer and A. H. Nielsen, J. Chem. Phys. **9**, 847 (1941).
[19] W. H. Shaffer, J. Chem. Phys. **10**, 1 (1942).
[20] S. Silver, J. Chem. Phys. **10**, 565 (1942).
[21] W. H. Shaffer and R. P. Schuman, J. Chem. Phys. **12**, 504 (1944).
[22] W. H. Shaffer and R. C. Herman, J. Chem. Phys. **12**, 494 (1944); *ibid.* **13**, 83 (1945).
[23] E. B. Wilson, Jr. and J. B. Howard, J. Chem. Phys. **4**, 260 (1936).
[24] H. H. Nielsen, Phys. Rev. **60**, 794 (1941); *ibid.* **61**, 540 (1942).

the vibration-rotation energies of the tetrahedral X_2YZ_2 molecular model are worked out in considerable detail in Section IV.

II. THE HAMILTONIAN

Let the motion of the system of particles representing the molecule be described in terms of a moving system of coordinates whose origin is at the center of mass of the molecule. The moving system has an angular velocity $\boldsymbol{\omega}$ and a translational velocity $\mathbf{V}$. The position of the ith particle of the system is given relative to the moving origin by the vector $\mathbf{r}_i=\mathbf{r}_i(x_i,y_i,z_i)$. If $\mathbf{R}$ denotes the position of the moving origin relative to the space fixed origin, the position of the ith particle relative to the fixed origin is $\mathbf{R}+\mathbf{r}_i$, and by the well-known moving axes formulae, the velocity of the ith particle is given by the relation

$$\mathbf{V}_i=\dot{\mathbf{R}}+\dot{\mathbf{r}}_i+[\boldsymbol{\omega}\times\mathbf{r}_i]=\mathbf{V}+\mathbf{v}_i+[\boldsymbol{\omega}\times\mathbf{r}_i]. \quad (1)$$

The kinetic energy of the entire system is given by

$$\begin{aligned}T&=(1/2)\textstyle\sum_i m_i V_i^2\\&=(V^2/2)\textstyle\sum_i m_i+(1/2)\sum_i m_i v_i^2\\&+(1/2)\textstyle\sum_i m_i[\boldsymbol{\omega}\times\mathbf{r}_i]\cdot[\boldsymbol{\omega}\times\mathbf{r}_i]\\&+\mathbf{V}\cdot\{\textstyle\sum_i m_i\mathbf{v}_i\}+[\mathbf{V}\times\boldsymbol{\omega}]\cdot[\textstyle\sum_i m_i\mathbf{r}_i]\\&+2\boldsymbol{\omega}\cdot\{\textstyle\sum_i m_i[\mathbf{r}_i\times\mathbf{v}_i]\}. \quad (2)\end{aligned}$$

Following Eckart[25] it is convenient to define the rotating system by imposing the conditions

$$\textstyle\sum_i m_i\mathbf{v}_i=0 \quad \text{or} \quad \sum_i m_i\mathbf{r}_i=0, \quad (3a)$$

and

$$\textstyle\sum_i m_i[\mathbf{r}_{0i}\times\mathbf{v}_i]=0, \quad (3b)$$

where $\mathbf{r}_{0i}$ denotes the equilibrium position of the ith particle relative to the moving system. Equation (3a) fixes the origin of the moving system at the center of mass of the molecule while Eq. (3b) implies that the internal vibratory motions do not produce any rotational angular momentum of the molecule as a rigid framework, relative to the moving system. The latter condition means that there is no rotation of the system as a whole relative to the body-fixed axes, i.e., the body-fixed axes rotate with the molecule. However, the particles may still execute rotations on infinitesimal orbits about their positions of equilibrium. The position vector $\mathbf{r}_i$ is given by

$$\mathbf{r}_i=\mathbf{r}_{0i}+\boldsymbol{\delta}_i, \quad (4)$$

where $\boldsymbol{\delta}_i$ is the displacement of the ith particle from its equilibrium position. After substitution of the relations given in Eqs. (3a), (3b), and (4) into Eq. (2), the kinetic energy becomes

$$\begin{aligned}T&=(1/2)V^2\textstyle\sum_i m_i\\&+(1/2)\textstyle\sum_i m_i[\boldsymbol{\omega}\times\mathbf{r}_i]\cdot[\boldsymbol{\omega}\times\mathbf{r}_i]\\&+(1/2)\textstyle\sum_i m_i v_i^2+\boldsymbol{\omega}\cdot\{\sum_i m_i[\boldsymbol{\delta}_i\times\mathbf{v}_i]\}. \quad (5)\end{aligned}$$

The first term is the translational energy of the system and can be omitted since it is of no interest in connection with band spectra, the second term is the rotational energy, the third term is the vibrational kinetic energy, and the last term gives the energy associated with the coupling between vibration and rotation.

Finally, as is well known, the classical Hamiltonian form of the kinetic energy of the molecular system is given by[23,26]

$$\begin{aligned}2T&=\mu_{xx}(P_x-p_x)^2+\mu_{yy}(P_y-p_y)^2\\&+\mu_{zz}(P_z-p_z)^2+2\mu_{xy}(P_x-p_x)(P_y-p_y)\\&+2\mu_{yz}(P_y-p_y)(P_z-p_z)\\&+2\mu_{zx}(P_z-p_z)(P_x-p_x)+\textstyle\sum_k p_k^2, \quad (6)\end{aligned}$$

where the components of total angular momentum, P_α, are defined as $P_\alpha=\partial T/\partial\omega_\alpha$; the momenta p_k conjugate to the normal coordinates Q_k as $p_k=\partial T/\partial\dot{Q}_k$; and the components of internal angular momentum, p_α, as $p_x=\sum_k X_k p_k$, $p_y=\sum_k Y_k p_k$ and $p_z=\sum_k Z_k p_k$. The $(3N-6)$ normal coordinates Q_k may be defined in terms of the components

$$x_k'/m_k^{\frac{1}{2}}, \quad y_k'/m_k^{\frac{1}{2}} \quad \text{and} \quad z_k'/m_k^{\frac{1}{2}}$$

of the displacement vector $\boldsymbol{\delta}$ as follows:[27]

$$x_k'=\textstyle\sum_{k'} l_{kk'}Q_{k'}, \quad y_k'=\sum_{k'} m_{kk'}Q_{k'}$$

and

$$z_k'=\textstyle\sum_{k'} n_{kk'}Q_{k'}. \quad (6a)$$

[25] C. Eckart, Phys. Rev. **47**, 552 (1932).

[26] H. Margenau and G. M. Murphy, *The Mathematics of Physics and Chemistry* (D. Van Nostrand Company, Inc., New York, 1943).

[27] In general, it is convenient to define a suitable set of linearly independent, intermediate generalized coordinates of proper symmetry in terms of x', y', and z' and then to transform to the normal coordinates. For illustrations of this procedure see, for example, some of references 10–24.

The quantities X_h, Y_h, and Z_h are defined by means of the following equations:

$$X_h=\sum_{h',h''}(n_{h'h}m_{h'h''}-m_{h'h}n_{h'h''})Q_{h''},$$

$$Y_h=\sum_{h',h''}(l_{h'h}n_{h'h''}-n_{h'h}l_{h'h''})Q_{h''}, \tag{6b}$$

$$Z_h=\sum_{h',h''}(m_{h'h}l_{h'h''}-l_{h'h}m_{h'h''})Q_{h''}.$$

The quantities $\mu_{\alpha\beta}$ are defined as

$$\begin{aligned}
\mu_{xx}&=(I_y'I_z'-I_{yz}'^2)\Delta^{-1},\\
\mu_{yy}&=(I_x'I_z'-I_{zx}'^2)\Delta^{-1},\\
\mu_{zz}&=(I_x'I_y'-I_{xy}'^2)\Delta^{-1},\\
\mu_{xy}&=\mu_{yx}=(I_z'I_{xy}'+I_{yz}'I_{zx}')\Delta^{-1},\\
\mu_{xz}&=\mu_{zx}=(I_{xy}'I_{yz}'+I_y'I_{zx}')\Delta^{-1},\\
\mu_{yz}&=\mu_{zy}=(I_x'I_{yz}'+I_{xy}'I_{zx}')\Delta^{-1},
\end{aligned} \tag{7a}$$

where

$$\Delta=\mu^{-1}=\begin{vmatrix} I_x' & -I_{xy}' & -I_{xz}' \\ -I_{xy}' & I_y' & -I_{yz}' \\ -I_{xz}' & -I_{yz}' & I_z' \end{vmatrix}, \tag{7b}$$

and

$$I_x'=I_x-\textstyle\sum_h X_h^2, \quad I_{xy}'=I_{xy}+\sum_h X_hY_h, \quad \text{etc.}$$

The quantities I_x, I_{xy}, etc. are the instantaneous moments and products of inertia, respectively.

The derivation of the quantum-mechanical Hamiltonian from the classical Hamiltonian form of the energy has been discussed by Podolsky and others.[23,28–33] According to Wilson and Howard[23] the appropriate Hamiltonian operator[34] for the general case of a polyatomic molecule which corresponds to the classical Hamiltonian, is given by

$$H=(1/2)\sum_{\alpha,\beta}\mu_{\alpha\beta}P_\alpha P_\beta-\sum_\alpha h_\alpha P_\alpha$$
$$+(1/2)\sum_{\alpha,\beta}\mu^{\frac{1}{4}}p_\alpha\mu_{\alpha\beta}\mu^{-\frac{1}{2}}p_\beta$$
$$+(1/2)\sum_h\mu^{\frac{1}{4}}p_h\mu^{-\frac{1}{2}}p_h+U, \tag{8a}$$

where the momenta P_α, p_α, and $p_h=-i\hbar\partial/\partial Q_h$ are to be represented by their respective quantum-mechanical operators[23] and

$$h_\alpha=(1/2)\textstyle\sum_\beta\{2\mu_{\alpha\beta}p_\beta+(p_\beta\mu_{\alpha\beta})$$
$$+\mu_{\alpha\beta}\mu^{\frac{1}{4}}(p_\beta\mu^{-\frac{1}{4}})\}, \tag{8b}$$

in which p_β operates only on the quantities in the parentheses and summation over α or β indicates the summation over x, y, and z. The quantities $\mu_{\alpha\beta}$ and μ are as previously defined in Eqs. (7a) and (7b) but must be treated as operators since they are functions of the normal coordinates; U is the potential energy.

At this point it is convenient to introduce the dimensionless normal coordinate q_h defined by the relation

$$Q_h=(h/2\pi c)^{\frac{1}{2}}\omega_h^{-\frac{1}{2}}q_h, \tag{9}$$

where h is Planck's constant divided by 2π, c is the velocity of light in cm/sec., and ω_h is the frequency in cm^{-1}. During the remainder of this paper we shall employ $p_h=\partial T/\partial\dot{q}_h$ to represent the momentum conjugate to q_h. The momentum conjugate to Q_h is related to the momentum conjugate to q_h through a relation similar to Eq. (9), namely,

$$p_Q=(2\pi c/h)^{\frac{1}{2}}\omega_h^{\frac{1}{4}}p_q. \tag{9a}$$

In terms of the dimensionless normal coordinates q_h the potential energy U, may be written to second-order approximation as

$$U=U_0(q_hq_{h'})+U_1(q_hq_{h'}q_{h''})$$
$$+U_2(q_hq_{h'}q_{h''}q_{h'''})+\cdots. \tag{10}$$

The potential function given in Eq. (10) includes all the various combinations of the q_h which make U totally symmetric with respect to all the covering operations of the molecule. The Hamiltonian may be expanded and separated into

---

[28] B. Podolsky, Phys. Rev. **32**, 812 (1928).
[29] E. C. Kemble, *Fundamental Principles of Quantum Mechanics* (McGraw-Hill Book Company, Inc., New York, 1937), Chapter VII, pp. 237–240.
[30] R. Courant and D. Hilbert, *Methoden Mathematischer Physik* (Julius Springer Verlag, Berlin, 1931).
[31] E. Schrödinger, Ann. d. Physik **79**, 747 (1926).
[32] J. H. Van Vleck, Phys. Rev. **33**, 467 (1929).
[33] O. M. Jordahl, Phys. Rev. **45**, 87 (1934).
[34] According to B. T. Darling and D. M. Dennison, the Hamiltonian operator is given by:

$$H=(1/2)\sum_{\alpha,\beta}\mu^{\frac{1}{4}}(P_\alpha-p_\alpha)\mu_{\alpha\beta}\mu^{-\frac{1}{2}}(P_\beta-p_\beta)\mu^{\frac{1}{4}}$$
$$+(1/2)\sum_h\mu^{\frac{1}{4}}p_h\mu^{-\frac{1}{2}}p_h\mu^{\frac{1}{4}}+U.$$

This form is Hermitian while that given by Wilson and Howard is not; however, the two forms of H are entirely equivalent to second-order approximation.

orders of magnitude in the following manner. Since p_h is the differential operator $-i\hbar\partial/\partial q_h$ and p_h does not commute with q_h, the term $(hc/2\hbar^2)\sum_h \omega_h\mu^{\frac{1}{2}}p_h\mu^{-\frac{1}{2}}p_h$ in Eq. (8a) becomes, upon expansion,

$$(hc/2\hbar^2)\sum_h \omega_h[p_h^2+\mu^{\frac{1}{2}}(p_h\mu^{-\frac{1}{2}})p_h].$$

The term

$$(1/2)\sum_{\alpha,\beta}\mu^{\frac{1}{2}}p_\alpha\mu_{\alpha\beta}\mu^{-\frac{1}{2}}p_\beta$$

is equivalent to

$$(1/2)\sum_{\alpha,\beta}\mu_{\alpha\beta}p_\alpha p_\beta+(1/2)\mu^{\frac{1}{2}}\sum_{\alpha,\beta}(p_\alpha\mu_{\alpha\beta}\mu^{-\frac{1}{2}})p_\beta.$$

It can be shown that the second term in the last expression contains third- and higher order terms only and need not be considered further. The expression $\sum_\alpha h_\alpha P_\alpha$ yields

$$\sum_{\alpha,\beta}(\mu_{\alpha\beta}p_\beta)P_\alpha+(1/2)\sum_{\alpha,\beta}(p_\beta\mu_{\alpha\beta})P_\alpha+(1/2)\sum_{\alpha,\beta}\mu_{\alpha\beta}\mu^{\frac{1}{2}}(p_\beta\mu^{-\frac{1}{2}})P_\alpha,$$

in which the last part leads to third- and higher order terms only and the second part is zero. Thus, up to second-order approximation the Hamiltonian may be simplified to read[35]

$$\begin{aligned}H=&(1/2)\sum_{\alpha,\beta}\mu_{\alpha\beta}P_\alpha P_\beta-\sum_{\alpha,\beta}(\mu_{\alpha\beta}p_\beta)P_\alpha\\&+(1/2)\sum_{\alpha,\beta}\mu_{\alpha\beta}p_\alpha p_\beta+(hc/2\hbar^2)\sum_h\omega_h p_h^2\\&+(hc/2\hbar^2)\sum_h\omega_h\mu^{\frac{1}{2}}(p_h\mu^{-\frac{1}{2}})p_h\\&+U_0+U_1+U_2+\cdots.\end{aligned}\quad(11)$$

After substitution of the explicit expressions for $\mu_{\alpha\beta}$, μ, etc. (for example see Eq. (14)) as functions of the q_h into Eq. (11), the Hamiltonian will consist of the following types of terms. The zero-order part will be

$$H_0=(1/2)\sum_\alpha P_\alpha^2/I_{e\alpha}+(hc/2)\sum_h\omega_h[p_h^2/\hbar^2+q_h^2],$$

while the first-order Hamiltonian, H_1, contains terms of the type $q_hP_\alpha^2$, $p_\alpha P_\alpha$, p_h, and $q_hq_{h'}q_{h''}$. The first type of term in H_1 represents the first-order effect of the vibration on the change of the moment of inertia, the second term represents the Coriolis interaction between the internal angular momentum of vibration and the rotational angular momentum, the third term contributes to the zero-point energy, while the remaining term results from the anharmonicity of the oscillations. In a similar manner the second-order Hamiltonian, H_2, is found to contain such terms as $q_h^2P_\alpha^2$, p_α^2, $q_hq_{h'}q_{h''}q_{h'''}$, and q_hp_h which represent the second-order effect of the oscillation on the moment of inertia, the energy associated with the internal angular momenta, second-order terms arising from the anharmonicity of the vibration, while the last term contributes to the zero-point energy.

III. CALCULATION OF THE VIBRATIONAL ENERGY

In actual practice the first-order Hamiltonian is frequently so complicated that it is an extremely tedious and difficult problem to calculate by means of perturbation theory[36,37] the second-order energy corrections which arise from terms in H_1 having non-diagonal matrix elements. The calculation of the second-order energy corrections can be facilitated by the introduction of a contact transformation[32,33,38] which eliminates from the first-order Hamiltonian those terms which have matrix elements connecting a particular unperturbed vibrational energy level with other unperturbed levels, and places appropriate terms in the second-order Hamiltonian for consideration in perturbation calculations. The detailed application of the contact transformation to the calculation of vibration-rotation energies of polyatomic molecules has been developed by Thomas,[39] Shaffer, Nielsen, and Thomas,[13] and others.[16,40] As is well known, the various portions of the transformed Hamiltonian, H', are given by[38]

$$\begin{aligned}H_0'&=H_0,\\H_1'&=H_1-i(H_0S-SH_0),\\H_2'&=H_2+(i/2)[S(H_1+H_1')-(H_1+H_1')S],\end{aligned}\quad(12)$$

[35] It must be remembered that upon the introduction of the expressions for $\mu_{\alpha\beta}$, $\mu^{\frac{1}{2}}$, etc., there will appear terms that are higher than the second order that should be rejected in this approximation.

[36] L. Pauling and E. B. Wilson, Jr., *Introduction to Quantum Mechanics* (McGraw-Hill Book Company, Inc., New York, 1935).

[37] E. U. Condon and G. H. Shortley, *The Theory of Atomic Spectra* (Cambridge University Press, Teddington, 1935).

[38] The details of the contact transformation have been discussed by Kemble. See reference 29, Chapter XI, pp. 394–396.

[39] L. H. Thomas, J. Chem. Phys. **10**, 532, 538 (1942).

[40] H. H. Nielsen, Phys. Rev. **68**, 181 (1945).

TABLE I. Commutation rules.

$$
\begin{aligned}
p^n q - q p^n &= -ni\hbar p^{n-1}, \quad n \geqq 1 \\
pq^n - q^n p &= -ni\hbar q^{n-1} \\
q^n pq - qpq^n &= (n-1)i\hbar q^n \\
pqp^n - p^n qp &= (n-1)i\hbar p^n \\
p^3q^2 - q^2p^3 &= -3i\hbar(p^2q + qp^2) \\
p^2q^3 - q^3p^2 &= -3i\hbar(pq^2 + q^2p) \\
p^2qpq - qpqp^2 &= -2i\hbar(p^2q + qp^2) \\
p^2q^2 - q^2p^2 &= -2i\hbar(pq + qp) \\
p^3q^3 - q^3p^3 &= -3i\hbar[(3/2)(p^2q^2 + q^2p^2) + \hbar^2]
\end{aligned}
$$

where S is a function of the canonically conjugate variables p_h and q_h.

The terms in H_1 which can be removed, consist of functions of the conjugate variables p_h and q_h, multiplied by a coefficient which is either a constant or a function of the angular momentum operators P_α. To second-order approximation the rotational operators can be considered as constant operators so far as the transformation is concerned but their non-commutative properties must be observed carefully. One can find S as a function of the p_h and q_h by setting

$$H_0 = (hc/2)\textstyle\sum_h \omega_h[p_h^2/\hbar^2 + q_h^2],$$

since the zero-order part of the rotational Hamiltonian H_{0R} is a constant for purposes of the transformation, and by imposing the condition $H_1 = i(H_0S - SH_0)$. Suitable functions S_ρ, required for the removal of various types of terms occurring in the first-order Hamiltonian, can be determined from a consideration of the commutation rules, some of which are given in Table I for convenience. The functions S_ρ listed in Table II will remove from the first-order part to the second-order part of the Hamiltonian all types of terms except those Coriolis interaction terms which involve only one fundamental frequency. This type of interaction will occur only in the event of a degeneracy. The index τ is used to denote the type of term $H_{1;\tau}$ in H_1 which is being removed, while the index ρ designates the function S_ρ which is required to remove the term $\tau = \rho$. In Table III are given the terms[41] that are transformed into H_2'. Note that the S_ρ required to remove a term for H_1 will operate on all the other terms in H_1 and, in general, transform a number of terms into H_2'. Only those terms, transformed into H_2', are listed which contribute to second-order approximation. The diagonal matrix elements of the terms transformed into H_2' are also listed in Table III. In Table III the terms transformed into H_2' are designated by the notation $H'_{2;\tau,\rho}$. By this symbolism we mean the term placed in H_2' when the function S_ρ operates on terms of the type τ in H_1. Note that ρ and τ may or may not be equal. The terms transformed into H_1' are designated as $H'_{1;\tau}$. The second-order corrections to the vibrational energy consist of the diagonal matrix elements listed in Table III, the diagonal matrix elements of H_2 and contributions, if any,

TABLE II. Transformation functions S_ρ required to remove the types of terms, $H_{1;\tau}$, occurring in H_1, together with the corresponding values of $i(H_0S_\rho - S_\rho H_0) = H_{1;\tau}$.

ρ	S_ρ	$H_{1;\tau} = i(H_0S_\rho - S_\rho H_0)$
1	$-(a_1/\hbar hc\omega_h)p_h$	a_1q_h
2	$(a_2\hbar/hc\omega_h)q_h$	a_2p_h
3	$-(2a_3/\hbar hc\omega_h)(p_h^3/3\hbar^2 + q_hp_hq_h/2)$	$a_3q_h^3$
4	$-(a_4\hbar/hc)(\omega_h^2 - \omega_{h'}^2)^{-1}(\omega_{h'}q_hq_{h'} + \omega_hp_hp_{h'}/\hbar^2)$	$a_4q_hp_{h'}$
5	$-(a_5/\hbar hc\omega_{h'})(4\omega_h^2 - \omega_{h'}^2)^{-1}[(2\omega_h^2 - \omega_{h'}^2)q_h^2p_{h'} + \omega_h\omega_{h'}(p_hq_h + q_hp_h)q_{h'} + 2\omega_h^2p_h^2p_{h'}/\hbar^2]$	$a_5q_h^2q_{h'}$
6	$-(a_6\hbar/hc)(\omega_h - \omega_{h'})^{-1}(q_hq_{h'} + p_hp_{h'}/\hbar^2)$	$a_6(q_hp_{h'} - q_{h'}p_h)$
7	$-(a_7\hbar/hc)[(\omega_h\omega_{h'})^{\frac{1}{2}}(\omega_h^2 - \omega_{h'}^2)]^{-1}[(\omega_h^2 + \omega_{h'}^2)q_hq_{h'} + 2\omega_h\omega_{h'}p_hp_{h'}/\hbar^2]$	$a_7[(\omega_{h'}/\omega_h)^{\frac{1}{2}}q_hp_{h'} - (\omega_h/\omega_{h'})q_{h'}p_h]$
8	$-(a_8D_{hh'h''}/\hbar hc)[\omega_h(\omega_h^2 - \omega_{h'}^2 - \omega_{h''}^2)p_hq_{h'}q_{h''} + \omega_{h'}(\omega_{h'}^2 - \omega_h^2 - \omega_{h''}^2)q_hp_{h'}q_{h''} + \omega_{h''}(\omega_{h''}^2 - \omega_h^2 - \omega_{h'}^2)q_hq_{h'}p_{h''} - 2\omega_h\omega_{h'}\omega_{h''}p_hp_{h'}p_{h''}/\hbar^2]$	$a_8q_hq_{h'}q_{h''}$
	$D_{hh'h''} = [(\omega_h + \omega_{h'} + \omega_{h''})(\omega_h - \omega_{h'} - \omega_{h''})(\omega_h - \omega_{h'} + \omega_{h''})(\omega_h + \omega_{h'} - \omega_{h''})]^{-1}$	

[41] In Table III the column giving $H_{1;\tau} + H'_{1;\tau}$ is obviously equal to $H_{1;\tau}$ since this table refers to the case in which $H'_{1;\tau}$ is made equal to zero.

TABLE III. Tabulation of the individual terms $H'_{2;\tau,\rho}$ transformed into H_2' together with their matrix elements diagonal in the vibrational quantum numbers.*

ρ	τ	$H_{1;\tau}+H'_{1;\tau}$	$H'_{2;\tau,\rho}=(i/2)[S_\rho(H_{1;\tau}+H'_{1;\tau})-(H_{1;\tau}+H'_{1;\tau})S_\rho]$	$(\Gamma\|H'_{2;\tau,\rho}\|\Gamma)$
1	1	a_1q_h	$-(a_1^2/2hc\omega_h)$	$-(a_1^2/2hc\omega_h)$
1	1	$a_1'q_h$	$-(a_1a_1'+a_1'a_1)(4hc\omega_h)^{-1}$	$-(a_1a_1'+a_1'a_1)(4hc\omega_h)^{-1}$
1	3	$a_3q_h^3$	$-(3a_1a_3q_h^2/2hc\omega_h)$	$-(3a_1a_3/2hc\omega_h)(v_h+1/2)$
1	5	$a_5'q_hq_{h'}^2$	$-(a_1a_5'q_{h'}^2/2hc\omega_h)$	$-(a_1a_5'/2hc\omega_h)(v_{h'}+1/2)$
2	2	a_2p_h	$-(a_2^2\hbar^2/2hc\omega_h)$	$-(a_2^2\hbar^2/2hc\omega_h)$
3	1	a_1q_h	$-(3a_1a_3q_h^2/2hc\omega_h)$	$-(3a_1a_3/2hc\omega_h)(v_h+1/2)$
3	3	$a_3q_h^3$	$-(a_3^2/hc\omega_h)[(3/2\hbar^2)(p_h^2q_h^2+q_h^2p_h^2)+1+(3/2)q_h^4]$	$-(a_3^2/hc\omega_h)[(15/4)(v_h+1/2)^2+7/16]$
3	5	$a_5'q_hq_{h'}^2$	$-(3a_3a_5'q_h^2q_{h'}^2/2hc\omega_h)$	$-(3a_3a_5'/2hc\omega_h)(v_h+1/2)(v_{h'}+1/2)$
4	4	$a_4q_hp_{h'}$	$(a_4^2\hbar^2/2hc)(\omega_h^2-\omega_{h'}^2)^{-1}[\omega_{h'}q_h^2-\omega_hp_{h'}^2/\hbar^2]$	$(a_4^2\hbar^2/2hc)(\omega_h^2-\omega_{h'}^2)^{-1}[\omega_{h'}(v_h+1/2)-\omega_h(v_{h'}+1/2)]$
4	6	$a_6(q_hp_{h'}-q_{h'}p_h)$	$(a_4a_6\hbar^2/2hc)(\omega_h^2-\omega_{h'}^2)^{-1}[\omega_{h'}(q_h^2-q_{h'}^2)+(\omega_h/\hbar^2)(p_h^2-p_{h'}^2)]$	$(a_4a_6\hbar^2/2hc)(\omega_h-\omega_{h'})^{-1}(v_h-v_{h'})$
5	1	$a_1'q_{h'}$	$-(a_1'a_5q_h^2/2hc\omega_{h'})$	$-(a_1'a_5/2hc\omega_{h'})(v_h+1/2)$
5	3	$a_3'q_{h'}^3$	$-(3a_3'a_5q_h^2q_{h'}^2/2hc\omega_{h'})$	$-(3a_3'a_5/2hc\omega_{h'})(v_h+1/2)(v_{h'}+1/2)$
5	5	$a_5q_h^2q_{h'}$	$-(a_5^2/2hc\omega_{h'})(4\omega_h^2-\omega_{h'}^2)[(2\omega_h^2-\omega_{h'}^2)q_h^4+4\omega_h\omega_{h'}q_h^2q_{h'}^2+(\omega_h^2/\hbar^2)(p_h^2q_h^2+q_h^2p_h^2)]$	$-(a_5^2/4hc\omega_{h'})E_{hh'}(v_h+1/2)^2+(3a_5^2/16hc)H_{hh'}-(a_5^2/hc)F_{hh'}(v_h+1/2)(v_{h'}+1/2)$
5	5	$a_5''q_{h''}^2q_{h'}$	$-(a_5a_5''q_{h''}^2q_h^2/2hc\omega_{h'})$	$-(a_5a_5''/2hc\omega_{h'})(v_{h''}+1/2)(v_h+1/2)$
6	4	$a_4q_hp_{h'}$	$(a_4a_6\hbar^2/2hc)(\omega_h-\omega_{h'})^{-1}[q_h^2-p_{h'}^2/\hbar^2]$	$(a_4a_6\hbar^2/2hc)(\omega_h-\omega_{h'})^{-1}(v_h-v_{h'})$
6	6	$a_6(q_hp_{h'}-q_{h'}p_h)$	$(a_6^2\hbar^2/2hc)(\omega_h-\omega_{h'})^{-1}[(q_h^2+p_h^2/\hbar^2)-(q_{h'}^2+p_{h'}^2/\hbar^2)]$	$(a_6^2\hbar^2/hc)(\omega_h-\omega_{h'})^{-1}(v_h-v_{h'})$
7	7	$a_7[(\omega_{h'}/\omega_h)^{\frac{1}{2}}q_hp_{h'}-(\omega_h/\omega_{h'})^{\frac{1}{2}}q_{h'}p_h]$	$a_7^2\hbar^2[2hc(\omega_h^2-\omega_{h'}^2)]^{-1}[(3\omega_h^2+\omega_{h'}^2)(q_h^2/\omega_h)-(3\omega_{h'}^2+\omega_h^2)(q_{h'}^2/\omega_{h'})]$	$(a_7^2\hbar^2/2hc)[\omega_h^{-1}J_{hh'}(v_h+1/2)+\omega_{h'}^{-1}J_{h'h}(v_{h'}+1/2)]$
8	8	$a_8q_hq_{h'}q_{h''}$	$-(a_8^2D_{hh'h''}/2hc)[\omega_h(\omega_h^2-\omega_{h'}^2-\omega_{h''}^2)q_{h'}^2q_{h''}^2+\omega_{h'}(\omega_{h'}^2-\omega_{h''}^2-\omega_h^2)q_h^2q_{h''}^2+\omega_{h''}(\omega_{h''}^2-\omega_h^2-\omega_{h'}^2)q_h^2q_{h'}^2+\omega_h\omega_{h'}\omega_{h''}/2]$	$-(a_8^2/hc)[C_{hh'h''}(v_{h'}+1/2)(v_{h''}+1/2)+C_{h'h''h}(v_h+1/2)(v_{h''}+1/2)+C_{h''hh'}(v_h+1/2)(v_{h'}+1/2)+(\omega_h\omega_{h'}\omega_{h''}D_{hh'h''}/4)]$
			$C_{hh'h''}=\omega_h(\omega_h^2-\omega_{h'}^2-\omega_{h''}^2)D_{hh'h''}/2$	$F_{hh'}=2\omega_h(4\omega_h^2-\omega_{h'}^2)^{-1}$
			$D_{hh'h''}=[(\omega_h+\omega_{h'}+\omega_{h''})(\omega_h-\omega_{h'}-\omega_{h''})(\omega_h-\omega_{h'}+\omega_{h''})(\omega_h+\omega_{h'}-\omega_{h''})]^{-1}$	$H_{hh'}=\omega_{h'}(4\omega_h^2-\omega_{h'}^2)^{-1}$
			$E_{hh'}=(8\omega_h^2-3\omega_{h'}^2)(4\omega_h^2-\omega_{h'}^2)^{-1}$	$J_{hh'}=(3\omega_h^2+\omega_{h'}^2)(\omega_h^2-\omega_{h'}^2)^{-1}$

* See reference 42.

TABLE IV. Diagonal matrix elements of $f(g)$ for the linear oscillator.*

$f(g)$	$(v\|f(g)\|v)$
q, p	0
q^2, $p^2/\hbar^2$	$(v+1/2)$
pg, $-qp$	$-i\hbar/2$
q^4, $p^4/\hbar^4$	$[(3/2)(v+1/2)^2+3/8]$
p^2q^2, q^2p^2	$[(1/2)(v+1/2)^2-3/8]\hbar^2$

* For additional matrix elements see reference 8.

of the non-zero matrix elements of terms remaining in H_1'. For the sake of convenience some of the harmonic oscillator matrix elements are given in Table IV.

In the case of terms of the type $a_8q_hq_{h'}q_{h''}$ and $a_7[(\omega_{h'}/\omega_h)^{\frac{1}{2}}q_hp_{h'}-(\omega_h/\omega_{h'})^{\frac{1}{2}}q_{h'}p_h]$ the terms transformed into H_2' have resonance denominators which may become very large in the event of an accidental degeneracy and the functions S_7 and S_8 cannot be applied. Special transformation functions for these cases have been discussed by Nielsen[40] and are given in the Appendix.

As an example of how the transformation is employed, consider a term in H_1 of the form $H_{1;3}=a_3q_h^3$ where a_3 is the anharmonicity constant $hc\beta_{hhh}$. Employing S_3 given in Table II we find with the aid of the relations given in Table I that $i(H_0S_3-S_3H_0)=a_3q_3^3$ and, therefore, $H'_{1;3}=H_{1;3}-i(H_0S_3-S_3H_0)=0$. The term

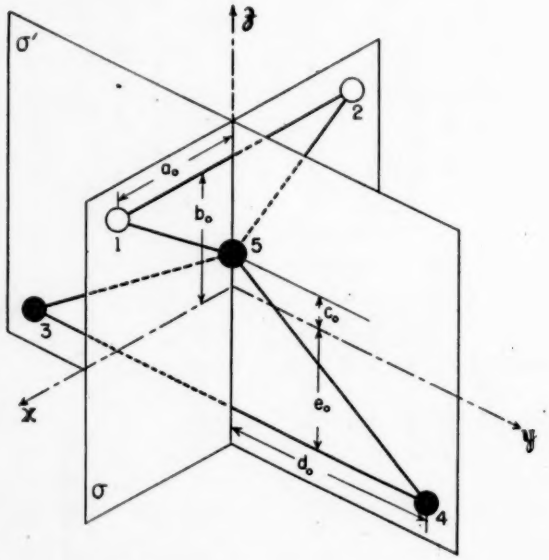

FIG. 1.

$H'_{2;3,3}$ transformed into H_2' is given in Table III together with its matrix element diagonal in the vibrational quantum numbers. Note that S_3, operating on the terms a_1q_h and $a_5'q_hq_{h'}$ places additional terms in H_2', namely, $H'_{2;1,3}$ and $H'_{2;5,3}$. However, S_3 operating on all the other terms gives either zero or terms which contribute in approximations higher than the second.

In cases where there are no accidental degeneracies the vibrational energy, E_v, is given by

$$E_v=hcG. \tag{13}$$

The quantity G in Eq. (19) is defined as

$$G=G_0+\sum_h\omega_h(v_h+1/2)+\sum_h[G_{hh}(v_h+g_h/2)^2+\sum_{h'<h}G_{hh'}(v_h+g_h/2)(v_{h'}+g_{h'}/2)], \tag{13a}$$

where g_h is the order of the degeneracy of mode ω_h. Thus, the purely vibrational contribution to the eigenvalues of the vibration-rotation Hamiltonian may be written directly by collecting all the matrix elements of terms appearing in H_2' which do not involve the angular momentum operators P_α. The first summation term in Eq. (13a) arises from H_0, while the remaining summation terms as well as G_0, the zero-point energy, may be obtained by inspection of Table III and the additional evaluation of the simple diagonal matrix elements of the quartic potential function[42] and other types of terms originally present in H_2. The latter may be found in Table IV. In the event of a degeneracy the contributions to the energy will include the matrix elements of terms remaining in H_1'. These matrix elements must be evaluated by the methods of degenerate perturbation theory.[36,37]

IV. AN ILLUSTRATION—THE TETRAHEDRAL X_2YZ_2 MOLECULAR MODEL

For the purposes of illustration consider the calculation of the vibration energies of the tetrahedrally symmetric X_2YZ_2 molecular model. This problem was worked out recently by the authors.[22] The equilibrium configuration of the

[42] To second-order approximation the quartic potential energy terms must be of even degree in all coordinates, i.e., terms of the type q_h^4, $q_h^2q_{h'}^2$, etc. will contribute, while terms odd in one or more coordinates such as $q_h^3q_{h'}$, $q_h^2q_{h'}q_{h''}$, etc. will not.

model assumed is shown in Fig. 1. In what follows only those quantities are given which are required to carry out the expansion of the Hamiltonian and the contact transformation; the others may be found in the references cited.

The coefficients $\mu_{\alpha\beta}$, $\mu^{\frac{1}{2}}$, and $\mu^{-\frac{1}{2}}$ which appear in the Hamiltonian can be found from Eqs. (7a) and (7b) after determining the quantities I_x, I_{xy}, X_h, etc. as functions of the dimensionless normal coordinates to second-order approximation. These coefficients are as follows:

$$\begin{aligned}
\mu_{xx}&=I_{ex}^{-1}\{1-\textstyle\sum_i \omega_i^{-\frac{1}{2}}a_iq_i\\
&\quad+\textstyle\sum_h \omega_h^{-1}(a_h^2-a_{hh}+d_h^2+f_h^2)q_h^2+\cdots\},\\
\mu_{yy}&=I_{ey}^{-1}\{1-\textstyle\sum_i \omega_i^{-\frac{1}{2}}b_iq_i\\
&\quad+\textstyle\sum_h \omega_h^{-1}(b_h^2-b_{hh}+d_h^2+e_h^2)q_h^2+\cdots\},\\
\mu_{zz}&=I_{ez}^{-1}\{1-\textstyle\sum_i \omega_i^{-\frac{1}{2}}c_iq_i\\
&\quad+\textstyle\sum_h \omega_h^{-1}(c_h^2-c_{hh}+e_h^2+f_h^2)q_h^2+\cdots\},\\
\mu_{xy}&=(I_{ex}I_{ey})^{-\frac{1}{2}}\{\textstyle\sum_j \omega_j^{-\frac{1}{2}}d_jq_j\\
&\quad+\textstyle\sum_h \omega_h^{-1}(e_hf_h-a_hd_h-b_hd_h)q_h^2+\cdots\},\\
\mu_{yz}&=(I_{ey}I_{ez})^{-\frac{1}{2}}\{\textstyle\sum_l \omega_l^{-\frac{1}{2}}e_lq_l\\
&\quad+\textstyle\sum_h \omega_h^{-1}(d_hf_h-b_he_h-c_he_h)q_h^2+\cdots\},\\
\mu_{zx}&=(I_{ex}I_{ez})^{-\frac{1}{2}}\{\textstyle\sum_k \omega_k^{-\frac{1}{2}}f_kq_k\\
&\quad+\textstyle\sum_h \omega_h^{-1}(d_he_h-a_hf_h-c_hf_h)q_h^2+\cdots\},
\end{aligned}\tag{14}$$

while

$$\begin{aligned}
\mu^{-\frac{1}{2}}=\Delta^{\frac{1}{2}}&=(I_{ex}I_{ey}I_{ez})^{\frac{1}{2}}\\
&\times\{1+(1/2)\textstyle\sum_i \omega_i^{-\frac{1}{2}}(a_i+b_i+c_i)q_i\\
&+(1/2)\textstyle\sum_h \omega_h^{-1}[-(a_h^2+b_h^2+c_h^2)/4\\
&-(d_h^2+e_h^2+f_h^2)+(a_hb_h+a_hc_h+b_hc_h)/2\\
&\qquad+a_{hh}+b_{hh}+c_{hh}]q_h^2+\cdots\},
\end{aligned}\tag{14a}$$

and

$$\begin{aligned}
\mu^{\frac{1}{2}}=\Delta^{-\frac{1}{2}}&=(I_{ex}I_{ey}I_{ez})^{-\frac{1}{2}}\\
&\times\{1-(1/2)\textstyle\sum_i \omega_i^{-\frac{1}{2}}(a_i+b_i+c_i)q_i\\
&+(1/2)\textstyle\sum_h \omega_h^{-1}[(3/4)(a_h^2+b_h^2+c_h^2)\\
&+(d_h^2+e_h^2+f_h^2)+(1/2)(a_hb_h+a_hc_h+b_hc_h)\\
&\qquad-(a_{hh}+b_{hh}+c_{hh})]q_h^2+\cdots\}.
\end{aligned}\tag{14b}$$

The notation adopted is that the subscript h denotes any one of the nine normal coordinates; i assumes the values 1, 2, 3, 4 and denotes a coordinate of symmetry type A_1; j assumes the value 5 and denotes the single coordinate of type A_2; k assumes the values 6, 7 and denotes coordinates of type B_1; and l assumes the values 8, 9 and denotes coordinates of type B_2. Of the coefficients a_h, a_{hh}, etc. occurring in Eq. (14) the following vanish:

$$\begin{aligned}
&a_j=b_j=c_j=0;\quad a_k=b_k=c_k=0;\\
&a_l=b_l=c_l=0;\quad d_i=e_i=f_i=0;\\
&e_j=f_j=0;\quad d_k=e_k=0;\quad d_l=f_l=0.
\end{aligned}\tag{14c}$$

In terms of the dimensionless normal coordinates the cubic and quartic[42] anharmonic potential functions are given by the following expressions:[43]

$$\begin{aligned}
U_1/hc&=\textstyle\sum_i \beta_{iii}q_i^3+\sum_i\sum_{i'}\beta_{iii'}q_i^2q_{i'}\\
&\quad+\textstyle\sum_i\sum_{i'}\sum_{i''}\beta_{ii'i''}q_iq_{i'}q_{i''}\\
&\quad+\textstyle\sum_i\sum_j\beta_{iij}q_iq_j^2+\sum_i\sum_k\beta_{ikk}q_iq_k^2\\
&\quad+\textstyle\sum_i\sum_k\sum_{k'}\beta_{ikk'}q_iq_kq_{k'}\\
&\quad+\textstyle\sum_i\sum_l\beta_{ill}q_iq_l^2\\
&\quad+\textstyle\sum_i\sum_l\sum_{l'}\beta_{ill'}q_iq_lq_{l'}\\
&\qquad+\textstyle\sum_j\sum_k\sum_l\beta_{jkl}q_jq_kq_l
\end{aligned}\tag{15a}$$

and

$$\begin{aligned}
U_2/hc&=\textstyle\sum_i\gamma_{iiii}q_i^4+\sum_i\sum_{i'}\gamma_{iii'i'}q_i^2q_{i'}^2\\
&+\textstyle\sum_j\gamma_{jjjj}q_j^4+\sum_k\gamma_{kkkk}q_k^4\\
&+\textstyle\sum_k\sum_{k'}\gamma_{kkk'k'}q_k^2q_{k'}^2+\sum_l\gamma_{llll}q_l^4\\
&+\textstyle\sum_l\sum_{l'}\gamma_{ll'l'}q_l^2q_{l'}^2+\sum_i\sum_j\gamma_{iijj}q_i^2q_j^2\\
&+\textstyle\sum_i\sum_k\gamma_{iikk}q_i^2q_k^2+\sum_i\sum_l\gamma_{iill}q_i^2q_l^2\\
&+\textstyle\sum_j\sum_k\gamma_{jjkk}q_j^2q_k^2+\sum_j\sum_l\gamma_{jjll}q_j^2q_l^2\\
&\qquad+\textstyle\sum_k\sum_l\gamma_{kkll}q_k^2q_l^2.
\end{aligned}\tag{15b}$$

The components of internal angular momentum are expressed in terms of the dimensionless normal coordinates q_h and conjugate momenta p_h as follows:[44]

---

[43] Primed and unprimed subscripts in a given summation are used to denote different coordinates of the same symmetry type. Each combination of subscripts may occur only once, i.e., permutations of a given combination of subscripts are not allowed; for example β_{123} is the same as β_{132}, β_{213}, etc. The coefficients β and γ are expressed in cm^{-1}.

[44] The Coriolis parameters ξ, η and ζ are given explicitly in reference 22.

$$
\begin{aligned}
p_x &= \sum_k \xi_{k5}[(\omega_5/\omega_k)^{\frac{1}{2}} q_k p_5 - (\omega_k/\omega_5)^{\frac{1}{2}} q_5 p_k] \\
&\quad + \sum_l \sum_i \xi_{li}[(\omega_l/\omega_i)^{\frac{1}{2}} q_i p_l - (\omega_i/\omega_l)^{\frac{1}{2}} q_l p_i], \\
p_y &= \sum_l \eta_{l5}[(\omega_5/\omega_l)^{\frac{1}{2}} q_l p_5 - (\omega_l/\omega_5)^{\frac{1}{2}} q_5 p_l] \\
&\quad + \sum_k \sum_i \eta_{ki}[(\omega_k/\omega_i)^{\frac{1}{2}} q_i p_k - (\omega_i/\omega_k)^{\frac{1}{2}} q_k p_i], \\
p_z &= \sum_i \zeta_{i5}[(\omega_5/\omega_i)^{\frac{1}{2}} q_i p_5 - (\omega_i/\omega_5)^{\frac{1}{2}} q_5 p_i] \\
&\quad + \sum_k \sum_l \zeta_{kl}[(\omega_k/\omega_l)^{\frac{1}{2}} q_l p_k - (\omega_l/\omega_k)^{\frac{1}{2}} q_k p_l].
\end{aligned} \tag{16}
$$

The Hamiltonian may now be expressed to second-order approximation by the substitution of Eqs. (14), (15), and (16) into Eq. (11), remembering that we are dealing with operators. After expanding and dropping all terms higher than the second order, we obtain the following expressions for the various portions of the Hamiltonian:

$$
\begin{aligned}
H_0 &= (hc/2)\Big\{\sum_{h=1}^{9} \omega_h[p_h^2/\hbar^2 + q_h^2] \\
&\quad + (2/\hbar^2)[B_{ex}P_x^2 + B_{ey}P_y^2 + B_{ez}P_z^2]\Big\}, \qquad (17a)
\end{aligned}
$$

$$
\begin{aligned}
H_1 &= (hc/\hbar^2)\Big\{\sum_{i=1}^{4} \omega_i^{-\frac{1}{2}} q_i[a_i B_{ex}P_x^2 + b_i B_{ey}P_y^2 \\
&\quad + c_i B_{ez}P_z^2] + \omega_5^{-\frac{1}{2}} q_5 d_5 B_{ex}^{\frac{1}{2}} B_{ey}^{\frac{1}{2}} (P_x P_y + P_y P_x) \\
&\quad + \sum_{l=8}^{9} \omega_l^{-\frac{1}{2}} q_l e_l B_{ey}^{\frac{1}{2}} B_{ez}^{\frac{1}{2}} (P_y P_z + P_z P_y) \\
&\quad + \sum_{k=6}^{7} \omega_k^{-\frac{1}{2}} q_k f_k B_{ez}^{\frac{1}{2}} B_{ex}^{\frac{1}{2}} (P_z P_x + P_x P_z) \\
&\quad - 2(B_{ex}p_x P_x + B_{ey}p_y P_y + B_{ez}p_z P_z)\Big\} \\
&\quad - (i\pi c/2)\sum_{i=1}^{4} \omega_i^{\frac{1}{2}} (a_i + b_i + c_i) p_i + U_1, \qquad (17b)
\end{aligned}
$$

and

$$
\begin{aligned}
H_2 &= (hc/\hbar^2)\Big\{\sum_{h=1}^{9} \omega_h^{-1} q_h^2[(a_h^2 - a_{hh} + d_h^2 \\
&\quad + f_h^2) B_{ex}P_x^2 + (b_h^2 - b_{hh} + e_h^2 + d_h^2) B_{ey}P_y^2 \\
&\quad + (c_h^2 - c_{hh} + e_h^2 + f_h^2) B_{ez}P_z^2] \\
&\quad + (B_{ex}p_x^2 + B_{ey}p_y^2 + B_{ez}p_z^2)\Big\} \\
&\quad - (i\pi c/2)\sum_h [a_{hh} + b_{hh} + c_{hh} - (a_h^2 + b_h^2 + c_h^2)/2 \\
&\quad - (d_h^2 + e_h^2 + f_h^2)] q_h p_h + U_2, \qquad (17c)
\end{aligned}
$$

in which the equilibrium rotational constants are $B_{ex} = (h/8\pi^2 c I_{ex})$, $B_{ey} = (h/8\pi^2 c I_{ey})$, $B_{ez} = (h/8\pi^2 c I_{ez})$ and if c is the velocity of light in cm/sec., ω_h is given in cm^{-1}.

To perform the contact transformation of the Hamiltonian given in Eq. (17), we set up the function S given by $S = \sum_\rho S_\rho$, where the S_ρ are the functions required for the removal of the various types of terms, $\tau = \rho$, appearing in H_1. The X_2YZ_2 tetrahedrally symmetric molecular model has no real degeneracies and it shall be assumed that there are no accidental degeneracies. The complete function S required to remove all the terms in H_1 will not be given explicitly since the terms added to H_2' as well as their matrix elements diagonal in the vibrational quantum numbers may be determined directly from Table III.

In the following discussion of the use of Table III we employ the notation $H_{1;\tau}$ for terms of type τ in H_1 and $H'_{2;\tau,\rho}$ for the terms transformed into H_2' as previously described in Section III. Inspection of the first-order Hamiltonian of the X_2YZ_2 molecular model shows that there are terms of the type $\tau = 1, 2, 3, 5, 7$, and 8. All of these terms can be transformed out of H_1' subject to the condition that there are no accidental degeneracies. Consider terms of the type $\tau = 1$ which are linear in the normal coordinate q_h. There are 6 such terms, of two kinds, which are designated as follows:

$$H_{1;1a} = (hc/\hbar^2)\omega_i^{-\frac{1}{2}} a_i B_{ex} P_x^2 q_i,$$

while $H_{1;1b}$ and $H_{1;1c}$ represent the similar terms in $P_y^2 q_i$ and $P_z^2 q_i$, respectively;

$$H_{1;1d} = (hc/\hbar^2)\omega_5^{-\frac{1}{2}} d_5 B_{ex}^{\frac{1}{2}} B_{ey}^{\frac{1}{2}} (P_x P_y + P_y P_x) q_5,$$

while $H_{1;1e}$ and $H_{1;1f}$ represent the similar terms in $(P_y P_z + P_z P_y) q_l$ and $(P_z P_x + P_x P_z) q_k$. The functions $S_{1a}, \cdots S_{1d}, \cdots$ required for the removal of each of the above terms may be found in Table II for $\rho = 1$. According to Table III, these functions operating on the terms they are intended to remove give rise to the following matrix elements:

$$
\begin{aligned}
&-(hc/\hbar^4)(a_i^2/2\omega_i^2) B_{ex}^2 P_x^4, \cdots \\
&\quad -(hc/\hbar^4)(d_5^2/2\omega_5^2) B_{ex} B_{ey} (P_x P_y + P_y P_x)^2, \cdots.
\end{aligned}
$$

In addition, matrix elements appear because

each function S_1 operates on terms linear in q_h other than the one it removes from H_1'. Thus, we obtain matrix elements of the type

$$-(hc/h^4)(a_ib_i/2\omega_i^2)B_{ez}B_{ey}(P_x^2P_y^2+P_y^2P_x^2), \cdots$$

which are the sum of the matrix elements of $H'_{2;1a,1b}$ and $H'_{2;1b,1a}$, etc. These matrix elements are given in the second line of Table III. It is important to note that the coefficients of q_h are angular momentum operators which do not commute. The matrix elements of the type $P_x^2(P_xP_y+P_yP_x)+(P_xP_y+P_yP_x)P_x^2$, $\cdots$ and

$$(P_xP_y+P_yP_x)(P_yP_z+P_zP_y)+(P_yP_z+P_zP_y)(P_xP_y+P_yP_x), \cdots$$

do not occur for this particular molecular model because of the zero value of the coefficients listed in Eq. (14c). The matrix elements considered up to this point are associated with the centrifugal stretching of the molecule. Each function S_1 will also operate on terms of type $\tau=3$ and 5, and therefore introduce the terms $H'_{2;3,1}$ and $H'_{2;5,1}$ into H_2'. These terms will combine with $H'_{2;1,3}$ and $H'_{2;1,5}$, respectively, and lead to matrix elements of the following kind:

$$(hc/h^2)(3a_i\beta_{iii}/\omega_i^4)B_{ez}P_z^2(v_i+1/2), \cdots$$

and

$$(hc/h^2)(a_i\beta_{ihh}/\omega_i^4)B_{ez}P_z^2(v_h+1/2), \cdots, \quad h=i', j, k, l.$$

The matrix elements of this type which involve the operators $(P_xP_y+P_yP_x)$, $\cdots$ are all zero because of the conditions specified in Eq. (14c). The matrix elements associated with the terms p_h in H_1 are constants and contribute to the zero-point energy only. The matrix elements of the terms $H'_{2;3,3}$, apart from constants, are of the form $-(15hc\omega_i^{-1}\beta^2_{iii}/4)(v_i+1/2)^2$, while the matrix elements of $H'_{2;5,3}$ combine with those of $H'_{2;3,5}$ to yield terms of the type

$$-(3hc\omega_i^{-1}\beta_{iii}\beta_{hhi})(v_i+1/2)(v_h+1/2), \quad h=i', j, k, l,$$

and the matrix elements of $H'_{2;5,5}$ are as shown in Table III. The matrix elements that arise from the removal of the Coriolis terms and the anharmonic potential energy terms of the type $q_hq_{h'}q_{h''}$, also follow directly from Table III. Since from Eq. (12)

$$H_2'=H_2+\sum_{\tau,\rho}H'_{2;\tau,\rho},$$

it is necessary to evaluate the matrix elements of the terms originally in H_2. These matrix elements can be found in Table IV.

Upon completion of the above procedure, the purely vibrational contribution E_v to the eigenvalues of the vibration-rotation Hamiltonian can be written in the form, $E_v=hcG$, where G is the vibrational term in Eq. (13a). The quantities G_0, G_{hh} and $G_{hh'}$ are given by the following relations,[45] in which the subscript notation is that which was described earlier:

$$\begin{aligned}
G_0&=(1/4)\textstyle\sum_h\{(a_{hh}+b_{hh}+c_{hh})\\
&-(3/8)(a_i^2+b_i^2+c_i^2)\\
&+(1/4)(a_ib_i+b_ic_i+c_ia_i)\\
&-(d_j^2+e_i^2+f_k^2)+(3/2)\gamma_{hhhh}\}\\
&-(1/16)\textstyle\sum_h\{7\omega_i^{-1}\beta^2_{iii}+4\omega_i\omega_{i'}\omega_{i''}D_{ii'i''}\beta^2_{ii'i''}\\
&+4\omega_i\omega_k\omega_{k'}D_{ikk'}\beta^2_{ikk'}+4\omega_i\omega_l\omega_{i'}D_{ill'}\beta^2_{ill'}\\
&+4\omega_j\omega_k\omega_l\beta^2_{jkl}-3H_{ii'}\beta^2_{iii'}\\
&-3H_{ji}\beta^2_{jji}-3H_{ki}\beta^2_{kki}-3H_{li}\beta^2_{lli}\}\\
&-(1/2)\sum_{hh'}\{(\xi^2_{kj}+\xi^2_{li})B_{ez}+(\eta^2_{lj}+\eta^2_{ki})B_{ey}\\
&\qquad+(\zeta^2_{ij}+\zeta^2_{kl})B_{ex}\},\\
G_{ii}&=(1/4)\{6\gamma_{iiii}-15\omega_i^{-1}\beta^2_{iii}\\
&\qquad-\textstyle\sum_{i'}\omega_i^{-1}E_{ii'}\beta^2_{iii'}\},\\
G_{jj}&=(1/4)\{6\gamma_{jjjj}-\textstyle\sum_i\omega_i^{-1}E_{ji}\beta^2_{jji}\},\\
G_{kk}&=(1/4)\{6\gamma_{kkkk}-\textstyle\sum_i\omega_i^{-1}E_{ki}\beta^2_{kki}\},\\
G_{ll}&=(1/4)\{6\gamma_{llll}-\textstyle\sum_i\omega_i^{-1}E_{li}\beta^2_{lli}\},\\
G_{ii'}&=\{\gamma_{iii'i'}-3\omega_i^{-1}\beta_{iii}\beta_{ii'i'}-3\omega_{i'}^{-1}\beta_{i'i'i'}\beta_{i'ii}\\
&\qquad-\textstyle\sum_{i''}(\omega_{i''}^{-1}\beta_{iii''}\beta_{i'i'i''})-F_{ii'}\beta^2_{iii'}\\
&\qquad-F_{i'i}\beta^2_{i'i'i}-\textstyle\sum_{i''}C_{i''ii'}\beta^2_{ii'i''}\},\\
G_{ij}&=\{\gamma_{iijj}-3\omega_i^{-1}\beta_{iii}\beta_{jji}-F_{ji}\beta^2_{jji}\\
&\qquad+K_{ij}\zeta^2_{ij}B_{ez}\},\\
G_{ik}&=\{\gamma_{iikk}-3\omega_i^{-1}\beta_{iii}\beta_{kki}-F_{ki}\beta^2_{kki}\\
&\qquad+K_{ki}\eta^2_{ki}B_{ey}-\textstyle\sum_{k'}C_{k'ki}\beta^2_{ikk'}\},
\end{aligned} \tag{18}$$

[45] For the definitions of the constants employed, see Table III.

$$G_{il}=\{\gamma_{iill}-3\omega_i^{-1}\beta_{iii}\beta_{lli}-F_{li}\beta^2_{lli}+K_{li}\xi^2_{li}B_{ex}-\sum_{l'}C_{l'li}\beta^2_{ill'}\},$$

$$G_{jk}=\{\gamma_{jjkk}+K_{jk}\xi^2_{jk}B_{ex}-\sum_l C_{ljk}\beta^2_{jkl}\},$$

$$G_{jl}=\{\gamma_{jjll}+K_{jl}\eta^2_{jl}B_{ey}-\sum_k C_{klj}\beta^2_{jkl}\},$$

$$G_{kl}=\{\gamma_{kkll}+K_{kl}\zeta^2_{kl}B_{ez}-\sum_j C_{jkl}\beta^2_{jkl}\},$$

$$G_{kk'}=\{\gamma_{kkk'k'}-\sum_i C_{ikk'}\beta^2_{ikk'}\},$$

$$G_{ll'}=\{\gamma_{ill'l'}-\sum_i C_{ill'}\beta^2_{ill'}\}.$$

The effective rotational Hamiltonian H_R, which results from the contact transformation and subsequent diagonalization with respect to the vibrational coordinates, has the form:

$$\begin{aligned}H_R=&(hc/\hbar^2)\{B_{vx}P_x^2+B_{vy}P_y^2+B_{vz}P_z^2\}\\&-(hc/\hbar^4)\{\tau_1P_x^4+\tau_2P_y^4+\tau_3P_z^4\\&+\tau_4(P_xP_y+P_yP_x)^2+\tau_5(P_yP_z+P_zP_y)^2\\&+\tau_6(P_zP_x+P_xP_z)^2+\tau_7(P_x^2P_y^2+P_y^2P_x^2)\\&+\tau_8(P_x^2P_z^2+P_z^2P_x^2)\\&+\tau_9(P_y^2P_z^2+P_z^2P_y^2)\},\end{aligned}\tag{19}$$

where

$$\begin{aligned}\tau_1&=B_{ex}^2\textstyle\sum_i(a_i^2/2\omega_i^2);\\ \tau_2&=B_{ey}^2\textstyle\sum_i(b_i^2/2\omega_i^2);\\ \tau_3&=B_{ez}^2\textstyle\sum_i(c_i^2/2\omega_i^2);\\ \tau_4&=B_{ex}B_{ey}\textstyle\sum_j(d_j^2/2\omega_j^2);\\ \tau_5&=B_{ey}B_{ez}\textstyle\sum_l(e_l^2/2\omega_l^2);\\ \tau_6&=B_{ex}B_{ez}\textstyle\sum_k(f_k^2/2\omega_k^2);\\ \tau_7&=B_{ex}B_{ey}\textstyle\sum_i(a_ib_i/2\omega_i^2);\\ \tau_8&=B_{ex}B_{ez}\textstyle\sum_i(a_ic_i/2\omega_i^2);\\ \tau_9&=B_{ey}B_{ez}\textstyle\sum_i(b_ic_i/2\omega_i^2).\end{aligned}\tag{19a}$$

The effective rotation constants are, to second-order approximation,

$$B_{vx}=B_{ex}\Big\{1+\sum_{h=1}^{9}\alpha_h(v_h+1/2)\Big\},$$

$$B_{vy}=B_{ey}\Big\{1+\sum_{h=1}^{9}\beta_h(v_h+1/2)\Big\},\tag{20}$$

$$B_{vz}=B_{ez}\Big\{1+\sum_{h=1}^{9}\gamma_h(v_h+1/2)\Big\},$$

where[45] if $A=[3\beta_{iii}+\beta_{ii'i'}+\beta_{ijj}+\beta_{ikk}+\beta_{ill}]$,

$$\begin{aligned}\alpha_i&=\omega_i^{-1}\{a_i^2-a_{ii}+\omega_i^{-1}a_iA+2B_{ex}\textstyle\sum_l J_{il}\xi^2_{li}\},\\ \beta_i&=\omega_i^{-1}\{b_i^2-b_{ii}+\omega_i^{-1}b_iA+2B_{ey}\textstyle\sum_k J_{ik}\eta^2_{ki}\},\\ \gamma_i&=\omega_i^{-1}\{c_i^2-c_{ii}+\omega_i^{-1}c_iA+2B_{ez}\textstyle\sum_j J_{ij}\zeta^2_{ji}\},\\ \alpha_j&=\omega_j^{-1}\{d_j^2-a_{jj}+2B_{ex}\textstyle\sum_k J_{jk}\xi^2_{kj}\},\\ \beta_j&=\omega_j^{-1}\{d_j^2-b_{jj}+2B_{ey}\textstyle\sum_l J_{jl}\eta^2_{jl}\},\\ \gamma_j&=\omega_j^{-1}\{-c_{jj}+2B_{ez}\textstyle\sum_i J_{ji}\zeta^2_{ji}\},\\ \alpha_k&=\omega_k^{-1}\{f_k^2-a_{kk}+2B_{ex}\textstyle\sum_j J_{kj}\xi^2_{kj}\},\\ \beta_k&=\omega_k^{-1}\{-b_{kk}+2B_{ey}\textstyle\sum_i J_{ki}\eta^2_{ki}\},\\ \gamma_k&=\omega_k^{-1}\{f_k^2-c_{kk}+2B_{ez}\textstyle\sum_l J_{kl}\zeta^2_{kl}\},\\ \alpha_l&=\omega_l^{-1}\{-a_{ll}+2B_{ex}\textstyle\sum_i J_{li}\xi^2_{li}\},\\ \beta_l&=\omega_l^{-1}\{e_l^2-b_{ll}+2B_{ey}\textstyle\sum_j J_{lj}\eta^2_{lj}\},\\ \gamma_l&=\omega_l^{-1}\{e_l^2-c_{ll}+2B_{ez}\textstyle\sum_k J_{lk}\zeta^2_{lk}\}.\end{aligned}\tag{20a}$$

The eigenvalues of the rotational part, H_R, of the Hamiltonian can be evaluated from a secular determinant which is a modified form of the one given by Wang[46] for the rigid asymmetric rotator. This part of the problem is involved and is best treated separately for each individual case. It suffices to say that the non-vanishing matrix elements of the secular determinant have been worked out for the X_2YZ_2 tetrahedrally symmetric model.[22] The eigenvalues of H_R that are obtained can be expressed in the form $E_R=hcF$, where F is the rotational term.[12,47]

V. APPENDIX

According to Nielsen,[40] the removal of the term $a_8q_hq_{h'}q_{h''}$ from H_1' when there is an accidental degeneracy, $\omega_h+\omega_{h'}\approx\omega_{h''}$, may be accomplished if the function S_8 is given in the following modified form:

$$\begin{aligned}S_8^*=(a_8/4\hbar hc)\{&(\omega_h^2+\omega_{h'}^2+\omega_{h''}^2-2\omega_h\omega_{h'}\\&+2\omega_h\omega_{h''}+2\omega_{h'}\omega_{h''})(p_hp_{h'}p_{h''}/\hbar^2)\\&-(\omega_h^2+\omega_{h'}^2-3\omega_{h''}^2-2\omega_h\omega_{h'}\\&-2\omega_h\omega_{h''}-2\omega_{h'}\omega_{h''})(q_hq_{h'}p_{h''})\\&+(\omega_h^2-3\omega_{h'}^2+\omega_{h''}^2+2\omega_h\omega_{h'}\\&+2\omega_h\omega_{h''}-2\omega_{h'}\omega_{h''})(q_hp_{h'}q_{h''})\\&+(-3\omega_h^2+\omega_{h'}^2+\omega_{h''}^2+2\omega_h\omega_{h'}\\&-2\omega_h\omega_{h''}+2\omega_{h'}\omega_{h''})(p_hq_{h'}q_{h''})\}\\&\times\{(\omega_h+\omega_{h'}+\omega_{h''})(\omega_h-\omega_{h'}+\omega_{h''})\\&\times(\omega_h-\omega_{h'}-\omega_{h''})\}^{-1}.\end{aligned}$$

[46] S. C. Wang, Phys. Rev. **34**, 243 (1929).
[47] H. H. Nielsen, Phys. Rev. **59**, 565 (1941).

A detailed calculation shows that

$$H'_{1;8}=(a_8/4)\{(q_hp_{h'}+p_hq_{h'})(p_{h''}/\hbar^2)$$
$$-(p_hp_{h'}/\hbar^2-q_hq_{h'})q_{h''}\}$$

and

$$H'_{2;8,8}=(i/2)[S_8^*(H'_{1;8}+H_{1;8})-(H'_{1,8}+H_{1;8})S^*]$$
$$=(a_8^2/4hc)\{i(\omega_h^2+\omega_{h'}^2+\omega_{h''}^2$$
$$-2\omega_h\omega_{h'}+2\omega_h\omega_{h''}+2\omega_{h'}\omega_{h''})$$
$$\times(p_hq_hp_{h'}q_{h'}p_{h''}q_{h''}$$
$$-q_hp_hq_{h'}p_{h'}q_{h''}p_{h''})/\hbar^3$$
$$-(\omega_h^2+\omega_{h'}^2-3\omega_{h''}^2-2\omega_h\omega_{h'}$$
$$-2\omega_h\omega_{h''}-2\omega_{h'}\omega_{h''})q_h^2q_{h'}^2$$
$$+(\omega_h^2-3\omega_{h'}^2+\omega_{h''}^2+2\omega_h\omega_{h'}$$
$$+2\omega_h\omega_{h''}-2\omega_{h'}\omega_{h''})q_h^2q_{h''}^2$$
$$+(-3\omega_h^2+\omega_{h'}^2+\omega_{h''}^2+2\omega_h\omega_{h'}$$
$$-2\omega_h\omega_{h''}+2\omega_{h'}\omega_{h''})q_{h'}^2q_{h''}^2\}$$
$$\times\{(\omega_h+\omega_{h'}+\omega_{h''})(\omega_h-\omega_{h'}+\omega_{h''})$$
$$\times(\omega_h-\omega_{h'}-\omega_{h''})\}^{-1}.$$

The function S_8 has been modified so as to prevent the appearance of the resonance denominator $(\omega_h+\omega_{h'}-\omega_{h''})$ in the term $H'_{2;8,8}$, transformed into H_2' and retain the term $H'_{1;8}$ in H_1'. In the event of an accidental degeneracy $\omega_h+\omega_{h'}\approx\omega_{h''}$, or $\omega_{h''}=\omega_{h'}+\omega_h-\delta$, the zero-order Hamiltonian becomes

$$H_0=(hc/2)\{\omega_h(p_h^2/\hbar^2+q_h^2)+\omega_{h'}(p_{h'}^2/\hbar^2+q_{h'}^2)$$
$$+(\omega_h+\omega_{h'})(p_{h''}^2/\hbar^2+q_{h''}^2)\}$$

and the term $(\delta\hbar/2)(p_{h''}^2/\hbar^2+q_{h''}^2)$ is incorporated in H_1' given above.

For the removal of the Coriolis resonance interaction term $a_7[(\omega_{h'}/\omega_h)^{\frac{1}{2}}q_hp_{h'}-(\omega_h/\omega_{h'})^{\frac{1}{2}}q_{h'}p_h$ when there is an accidental degeneracy, Nielsen[40] has shown that

$$S_7^*=(a_7\hbar/2hc)(\omega_h-\omega_{h'})[\omega_h^{\frac{1}{2}}\omega_{h'}^{\frac{1}{2}}(\omega_h+\omega_{h'})]^{-1}$$
$$\times(q_hq_{h'}^*-p_hp_{h'}/\hbar^2).$$

The following terms are transformed into H':

$$H'_{1;7}=a_7[(\omega_h+\omega_{h'})/(2\omega_h^{\frac{1}{2}}\omega_{h'}^{\frac{1}{2}})](q_hp_{h'}-q_{h'}p_h)$$

and

$$H'_{2;7,7}=(i/2)[S_7^*(H'_{1,7}+H_{1;7})$$
$$-(H'_{1;7}+H_{1;7})S_7^*]$$
$$=(a_7^2\hbar^2/8hc)(\omega_h-\omega_{h'})(\omega_h\omega_{h'})^{-\frac{1}{2}}(\omega_h+\omega_{h'})^{-1}$$
$$\times\{[3(\omega_{h'}/\omega_h)^{\frac{1}{2}}+(\omega_h/\omega_{h'})^{\frac{1}{2}}]q_h^2$$
$$-[(\omega_{h'}/\omega_h)^{\frac{1}{2}}+3(\omega_h/\omega_{h'})^{\frac{1}{2}}](p_h^2/\hbar^2)$$
$$-[3(\omega_h/\omega_{h'})^{\frac{1}{2}}+(\omega_{h'}/\omega_h)^{\frac{1}{2}}]q_{h'}^2$$
$$+[(\omega_h/\omega_{h'})^{\frac{1}{2}}+3(\omega_{h'}/\omega_h)^{\frac{1}{2}}](p_{h'}^2/\hbar^2)\}.$$

If $\omega_h\approx\omega_{h'}$, so that $\omega_{h'}=\omega_h+\delta$, the zero-order Hamiltonian becomes

$$H_0=(hc\omega_h/2)[(p_h^2/\hbar^2+q_h^2)+(p_{h'}^2/\hbar^2+q_{h'}^2)],$$

and the first-order transformed Hamiltonian will contain, in addition to the expression given earlier, the term

$$(hc\delta/2)(p_{h'}^2/\hbar^2+q_{h'}^2).$$

The matrix elements of the terms remaining in H_1' can be found in Nielsen's paper,[40] while the matrix elements of $H'_{2;7,7}$ and $H'_{2;8,8}$ can be found in the reference cited or from Table IV.

Catalytic Isomerization of Butene-1 to Butene-2*

JOHN TURKEVICH AND ROBERT KINSEL SMITH
Department of Chemistry, Princeton University, Princeton, New Jersey

(Received January 5, 1948)

A study has been made of the interconversion of butene-1 and butene-2 on a variety of catalysts, both liquid and solid. This work was paralleled by the study of the exchange of radioactive hydrogen and tritium between the catalysts and the hydrocarbons, butene, propylene, and ethylene. A mechanism based on hydrogen transfer by the catalyst is proposed to explain the results and this mechanism is extended to apply to the action of catalysts in alkylation, cracking, and polymerization reactions.

THE butenes represent one of the simplest systems for the study of molecular rearrangements. There are three such transformations possible. The first is the *cis-trans*-transformation of the butene-2. This has been studied by G. B. Kistiakowski and W. R. Smith.[1] Another type of transformation is the migration of the double bond between the first and second position. A study of thermal reaction has been reported from this laboratory where references are given to previous work.[2] The catalytic reaction has been studied on copper at red heat on aluminum sulfate at 250–300°C,[3] on calcium oxide at 420°C and on quartz at 550°C,[4] on perchloric acid at 21°C, zinc chloride at 100°C, benzene sulfonic acid and pure phosphoric acid at room temperature, and phosphoric acid on silica gel at 249°C.[5] The kinetics of this transformation on nickel catalysts were studied by Twigg.[6]

TABLE I.

	Vapor pressure	Infra-red
Sample 1	81.5 percent	82 percent
Sample 2	67.0 percent	68 percent

These studies were supplemented with an investigation of the rate of hydrogenation and the rate of deuterium exchange. It is significant that no isomerization was found in the absence of hydrogen. The third type of isomerization that butene may undergo is the carbon skeleton transformation of butylene into isobutylene and vice versa. Serebryakova, Rudkovskii, and Frost[7] found that dehydrating catalysts such as various clays, aluminum sulfate, alumina, and phosphoric acid either on carbon or fire clay at 300°C produced isobutylene from normal butenes. Peski and Lorang[8] report that hydrated catalysts consisting of phosphorus oxyacids supported on different silicious materials are effective for this type of transformation. Furthermore, thorium and aluminum hydrated oxides are useful in the preparation of branched chain isomers in the temperature range of 600°C to 1000°C.[9]

Finally, aluminum silicate catalysts from 400 to 600°C are recommended as catalysts for this transformation.[10]

The purpose of this investigation is to make a comprehensive study of the catalytic transformation of butene-1 to butene-2 and vice versa.

THERMODYNAMICS

The thermodynamic properties of the transformation of the double bond between the two normal butenes has been reported previously.[11]

* Submitted by Robert K. Smith in partial fulfillment of the requirements for a degree of Doctor of Philosophy at Princeton University, September 1943. Preliminary communication, Nature **157**, 879 (1946).

[1] G. B. Kistiakowski and W. R. Smith, J. Am. Chem. Soc. **58**, 766 (1936).

[2] W. Walter McCarthy and John Turkevich, J. Chem. Phys. **12**, 461 (1945).

[3] Perkin, Weizmann, Mathews, and Strange, Brit. Pat. 9722 (1911); Bull. soc. chim. Belg. **29**, 192 (1920).

[4] F. Runge and Mueller Conrade, U. S. Pat. 1,914,672 (1933).

[5] Ipatieff, Pines, and Schaad, J. Am. Chem. Soc. **56**, 2696 (1934).

[6] G. H. Twigg, Proc. Roy. Soc. **A178**, 106 (1941).

[7] Serebryakova, Rudkovskii, and Frost, Comptes Rendus (Doklady) Acad. Sci. USSR (13) **4**, 373 (1936).

[8] Peski and Lorang, Can. Pat. 384,317 (1939).

[9] Thomas and Bloch, U. S. Pat. 2,216,284 (1941).

[10] Egloff, Morrell, Thomas, and Bloch, J. Am. Chem. Soc. **61**, 3571 (1939); A. U. Frost, J. Phys. Chem. U.S.S.R. **14**, 1313 (1940).

[11] W. Walter McCarthy and John Turkevich, J. Chem. Phys. **12**, 405 (1944).

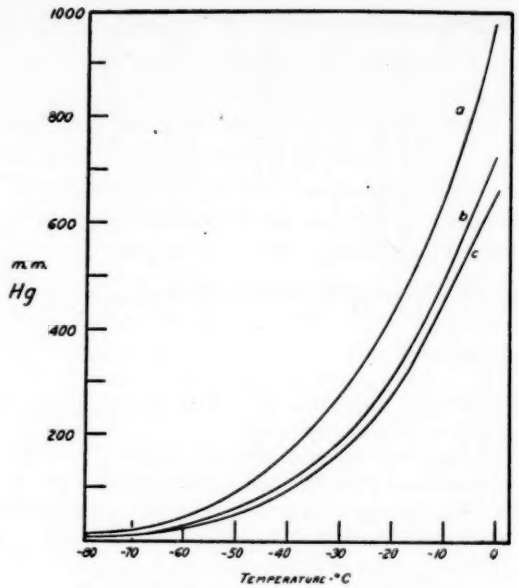

FIG. 1. Vapor pressure of the butene.

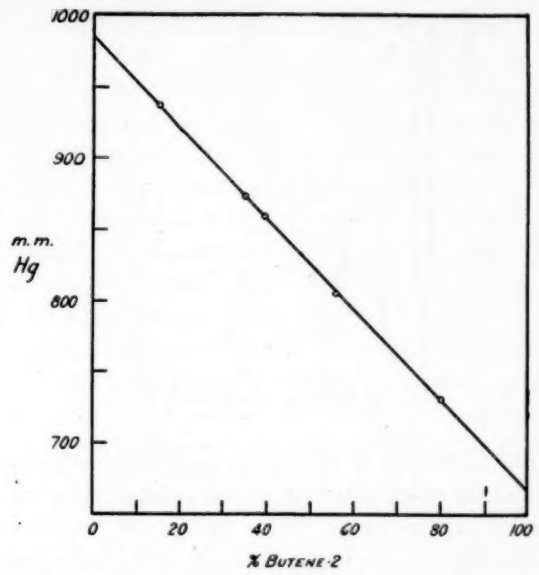

FIG. 2. Vapor pressure of binary mixtures of *n* butenes.

ANALYSIS

Data compiled by previous workers on the isomerization of butenes indicates that identification of resulting gases is one of the most difficult problems in this research. The investigation of the kinetics of the reaction requires, however, that the analysis be made with an accuracy of one percent. The narrow range over which the products boil prevents quantitative separation of the isomers by low temperature distillation. The possibility of isomerization by liquid solvents threw doubt on the use of preferential absorption by solvents.

Measurement of the vapor pressure of the product offers, however, a simple, rapid method of analysis (Fig. 1) whenever there is no cracking or carbon skeleton isomerization. Twigg[6] used the vapor pressure at −80°C as a method of analysis. His method was modified in that a temperature of 0°C was used. This choice permitted better control of the temperature bath, faster attainment of equilibrium, and a wider range in the vapor pressure variation. It should be pointed out that the assumption was made that whenever there was a butene-1 to a butene-2 transformation the resultant butene-2 was an equilibrium mixture of *cis*- and *trans*-butenes. The calibration curve, Fig. 2, was obtained by assuming a linear dependence of the vapor pressure on the composition. This was checked by synthetic mixtures (shown on the graph). Furthermore, infra-red spectrophotometry was used to establish the validity of this method. Utilizing a method developed by Mr. W. W. McCarthy based on the distinction between the two isomers in the 5.45-μ band, the results in Table I were obtained.

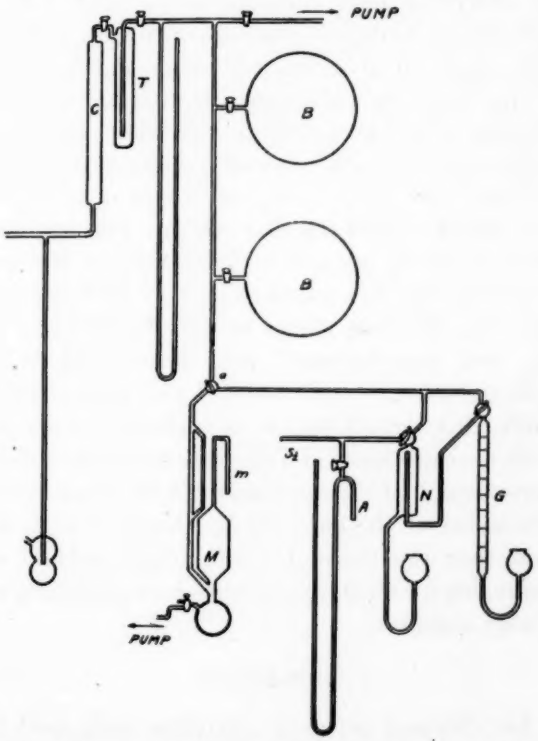

FIG. 3. Vacuum apparatus for measuring vapor pressure.

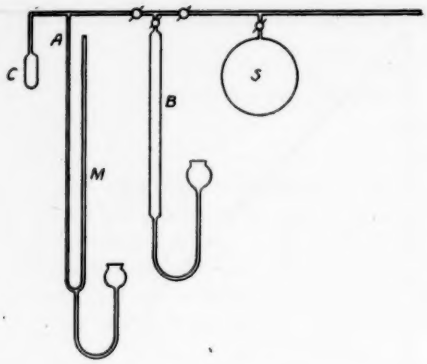

FIG. 4. Adsorption apparatus.

The accuracy of the vapor pressure method is estimated to be better than one percent since one percent corresponds to a difference of three millimeters in the vapor pressure. The procedure used in carrying out the analysis will be discussed after the description of the apparatus.

The use of thermal conductivity as a method of analysis was also explored. Twigg[6] suggested that the thermal conductivity of the butene-1 and equilibrium butene-2 were about the same but that thermal conductivity of *cis*-butene-2 differs from that of *trans*-butene-2. Using apparatus to be described later, measurements were standardized by hydrogen, helium, nitrogen, ethane, and argon to give the calibration curve. Since Twigg gives no values for the thermal conductivities of the two gases, the following values are of interest. With the thermal conductivity of air $=5.80\times10^{-5}$ cal./cm deg. sec., that of butene-1 was found to be 4.6×10^{-5} cal./cm deg. sec. and that of an 86 percent *cis*-butene-2, 14 percent *trans*-mixture was found to be 4.4×10^{-5} cal./cm deg. sec. Absolute values for the conductivity of *cis*- and *trans*-butene-2 were determined to be 4.35 and 4.6×10^{-5} cal./cm deg. sec., respectively. Since this determination is intimately tied up with measurements of a *cis-trans*-transformation, presentation of the argument will be given in the discussion of the data. In conclusion it may be said that the thermal conductivity method of analyzing for *cis-trans*-mixtures is as promising as Twigg suggests.

APPARATUS

Six different types of apparatus were used in the study of the isomerization of the butenes.

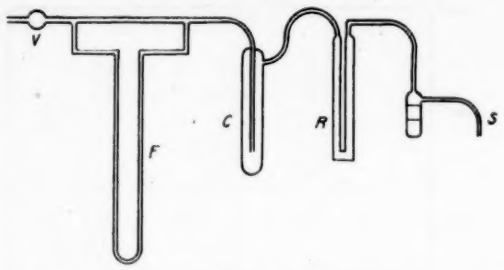

FIG. 5. Apparatus for catalytic flow measurements.

These were:

1. A vacuum apparatus for filling reaction flasks and analysis by vapor pressure.
2. An apparatus for measuring adsorption.
3. Apparatus for studies using liquid catalysts.
4. A flow system apparatus for studying catalytic transformation on solids.
5. Thermal conductivity apparatus.
6. Counting chamber for radioactive hydrogen.

The vacuum apparatus used is shown in Fig. 3. This served both in a storage and purification capacity and for analysis by vapor pressure. Manipulation of the gases first involved passage through the calcium chloride tube, *C*, from the original tank of butene. The gas was condensed in trap, *T*, by liquid air and the entire system completely evacuated. The bulbs, *B*, and the stopcock, *a*, were closed and the butene allowed to warm. About one-third of the liquid was removed by distillation, whereupon the remainder was stored in one of the bulbs, *B*. The construction of the apparatus permitted vapor pressure measurements to be made both at -80°C and 0°C. The former involved admission of the gas to the bulb, *M*. Stopcock *a* was closed and the gas condensed with liquid nitrogen in small bulb, *m*. Non-condensable gases were removed by evacuation, stopcock *a* was again closed, and the dry ice temperature bath placed around *m*. Mercury was permitted to rise from the storage bulb and the vapor pressure was measured by the difference of the height of the mercury in the two capillaries. The procedure at 0°C was essentially the same. Gas was condensed in bulb *A* and impurities pumped out. An ice bath was then placed around *A* and the vapor pressure read on the manometer. Synthetic mixtures for calibration were made by measuring definite amounts of the isomers in *G* and mixing them in *N* before condensing in the bulb *A*. Stopcock grease made of 25 g of glycerine,

7 g of dextrin, and 3.5 g of mannite was used to prevent action by the hydrocarbons which would have occurred on ordinary grease. This was made by adding solids to nearly boiling glycerine and cooling with continuous stirring.

The adsorption apparatus is shown in Fig. 4 and was connected with the vacuum system. Conventional designs were followed in the construction of this system. Gas was admitted to the burette, *B*, after the entire system had been evacuated. Capillary tubing was used in connecting *B* to the adsorption chamber, *C*. The dead space was only 0.5 cc as measured from the stopcock to point *A* and the top of the chamber. *C* was enclosed in an electrically heated furnace wherein the temperature was controlled by a gas thermometer operating a mercury contact.

The apparatus used for the investigation of liquid reagents consisted of a one-liter glass bulb to one end of which was attached a stopcock and a ground glass joint which would fit S_2 in Fig. 3. This was shaken by a motor-driven frame on which the bulb was eccentrically mounted. The frame was rotated about one hundred revolutions per minute. The entire system was enclosed in an asbestos box which held the temperature within 0.5 degrees of the desired value.

Solid catalysts were investigated by means of the flow system shown in Fig. 5. The gases were admitted to the system through the ventile valve, *V*, which accurately controlled the flow as measured on the flow meter, *F*. The gas was passed over calcium chloride, *C*, and thence into the catalyst chamber, *R*. This was surrounded by an electric furnace whose temperature was controlled within one degree. After leaving the system the gases were collected by a small trap which fit the ground glass joint, *S*. Liquid air was used to condense the gases which were then transferred to the vapor pressure system by connecting the trap to S_2 in Fig. 3. The analysis was then made in the usual way.

This flow system was modified by the insertion of thermal conductivity bulbs between *C* and *R* and between *R* and *S*. As these were soft glass they were connected through ground glass joints. This modification played no part as far as the isomerization was concerned. Thermal conductivity cells were constructed from elongated GE 25-watt light bulbs with sealed on lead-in tubes. A constant amperage of 55 milliamperes and a standard Wheatstone bridge arrangement were used. To avoid temperature fluctuations one resistance in the bridge was replaced by a "standard" thermal conductivity cell.

The experiments with radioactive phosphoric acid were carried out in the same bulb that was used for previous experiments with phosphoric acid. The radioactivity exchange was measured by drawing off periodically small samples of the butene into the Geiger-Mueller counting tube. This was constructed in the following way. A brass tube, 2″×10″, was turned on a lathe so that glass caps could be inserted and sealed with

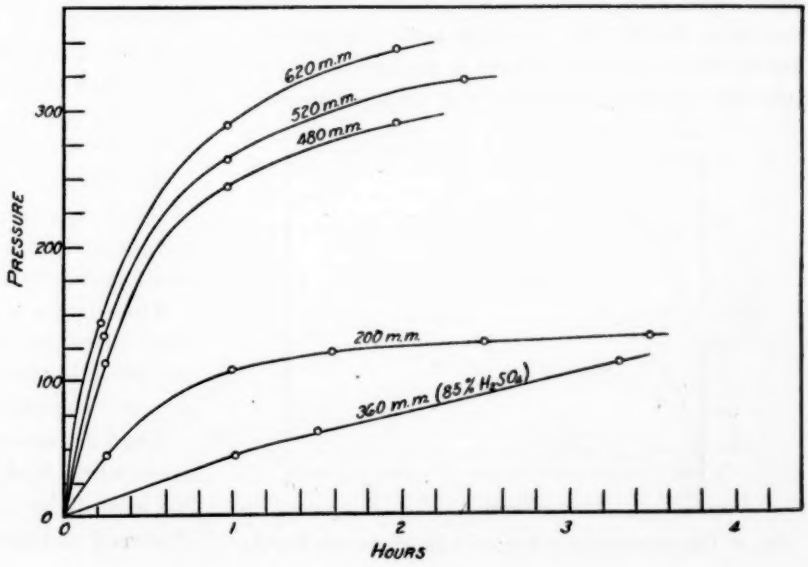

FIG. 6. Pressure of butene-2 due to isomerization of butene-1 over 96 percent H_2SO_4.

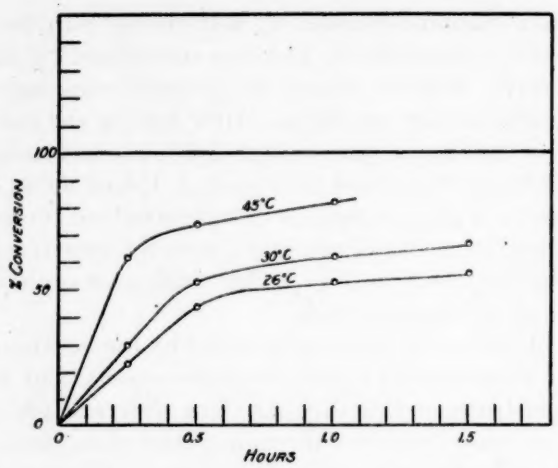

FIG. 7. Temperature dependence of isomerization on H_2SO_4.

Picein on each end. A fine tungsten wire was passed through capillaries in the center of each cap. One cap had a stopcock with a ground glass joint which could be connected at S_2 in Fig. 3. The counter was inserted onto a standard circuit constructed by Herbach and Rademann, GL-532 DeLuxe high speed Geiger-Mueller counter. It was found that 7.5 mm of butene and 27.5 mm of argon gave a plateau over a 50-volt range at a potential across the tube of from eight to nine hundred volts. This was used as the standard gas mixture.

MATERIALS

The butenes used in this series of experiments were obtained from Matheson Chemical Company, East Rutherford, New Jersey, through the courtesy of M. W. Kellogg and Company of Jersey City. Butene-1 had a vapor pressure of 988 mm at 0°C and butene-2 a vapor pressure (670 mm) corresponding to 14 percent *trans*-butene-2 and 86 percent *cis*-butene-2.

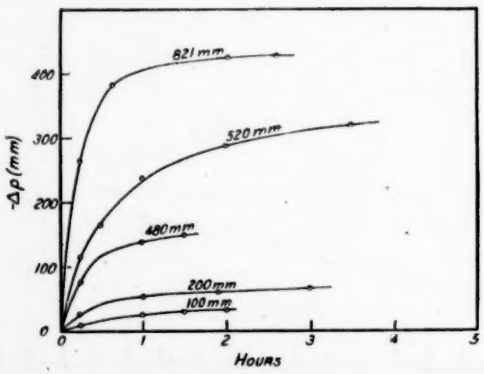

FIG. 8. Polymerization of butene-1 on 96 percent H_2SO_4.

The sulfuric acid used in the kinetic experiments was C.P. sulfuric acid, Grasselli Division of DuPont. The phosphoric acid used was made from phosphoric pentoxide and C.P. phosphoric acid (85 percent). The other materials tested as liquid catalysts were chemically pure materials used as obtained from the storeroom.

The aluminum sulfate was prepared from hydrated C.P. material by heating for twenty-four hours at 350 to 400°C. This processing drove off the water and increased the surface area tremendously. The material was broken into fine crystals for the adsorption experiments.

The copper pyrophosphate and aluminum silicate were commercial catalysts which were used without previous treatment. These were broken so that the majority of the material would be from 4 to 8 mesh in size.

The other sulfate catalysts were used as obtained from the storeroom. These were reagent grade materials. The water was driven off the nickel sulfate before using by the same treatment that was given aluminum sulfate.

The alumina which was used was Alorco Activated Alumina which had been heated to 400°C for several hours to remove the larger part of the adsorbed water. During the investigation more water came from the alumina which changed the characteristics of the material as will be shown later.

The chromic oxide catalyst was used through the kindness of Mr. George Gordon. This had been prepared by precipitation on alumina of the oxide with subsequent ignition. The original material did not possess as great a degree of activity as the final catalyst.

The thoria was prepared by the precipitation of the hydroxide from dilute solutions of thorium nitrate and ammonium hydroxide. The material was ground to the desired size and dried at 350°C.

The silica was commercial silica gel which had been dried at 150°C. The material was quite stable, however, and no change in catalytic activity was observed on heating up to 300°C.

The calcium oxide used was reagent calcium oxide which had been ground to the desired form. No loss of the catalytic activity or cracking was observed at the temperatures used.

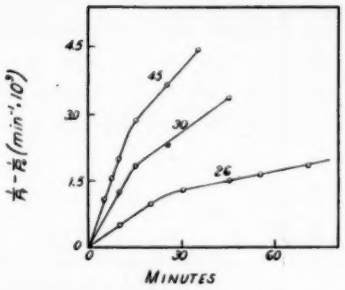

FIG. 9. Temperature dependence of polymerization on H_2SO_4.

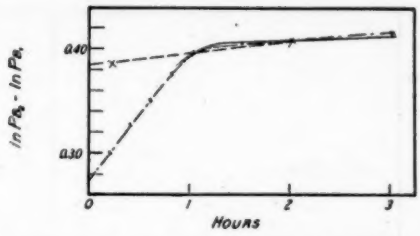

FIG. 11. Isomerization on sulfuric acid.

The radioactive phosphoric acid was prepared by adding 2.5 g of distilled water to 7 g of C.P. phosphoric pentoxide. This was thoroughly mixed and then 0.2 cc of radioactive water, $6.\times10^8$ counts/mole/min. were added. The radioactive water was part of a sample prepared by J. G. Hamilton of the University of California. This was made from treatment of lithium chloride with radiation from the cyclotron.

RESULTS

Experimental investigation of the isomerization of butene-1 was approached in the following ways. Reactions were studied with liquid catalysts and, in the case of one, were supplemented by a study of the exchange reaction. Another phase of the work consisted of the study of solid contact catalysts. This in its turn was supplemented by study of the adsorption characteristics of one such catalyst. Finally, an attempt was made to study *cis-trans*-isomerization. The results of this experimental work will be presented in the above order with a discussion following each.

LIQUID CATALYSTS

The static system was used to study the following liquid catalysts: sulfuric acid, phosphoric acid, hydrochloric acid, trichloroacetic acid, acetic acid, acetic anhydride, and aqueous solutions of zinc chloride and phenylsulfonic acid. The last six named above had no catalytic activity measureable within a period of three days at room temperature and warrant no further consideration. On the other hand, sulfuric and phosphoric acid showed considerable activity and their behavior was studied in some detail. The results on sulfuric acid are presented in Figs. 6 to 11. Examination of the isomerization curves for different starting pressures of butene-1 suggest that the rate of isomerization is directly dependent upon the amount of butene-1 present. To effect the isomerization of fifty percent of the material required about the same period of one hour at 200 mm as at 480 mm (Fig. 6). However, the additional fact is noted that a change in slope occurs when the logarithm of the amount reacted is plotted against the time. (Figure 11.) This suggests the possibility of two simultaneous processes, one of which is stopped through removal of reacting material. Birch and Dunstan[12] have noted a similar situation in alkylation with sulfuric acid as catalyst. As the reaction progresses the sulfuric acid turns from a gold-brown to a deep red color. The kinetics of the process are quite complicated. To check the hypothesis of the two stage process, a sulfuric acid catalyst which

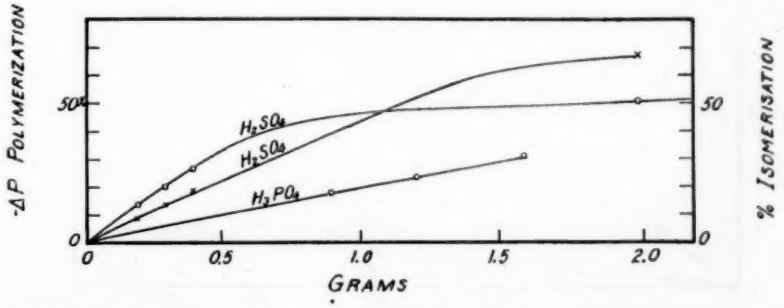

FIG. 10. Effect of amount of catalyst on isomerization and polymerization.
× Polymerization
0 Isomerization

[12] Birch and Dunstan, Trans. Faraday Soc. **35**, 1013 (1938).

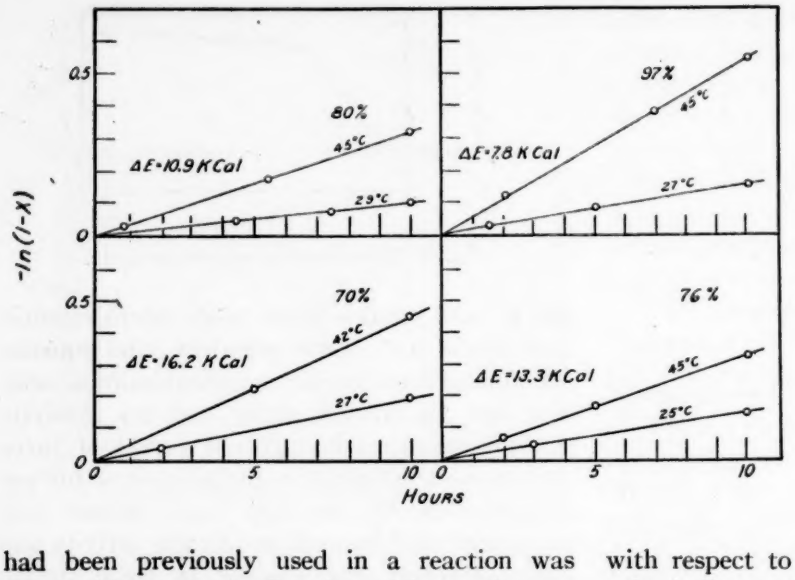

FIG. 12. Dependence of rate of isomerization on concentration of phosphorous pentoxide.

had been previously used in a reaction was thoroughly pumped off and used in another reaction. The resulting rate curve for the second reaction is shown as a horizontal line in Fig. 11. The curved line represents the rate curve for the original reaction. It is seen that the second stage of the first reaction represents the over-all process for the second and subsequent reactions using the changed catalyst. The temperature dependence of the isomerization process on sulfuric acid is indicated in Fig. 7. From this data the activation energy of the primary process is found to be 18 kcal., while that for the second process is of the order of 10–15 kcal.

The isomerization process is accompanied by polymerization. The latter was measured by drop in pressure and found to be bimolecular with respect to the butene present and unimolecular with respect to sulfuric acid. Experimental results indicate a break in the curve of the same type as the break in the isomerization curve. This lends confirmatory evidence to the assumption that two forms of catalyst are effective in the system. It is assumed that the free acid is the first form while the butyl hydrogen sulfate is the second form.

The reaction of butenes with phosphoric acid is presented in Figs. 12 and 13. These experiments are much more simple than the foregoing group with sulfuric acid. To begin with, at the pressure of the butenes used, the polymerization catalyzed by the acid occurred so slowly that its effect upon the actual isomerization reaction was negligible. The rate of isomerization was found to be proportional to the amount of the catalyst. The catalyst did not deteriorate in activity as did the

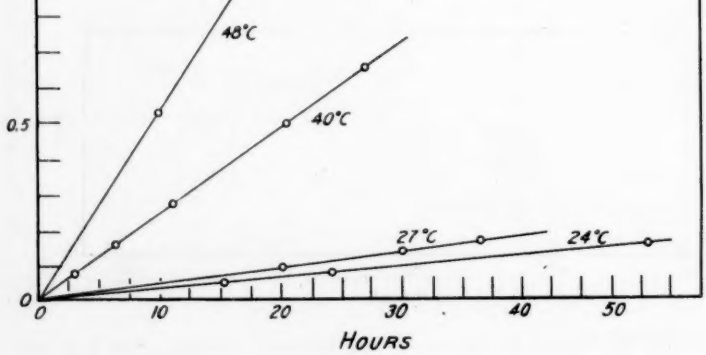

FIG. 13. Isomerization of butene-1 on radioactive phosphoric acid.

sulfuric acid for, as the figures indicate, the logarithm of the unreacted butene-1 plotted against the time of reaction produces a straight line in accordance with the integrated form of the equation

$$dP_2/dt = K(P_1 - P_2),$$

where P_2 = partial pressure of butene-2 and P_1 = partial pressure of butene-1.

The rate constants derived are presented in Fig. 12 in terms of grams of catalyst per liter. Various compositions of the catalyst were tried and the activation energies measured. As can be seen, the activation energy decreases with increasing phosphoric anhydride content. The reaction of radioactive phosphoric acid TH_2PO_4 with butene-2 is presented in Figs. 13–15. Figure 13 presents the rates at which isomerization occurred at various temperatures, Fig. 14, the increase of radioactivity of butenes, (8 mm of product gas in counter), while Fig. 16 represents the logarithm of the rates of isomerization and of the exchange plotted against the reciprocal of the absolute temperature. The activation energy for the isomerization reaction is 14.2 kcal. while that for the exchange is 17.8 kcal., giving a difference in activation energy of 3.6 kcal. Comparison of the absolute rates of the two reactions at 27°C shows that for 18 percent conversion for the butene-1 to butene-2 there is 0.15 percent exchange of tritium. Thus the rate of exchange is slower than the rate of isomerization. This difference in rates corresponds to a difference in activation rates for the two processes of 2.9 kcal., a result in good agreement with the value of 3.6 obtained from temperature coefficients. The values obtained this way are consistent with an expected difference in the zero point energies of bonded hydrogen and tritium. When a correction is made for this difference in activation, it is seen that these results indicate that every isomerization is accompanied by an exchange and that the two processes take place by the same mechanism. The difference in activation energy for the two processes emphasizes the fact that in these reactions we are dealing with covalently bonded hydrogen and tritium and not with hydrogen or tritium *ions*.

Butene-1 was treated with radioactive water for 75 hrs. to determine whether or not there was any exchange between the tritium in the water and the hydrogen of the butene. No exchange was found.

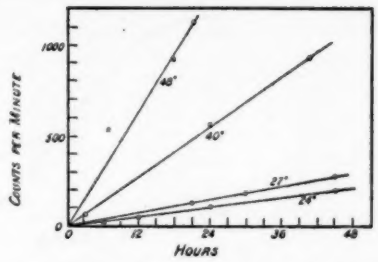

FIG. 14. Exchange of butene-1 on radioactive phosphoric acid.

Butene-1 was also treated with tritium hydrochloric acid, 10 cc conc. HCl with 0.2 cc of tritium water. No exchange was observed. The absence of exchange indicates that the tritium ion is not a sufficient condition for exchange.

Ethylene was shaken with tritium phosphoric acid for 48 hours at 50°C. A total count of 306 per minute was observed against a background of 300 per minute. The difference is within experimental error and shows that ethylene does not exchange with tritium phosphoric acid.

Propylene, at 500 mm, was treated with the same sample of tritium phosphoric acid as was used for the ethylene experiment. The results are found in Table II.

The difference in E^* between that for butene exchange (17.8 kcal.) and propene (19.6 kcal.) may be due to the energy difference in the removal of hydrogen from the methylene grouping as compared with the removal of hydrogen from a methyl group.

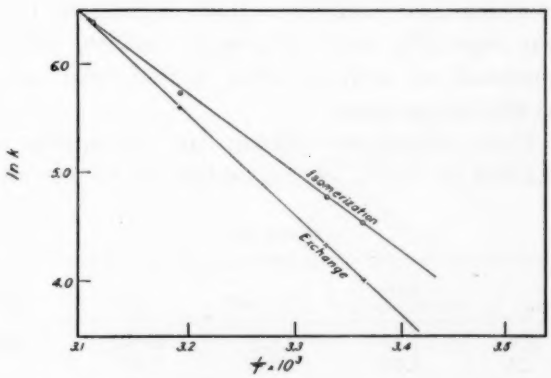

FIG. 15. Temperature dependence of exchange and isomerization reaction.

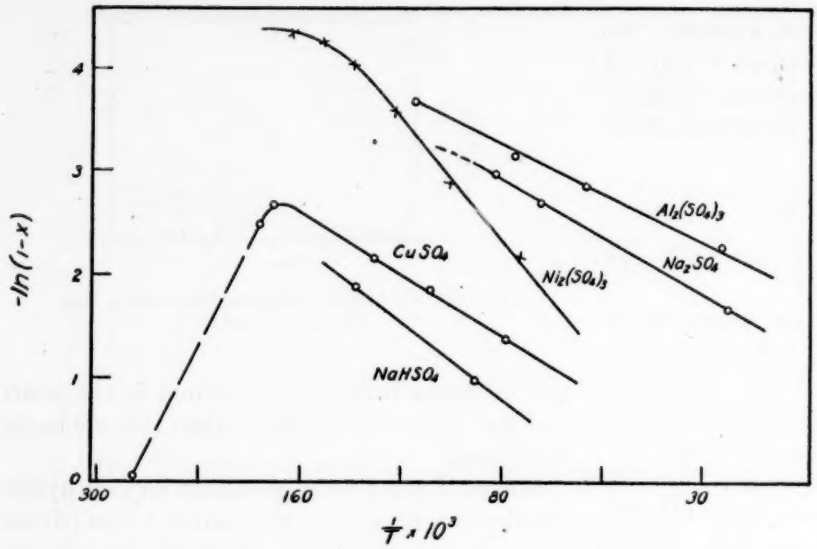

FIG. 16. Isomerization of butene-1 on sulfate catalysts.

SOLID CATALYSTS

The flow system shown in Fig. 4 was used to study the effect of solids upon butene-1 at various temperatures. The catalysts investigated were aluminum sulfate, upon which supplementary adsorption experiments were performed, copper sulfate, sodium sulfate, sodium hydrogen sulfate, nickel sulfate, copper pyrophosphate, aluminum silicate, alumina, silica gel, thoria, chromic oxide on alumina, and calcium oxide.

These catalysts, with the exceptions noted below, were studied at a nearly constant flow velocity of seven seconds contact time. The results are plotted in Figs. 16 and 17. The particular catalyst involved is indicated for each set of points.

The sulfate catalysts shown in Fig. 16 were observed to eliminate water at the temperatures at which their catalytic activity decreased. This was especially true for copper sulfate, which possessed no activity when it had been completely dehydrated.

Using aluminum silicate, an asymptote is reached at 125°C corresponding to 85 percent conversion of butene-1 to butene-2. This result does not correspond to equilibrium but was caused by decrease in catalytic activity by decomposition of the butene on the surface.

TABLE II.

Temp. °K	Rate (counts/min. hr.)	$1/K \times 10^3$	$\ln k$	E^*
320	2.33	3.125	0.846	19.6
324	3.46	3.086	1.225	

* J. O. Smith, Jr. and H. S. Taylor, J. Chem. Phys. 7, 390 (1939).

CIS-TRANS-ISOMERIZATION

The results of the study of *cis-trans*-isomerization were curtailed by lack of *cis*-butene-2. It was found that activated charcoal isomerized 85 percent *cis*-butene-2 as follows:

Time	0.	2 days	3 days
percent *cis*	86	72	60

The reaction was performed at −80°C in the liquid phase. No butene-1 was formed as determined by infra-red measurements performed by Mr. W. W. McCarthy.

No such isomerization was observed on this catalyst using contact time of seven seconds and at room temperature.

Using a catalyst of nickel supported on porcelain, no butene-1 was formed and the results listed in Table III were obtained for the conversion of butene-2 from *cis* to *trans*. Starting material: 14 percent *trans*-butene-2.

The activation energy from the first two values is about four kilocalories.

ADSORPTION

The investigation of the adsorption characteristics of aluminum sulfate for butene was carried out to see whether or not any connection existed

TABLE III.

Temperature	Flow	Percent *trans* (vapor press.)	(Thermal cond.)
65°C	20 sec.	22 percent	22.5 percent
88°C	20 sec.	33 percent	36 percent
116°C	20 sec.	28 percent	
*124°C	20 sec.	14 percent	13 percent
**124°C	20 sec.	40 percent	

* Catalyst poisoned by butene adsorption.
** Catalyst cleaned by hydrogen before using. Possible butane and butene-1 formation.

between this phenomenon and the isomerization process. The apparatus has been previously described. The dead space of the system was measured by nitrogen which was assumed sufficiently inert at the temperatures involved so that no appreciable adsorption would occur. The measurements were made on a 3-g sample by admitting a known quantity of butene at a regulated temperature and allowing the system to reach equilibrium. At the measurements below 80°C this was rapid and the isotherms which are plotted in Fig. 18 follow Langmuir's derived equations. From these data the heat of adsorption was calculated to be 1020 cal. per mole adsorbed.

At higher temperatures, equilibrium was more slowly attained so observations were made as to the time required to adsorb 1.8 cc of gas at the temperatures and pressures indicated in Table IV. The pressure did not vary by more than 25 mm during this process so that for the purpose of the experiment no special precautions were taken in setting up a constant pressure apparatus. The rates obtained are tabulated below in terms of cc adsorbed per hour. The activation energy of adsorption was then obtained by using these values as rate constants and plotting their logarithms against the reciprocal temperature.

TABLE IV.

Exp.	Temperature	Pressure	Rate	E^*
A-13	82°C	760 mm	0.09	3 kcal.
A-14	92°C	760 mm	0.10	8
A-15	131°C	770 mm	0.36	8.3 kcal.
A-4	136°C	760 mm	0.39	8.3 kcal.
A-16	161°C	765 mm	0.72	8 kcal.

DISCUSSION

Several mechanisms have been proposed for the migration of the double bond in hydrocarbons. Ipatieff and Carson[13] postulated in their mechanism for the polymerization of butenes by phosphoric acid that an ester is first formed and then reacts with another butene molecule to form the dimer. If, however, the olefine leaves the catalyst before reaction with another molecule, isomerization can take place.

$$C_4H_8(-1)+H_3PO_4=CH_3\cdot CHOPO_3H\cdot CH_2\cdot CH_3$$
$$=H_3PO_4+C_4H_8(-2).$$

The second mechanism is that of Whitmore.[14] It consists of the addition of the hydrogen ion to one point of the molecule and its subsequent elimination at another point.

$$C_4H_8(-1)+H^+\rightleftarrows(CH_3\cdot CH_2\cdot CH\cdot CH_3)^+$$
$$\rightleftarrows H^++C_4H_8(-2).$$

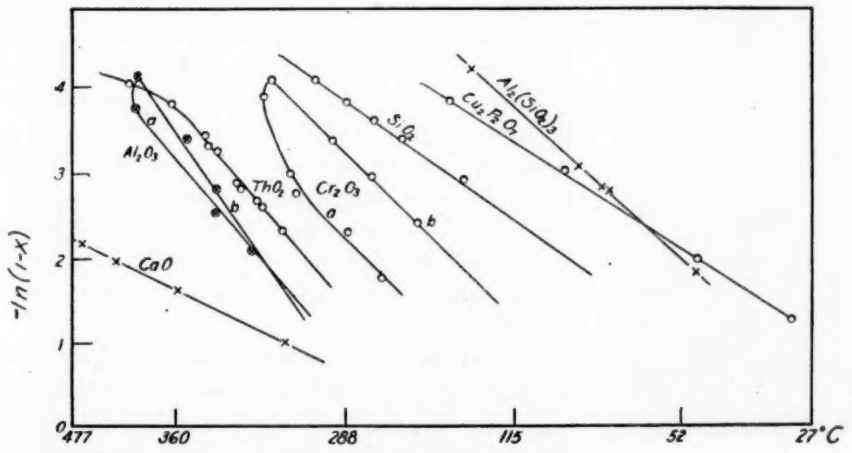

FIG. 17. Isomerization of butene-1 on oxide catalysts. (a) activity on heating, (b) activity on cooling.

[13] Ipatieff and Carson, Ind. Eng. Chem. **27**, 1069 (1935).
[14] Whitmore, J. Am. Chem. Soc. **54**, 3264 (1932).

The third mechanism is that of Farkas and Farkas.[15] These workers postulate a complex of two molecules of butene with phosphoric acid,

$$H_3PO_4+2C_4H_8 \rightleftarrows (H_3PO_4 \cdot 2C_4H_8).$$

Since the identity of the double bond is lost in the complex, a shift of the double bond may result when the complex breaks up.

Before attempting to formulate a theory the experimentally observed facts shall be reviewed. Experiments with sulfuric and phosphoric acids have shown that the rate of reaction is proportional to the amount of the catalyst when the latter is small and that ester formation retards the rate of double bond migration. This would indicate that the rate determining step is the interaction of the acid with the butene and not the decomposition of the complex. The study of the behavior of butene-1 with radioactive phosphoric acid indicates the similarity of the isomerization and the exchange reaction. From the temperature dependence of the rates of the reaction a difference of activation energies of 3.6 kcal. has been found for the two reactions; this difference might be correlated with the difference in the zero-point energies of hydrogen and tritium. A difference of zero-point energy can only exist for bonded hydrogen and tritium. There would be no zero-point energy difference between the hydrogen ion and the tritium ion. The presence of such an activation energy difference is difficult to reconcile with the theory of the addition of the hydrogen ion to the double bond.

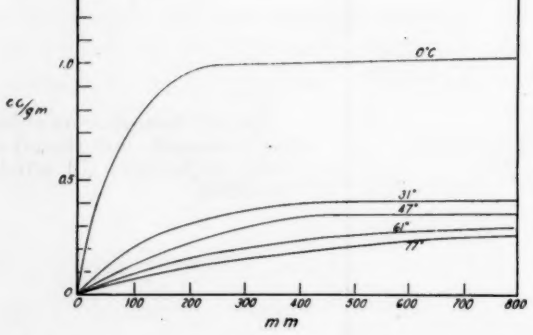

FIG. 18. Absorption of butene on aluminum sulfate.

[15] Farkas and Farkas, Ind. Eng. Chem. **33**, 785 (1941).

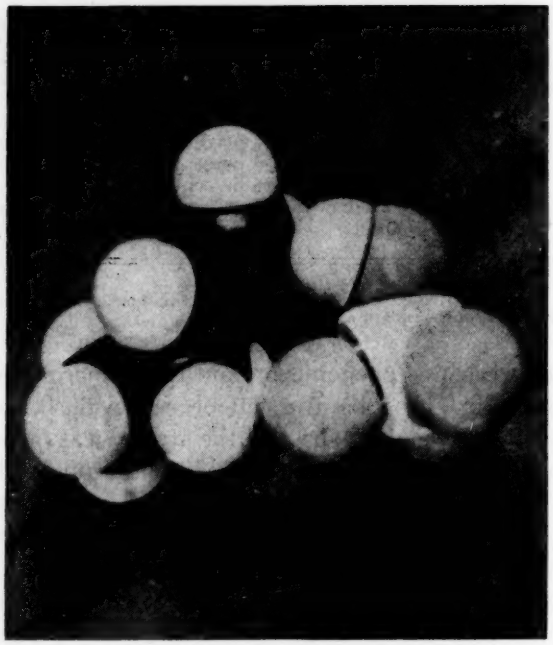

FIG. 19. Isomerization.

The failure of the ethylene to exchange with radioactive phosphoric acid again emphasizes the difficulty of formulating the process in terms of either the hydrogen ion or ester formation. The failure of radioactive hydrogen chloride to produce any exchange with butene-1 reemphasizes the fact that the tritium ion and, therefore, the hydrogen ion do *not* add readily to carbon-carbon double bonds. This is further substantiated by the inability of the trichloracetic acid, a relatively strong acid, to isomerize butene-1. The increase in the activation energy of isomerization with increase in the water content of the phosphoric acid indicates that the more dilute solutions where the hydrogen ion concentration is higher, are less efficient catalysts. Furthermore, in concentrated phosphorus pentoxide solutions, the hydrogen is probably present more in the covalent hydroxyl bond than as the hydrogen ion. The Raman spectra have shown this to be the case in concentrated sulfuric and perchloric acid,[16] substances which are known to be good isomerization catalysts.

It is on the above grounds that we feel that the mechanisms previously proposed are inadequate for explaining the facts of the double bond migra-

[16] Simon, Zeits. f. angew. Chemie **51**, 783 (1935).

tion in the butenes. We therefore propose the following "Hydrogen Switch" mechanism. When a sulfuric acid molecule approaches a butene-1 molecule the approach is postulated to take place in such a way that one of the hydrogen atoms of the sulfuric acid approaches the end carbon atom while the oxygen atom having no hydrogen on it approaches the hydrogen atom on the third carbon atom in the butene-1 molecule. It is found by means of molecular models that the sulfuric acid "fits" the butene molecule in this way (see Fig. 19).

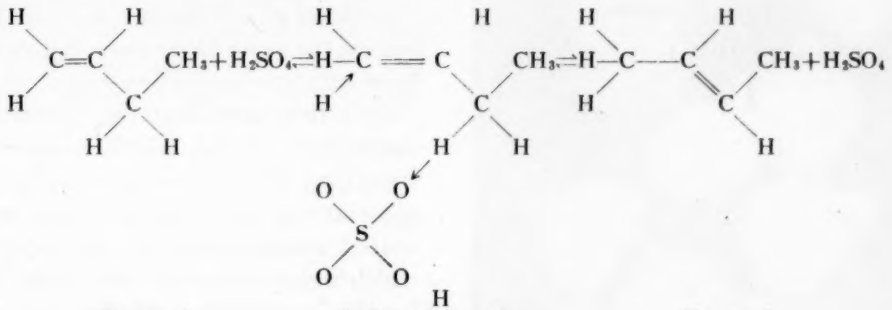

An activated complex is formed with no bond distortion in either butene or the catalyst molecule. The electron cloud which travels at least two thousand times faster than the nuclei may migrate to the middle of the butene molecule. When the sulfuric acid breaks away from the complex it may take with it the hydrogen atom from the third carbon atom and leave a hydrogen atom on the first carbon atom. The result is butene-2. The mechanism is reversible, producing either butene-1 or butene-2 consistent with the thermodynamic requirements. The sulfuric acid thus acts as both a donor and acceptor of the hydrogen atoms, the hydrogen lost by the hydroxyl is gained by the "double bonded" oxygen atom. This process of hydrogen transfer takes place in one elementary act, the energy requirements of the loss being compensated by the energy requirements of the addition of the hydrogen atom. *The critical demand on the catalyst is that it be able to furnish a hydrogen and accept a hydrogen at a distance of approximately 3.5*A. This distance is the distance between the hydrogen on the first carbon and the third carbon atom in an aliphatic chain.

This mechanism is in harmony with known experimental facts. The rate will be proportional to the amount of the catalyst when that is small. Furthermore, when an ester is formed between the butene and the acid molecule, the process will be slower because there are less hydrogen atoms available in the ester as donors. The mechanism of the exchange reaction is the same as the mechanism of the isomerization. The rate of the exchange reaction using tritium will be smaller

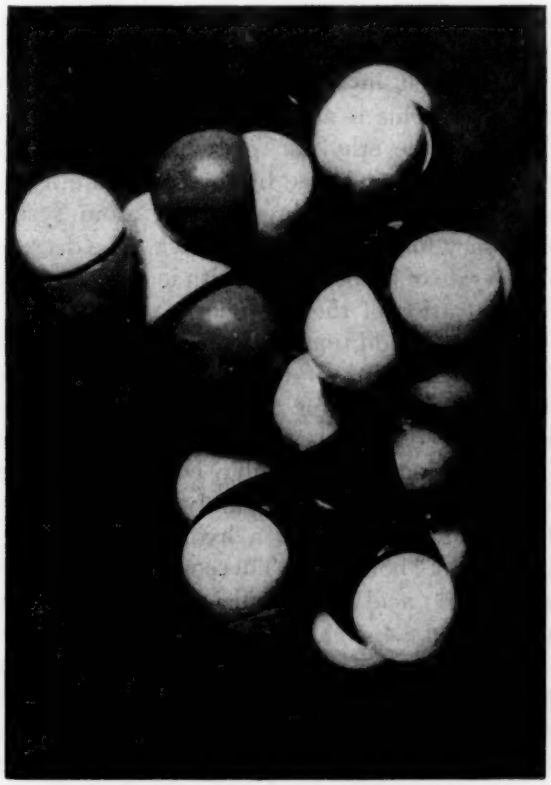

FIG. 20. Polymerization.

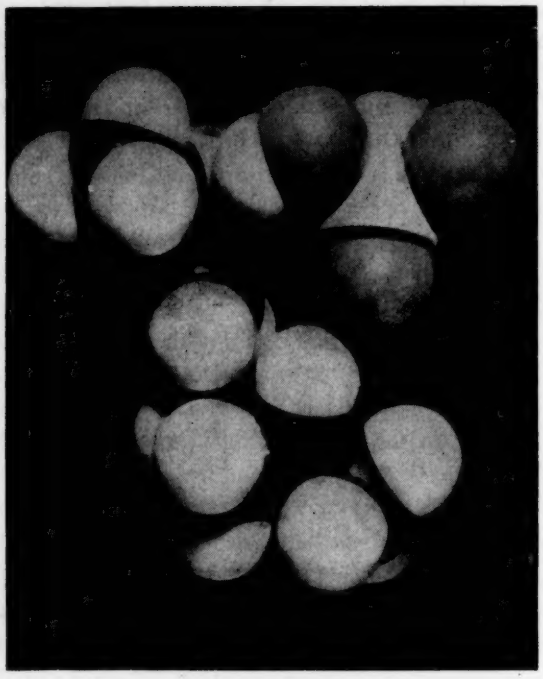

FIG. 21. Alkylation.

since the difference in zero-point energies of covalently bonded hydrogen and tritium should express itself in the activation energy of the processes. This is actually found to be so. The failure of the ethylene to exchange with phosphoric acid is explained by the fact that ethylene does not have the three carbon atom system necessary for the hydrogen switch. The decrease in the rate of isomerization with increase in water concentration of the phosphoric acid solution is due to the addition of water to the "double bonded" oxygens of the phosphoric acid thus muzzling the acceptor part of the catalyst. Thus the ability of various substances to carry out the isomerization of the double bond is associated with the presence in a catalyst molecule of a hydrogen acceptor and a hydrogen donor at a distance of about 3.5A. This condition is satisfied by sulfuric acid 3.45A, silicic acid 3.50A, phosphoric acid 3.46A, and perchloric acid 3.41A.[17]

The action of moist aluminum chloride or bromide is interpreted as due to $HAlCl_4$ with 3.46A and $HAlBr_4$ with 3.58A between the hydrogen donor and the hydrogen acceptor centers on the molecule. Isomerization using nickel and hydrogen is formulated as being due to a reaction of the following type:

$$\begin{matrix} H & & H \\ Ni-Ni+C_4H_8(-1)=Ni-Ni+C_4H_8(-2). \end{matrix}$$

The nickel-nickel distance is 3.52A. Other metals having the same atom-atom distance should also have catalytic properties.

It is thus seen that the "Hydrogen Switch" mechanism is one which requires very little stretching of the hydrogen bonds in either the substrate or the catalyst, is one which gives a spatial interpretation of specificity and is one which neatly balances the energy requirements for the isomerization process. The following are some reactions by which it is hoped to further test this mechanism. If propylene be reacted with deuterated sulfuric acid, the hydrogen exchange will take place on the first and third carbon atom of the chain and there will be no exchange on the middle carbon atom, giving—in the case of propylene—$CD_2=CHCD_3$. Furthermore, this mechanism would predict that there would be no shift of the double bond using the above catalysts for hydrocarbons where there is a tertiary carbon

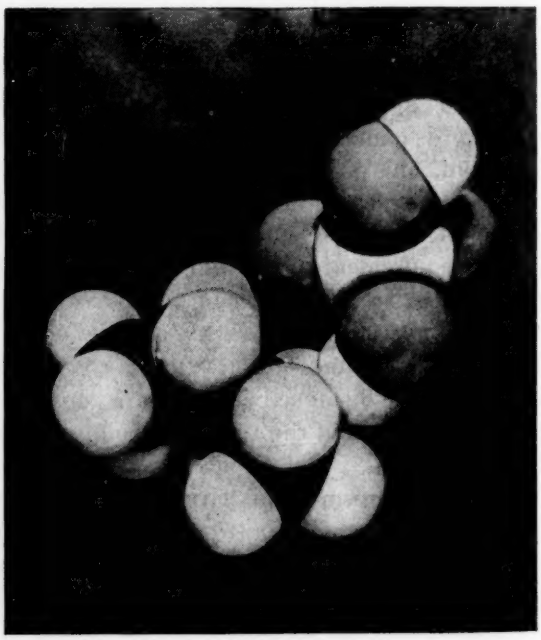

FIG. 22. Cracking.

[17] L. Pauling, *The Nature of the Chemical Bond* (Cornell University Press, Ithaca, New York, 1941).

atom in position three from the carbon atom containing the farther end of the double bond as in $R_3C-CH=CH_2$. There is partial substantiation of this view in the observation of Whitmore *et al.*[14] that there are only two isomers in the dimer of polymerization of isobutylene, namely 224 trimethyl pentene-3 or pentene-4. Furthermore, treatment with deuterated sulfuric acid should yield as the final product $(CH_3)_3C-CD=C(CD_3)^2$ and $(CH_3)_3C-CD_2-C(CD_3)=CD_2$.

Furthermore, it would be of interest to test for catalytic activity such metals as platinum, palladium, silver, gold, copper, cobalt, iron and others.

It is possible to extend the hydrogen switch mechanism to formulate not only double bond migrations but polymerizations, alkylation, and cracking. Thus polymerization is formulated as a hydrogen switch between two molecules of the olefine (Fig. 20).

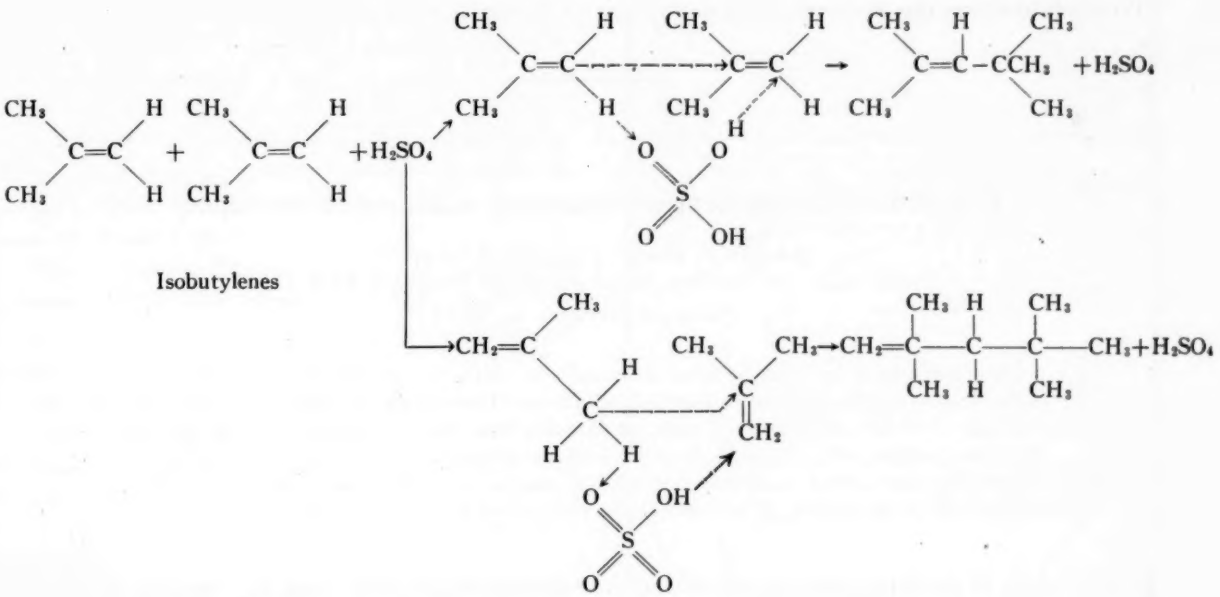

Alkylation (Fig. 21) is formulated as a hydrogen switch between the paraffin and the olefine. The hydrogen is transferred in this case from the paraffin to the olefine by means of the catalyst

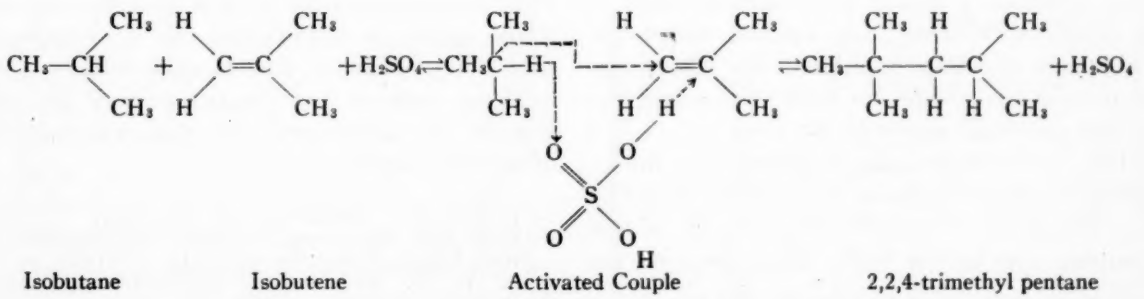

Cracking is visualized as the reverse of alkylation. Thus a carbon-carbon bond is broken as the catalyst (silicic acid or alumino silicic acid) removes the hydrogen from one carbon atom and transfers it to a carbon atom one removed from the first one, Fig. 22.

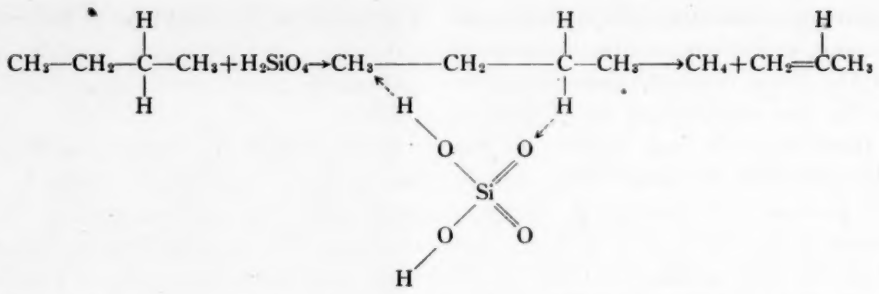

A more detailed presentation of this unitary mechanism of catalytic hydrocarbon reactions will be a subject of a subsequent communication by the senior author.

We wish to thank the M. W. Kellogg Company for financial assistance in this work.

THE JOURNAL OF CHEMICAL PHYSICS VOLUME 16, NUMBER 5 MAY, 1848

The Ultraviolet Absorption Spectrum of Benzonitrile Vapor*

ROBERT C. HIRT** AND JOHN P. HOWE***
Metcalf Research Laboratory, Brown University, Providence, Rhode Island

(Received December 31, 1947)

The ultraviolet absorption spectrum of benzonitrile vapor has been investigated, and many of the observed bands have been accounted for in terms of ground and excited state frequencies. The data obtained were compared with the data available from infra-red absorption spectra, the Raman effect, and early work on ultraviolet absorption spectra. The spectrum of benzonitrile vapor was shown to resemble closely the spectra of other monosubstituted benzenes, particularly in the spacing of the excited state bands from the zero-zero band.

THIS study of the ultraviolet absorption spectrum of benzonitrile vapor has the aim of extending the analyses of the spectra of monosubstituted benzenes. Since the initiation of this work, the spectra of several other monosubstituted benzenes have been reported and their main features analyzed. The present work is consistent with these analyses and allows the assignment of a large fraction of the vibrational frequencies and modes for both the ground and excited electronic states of the molecule.

The C−C≡N grouping is known to be linear, and the symmetry class of benzonitrile should be C_{2v}. Vibrational frequencies characteristic of this grouping are known from comparison of the Raman effect and infra-red spectra of organic cyanides as well as of HCN and cyanogen. Therefore a key exists as to some of the vibrational frequencies introduced by the substituent group. Since the nitrile group possesses an unshared pair of electrons which may resonate with those in the ring, an intensification as well as a shift of the whole spectrum toward the red, as compared with that of benzene, may be expected.

Many authors have reported work on the Raman effect, infra-red, and ultraviolet spectra of benzonitrile.[1–8]

* Abstract from a thesis by Robert C. Hirt presented in partial fulfillment of the requirements for the degree of Doctor of Philosophy at Brown University, June 1947, covering work done during the years 1940–42 and 1946–47.

** Present address: Physics Division, American Cyanamid Company, Stamford, Connecticut.

*** Present address: Research Laboratories, General Electric Company, Schenectady, New York.

[1] J. E. Purvis, J. Chem. Soc. **107**, 496 (1915).
[2] H. E. Acly, Zeits. f. physik. Chemie **135**, 251 (1928).
[3] Koiti Masaki, Chem. Soc. Japan **11**, 346 (1936).
[4] K. W. F. Kohlrausch, *Ramanspektren* (Edwards Brothers, Inc., Ann Arbor, 1945).
[5] J. Simons, Finska Vetenskap-Soc., Comm. Phys.-Math. **6**, No. 13 (1932).
[6] J. Lecompte, J. de phys. et rad **8**, 489 (1937).
[7] P. Barchewitz and M. Parodi, J. de phys. et rad. **10**, 143 (1939).
[8] P. Barchewitz and M. Parodi, Comptes Rendus **209**, 30 (1939).

EXPERIMENTAL

The absorption spectrum of benzonitrile vapor was photographed with a Hilger Littrow spectrograph having quartz optical parts and a dispersion of 48 wave numbers per millimeter in the region of 2740A (36,500 cm^{-1}). A hydrogen discharge tube used end-on was the light source. This tube was of the flowing type, hydrogen being introduced through a palladium thimble and pumped out by a Cenco Hyvac pump.

Absorption cells having lengths of 83 and 152 cm and quartz windows were used. The longer cell was equipped to operate as a flowing, rather than static, cell with a bulb at either end. One bulb held pure liquid benzonitrile, and the other was cooled by a dry ice-isopropyl alcohol bath. This flowing arrangement was used to avoid accumulation of decomposition products in the cell and on the cell windows.

The cells could be placed in an electrically heated furnace and the pressure controlled by the temperature of the bulb which contained the liquid.

Benzonitrile obtained from the Eastman Kodak Company was dried over calcium chloride and by passing the vapors over activated alumina. The liquid was twice distilled under reduced pressure, and introduced into the cells by vacuum distillation.

Measurement of the observed bands were made on microphotometer tracings prepared on a microphotometer-comparator nearly identical with that described by Leighton, Smith, and Henson.[9] Eastman Kodak plates of types 40, 33, and 103–0 were used both for photographing the spectra and the tracings. A drawing of the benzonitrile vapor absorption spectrum made from these tracings is shown in Fig. 1. The tracings were usually eight times the size of the original spectrum. A standard Pfund iron arc was used as a wave-length standard. The wave-lengths of the observed bands were corrected to vacuum and converted into wave numbers (cm^{-1}).

The Raman effect spectrum of benzonitrile (see Table II) was photographed with a Hilger spectrograph having glass optical parts, using four H-11 mercury lamps as light sources. Measure-

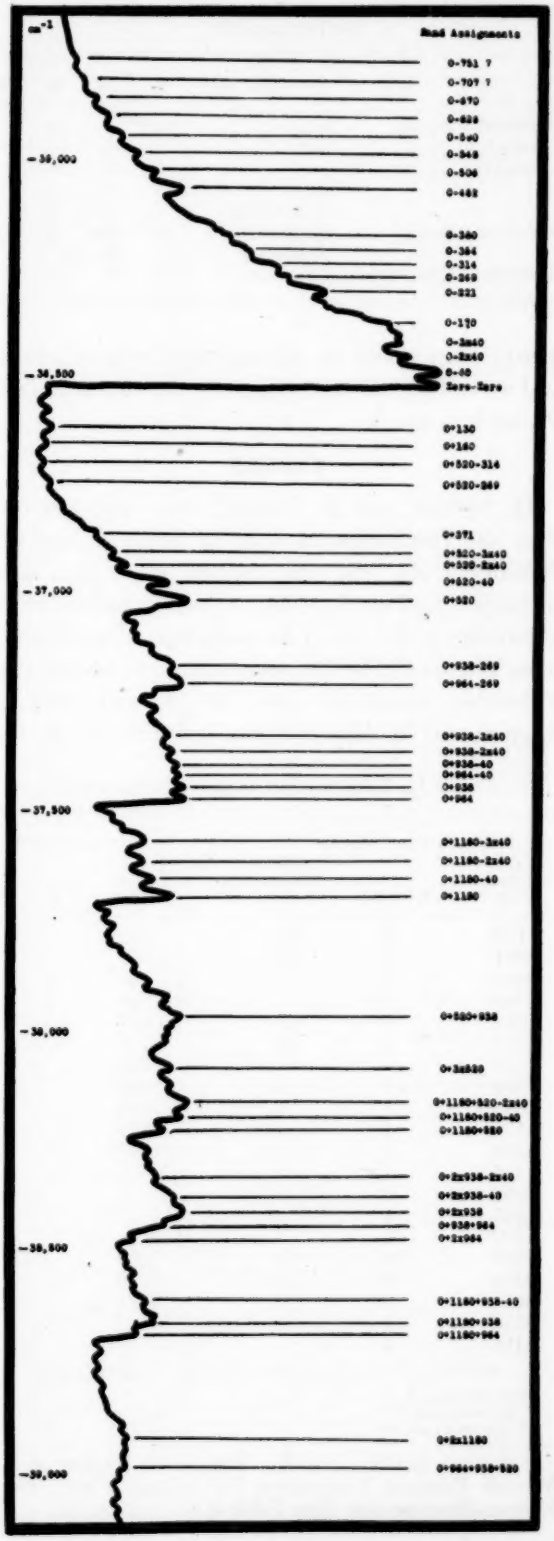

FIG. 1. Ultraviolet absorption spectrum of benzonitrile vapor (composite drawing of several microphotometer tracings).

[9] P. A. Leighton, S. Smith, and F. C. Henson, Rev. Sci. Inst. 5, 431 (1934).

TABLE I. Symmetry elements and selection rules for benzonitrile.

	Symmetry class	A_1	A_2	B_1	B_2
Essential	I	+	+	+	+
Symmetry	C_2^y	+	+	−	−
Elements	σ_h	+	−	+	−
	σ_v	+	−	−	+
	Translation	T_y		T_x	T_z
Selection rules	Raman effect	p	dp	dp	dp
	Infra-red	a	ia	a	a
Number of vibrations	(13 atoms)	13	3	10	7

ments were made on microphotometer tracings, and wave-lengths determined by use of a standard Pfund iron arc.[10]

THEORY

H. Sponer and E. Teller[11] have pointed out that the fundamental state of benzene has the symmetry A_{1g} and the excited state B_{2u}. The transition is then $A_{1g}\rightarrow B_{2u}$, which is forbidden in symmetry class D_{6h}. The reduction of symmetry from D_{6h} to C_{2v} by monosubstitution makes this forbidden transition into an allowed one, as Sponer and Wollman[12] have pointed out in the case of monochlorobenzene. Thus the spectra of monosubstituted benzenes would be expected to show certain features of the forbidden benzene spectrum, due to the presence of the ring, together with other features of an allowed spectrum arising from the reduction in symmetry.

By analogy to the Sponer-Wollman treatment of monochlorobenzene, the electronic transition for benzonitrile is $A_1\rightarrow B_1$, with the electronic moment lying in the plane of the ring and perpendicular to the axis of substitution. This is allowed, and should give rise to a strong band in the ultraviolet spectrum.

Table I presents the symmetry elements and selection rules for molecules of symmetry class C_{2v}. It resembles that of Sponer and Stücklen[13] for pyridine.

TABLE II. Raman effect data on benzonitrile.

Kohlrausch* and Simons**			This research***	
Wave-number shift	Intensity	Depolarization (percent)	Wave-number shift	Intensity
170	8	85	170	10
381	2	35	378	3
460	6		460	6
549	5		548	5
624	5	84	623	5
751	3	15	752	4
765	5		764	6
998	15	4	1001	10
1023	3		1026	3
1178	8		1178	7
1190	8	24	1192	7
1310	1			
1353	0			
1447	1			
1493	2			
1597	10	88	1598	10
2224	10	23	2229	10
3071	8	30	3071	8
3146	1			
3196	1			

* See reference 4.
** See reference 5.
*** See reference 10.

DISCUSSION

The most prominent feature of the ultraviolet absorption spectrum of benzonitrile vapor is the group of bands culminating in the very strong band with an extremely sharp edge on the ultraviolet side which occurs at 36,516 cm^{-1} (2737.7A). This band has been taken as the zero-zero (0→0) band. Sponer[11] and Masaki[3] also took this to be the zero-zero band.

Certain bands to the lower-wave number (red) side of the 0→0 band have been attributed to transitions from a given vibrational level of the ground state to the excited state with no vibrations active. These are shown in the "Assignments" column of Table III, and are compared to the Raman effect data, the infra-red data, and to Masaki's assignments in Table IV.

Bands at 269 and 380 cm^{-1} to the red of the 0→0 band correspond to the infra-red bands at 264 and 384 cm^{-1} reported by Barchewitz and Parodi,[7,8] and attributed by them to the nitrile group, having been found in other nitriles. Bands were found at 314, 460, 506, 548, 626, and 670 cm^{-1} to the red of the 0→0 band, and ascribed to transitions from ground state vibrational levels of these values. The 548 band is due to the ω_6'' vibration (Sponer's notation) or 6a (Wilson's notation).[14] The band at 626 separation is due to

[10] We are indebted to Dr. Robert C. Taylor of the Metcalf Research Laboratory for assistance with these Raman effect spectra. (See Table II.)

[11] H. Sponer and E. Teller, Rev. Mod. Phys. **13**, 76 (1941).

[12] H. Sponer and S. Wollman, J. Chem. Phys. **9**, 816 (1941).

[13] H. Sponer and H. Stücklen, J. Chem. Phys. **14**, 101 (1946).

[14] For notation and modes of benzene ring vibrations, see K. S. Pitzer and D. W. Scott, J. Am. Chem. Soc. **65**, 803–829, (1943), and E. Bright Wilson, Phys. Rev. **45**, 706 (1934).

TABLE III. Observed ultraviolet bands of benzonitrile.

Wave number of band	Difference from 0→0 band	Intensity	Assignment of band
35,653	863	*vf*	
35,675	841	*vf*	0−838 ?
35,704	812	*vf*	
35,743	773	*vf*	0−765 ?
35,775	741	*vf*	0−751 ?
35,809	707	*vf*	
35,847	669	*f*	0−670
35,890	626	*vw*	0−626
35,926	590	*vw*	
35,968	548	*w*	0−548
36,010	506	*w*	0−3×170 ?
36,054	462	*wm*	0−462
36,136	380	*vw*	0−380
36,162	354	*w*	
36,202	314	*wm*	0−314
36,233	283	*wm*	
36,247	269	*m*	0−269
36,295	221	*ms*	0+160−381
36,346	170	*ms*	0−170
36,364	152	*s*	0+160−314
36,382	134	*vs*	0+130−269
36,397	119	*vs*	0−3×40
36,434	82	*vs*	0−2×40
36,458	58	*s*	
36,476	40	*vvs*	0−40
36,516	0	*vvs*	0→0
36,547	31	*vw*	
36,596	80	*vw*	
36,640	124	*vw*	0+130
36,676	160	*vw*	0+160
36,722	206	*vw*	0+520−314
36,767	251	*vw*	0+520−269
36,826	310	*w*	
36,887	371	*w*	0+371
36,922	406	*wm*	0+520−3×40
36,956	440	*m*	0+520−2×40
36,997	481	*ms*	0+520−40
37,036	520	*ms*	0+520
37,058	542	*wm*	
37,090	574	*w*	
37,114	598	*w*	
37,147	631	*wm*	
37,180	664	*m*	0+938−269
37,217	701	*m*	0+964−269
37,241	725	*wm*	
37,277	761	*w*	
37,340	824	*wm*	0+938−3×40
37,376	860	*m*	0+938−2×40
37,439	923	*ms*	0+964−40
37,454	938	*s*	0+938
37,480	964	*ms*	0+964
37,523	1007	*w*	
37,544	1028	*w*	
37,572	1056	*wm*	0+1180−3×40
37,619	1103	*wm*	0+1180−2×40
37,656	1140	*m*	0+1180−40
37,696	1180	*s*	0+1180
37,731	1215	*vw*	
37,763	1247	*vw*	
37,786	1270	*vw*	
37,811	1295	*w*	
37,855	1339	*wm*	
37,883	1367	*wm*	
37,916	1400	*w*	
37,957	1441	*ms*	
37,978	1462	*m*	0+520+938
37,993	1477	*wm*	
38,014	1498	*wm*	
38,071	1555	*wm*	0+3×520
38,110	1594	*wm*	
38,144	1628	*wm*	
38,176	1660	*m*	0+520+1180−40
38,207	1691	*wm*	0+520+1180
38,252	1736	*vw*	
38,277	1761	*vw*	
38,310	1794	*w*	0+2×938−2×40
38,358	1842	*wm*	0+2×938−40
38,377	1861	*wm*	
38,393	1877	*ms*	0+2×938
38,416	1900	*m*	0+938+964
38,448	1932	*w*	0+2×964
38,497	1981	*f*	0+2×520+938 ?
38,525	2009	*vw*	0+2×520+964 ?

TABLE III.—*Continued.*

Wave number of band	Difference from 0→0 band	Intensity	Assignment of band
38,588	2072	*wm*	0+938+1180−40
38,620	2104	*wm*	
38,632	2116	*m*	0+938+1180
38,653	2137	*m*	0+964+1180
38,696	2180	*f*	
38,768	2252	*f*	
38,854	2338	*f*	
38,881	2365	*vw*	0+2×1180
38,905	2389	*f*	
38,936	2420	*f*	0+520+938+964
38,960	2444	*vw*	0+520+2×964
39,008	2492	*vw*	0+130+2×1180 ?
39,042	2526	*vw*	
39,096	2580	*w*	
39,121	2605	*w*	
39,149	2633	*vw*	0+520+938+1180 ?
39,192	2676	*vw*	
39,209	2693	*vw*	
39,224	2708	*f*	
39,265	2749	*f*	
39,287	2771	*f*	
39,325	2809	*f*	
39,340	2824	*vw*	0+3×938
39,363	2847	*vw*	0+2×938+964 ?
39,397	2881	*f*	0+520+2×1180 ?
39,418	2902	*f*	0+3×964
39,442	2926	*f*	
39,490	2974	*f*	0+2×520+2×964 ?
39,558	3042	*f*	
39,570	3054	*f*	0+2×938+1180 ?
39,597	3081	*f*	0+938+964+1180
39,629	3113	*f*	0+2×964+1180 ?
39,641	3125	*f*	
39,655	3149	*f*	
39,728	3212	*f*	
39,746	3230	*f*	
39,772	3256	*f*	
39,795	3279	*f*	
39,809	3293	*f*	0+938+2×1180 ?
39,818	3302	*f*	
39,834	3318	*f*	0+964+2×1180 ?
39,849	3333	*f*	0+520+3×938 ?
39,864	3349	*vf*	
39,939	3423	*f*	
39,947	3431	*f*	
39,972	3456	*f*	
40,006	3490	*vf*	
40,038	3522	*f*	0+3×1180
40,084	3568	*f*	
40,111	3595	*f*	
40,142	3626	*f*	
40,176	3660	*vf*	
40,183	3667	*vf*	
40,219	3703	*f*	
40,251	3735	*f*	
40,261	3745	*f*	
40,270	3754	*vf*	0+4×938 ?
40,287	3771	*vf*	
40,312	3796	*f*	
40,325	3809	*vf*	0+2×938+2×964 ?
40,358	3842	*f*	
40,382	3866	*f*	0+4×964 ?
40,412	3896	*f*	
40,484	3968	*f*	
40,533	4017	*f*	
40,559	4043	*f*	
40,592	4076	*f*	
40,626	4110	*f*	
40,648	4132	*f*	
40,662	4146	*f*	
40,701	4185	*f*	
40,731	4215	*f*	
40,777	4261	*f*	
40,860	4344	*vf*	
40,977	4461	*f*	
41,177	4661	*f*	
41,263	4747	*f*	0+4×1180 ?
41,340	4826	*vf*	
41,413	4897	*vf*	
41,466	4950	*vf*	
41,485	4969	*vf*	
41,509	4993	*vf*	
41,521	5005	*vf*	
41,533	5017	*vf*	

the ring frequency ω_4'' (or 6*b*). Both the 6*a* and 6*b* vibrations have the value of 606 in benzene, but split in the monosubstituted benzenes.

Measurements at higher temperatures and pressures indicate that there is still some absorp-

TABLE IV. Comparison of ground state frequencies obtained from Raman effect, infra-red, and ultraviolet spectra data on benzonitrile.

Infra-red		Raman effect		Ultraviolet	
Barchewitz and Parodi*,**	Lecompte***	Kohlrausch†	This research††	Masaki†††	This research
—	—	170	170	—	170
206	—	—	—	—	—
264	—	—	—	—	269
323	—	—	—	—	314
384	—	381	378	—	380
—	—	460	460	459	462
—	548	549	548	547	548
—	616	624	623	616	626
—	676	—	—	—	670
—	686	—	—	—	—
—	754	751	752	—	741
—	—	765	764	—	773
—	838	—	—	—	841
—	922	—	—	—	—
—	1002	998	1001	1009	—

* See reference 7.
** See reference 8.
*** See reference 6.
† See reference 4.
†† See reference 10.
††† See reference 3.

tion below 35,846 cm^{-1}, but the identification of the individual bands is uncertain because of the diffuseness and low intensities. Diffuse bands were found at separations from the 0→0 band of 707, 741, 773, 812, 841, and 863 cm^{-1}. The symmetric ring "breathing" frequency, ω_1'', could not be identified even on plates made with the highest pressures, though Masaki reported a band at 1009 cm^{-1} separation.

A very strong band is found at 40 cm^{-1} from the 0→0 band. This has been ascribed to a difference frequency which occurs between a ground state vibration and that same vibration in the excited state, that is, a so-called 1→1 type of transition. It is closely analogous to the 60 cm^{-1} difference that is so prominent in the spectrum of monochlorobenzene[12] and to the 59 cm^{-1} difference in toluene.[15] The lowest frequency found in the Raman effect is 170 cm^{-1}. This is a strong band, with an intensity of 8, and is 85 percent depolarized. A relatively strong anti-Stokes line of this frequency was observed by us[10] with only a 3-hr. exposure. It would seem preferable to correlate this 40-difference frequency with the lowest frequency of vibration of the molecule, for it must arise from a vibrational frequency having a high Boltzmann factor to appear so strongly and so often as a difference frequency in the ultraviolet spectrum.

A medium-strong band was found 170 cm^{-1} to the red of the 0→0, as a shoulder on a stronger group of bands. A band which corresponds to the upper state frequency of this vibration would be expected at a separation of 170−40=130 to the ultraviolet of the 0→0 band. A weak, though quite distinct, band is found at a value of 124 cm^{-1} above the 0→0.

This ground state frequency of 170 cm^{-1} is believed to be that of the bending of the nitrile "tail" of the molecule out of the plane of the ring, i.e., as a "warping" of the most distant atoms of the molecule out of the plane of the ring. This motion would belong to a B_2 symmetry. According to Table I, this frequency should appear depolarized in the Raman effect. This it does, with a depolarization of 85 percent.

Vibrations of class B_2 should be active in infrared absorption. The data of Barchewitz and Parodi, unfortunately, only extend as low as 180 cm^{-1}, so the question of the presence of an infrared band at or near 170 cm^{-1} must go unanswered.

This difference frequency of 40 appears quite often in the ultraviolet spectrum, and also its multiples of 2×40 and 3×40. Each major upper state band has its train of 40, 2×40, and 3×40 bands to the red. It should be noted that these multiples are actually 2×130–2×170 and 3×130–3×170.

The first major band to the ultraviolet side of the 0→0 band occurs at 37,036 cm^{-1}, or 520 distant. This is assigned to an upper state vibrational frequency of 520. This would be the ω_6', or 6*b*, vibration. This is a characteristic frequency of the benzene ring and is not appreciably changed by the nature of the monosubstituted group. F. A. Matsen[16] showed that a number of monosubstituted benzenes had this upper state frequency between 505 and 528 cm^{-1}.

At separations of 938 and 964 cm^{-1} from the 0→0 band, two very strong bands were found, with weaker bands to their red sides. The stronger band at 938 is assigned to the ω_1', or 1, symmetric ring "breathing" frequency. The 964 band is assigned to the ω_2', or 18*a*, mode of vibration.

[15] N. Ginsburg and F. A. Matsen, J. Chem. Phys. **14**, 511 (1946).

[16] F. A. Matsen, talk before the Symposium on Color and Electronic Spectra of Complex Molecules, Chicago, Illinois, December 30, 1946, and F. A. Matsen, W. W. Robertson, and R. L. Chuoke, Chem. Rev. **41**, 273 (1947).

Bands of the 40-difference frequency and its multiples were found to the red of the 938 band, but the weaker corresponding band for the 964 were obscured by those of the 938.

A strong band at 1180 separation is assigned to the upper state frequency of the $7a$ vibration. This was the highest wave number band having the very sharp ultraviolet edge. The 40-multiple series was very prominent to the red of this band.

The stronger bands observed appeared to have a doublet nature. However, the resolving power of the spectrograph and plates used was not sufficient to permit full resolution of these doublets. The width of the bands measured 2.4 cm^{-1}, which corresponds to the value of 2.7 cm^{-1} earlier reported by Acly.[2] The granularity of the plates used was sufficient to impair the accuracy of these measurements.

A prominent band appears at 231 cm^{-1} to the red of the 0→0 band. It cannot be accounted for in terms of a ground state frequency, and it appears feasible to assign it to a difference frequency arising from a 1→1 transition from 381 to 160 cm^{-1}. A weak, though prominent, band occurs at 160 cm^{-1} to the ultraviolet of the 0→0, and a band at 381 cm^{-1} to the red, which corresponds to a value of 384 in infra-red absorption and 381 in the Raman effect, 36 percent depolarized. This is ascribed to a mode of vibration similar to that of $16a$ in benzene, with the nitrile group bending out of the plane of the ring, and the ring proper describing a "buckling" motion. This mode would have twice the number of nodes of that causing the 40-cm^{-1} difference, and it is noted that 381 is very roughly twice 170, in comparing the ground state frequencies.

Both these modes of vibration from which arise the difference frequencies of 40 and 221 belong to class B_2. $B_2 \rightarrow B_2$ transitions are allowed, and should appear strongly, as they are found to do. However, examination of the selection rules shows that transitions from a non-vibrating ground state, A_1, to a B_2 vibrating upper state should not occur, nor should $B_2 \rightarrow A_1$. Weak bands are observed, however, to which it is convenient to make such assignments. The distortions from the C_{2v} symmetry caused by the participation of the nitrile "tail" of the molecule in the vibrations of the molecule probably make such transitions possible, with low intensities.

TABLE V. Comparison of excited (upper) state frequencies for various monosubstituted benzenes.

Molecule	Excited state frequencies							Reference
(Wilson notation)	—	6a	6b	12	1	18a	7a	14
Benzonitrile	371	—	520	—	938	964	1180	this work
Chlorobenzene	372	—	521	—	931	966	1190	12
Bromobenzene	—	—	518	—	931	962	1208	a
Fluorobenzene	332	410	517	779	915	966	1218	b
Toluene	—	—	527	—	930	964	1189	c
Phenol	374	476	562	783	935	975	1273	d
Deuterophenol	—	471	550	772	933	959	1268	d
Aniline	338	492	567	797	953	984	1184	d
Deuteroaniline	—	481	563	787	953	964	—	d
Methylaniline	—	442	550	775	954	973	—	d
D-methylaniline	—	426	544	780	953	965	—	d
Anisol	—	—	527	759	934	954	1270	d
Ethylbenzene	—	—	527	—	940	—	1235	16
N-propylbenzene	339	—	527	—	949	—	1258	16
Isopropylbenzene	353	—	516	—	944	—	1234	16
N-butylbenzene	366	—	540	—	949	—	1273	16
S-butylbenzene	343	—	505	—	946	—	1229	16
T-butylbenzene	333	—	510	—	955	—	1290	16
Phenyl-cyclo-hexane	318	—	523	—	934	—	1184	16

[a] K. Asagoe and Y. Ikemoto, Phys.-Math. Soc. Japan 22, 677 (1940).
[b] S. H. Wollman, J. Chem. Phys. 14, 123 (1946).
[c] N. Ginsburg, W. W. Robertson, and F. A. Matsen, J. Chem. Phys. 14, 511 (1946).
[d] N. Ginsburg and F. A. Matsen, paper presented before the Symposium on Color and Electronic Spectra of Complex Molecules, Chicago, Illinois, December 30, 1946.

Progressions and combinations of the totally symmetric A_1 frequencies are allowed, and appear prominently in the ultraviolet spectrum. This is noticeable in Table III and Fig. 1. The bands farther toward the ultraviolet become increasingly complicated and less distinct because of these combinations and dissociation. Above 40,000 cm^{-1} the bands are indistinct, although some bands were observed as high as 41,533 cm^{-1}. Assignments of these higher wave number bands are necessarily uncertain, however well the assignment may fit.

The benzonitrile molecule, having an unshared pair of electrons on its substituent group, should have its 0→0 band displaced toward higher wavelengths from the theoretical position of the 0→0 band of benzene, like other molecules whose substituent groups may contribute to resonance with the ring. It occurs at 36,516 cm^{-1}, near those of bromobenzene (36,997) and phenol (36,349).

A comparison of the upper state vibrational frequencies with those of other monosubstituted benzenes is shown in Table V.

The authors wish to express their gratitude to Professor Paul C. Cross for his many helpful suggestions in connection with this investigation.

The Variation of the Complex Dielectric Constant with Frequency

H. C. BOLTON
University College, Nottingham, England
(Received January 5, 1948)

The locus of the complex dielectric constant for the dispersion region of a polar dielectric is found in the "complex dielectric constant plane" following the equation of Onsager (1936), and is compared with the approximate solution of Cole (1938). The curve is plotted for the polar liquids, water, ethyl alcohol, and tertiary butyl alcohol, and compared with the curve deduced from Debye's equation. Calculations are made of the values of the relaxation times. The values of the molecular volume deduced from the Debye expression for the relaxation time are compared with those deduced from the van der Waals b coefficient.

INTRODUCTION

THE equation of Debye[1] for the dielectric constant ϵ of a polar substance at any frequency $\omega/2\pi$ is

$$\frac{\epsilon-1}{\epsilon+2}=\frac{4\pi}{3}N\left[\alpha+\frac{\mu_0^2}{3kT}\frac{1}{1+i\omega\tau}\right]. \tag{1}$$

N is the number of dipoles per cc, α the molecular polarizability, μ_0 the dipole moment in the absence of interaction effects, k Boltzmann's constant, T the absolute temperature, and τ the "relaxation time" of the dipole. Equation (1) reduces to $\epsilon-\epsilon_0=(\epsilon_1-\epsilon_0)/(1+ix)$, where ϵ_1 is the statical dielectric constant, measured at frequencies low enough so that $\omega\tau\ll1$, ϵ_0 is the optical dielectric constant, given by the square of the refractive index measured for the D line, and x is a parameter given by

$$x=\frac{\epsilon_1+2}{\epsilon_0+2}\omega\tau. \tag{2}$$

It is customary to write $\epsilon=\epsilon'-i\epsilon''$, and K. S. Cole and R. H. Cole[2] showed that the locus of (ϵ',ϵ'') considered as a point in the complex dielectric constant plane is a circle with center on the real axis $[(\epsilon_1+\epsilon_0)/(2),0]$ and radius $(\epsilon_1-\epsilon_0)/2$. It was also pointed out by Cole and Cole that the experimental locus of (ϵ',ϵ'') lay below the Debye curve in many cases and could then be fitted by a circular arc with a center below the real axis.

[1] P. Debye, *Polar Molecules* (Chemical Catalog Company, New York, 1929).
[2] K. S. Cole and R. H. Cole, J. Chem. Phys. 9, 341 (1941).

THE USE OF ONSAGER'S EQUATION

The equation of Onsager[3] for ϵ_1 was suggested as an alternative expression for polar substances: the equation is

$$\frac{(\epsilon_1-\epsilon_0)(2\epsilon_1+\epsilon_0)}{\epsilon_1(\epsilon_0+2)^2}=\frac{4\pi}{9}N\frac{\mu_0^2}{kT},$$

and can be written as

$$\frac{(\epsilon_1-\epsilon_0)(2\epsilon_1+\epsilon_0)}{\epsilon_1(\epsilon_0+2)^2}=\beta, \tag{3}$$

where β is a constant. It is assumed that the term $1/(1+i\omega\tau)$, representing the relaxation of the dipoles, enters in the same way as in the Debye equation, and, thus, the Onsager equation for ϵ at any frequency $\omega/2\pi$ can be written

$$\frac{(\epsilon-\epsilon_0)(2\epsilon+\epsilon_0)}{\epsilon(\epsilon_0+2)^2}=\frac{\beta}{1+i\omega\tau}. \tag{4}$$

The problem is to obtain the locus of the point (ϵ',ϵ'') from Eqs. (3) and (4). A solution was given by R. H. Cole[4] by using the approximation

$$3\epsilon/(2\epsilon+\epsilon_0)\approx3/2, \tag{5}$$

and it was found to be a circle with the same center and radius as the Debye circle, but the parameter describing any point on it was simply $\omega\tau$ instead of Eq. (2). Cole also introduced a further factor q, following Van Vleck,[5] to describe the fact that the environment has a discrete structure and is not merely a continuum, but this is omitted in the following argument and the simple Onsager equation is considered.

[3] L. Onsager, J. Am. Chem. Soc. 58, 1486 (1936).
[4] R. H. Cole, J. Chem. Phys. 6, 385 (1938).
[5] J. H. Van Vleck, J. Chem. Phys. 5, 556 (1937).

Reference is made later to the modifications that Kirkwood[6] has suggested to describe this discrete nature of the dielectric. As will be expected from Eq. (5), the solution of Cole[4] and that given below agree for large values of ϵ/ϵ_0.

Combining Eqs. (3) and (4),

$$\frac{\gamma\epsilon}{(\epsilon-\epsilon_0)(2\epsilon+\epsilon_0)}=1+i\omega\tau, \tag{6}$$

where γ is a constant depending on the dielectric considered.

$$\gamma=[(\epsilon_1-\epsilon_0)(2\epsilon_1+\epsilon_0)]/\epsilon_1.$$

On substituting $\epsilon=\epsilon'-i\epsilon''$, rationalizing the denominator of the left-hand side, Eq. (6) becomes

$$R+iX=1+i\omega\tau,$$

where

$$R=\frac{\gamma[(2\epsilon'-\epsilon_0)(\epsilon'^2+\epsilon''^2)-\epsilon'\epsilon_0^2]}{(2\epsilon'^2-2\epsilon''^2-\epsilon'\epsilon_0-\epsilon_0^2)^2+(4\epsilon'\epsilon''-\epsilon''\epsilon_0)^2}=1, \tag{7}$$

and

$$X=\frac{\gamma[2\epsilon''(\epsilon'^2+\epsilon''^2)+\epsilon''\epsilon_0^2]}{(2\epsilon'^2-2\epsilon''^2-\epsilon'\epsilon_0-\epsilon_0^2)^2+(4\epsilon'\epsilon''-\epsilon''\epsilon_0)^2}=\omega\tau. \tag{8}$$

Equation (7) is the locus of the point (ϵ',ϵ''). The most convenient way of representing any point of the circle (corresponding to the parameter x of Debye) is through the value of $\omega\tau$. This is most directly given by

$$\omega\tau=\frac{X}{R}=\frac{2\epsilon''(\epsilon'^2+\epsilon''^2)+\epsilon''\epsilon_0^2}{(2\epsilon'-\epsilon_0)(\epsilon'^2+\epsilon''^2)-\epsilon'\epsilon_0^2}. \tag{9}$$

It will be seen that Eq. (7) contains two terms, ϵ_0 and γ, referring to the particular dielectric, but it can be generalized slightly by the substitutions

$$u=\epsilon'/\epsilon_0,\quad v=\epsilon''/\epsilon_0,$$
$$\delta=\gamma/\epsilon_0=[(\epsilon_1/\epsilon_0)-1][2(\epsilon_1/\epsilon_0)+1]/(\epsilon_1/\epsilon_0).$$

Equation (7) now becomes

$$\delta[(2u-1)(u^2+v^2)-u]=[2u^2-2v^2-u-1]^2+(4uv-v)^2, \tag{10}$$

in which only the one term δ represents the dielectric. In a similar manner Eq. (9) becomes

$$\omega\tau=\frac{2v(u^2+v^2)+v}{(2u-1)(u^2+v^2)-u}. \tag{11}$$

A solution of (10) is required giving real values of v for $1<u<\epsilon_1/\epsilon_0$, and it is obtained numerically.

For the purposes of calculation it is convenient to use the fact that Eq. (10) is a quadratic in v^2 and it can be written, after rearrangement, as

$$av^4+bv^2+c=0, \tag{12}$$

where

$$\begin{cases}a=4,\\ b=8u^2-u(4+2\delta)+(5+\delta),\\ c=4u^4-u^3(4+2\delta)+u^2(\delta-3)+u(\delta+2)+1.\end{cases}$$

The solution is given by

$$v^2=[-b\pm(b^2-4ac)^{\frac{1}{2}}]/2a. \tag{13}$$

It is found that

$$b^2-4ac=Fu^2-Gu+H,$$

where

$$\begin{cases}F=4(\delta^2+4\delta+36),\\ G=4(\delta^2+11\delta+18),\\ H=(\delta^2+10\delta+9).\end{cases}$$

At this stage a check can be applied to insure that the equation for the locus has been derived correctly. The curve of (u,v) must go through the points $(\epsilon_1/\epsilon_0,0)$ and $(1,0)$. Substituting

$$u=\epsilon_1/\epsilon_0=p \text{ (say)}$$

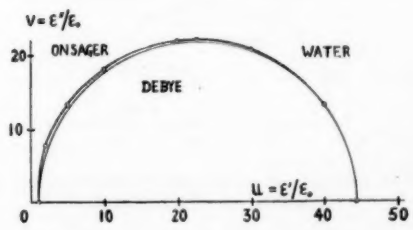

FIG. 1. The theoretical variation of the complex dielectric constant of water.

[6] J. G. Kirkwood, J. Chem. Phys. 7, 911 (1939).

in Eq. (13) it is found that $v^2=0$ (as required) and $\frac{1}{4}[(1/p)-6-4p^2]$. The second branch of the curve is here imaginary. Also, substituting $u=1$ in Eq. (13) it is found that $v^2=0$ (as required) and $\frac{1}{4}(\delta-9)$. The other branch of the curve can be real at this point, but in computation it is easy to see which branch is the physically possible one. A further check is given by considering what happens to the curve when $\delta=0$. First, the equation for v^2 becomes

$$v^2+(u-1)^2=0,$$

which is satisfied by the point (1,0). This is to be expected as the dielectric so considered is non-polar and loss-free. The other solution for v^2 is

$$v^2+(u+\tfrac{1}{2})^2=0,$$

satisfied by the point $(-\frac{1}{2},0)$ which is physically meaningless. In the following calculations only the physically significant solution is given, any imaginary branches of the curves being neglected.

COMPUTATION OF CURVE

Equation (13) has been used to plot the curve for water, ethyl alcohol, and tertiary butyl alcohol. These three dielectrics were chosen to see how the curve behaved for polar substances of large, medium, and small dielectric constant, and the data about them are reliable. In every case it was found that the positive sign in Eq. (13) gave the physical solution.

For water, the value of ϵ_1 was taken to be 78.5 at 25°C (Lattey, Gatty, and Davies[7]). $n_D=1.33$, $\epsilon_0=1.77$. Various values of u were taken between 1 and $\epsilon_1/\epsilon_0=44.3$ and the corresponding values of v were found. The points (u,v) are plotted in Fig. 1 and are seen to lie close to the Debye circle whose center is $(u=22.65, v=0)$ radius 21.65 and which is also drawn. As a whole the Onsager curve lies above the Debye circle but is closest to it for large u. This is to be expected as Cole[4] showed that the Onsager curve reduced to the circle if, essentially, ϵ_0 could be neglected in comparison with ϵ and this is true for the right-hand side of the curve for water.

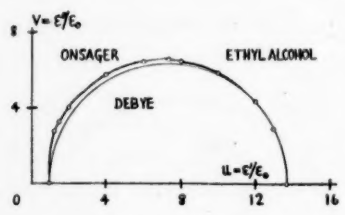

FIG. 2. The theoretical variation of the complex dielectric constant of ethyl alcohol.

[7] R. T. Lattey, O. Gatty, and W. G. Davies, Phil. Mag. **12**, 1019 (1931).

For ethyl alcohol, the value of ϵ_1 was taken to be 25.3 at 18°C (Akerlof[8]). $n_D=1.36$, $\epsilon_0=1.85$. Results are shown in Fig. 2.

Again for large u, the Onsager curve lies closely beside the Debye circle though the departure from it is more marked than for water. A similar comment applies to tertiary butyl alcohol for which ϵ_1 is 9.37 at 30°C.[8] $n_D=1.39$, $\epsilon_0=1.93$. The results are plotted in Fig. 3. In all three cases the Onsager curve lies above the Debye circle while Cole and Cole[2] showed that the experimental points lie below if not on it for the substances they considered. Considering only the curves as a whole, the Debye theory seems to be the more correct, especially for substances with small dielectric constants.

NUMERICAL COMPARISON WITH DEBYE'S EQUATION

A stricter comparison of the two theories is given if the parameters are considered for any point in the dispersion region. The point chosen is that midway between ϵ_0 and ϵ_1, namely, that for which $u=(1+\epsilon_1/\epsilon_0)/2$ and the value of $\omega\tau$ is calculated according to both theories. According to Debye, the midpoint of the semicircular arc is given when

$$x=1.$$

Hence from Eq. (2)

$$\omega\tau=(\epsilon_0+2)/(\epsilon_1+2).$$

To find the value of $\omega\tau$ according to Onsager's

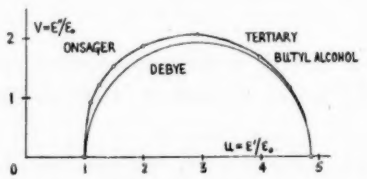

FIG. 3. The theoretical variation of the complex dielectric constant of tertiary butyl alcohol.

[8] G. Akerlof, J. Am. Chem. Soc. **54**, 4125 (1932).

TABLE I.

	$\omega\tau$ from Onsager	Debye
Water	0.99	0.047
Ethyl alcohol	0.97	0.14
Tertiary butyl alcohol	0.92	0.35

equation, the value of v has to be found from Eq. (13) in the usual manner and then both u and v are substituted in Eq. (11). Table I gives the values of $\omega\tau$ so calculated. It will be seen how good is Cole's approximation, since, as his parameter is $\omega\tau$, this implies that at the midpoint, $\omega\tau$ is unity. Table I shows the divergence between the two theories, but it is difficult to interpret numerical deductions from it. If Debye's equation for τ is used, namely,

$$\tau = 3\eta v/kT,$$

then the volume of the molecule is

$$v = (kT/3\eta)\tau,$$

η is the coefficient of "inner" viscosity generally taken to be the macroscopic viscosity. The values of τ are given by $\omega\tau$ for the midpoint of the dispersion region at the air wave-length λ_a.

$$v = (\lambda_a kT/6\pi c\eta)\cdot\omega\tau, \qquad (14)$$

where c is the velocity of light. It is customary to compare values of v found from dielectric measurements with those from van der Waals' equation. Table II gives the values of v calculated from the van der Waals b coefficient and from Debye and Onsager's theories, using Table I and Eq. (14). It has been assumed that b is $4\times$(volume of molecules in 1 cc). The unit of v is 10^{-24} cc. No value of λ_a for tertiary butyl alcohol was found in the literature. The observations of Bäz[9] and Slevogt[10] cover the major part of the dispersion region of ethyl alcohol.

Any deduction based on Debye's equation for τ cannot be very valuable. The two weaknesses

[9] See reference b to Table II.
[10] See reference c to Table II.

TABLE II.

	λ_a(cm)	Authority	v from Onsager	Debye	van der Waals
Water	1.5	Abadie[a]	12	0.6	14
Ethyl alcohol	28.9	Bäz,[b] Slevogt[c]	160	23	35

[a] P. Abadie, J. Faraday Soc. (1947).
[b] G. Bäz, Physik. Zeits. 40, 394 (1939).
[c] K. E. Slevogt, Ann der Physik 36, 141 (1939).

inherent in the equation are that the molecule is assumed to be spherical and that the viscosity coefficient entering into the damping of the rotation of the molecule is simply the macroscopic viscosity coefficient.

There is no need to assume Onsager's internal field to show that the locus of (ϵ',ϵ'') is a circle with parameter $\omega\tau$ because, as Fröhlich[11] has suggested, for some substances the internal field acting on each dipole may be just the electric field due to the potential distribution, no contribution being given by the volume polarization of the medium in such a case. Fröhlich showed that the Debye circle was given as before with the one difference that the parameter was

$$x = \omega\tau.$$

Again, $x=1$ at the midpoint of the semicircle. The extension made by Kirkwood[6] to Onsager's equation was to multiply β in Eq. (3) by a factor which was calculated from the "structure" of the liquid. As β does not appear explicitly in the equation for (u,v) neither will any multiplying factor, and the resulting analysis is unaffected. (The factor q introduced by Cole affects only the value of τ deduced from the circle.) It is perhaps best to leave τ as a time and not attempt to deduce anything from it. Too wide an application should not be expected for any one theory, and the internal field on an individual dipole in all probability varies according to the substance considered.

[11] H. Fröhlich, J. Inst. Elec. Eng. 91, 456 (1944).

On the Structure of a Catalyst Surface

ROBERT SIPS*
Frick Chemical Laboratory, Princeton University, Princeton, New Jersey
(Received January 20, 1948)

A method is described which makes it possible to calculate rigorously the distribution of the adsorption energies of the sites of a catalyst surface when the adsorption isotherms are known, if the adsorption is localized and there are no interactions. This method is applied to a Freundlich isotherm, and also to a new theoretical isotherm which reduces to the Freundlich type for small pressures, but exhibits saturation for large pressures. It is shown that this isotherm corresponds to a distribution function which differs very little from a Gaussian one. The case of atomic adsorption of gases is also considered.

I. INTRODUCTION

RECENT investigations by Taylor and his collaborators[1] have shown convincingly the heterogeneous nature of a catalyst surface. As a result, we should now consider the active surface of a catalyst as constituted by a collection of active centers, each of which is characterized by a separate energy of adsorption, and, therefore, the question arises of how to determine the statistical distribution of these centers. More precisely, we would now like to know the proportion of these centers associated with a definite value of the energy of adsorption.

This problem is not new and has already, in particular, been considered by J. Zeldowitsh[2] and by S. Z. Roginsky,[3] who gave approximate methods for solving it. Their solutions, however, are not valid in all cases and fail completely, for instance, in the important case where all the sites have the same adsorption energy.

In what follows, we describe a rigorous mathematical method which makes it possible to deduce the distribution function of the adsorption energy when the adsorption isotherm is known.

II. GENERAL METHOD

Let us suppose that the gas is adsorbed by the catalyst in the molecular state, that is, without dissociation. If then $N(q)dq$ is the number of active centers whose energy of adsorption per mole lies between q and $q+dq$, we shall assume that for the totality of these we can apply the Langmuir adsorption equation, so that the proportion of sites of adsorption energy q covered with molecules is given by

$$\theta(q)dq=\frac{N(q)dq}{1+(a/p)\exp(-q/RT)}, \qquad (1)$$

where p is the pressure and a is a constant which we shall assume to have the same value for all sites.

The total extent of covered surface will then be obtained if we integrate (1) over the whole range of possible values of q, that is, between $-\infty$ and $+\infty$, so that

$$\theta=\int_{-\infty}^{+\infty}\frac{N(q)dq}{1+(a/p)\exp(-q/RT)}. \qquad (2)$$

θ is now a function of p and T, and if we keep T constant, θ will be a function of the pressure only.

Suppose now that, as a result of an experimental investigation, we have obtained, with sufficient accuracy, one such adsorption isotherm. The question is: is the knowledge of $\theta(p)$ sufficient to determine the actual form of $N(q)$? We shall now prove that this is the case.

Considered from the purely mathematical point of view, the problem we have to solve is: does the integral equation

$$\theta(p)=\int_{-\infty}^{+\infty}\frac{N(q)dq}{1+(a/p)\exp(-q/RT)}$$

enable us to find the value of the function $N(q)$?

* Visiting Research Associate from Union Chimique Belge, Brussels, Belgium.

[1] H. S. Taylor and Shou Chu Liang, J. Am. Chem. Soc. 69, 1306 (1947).

[2] J. Zeldowitsh, Acta Physicochimica USSR 1, 961 (1934).

[3] S. Z. Roginsky, Comptes Rendus URSS 45, 61 (1944); *ibid.* 45, 194 (1944).

Let us replace a/p by y and $\exp(q/RT)$ by x. This gives the following form to the equation,

$$\theta(a/y) = RT \int_0^\infty \frac{N(RT \log x)dx}{x+y}. \quad (3)$$

The expression on the right-hand side of the equation is known as the Stieltjes transform of the function $RTN(RT \log x)$, and it is a well-known result of the theory of these transforms, that, if we have

$$f(y) = \int_0^\infty \frac{\varphi(x)}{x+y}dx, \quad (4)$$

then, provided the definite integral (4) exists,[4]

$$1/2[\varphi(x+)+\varphi(x-)] = \lim_{\eta \to 0+} \frac{f(-x-i\eta)-f(-x+i\eta)}{2\pi i}. \quad (5)$$

This form of the solution makes it necessary, of course, for us to know the form of the function $f(x)$ not only approximately, as given by experimentation, but with complete mathematical accuracy as we have to utilize its values for imaginary values of the variable. Actually, of course, this is no obstacle, because the experimental values may always be represented as exactly as we like by using analytical expressions.

Equation (5) may be expressed more simply by writing it in the following form,

$$\varphi(x) = \frac{f(xe^{-\pi i})-f(xe^{\pi i})}{2\pi i}. \quad (6)$$

III. APPLICATIONS

We shall now apply the preceding results to actual cases. It is well known that in many cases the experimental results may be expressed with a remarkable accuracy by using the Freundlich isotherm,

$$\theta(p) = Ap^c, \quad (7)$$

where A and c are constant at a definite temperature. We shall proceed to determine the corresponding distribution of active centers. In this case,

$$f(y) = A(a/y)^c = (Aa^c/RT)y^{-c}, \quad (8)$$

so that

$$\varphi(x) = \frac{Aa^c}{RT} \cdot \frac{x^{-c}e^{ixc}-x^{-c}e^{-ixc}}{2\pi i} = \frac{Aa^c}{RT} \cdot \frac{\sin \pi c}{\pi} x^{-c}$$

and

$$N(q) = \frac{Aa^c}{RT} \cdot \frac{\sin \pi c}{\pi} \cdot \exp(-cq/RT). \quad (9)$$

This shows that the Freundlich isotherm corresponds to an exponential distribution of the active centers, and it may easily be verified that

$$Ap^c = Aa^c \frac{\sin \pi c}{\pi RT} \int_{-\infty}^{+\infty} \frac{\exp(-cq/RT)}{1+(a/p)\exp(-q/RT)} \cdot dq.$$

The distribution (9) had, as a matter of fact, been previously proposed by Halsey and Taylor[5] to explain the results obtained by Frankenburg[6] on the adsorption of hydrogen by tungsten powder.

The procedure followed by Halsey and Taylor is just the opposite of that used in this paper. They chose *a priori* possible forms for $N(q)$ and introduced them in the integral until they found one which gave the right form for the isotherm. The preceding proof shows, in addition, however, that the distribution used by Halsey and Taylor is the only type of distribution capable of explaining the experimental results of Frankenburg.

Nevertheless, this exponential distribution cannot be the right one because if we try to evaluate the total number of active centers, which is given by

$$\int_{-\infty}^{+\infty} N(q)dq,$$

we find, if we use the value (9) for $N(q)$, that the integral is infinite. This, of course, is what we should expect if we admit the validity of the Freundlich isotherm, according to which the quantity of gas adsorbed increases indefinitely

[4] D. V. Widder, *The Laplace Transform* (Princeton University Press, Princeton, New Jersey, 1946), pp. 340, 341.

[5] G. Halsey and H. S. Taylor, J. Chem. Phys. 15, 640 (1947).

[6] W. G. Frankenburg, J. Am. Chem. Soc. 66, 1827 (1944); *ibid.* 66, 1838 (1944).

with the pressure. This is possible only if the number of available sites is itself infinite.

In fact, it is well known that, if the pressure is high enough, the catalyst surface becomes saturated, which means that for high values of p, θ tends asymptotically towards unity. The simplest way to express this is to assume that the actual form of the Freundlich isotherm is given by

$$\theta = Ap^c/(1+Ap^c). \tag{10}$$

If p is small, Ap^c is negligible compared with unity, and we obtain once again the form (7), while when p is very large, θ is practically equal to 1. We do not know whether or not this form of isotherm actually represents accurately any experimental results, but we think it worth while to find the kind of distribution of active centers to which it leads.

Using the same method as before, we must now find a solution for the following integral equation,

$$\frac{Ap^c}{1+Ap^c} = \int_{-\infty}^{+\infty} \frac{N(q)dq}{1+(a/p)\exp(-q/RT)}, \tag{11}$$

which, after changing the variables, becomes

$$\frac{(Aa)^c y^{-c}}{1+(Aa)^c y^{-c}} = RT \int_0^{+\infty} \frac{N(RT\log x)dx}{x+y}. \tag{12}$$

From this, using (6), we easily find

$$N(q) = \frac{1}{\pi RT} \cdot \frac{A_1 \exp(-cq/RT)\sin\pi c}{1+2A_1\exp(-cq/RT)\cos\pi c + A_1^2\exp(-2cq/RT)},$$

where $A_1 = Aa^c$. We shall now examine the properties of the distribution so obtained. First of all it is observed that for $q\to\infty$ and for $q\to-\infty$, $N(q)\to 0$, and that, furthermore, $N(q)$ is always positive. Consequently $N(q)$ takes a maximum value for a definite value of q, and by solving the equation

$$N'(q) = 0$$

we find that this maximum corresponds to

$$q = q_{\max} = (RT/c)\log A_1 = (RT/c)\log(Aa^c). \tag{13}$$

Using this, $N(q)$ may be given the following somewhat simpler form:

$$N(q) = (1/\pi RT) \cdot \frac{[\exp(c/RT)(q_m - q)]\sin\pi c}{1+2\cos\pi c\cdot\exp[(c/RT)(q_m-q)]+\exp[(2c/RT)(q_m-q)]}. \tag{14}$$

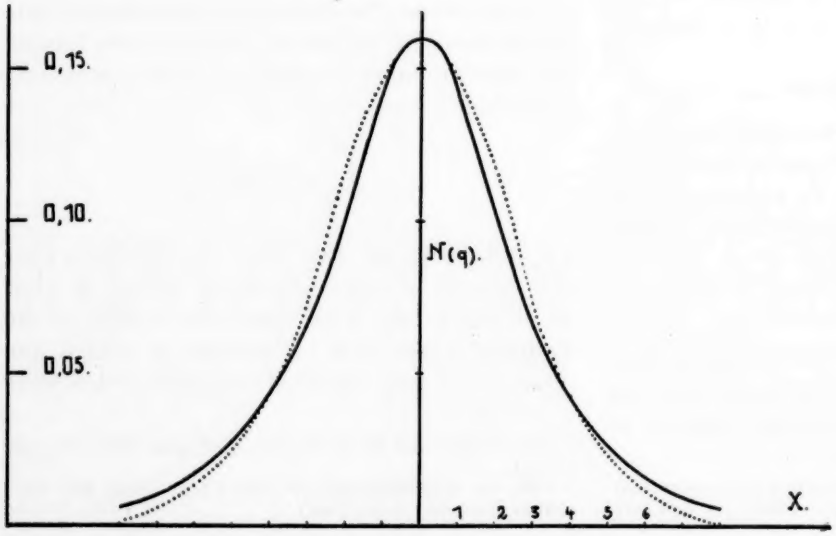

FIG. 1. ——— Distribution curve for $c=\frac{1}{2}$. ..... Equivalent Gaussian distribution.

We now see that if q is very large and positive

$$N(q)\sim(1/RT)\cdot\exp[(c/RT)(q_{max}-q)]$$
$$=(Aa^c/\pi RT)\cdot\sin\pi c\cdot\exp(-cq/RT),$$

which is exactly the form (9) obtained before, whereas if q is very large and negative,

$$N(q)\sim(1/RT)\exp[(c/RT)(q-q_{max})],$$

so that the two asymptotic curves are symmetric relative to the maximum ordinate $q=q_{max}$. The curve itself is symmetrical, of course, and the maximum value of $N(q)$ is given by

$$N(q_m)=\frac{1}{\pi RT}\cdot\frac{\sin\pi c}{2+2\cos\pi c}=\frac{1}{2\pi RT}\cdot tg\frac{\pi c}{2}. \quad (15)$$

We may use the distribution curve to calculate the total number of active centers. This will be given by

$$\int_{-\infty}^{+\infty}N(q)dq=\frac{1}{\pi RT}\int_{-\infty}^{+\infty}\frac{\exp[c/RT(q_{max}-q)]\cdot\sin\pi c}{1+2\cos\pi c\cdot\exp[c(q_{max}-q)/RT]+\exp[2c(q_{max}-q)/RT]}dq,$$

and the calculation shows that this is equal to 1. This, of course, is as it should be because, if in Eq. (11) we let p increase to infinity, we find that

$$\int_{-\infty}^{+\infty}N(q)dq=1.$$

The distribution (14) is astonishingly similar to a Gaussian distribution. In Fig. 1, we have represented the two curves

$$y_1(x)=\frac{1}{\pi}\cdot\frac{\exp(-x/2)}{1+e^{-x}}$$

corresponding to $c=\frac{1}{2}$, and where we have put $x=(q_m-q)/RT$, and the Gaussian distribution curve

$$y_2(x)=\frac{1}{2\pi}\cdot\exp(-x^2/4\pi),$$

where the constants have been chosen so that $y_1(0)=y_2(0)$, and

$$\int_{-\infty}^{+\infty}y_1(x)dx=\int_{-\infty}^{+\infty}y_2(x)dx=1.$$

As can be seen, the difference between the two curves is very small, and it is not improbable that in actual cases the curve is truly Gaussian.

Some of the calculated values for comparison follow:

x	$y_1(x)$	$y_2(x)$
0	0.160	0.160
1	0.141	0.147
2	0.103	0.116
4	0.042	0.043
8	0.006	0.001

It would be interesting to calculate the adsorption curve corresponding to a Gaussian distribution, but unfortunately this leads to intractable definite integrals.

It is, nevertheless, highly probable that the result would be a form of $\theta(p)$ which would not be very different from the one we have used.

It must be emphasized that in all the preceding calculations the values of c must lie between -1 and $+1$, for otherwise the integrals are not finite. Of course, in all physical cases, $c>0$. It is now interesting to see how the shape of the distribution curve varies when c takes different values, varying from 0 to 1.

The equations of the asymptotic curves show that when c increases, the distribution curve decreases more and more rapidly on each side of the maximum ordinate, so that the values of $N(q)$ not in the neighborhood of q_{max} become more and more negligible. For the limit, $c=1$, $N(q)$ is zero for $q\neq q_{max}$, and infinite for $q=q_{max}$, while the relation,

$$\int_{-\infty}^{+\infty}N(q)dq=1$$

still holds. This means that all the active centers have now the same adsorption energy and this gives us, as it should, the well-known Langmuir adsorption isotherm

$$\theta=\frac{1}{1+(a/p)\exp(-q/RT)}.$$

On the contrary, if c is very small, the distribu-

tion curve is very flat, and the limiting case is a uniform distribution of active centers

$$N(q) = \text{const.}$$

The relation (15) shows that this constant has the approximate value c/RT and tends to zero at the same time as c, which, of course, is necessary if the integral

$$\int_{-\infty}^{+\infty} N(q)dq$$

is to remain equal to 1.

Another form of isotherm which has been proposed and used, in particular by Temkin and Pyshev,[7] to explain the kinetics of catalytic decomposition of ammonia on iron catalysts, and which was later deduced theoretically by Brunauer, Love, and Keenan,[8] is the following

$$\theta = A \log cp, \tag{16}$$

where A and c are constants at a definite temperature. Using this form of θ we find for $f(y)$ the value,

$$f(y) = A \log(ac/y) = A \log ac - A \log y, \tag{17}$$

whence

$$\varphi(x) = [-A(\log x - \pi i) + A(\log x + \pi i)]/2\pi i = 1$$

and

$$N(q) = 1/RT. \tag{18}$$

We find here again the case of uniform distribution, but this result cannot be used as it is, because the integral

$$\int_0^{\infty} dx/(x+y)$$

is infinite. Nevertheless, if we take, as did Halsey and Taylor, $N = \text{const} = \alpha$, between $q = 0$ and $q = q_0$, and $N(q) = 0$ everywhere else, we find,

$$f(y) = \alpha \int_0^{q_0} dx/(x+y) = \alpha \log(y+q_0)/y,$$

and if q_0 is large as compared with y, we shall have approximately

$$f(y) = \alpha \log q_0 - \alpha \log y,$$

which is the same as (18) if we take $\alpha = A$, $q_0 = ac$. This shows that in a doubly promoted iron ammonia catalyst, the active centers must be more or less distributed according to the formula $N(q) = \text{constant}$.

IV. ATOMIC ADSORPTION

We have, so far, considered exclusively the case of molecular adsorption. If the molecule is adsorbed in the atomic state, for instance if a molecule X_2 is adsorbed as two separate atoms X, Eq. (1) must be replaced by

$$\theta(q)dq = \frac{N(q)dq}{1 + (b/\sqrt{p}) \exp(-q/2RT)}, \tag{19}$$

where q is the energy difference between two atoms X in the adsorbed state and a free molecule X_2 in the gas phase, θ is the proportion of the surface covered with atoms, and b is a constant. Equation (2) then becomes

$$\theta(p) = \int_{-\infty}^{+\infty} \frac{N(q)dq}{1 + (b/\sqrt{p}) \exp(-q/2RT)}. \tag{20}$$

If we now replace $(b/\sqrt{p})$ by y, and $\exp q/2RT$ by x, we find

$$\theta(b^2/y^2) = 2RT \int_0^{\infty} \frac{N(2RT \log x)}{x+y} dy \tag{21}$$

from which we can deduce the value of $N(q)$ in exactly the same way as before. Suppose, for instance, that we have a Freundlich isotherm

$$\theta(p) = Ap^c, \tag{22}$$

we find

$$f(y) = (A/2RT)(b^2/y^2)^c = (Ab^{2c}/2RT) \cdot y^{-2c}, \tag{23}$$

so that

$$\varphi(x) = (Ab^{2c}/2RT) \cdot (\sin 2\pi c/\pi) \cdot x^{-2c}$$

and

$$N(q) = (Ab^{2c}/2RT) \cdot (\sin 2\pi c/\pi) \cdot \exp(-cq/RT). \tag{24}$$

[7] Temkin and Pyzhev, Acta Physicochimica USSR **12**, 327 (1940).

[8] S. Brunauer, K. S. Love, and R. G. Keenan, J. Am. Chem. Soc. **64**, 751 (1942).

In the same way, an isotherm of the type (10) will lead to the following distribution

$$N(q)=\frac{1}{2\pi RT}\cdot\frac{\exp[(c/RT)(q_{\max}-q)]\sin 2\pi c}{1+2\cos 2\pi c\cdot\exp[(c/RT)(q_{\max}-q)]+\exp[(2c/RT)(q_{\max}-q)]}, \tag{25}$$

where

$$q_{\max}=(RT/c)\log\cdot Ab^{2c}. \tag{26}$$

One important difference between molecular and atomic adsorption is that in the former case c can vary between 0 and 1, while in the second case c can only vary between 0 and $\frac{1}{2}$. The first limiting case, $c=\frac{1}{2}$, corresponds to the case where all the sites have the same adsorption energy, while $c=0$ corresponds, exactly as in molecular adsorption, to a distribution law $N(q)=$constant.

THE JOURNAL OF CHEMICAL PHYSICS VOLUME 16, NUMBER 5 MAY, 1948

Study of the Berthelot Method for Determining the Tensile Strength of a Liquid

ARTHUR F. SCOTT, DAVID P. SHOEMAKER,* K. NOLEN TANNER,** AND JAMES G. WENDEL***
Reed College, Portland, Oregon

(Received January 20, 1948)

This paper describes an attempt to test directly the supposition that the high values for the tensile strengths of liquids as found by the Berthelot method are due to the trace of air ordinarily present in the Berthelot tube. A method is described for preparing Berthelot tubes in an evacuated system, using water from which air had been carefully removed. Measurements with these air-free tubes yielded 32 atmospheres as the average maximum hydrostatic tension that water can withstand. This value for the maximum tension is shown to be in good accord with evidence adduced recently by other investigators.

IN 1940 an attempt[1] was started in this laboratory to determine the effect of a variation of concentration on the tensile strengths of solutions of calcium nitrate. These experiments were made using the new bellows method described earlier that year by Vincent.[2] Before continuing or extending these measurements, it seemed necessary first to establish, if possible, the cause of the discordant results obtained by the various other methods for measuring the tensile strength of liquids. Accordingly, a series of experiments was started for the purpose of checking certain points in the classical Berthelot method. These experiments, which have been carried on intermittently for the past six years, are the subject of the present report.

The Berthelot method can be simply described. A strong walled capillary tube is filled with the liquid to be tested and is carefully sealed off in such a way as to leave only a small bubble of vapor and perhaps air. The liquid in the sealed tube is first expanded by warming until it completely fills the tube, and then cooled until the liquid column "breaks," usually with a distinct and characteristic clicking sound. The cooling process "stretches" the column of liquid, the amount of extension being equal to the volume of the vapor bubble formed when the liquid "breaks." The calculation of the tension existing in the liquid just before the "break" occurs involves two assumptions: (a) that the volume of the vapor bubble can be derived from the temperature increase necessary to cause the liquid to expand to fill the tube, and the known coefficient of expansion of the liquid, and (b) that

* Present address: Guggenheim Fellow at Copenhagen, Denmark.
** Present address: Chemistry Department, University of Rochester, Rochester, New York.
*** Present address: Mathematics Department, California Institute of Technology, Pasadena, California.

[1] A. F. Scott and M. Pound, J. Chem. Phys. **9**, 726 (1941).
[2] R. S. Vincent, Nature **145**, 970 (1940); Proc. Phys. Phys. Soc. London **53**, 126 (1941).

the extensibility of a liquid under tension is practically the same as its compressibility, thereby permitting the tension to be calculated from the computed volume of the extension and the known compressibility coefficient of the liquid. Some experimental evidence exists to support the second of these assumptions.[3] A reason for questioning the first assumption forms the basis of the present investigation and will be indicated below.

The values of the hydrostatic tension obtained by the Berthelot method[4] are uniformly and conspicuously higher than the corresponding values found by other methods. This disparity, it seemed to us, could arise from the effect a trace of air might have on the validity of the first assumption named in the preceding paragraph. If the small amount of air, which doubtless has been present in the liquids measured by the Berthelot method, accumulated in the vapor bubble, it seemed reasonable to suppose that considerable pressure might be required to dissolve the final bubble of air completely. Any excess of pressure resulting from this cause would act to increase the calculated or apparent tension of the liquid. Support for this line of reasoning was found in the results of measurements of tension by Meyer, who avoided the doubtful assumption of the Berthelot method. This investigator produced tensions in a liquid contained in a glass vessel by cooling the system as in the Berthelot method, but he measured the tension by the rotation of a glass spiral manometer which had been calibrated by positive pressure.

To test the idea that the high values of the Berthelot method have been due to the effect of a trace of air in the tube, we undertook the present series of experiments in which considerable pains have been taken to prepare air-free water and to fill Berthelot tubes with this water in the absence of air. Our experiments were planned also to give comparable measurements of tension over a considerable range of temperature.

Since our measurements were started, Vincent and Simmonds,[5] Temperley,[6] and Temperley and Chambers[7] have published valuable studies of the Berthelot method. These investigators, like ourselves, concluded that the weak point in the Berthelot method is the calculation of the extension of the liquid from the observed temperature difference, and they have reported new and interesting experiments which lend strong support to their and our supposition. More information concerning these experiments will be given later. To anticipate, it may be stated here that our experiments differ from the recent ones just referred to in that we have attempted to establish directly the effect of a trace of air in a Berthelot tube by producing tubes from which all air has been excluded.

EXPERIMENTAL

The apparatus used in the first stage of the preparation of the Berthelot tubes consisted basically of two parts: (a) the system for removing the dissolved gases from water, and (b) the capillary assemblies to be filled with the purified, gas-free water. The system used for removing dissolved gases was an adaptation of one described by Taylor.[8] Essentially it was an all-glass, total reflux still made from a 500-ml Erlenmeyer flask, a bubble-cap column, and a condenser. Following Taylor's suggestion, the Erlenmeyer kettle was fitted with a specially constructed side arm which, when warmed, acted as a "percolator" in that it ejected small portions of the water into the upper, vapor-filled part of the flask. This system was connected to the rest of the vacuum system through a glass-mercury valve of the Stock type.[9] At the start of an experiment, triple distilled water was placed in the Erlenmeyer flask and the system evacuated by means of a Hyvac pump. On warming the "percolator" bulb, the water in the flask was caused to boil without bumping and steady refluxing took place in the bubble-cap column. Periodically the vapors accumulating

[3] J. Meyer, Abhand. d. Deutschen-Bunsen Gesell. No. 6 (1911).

[4] For reviews of this question, see References 2, 5, 6, and 7.

[5] R. S. Vincent and G. H. Simmonds, Proc. Phys. Soc. London **55**, 376 (1943).

[6] H. N. V. Temperley, Proc. Phys. Soc. London **58**, 436 (1946).

[7] H. N. V. Temperley, and L. G. Chambers, Proc. Phys. Soc. London **58**, 420 (1946).

[8] R. K. Taylor, J. Am. Chem. Soc. **50**, 2937 (1928).

[9] A. Stock, Ber. **47**, 3109 (1914).

in the upper parts of the still were allowed to expand into a 1-l expansion chamber, where the partial pressure of the permanent gases could be measured by an attached McLeod-Taylor[10] gauge. This chamber would then be sealed off from the still with the mercury valve and reevacuated to a pressure of 10^{-6} mm with the Hyvac pump and a mercury diffusion pump, preparatory to again admitting water vapor and accumulated air from the fractionating column. Removal of air by this process was not considered satisfactory until the partial pressure of the permanent gases had been diminished to between 10^{-4} and 10^{-5} mm. To accomplish this generally required the continuous operation of the bubble-cap still for a period of several weeks. For some unexplained reason, we were never able to measure a reduction in the partial pressure of the permanent gases to less than 10^{-5} mm.

When the partial pressure of the permanent gases had remained at the minimum value for several days, a glass-mercury valve was opened to connect the still system with an evacuated (10^{-6} mm) manifold system containing about six capillary assemblies, and the water was distilled readily from the still into the assemblies. As each assembly was filled it was disconnected from the evacuated system by fusing the connecting tube at *b* (Fig. 1B), which had been constricted so that it could be sealed off safely.

The construction of the assemblies referred to in the preceding paragraph, and their manipulation to produce a filled Berthelot tube, will be described in some detail since the technique is new.

The first stage in the construction of a capillary assembly is shown in Fig. 1A. All the tubing was Pyrex glass. The capillary tubes which ultimately become the Berthelot tubes had internal diameters of 0.5 mm or 1.0 mm. In length they were generally about 120 mm. Although new Pyrex glass was used in the assemblies, they were always cleaned while in the stage shown in Fig. 1A by allowing them to stand in acid dichromate cleaning solution for about 48 hours. Following this treatment, the assembly was allowed to soak in distilled water and repeatedly

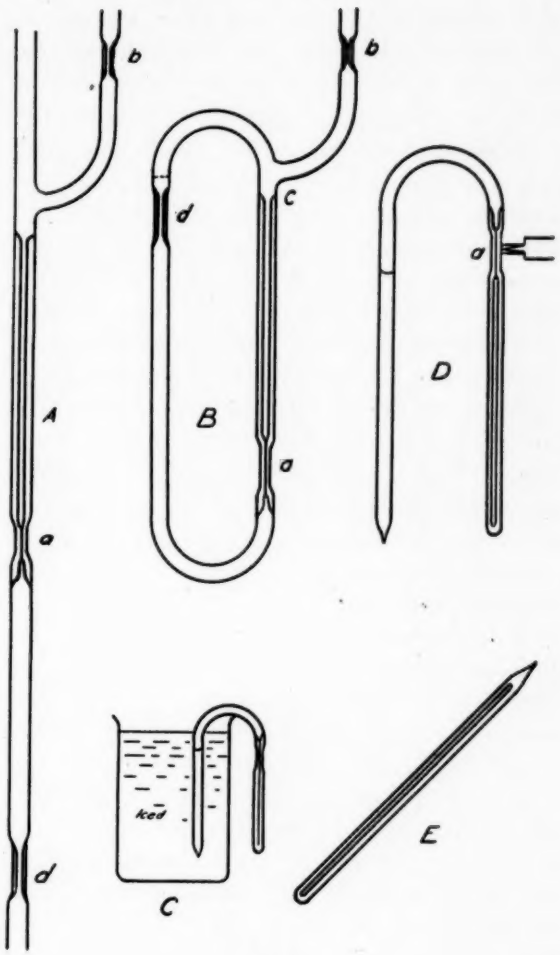

FIG. 1.

washed with distilled water until all trace of the cleaning solution was gone. After drying by draining, the glass tubes of the assembly were bent and sealed together to give the form shown in Fig. 1B. Usually six of these assembles were joined to the Pyrex glass manifold.

This manifold unit was connected on one hand to the mercury valve connecting with the percolator flask, and on the other hand to a mercury diffusion pump. This part of the system was evacuated to a pressure of about 10^{-6} mm. During the evacuation an oven was placed around the manifold unit, and the capillaries were kept at a temperature of about 250°C for at least 4 hours with the vacuum pump operating. When the evacuation of this part of the system was judged complete, the manifold unit was disconnected from the vacuum pump by sealing

[10] R. K. Taylor, J. Am. Chem. Soc. **52**, 3576 (1930).

off a constricted connecting tube, leaving the manifold unit available only through the mercury-glass valve to the bubble-cap column. While continuing to heat the capillary tube assemblies, a cold trap in the system was cooled with a dry ice and acetone bath to condense out as much mercury vapor as possible. The warmed portion of the apparatus was then allowed to return to room temperature. When the capillary tube assemblies had cooled, the valve between the manifold unit and the fractionating still was opened. After a small amount of water had been condensed in the cold trap over the mercury, an ice bath was placed around the capillary assemblies. When it appeared that the amount of water which had condensed in the assembly was about ten times that necessary to fill the capillary, the assembly was sealed off from the manifold at the constriction *b* (Fig. 1B).

Each assembly, after separation from the distillation apparatus, was subjected to the following series of operations to produce a Berthelot tube. First, with the assembly in the position shown in Fig. 1B the constriction *d* was fused and the loop opened by pulling out the glass. The capillary could then be sealed at *c* by carefully fusing the end of the capillary tube and pulling off the end of the assembly through which the tube had been filled. This left a U-shaped tube with the water sample in the bottom of the U. It may be noted here that great care was taken in making the seal at *c* to insure a stout and well shaped end to the tube. The U-tube was now inverted and suspended on the rim of a beaker, with the reservoir arm inside the beaker and the capillary tube outside (Fig. 1C). The beaker was filled with ice and water in order to condense all of the water sample in the reservoir arm. After this had been accomplished, the capillary tube was warmed with a smoky oxygen flame to remove such mercury vapor as may have been left in the capillary section. The next step was to reverse the arms of the inverted U-tube and immerse the capillary tube in the ice bath. Warming the water in the reservoir tube by means of an infra-red lamp resulted in the smooth distillation of the water into the capillary. The capillary tube was filled in this way with water to a point slightly above the constriction *a*. As soon as the capillary tube was filled, the inverted U-tube was transferred to another bath. This time both arms were immersed in the bath whose temperature was adjusted to be slightly less than the temperature desired as the "filling" temperature of the final Berthelot tube. Sufficient time was allowed for the tube and its contents to come into equilibrium with the bath. The tube was then raised so that the constriction *a* (Fig. 1D) was just clear of the surface of the bath and any water which was above the constriction was quickly distilled out by warming the tube at that point with a small flame. Following this operation the U-tube was transferred back to the ice water bath; both arms were immersed up to the point of the constriction. When the water in the capillary tube had contracted as far as it would go, the constricted tube was sealed off at *a* by means of a small pointed flame.

Two preparations of Berthelot tubes were carried out as described above, one in April, 1942, and the other in March, 1943. Of the six assemblies in the manifold unit at the start of each of these experiments, only four were carried through in the case of the older experiment and only three survived in the second preperation. The completed tubes of the 1942 preparation will be referred to hereafter as the "*A*" tubes; those of the 1943 preparation as the "*B*" tubes. The typical appearance of a completed Berthelot tube is shown in Fig. 1E. All completed tubes had good ends. A few of the "*A*" set of tubes had a droplet of mercury which was visible only by means of a magnifying glass. From the ease with which the tubes were filled in the final distillation step, it seems safe to conclude that the amount of permanent gases present was very small indeed.

Measurements of the "filling" and "breaking" temperatures of the different Berthelot tubes were made in a water bath. Of the various baths tried, the most satisfactory one was made from a 4-l beaker which was provided with a stirrer, a 500-watt heating unit, and a copper cooling coil through which cold water could be passed. It was found advantageous to add about 10 ml of Aerosol OT to eliminate the formation of bubbles on the Berthelot tube and the thermometer. In making a measurement, the Berthelot tube was fastened to a thermometer and immersed completely in the bath. For most of

the early measurements a tenth-degree thermometer was used, except at higher temperatures. For the 1947 series of measurements a 100° thermometer with tenth-degree markings was employed in all cases. Two methods were used for determining the filling temperature of a Berthelot tube. One was to raise the temperature very slowly and find the temperature at which the vapor bubble just disappeared as observed through a small magnifying glass. The other method was to make a series of cautious heating and cooling observations on the tube to find the lowest temperature at which the liquid would support tension upon being cooled. Our experience would indicate that these two methods of finding the filling temperature agree within the limits of observational error, provided the bath temperature is raised sufficiently slowly. The "breaking" temperature of a Berthelot tube was determined by allowing the bath to cool very slowly and noting the temperature at which the break occurred. With every tube except one, the rupture of the liquid column was made evident by a distinct "clicking" sound. In the case of the one tube (*A*-3), which did not produce an audible sound upon rupture, the breaking temperature was located by a long series of experiments in which the reappearance of the vapor bubble was observed visually. It is believed that the breaking temperature found in this way is almost as accurate as the determinations by the "clicking" signal.

RESULTS

Many measurements of the "filling temperature," T_f, and the "breaking temperature," T_b, of the seven Berthelot tubes have been made since their preparation. The history of tube *A*-4, which was prepared in April, 1942, is typical:

Date	Number of measurements
April 29, 1942	1
August 5, 1942	1
August 20, 1943	5
March 22, 1947	9

No two tubes have had exactly the same history. The treatment of a given tube was dependent to a large degree on the accumulated information of preceding experiments. The principal point of variation was the extent to which a tube was heated above T_f, the temperature at which the vapor bubble disappeared, before allowing the tube to cool to the "breaking temperature." In the first (April, 1942) measurements with the "*A*" set of tubes, the tubes were heated above the T_f temperature only a degree or two because preliminary tests had indicated that this procedure insured better adhesion of the liquid to the walls of the capillary. Subsequently, as it became apparent that the extent to which a tube was warmed above its T_f point had some effect on the T_b value obtained upon cooling the tube, more and more attention was paid to the heating above T_f in making measurements with a given tube.

A complete history of the treatment of each individual tube is not of sufficient importance to justify its presentation in this report. But the general conclusions reached as a result of these observations are important, and they will be summarized in the following paragraphs.

From the many measurements of T_f and T_b with the seven Berthelot tubes it appears that we can make three statements concerning the properties of these tubes as expressed in terms of T_f and T_b. First, so far as our measurements show, the T_f value of a tube remained practically constant during all the treatments to which it was subjected. Only the two high temperature tubes showed any change in T_f value, and these were not large enough to be significant. Second, the T_b value of a tube, on the other hand, varied with the treatment of the tube. This variation of T_b followed a fairly regular pattern. In the case of a tube which had been stored for some months, the first measurement of T_b (assuming that the tube had not been warmed more than a few tenths of a degree above T_f before being cooled) was always high, that is, ΔT was small. Repeated measurements of T_b of the same tube, using the same technique, yielded progressively lower values of T_b until eventually a limiting value was reached which we shall designate as T_b'. Now, if the foregoing procedure were varied by heating the tube a degree or more above T_f before instituting cooling, the same lowering of T_b would result, but the limiting value T_b' would be attained in fewer heating-cooling operations. Translated into other terms the phe-

TABLE I. Experimental data relating to Berthelot tubes containing water.

Tube	Dimensions of tube in mm l	r_0	r	Number of determinations total	1947	T_f °C	ΔT Values max. obs.	ave. 1947 series
A-1	144	3.0	0.5	16	13	31.8	10.4	9.2
A-2	130	3.0	0.25	16	13	42.1	3.9	3.2
A-3	148	3.0	0.25	12	10	40.0	3.2	3.0
A-4	107	3.0	0.25	16	9	91.8	4.9	3.6
B-1	138	3	0.5	31	14	58.1	2.7	2.0
B-2	98	3	0.5	8	5	94.5	2.4	1.1
B-3	166	3	0.5	15	8	42.9	3.4	2.2

TABLE II. Values of $f(T)$ at different temperatures.

T°C	$f(T)$ atmos./deg.
0	−7.61
10	2.04
20	4.64
30	6.96
40	8.97
50	10.71
60	12.17
70	13.48
80	14.59
90	15.43
100	16.18

nomenon just described means that when water in the Berthelot tube is subjected to positive pressure (obtained by warming the tube above T_f) it can withstand greater tension (lower T_b values), but that there is a maximum tension (limiting T_b' value) possible for each tube. The phenomenon could be accounted for by assuming either that the positive pressure leads to a better wetting of the tube—possibly at the point where the bubble had come to rest during the storage of the tube—or that the positive pressure reduced or eliminated the bubble forming nuclei in the liquid. Finally, there is a third property of the Berthelot tubes that should be mentioned. From the data on hand it appears that the T_b' value of most of the tubes underwent a definite change in the course of six or twelve months following their preparation. With some tubes T_b' increased; with others it decreased. The exact magnitude of the change is not certain because the treatment of the tubes in the early series of measurements is not comparable with the treatment in the last series. But there is little doubt that the change in T_b' in some cases was large enough to change the difference $T_f - T_b'$ that determines the magnitude of the calculated tension by a factor as large as two. It is important to note, however, that there is nothing in the experimental data to indicate that the properties of the tube changed to any appreciable degree after the first twelve months. The fact that T_b' values of the tubes did not all vary uniformly in one direction suggests strongly that the cause of this change is to be sought in changes taking place in the glass capillary tube rather than in the properties of the water. In view of the heat treatment to which the tubes were exposed during the last stages of preparation, certain characteristics of the glass—its volume, its elastic properties, and its surface properties—might be expected to change sharply during the early history of the tube. Indeed, it is rather surprising that such changes have not been noted before with Berthelot tubes.

A summary of our experimental data is presented in Table I. As mentioned before, the "*A*" set of tubes was prepared in April, 1942, and the "B" set in June, 1943. Under the heading "dimensions of tube" are given: l, the length of the finished tube; r_0 and r, the outside and inside radii of the capillary tubes, respectively. The "number of determinations" refers to the number of completed runs on the observation of T_f and T_b; under "total" is given the total number of completed observations; under "1947" is given the number of observations made in the spring of 1947. The temperatures given under "T_f" are the most probable values for the filling temperature of each tube. In the last two columns of the table are given the ΔT values, i.e., the differences $T_f - T_b$. Under "max. obs." is given the maximum ΔT value obtained for each tube after the tube had aged 12 months; under "ave. 1947 series" is given for each tube the accepted average ΔT value as found in the 1947 series of measurements.

The method of calculating the tensions produced in the Berthelot tubes can be derived from the following well-known relationship for a fluid at constant volume:

$$dP = \frac{\alpha}{\beta} dT, \tag{1}$$

where P and T denote pressure and temperature, respectively; α is the coefficient of expansion; and

β is the isothermal coefficient of compressibility. Allowance for the effect of temperature and tension on the volume of the tube containing the fluid leads to the expression:

$$dP=\left(\frac{\alpha-\sigma}{\beta-(1/\mu)}\right)dT. \qquad (2)$$

Here α and β have the same significance as above, and σ is the coefficient of expansion of the glass. The term $1/\mu$, in which μ is the modulus of rigidity, has been derived from Lame's equation[11] as a good approximation for the coefficient of extensibility of the cavity of a capillary tube when the radius of the bore of the capillary is small relative to its external radius.

If we represent the bracketed term in (2) as $f(T)$, we get, upon integrating (2) between the filling temperature T_f and the breaking temperature T_b,

$$\Delta P=\int_{T_b}^{T_f} f(T)dT. \qquad (3)$$

If it can be assumed that at the filling temperature the liquid in the Berthelot tube is under zero pressure, ΔP is the tension or negative pressure to which the liquid is subjected at T_b.

Numerical values of $f(T)$ for water have been computed for ten-degree intervals and are given in Table II. Values of α, β, σ, and μ used in computing $f(T)$ were taken from the compilation of Dorsey.[12]

Values of ΔP derived from our experimental data (Table I), as computed by graphical integration of Eq. (2) using the $f(T)$ values given in Table II, are summarized in Table III. The "average temperature" for each tube refers to the mean temperature of the range, T_f to T_b, in which the water in the tube is under tension. As before, the maximum ΔT value of column 3 refers to the maximum value obtained for a given tube after it had aged for one year.

Our measurements are not sufficiently numerous to reveal any variation of ΔP values with temperature, if, as might reasonably be supposed, such a variation exists. The present series of measurements establishes, however, quite definitely the order of magnitude of maximum hydrostatic tensions in Berthelot tubes from which practically all air has been excluded. Thus, taking the results of the 1947 series, which we regard as the most significant, we find

Average ΔP	Maximum ΔP	Minimum ΔP
32 atmos.	56.1 atmos.	17.3 atmos.

Our values are, therefore, a good hundred atmospheres less than the values heretofore reported for the maximum hydrostatic tension which water can withstand, as measured by the Berthelot method. In view of the fact that the only essential difference between our tubes and the Berthelot tubes used by other investigators is the complete absence of air from our tubes, it is hard to escape the conclusion that even a trace of air in a Berthelot tube can raise the apparent tension by something of the order of 100 atmospheres.

This is the same general conclusion arrived at by recent investigators of the same problem. Vincent and Simmonds[5] sought to avoid the possibility of pressure in the Berthelot tube caused by the presence of air in the tube by the simple and ingenious device of sealing the capillary with a frozen plug of the liquid (oil) in the tube rather than by fusing the glass of the capillary. With this method Vincent got considerably lower values for the hydrostatic tension and concluded that the higher values by the ordinary Berthelot method are to be regarded "as false on account of the high pressure which is liable to exist at the moment of disappearance of the final bubble, and which is assumed to be zero when calculating the tension." Temperley and Chambers'[7] modification of the usual Berthelot method consisted

TABLE III. Values of maximum tensions of water in Berthelot tubes.

Tube	Average temperature	Calculated values of ΔP atmos. from max. ΔT value	Calculated values of ΔP atmos. from ave. ΔT of 1947 series
A-1	26.6°	63.4	56.1
A-2	40.0°	34.0	28.7
A-3	38.4°	27.6	25.8
A-4	90.0°	75.1	54.7
B-1	57.1°	31.8	23.4
B-2	94.0°	37.8	17.3
B-3	41.8°	31.5	20.4

[11] A. E. H. Love, *A Treatise on the Mathematical Theory of Elasticity* (Cambridge University Press, Teddington, England, 1927), p. 142.

[12] N. E. Dorsey, *Properties of Ordinary Water Substance* (Reinhold Publishing Corporation, New York, 1940).

in measuring the change in volume of liquid between the filling and breaking temperature rather than calculating it from the thermal expansion of the liquid. This method yielded values for the maximum hydrostatic tension of water ranging from 16 to 68 atmospheres with a mean value of 32 atmospheres (the same as ours). Their conclusion was that "ordinary water, even if it contains dissolved air, can withstand static tensions of the order of 40 atmospheres." Temperley[6] alone continued these measurements with the Berthelot tube enclosed in an outer jacket connected to a capillary, which enabled him to measure the change in volume of the Berthelot tube when it was allowed to cool until the liquid broke. From the change in volume of the tube and from a knowledge of the dimensions of the tube, Temperley calculated the tension within the tube and found it to be of the order of 30 to 50 atmospheres. On the basis of his experiments Temperley observes "We therefore seem forced to the conclusion that the strength of water in the presence of glass is of the order of 30 to 50 atmospheres, and that the higher values reported by Dixon are due to the high pressures required to make the tubes fill in a reasonable time, which may in turn be traced to the low numerical values of diffusivities in liquids."

The results of our experiments reported in this paper, together with the supporting evidence found by Vincent and Simmonds, Temperley and Chambers, and Temperley, would appear to be decisive proof that the maximum hydrostatic tension which water can withstand in Berthelot tubes is close to 32 atmospheres. Our experiments show also that there is no marked variation of this maximum tension with the temperature of the water. The high values of hydrostatic tension found by other investigators using Berthelot tubes must be ascribed to the presence of a trace of air in the tube which could be dissolved in a reasonable time only by subjecting the air to positive pressure which would be accomplished by raising the filling temperature above that necessary to cause a bubble of water vapor alone to disappear. Finally, it may be noted also that the low value of the maximum hydrostatic tension, 32 atmospheres, is in excellent agreement with the value (34 atmospheres) obtained by Meyer whose method, which we described earlier, did not involve the assumptions of the Berthelot method.

THE JOURNAL OF CHEMICAL PHYSICS VOLUME 16, NUMBER 5 MAY, 1948

Energy of H_3^+ and H_3 by the Method of Molecular Orbitals

RALPH G. PEARSON
Department of Chemistry, Northwestern University, Evanston, Illinois
(Received January 26, 1948)

A calculation of the energies of H_3^+ and H_3 using MO's approximated as linear combinations of 1 S hydrogenic orbitals is made. The energy of H_3^+ is found to be -139 kcal. in good agreement with previous calculations and with the prediction of the crude MO method. The energy of H_3, however, is higher than the energy of three separated H atoms in disagreement with experiment and the prediction of the crude MO method. The poor form of the second MO is blamed for the discrepancy, different effective nuclear charges being needed for the two MO's, or for different nuclei.

INTRODUCTION

THE energies of the H_3^+ ion and the H_3 molecule were calculated by Hirschfelder, Eyring, and Rosen[1] using the HLSP method modified to include an effective nuclear charge and ionic terms. Their results can be used to set an upper limit for the energy of the H_3^+ ion which is not experimentally available. The H_3 molecule exists as the transition state of reactions such as

$$H+H_2 \rightarrow H_2+H \qquad (1)$$

[1] Hirschfelder, Eyring, and Rosen, J. Chem. Phys. **4**, 121, 130 (1936).

(as in the ortho-para conversion) and its energy is known with sufficient accuracy from the experimental activation energies of (1). The integrals evaluated in reference 1 make possible the ready calculation of H_3^+ and H_3 by the method of molecular orbitals[2] since no new integrals need appear if the MO's are approximated as a linear combination of atomic orbitals.

It is of interest to make these calculations for two reasons: first, the crude, approximate MO method predicts an energy for H_3^+ which is very close to the best value of reference 1 and presumably nearly correct, while the same method predicts an energy for H_3 which is obviously much too low; secondly, H_3^+ is the simplest example of a "resonating" molecule in that two equally probable valence bond structures,

(a) H−H H^+ and (b) H^+ H−H,

can be written and the correct electronic distribution corresponds to some "hybrid" of the above two structures.

CALCULATIONS

It is assumed that the three nuclei, A, B, and C, are arranged linearly and symmetrically and that the lowest MO is a function of the form

$$\psi_I = a\psi_A + b\psi_B + c\psi_C, \tag{2}$$

where ψ_A, etc., is a normalized $1s$ hydrogenic function, and that the next lowest MO is orthogonal to ψ_I. The coefficients a, b, and c, are varied to minimize the energy. B refers to the central nucleus.

As a first approximation let us solve the secular equation for a system of three such nuclei using the usual approximations of the crude MO method. We have[2]

$$\begin{vmatrix} q-w & \beta & 0 \\ \beta & q-w & \beta \\ 0 & \beta & q-w \end{vmatrix} = 0 \tag{3}$$

which gives $w_I = q+\sqrt{2}\beta$, $w_{II} = q$, $\psi_I = \sqrt{2}\psi_B + \psi_A + \psi_C$ and $\psi_{II} = \psi_A - \psi_C$ for the energies and wave functions of the two lowest MO's. The H_3^+ has two electrons in the lowest MO and a total energy of $2q+2\sqrt{2}\beta$ so that the energy of the ion (zero of energy being the separated atoms) is $2\sqrt{2}\beta$. The energy predicted for either structure (a) or (b) above is 2β so the "resonance energy" is 0.828β. If we evaluate β as one-half of the energy of the hydrogen molecule we find $\beta \simeq -50$ kcal., the energy of H_3^+ is -141 kcal., which is reasonably close to -155 kcal., the best value of reference 1, and the resonance energy is -41 kcal.

TABLE I. Energy of H_3^+ (zero of energy = separated atoms).

φ_I	Effective nuclear charge, z	Internuclear separation, R	Energy
$\psi_B+\psi_A+\psi_C$	1.3206	$1.51a_0$	−116.0 kcal.
$1.414\psi_B+\psi_A+\psi_C$	1.3340	1.50	−135.3
$1.667\psi_B+\psi_A+\psi_C$	1.3290	1.50	−138.9
$2\psi_B+\psi_A+\psi_C$	1.3175	1.52	−139.0
$2.5\psi_B+\psi_A+\psi_C$	1.1569	1.73	−52.9

For the H_3 molecule the third electron goes in the second MO and the total energy is $3q+2\sqrt{2}\beta$ and the molecular energy remains $2\sqrt{2}\beta$, a ridiculous result, as van Vleck and Sherman point out, since it indicates strong attraction between an H atom and an H_2 molecule. Experimentally there is a repulsion of the order of 5 to 10 kcal.[3] so that the energy should be about -100 kcal.

Going on to the more exact calculation of the energies, the wave function of H_3^+ is written as

$$\psi = \psi_{I(1)}\psi_{I(2)}, \tag{4}$$

where ψ_I is of the form of (2) with $a=c=1$ and the energy calculated by the variational method to determine the best value of b. All of the necessary integrals were recalculated in the closed form except the two electronic repulsions of the form $L(ab,bc)$ and $L(ab,ac)$, using the notation of Hirschfelder, Eyring, and Rosen. These integrals are given by them in graphical form for various values of $\rho = ZR$ where Z is the effective nuclear charge and R is the internuclear distance in units of a_0. Since the labor needed to minimize the energy with respect to ρ is considerable and values of the above two integrals cannot be read with any great accuracy except for integral values of ρ, it was decided to use a constant value of $\rho = 2$ throughout. This is the value of ρ which gives the best values of the energy for both H_3^+ and H_3 in the HLSP method.

[2] See J. H. Van Vleck and A. Sherman, Rev. Mod. Phys. 7, 167 (1935), for a discussion of the HLSP and MO methods.

[3] L. Farkas and A. Farkas, Proc. Roy. Soc. **152A**, 124 (1935).

With ρ given a definite value the energy is readily found as a function of Z only for any particular value of b. Minimizing with respect to Z gives the final value of the energy. Table I presents the results obtained.

For the H_3 molecule the wave function is written as

$$\psi=\psi_{I(1)}\psi_{I(2)}\psi_{II(3)} \tag{5}$$

where $\psi_I=2\psi_B+\psi_A+\psi_C$ and $\psi_{II}=\psi_A-\psi_C$. That is, ψ_I is the best function for the lowest MO and ψ_{II} is orthogonal to it. The wave function is more correctly written as a completely antisymmetric function,[4] for example, as a Slater determinant, but the actual calculation of the energy reduces to the form of (5) in any case.

Taking the same value of ρ as before, the energy of all three electrons is again found as a function of Z. The value of Z which minimizes the energy is $Z=1.0476$, and the total energy is $1.4534e^2/a_0$, which makes the H_3 molecule unstable with respect to the separated atoms by 29.2 kcal., a result far different from experiment (stable by 100 kcal.) and from the value (−141 kcal.) predicted by (3). Variation of either ρ or b will not help matters because the gain in energy of the lowest MO is greater than the decrease in energy of the higher. It appears that the only way of lowering the energy, if wave functions of the form ψ_I and ψ_{II} are used, would be to have one value of Z for ψ_I and another value for ψ_{II}, or else different effective nuclear charges for nucleus B and nuclei A and C. This would involve the calculation of several new integrals, however.

DISCUSSION

For the H_3^+ ion there is good agreement between the HLSP calculation, the crude MO, and the more precise MO calculation. If one compares the MO calculation with the HLSP calculation with no ionic terms, one finds the MO method somewhat superior, since the best value of reference 1 for the Wang approximation only is −130.9 kcal. The "resonance energy" of approximately −60 kcal. (compared to H_2 calculated by the same method) is due in part to the spreading of the electron density over the field of three nuclei with a resulting decrease in kinetic energy and increase in effective nuclear charge.[5] Another contributing factor to the stability of the ion is the advantageous position of an electron on the central nucleus. The potential energy of a single electron on nucleus B is some 180 kcal. lower than that of an electron on A or C. This is reflected in the high coefficient of ψ_B in (2). It is interesting to note that if we represent the "localized" MO's corresponding to valence bond structures (a) and (b) as $(\psi_A+\psi_B)$ and $(\psi_B+\psi_C)$, then the MO which is a linear combination of them, $(2\psi_B+\psi_A+\psi_C)$, is a much better approximation to the true wave function.

The high energy of H_3 must be attributed to the poor form of ψ_{II} which is actually antibonding. The neglect of the exchange integrals between non-adjacent atoms is responsible in part for the poor prediction of the crude MO method. (Exchange integrals between A and C are about one-fourth of the exchange integrals between B and C.) An equally large error is the neglect of the difference in the Coulombic energies according to whether an electron is on the central nucleus or on an end nucleus. The second MO with the electron concentrated on the two end nuclei is thus much higher in potential energy than the lowest orbital.

[4] M. Goeppert-Mayer and A. L. Sklar, J. Chem. Phys. **6**, 645 (1938).

[5] J. E. Lennard-Jones and C. A. Coulson, Trans. Far. Soc. **35**, 811 (1939).

THE JOURNAL OF CHEMICAL PHYSICS VOLUME 16, NUMBER 5 MAY, 1948

Sound Absorption and Velocity in Liquefied Argon, Oxygen, Nitrogen, and Hydrogen*

J. K. GALT**
Research Laboratory of Electronics, Massachusetts Institute of Technology, Cambridge, Massachusetts

(Received Feburary 4, 1948)

The pulse method has been applied to measure the velocity and absorption of sound in liquefied argon, oxygen, nitrogen, hydrogen at 44.4 Mc/sec. The experimentally determined attenuation (α) is compared with the calculated attenuation due to viscosity (α_{vis}) and the results indicate that relaxation processes are not an important mechanism for sound absorption in any of these gases, except perhaps for hydrogen. Measurements were also made at 14.8 Mc/sec., but the attenuations were too low for satisfactory precision. Indications, however, are that the attenuation varies as the frequency squared.

I. INTRODUCTION

MEASUREMENTS on pulses of ultrasonic vibrations have been used during and since the war to determine the absorption and velocity of sound in liquids.[1,2] Absorption is determined from the attenuation of the pulse as it traverses longer and longer paths in the liquid; velocity is determined by the increase in time required for the pulse to traverse the longer distances in the liquid. The oscilloscope presentation units developed for fire-control radar during the war render such measurements quite simple.

The present research is the application of this method to measurement of ultrasonic absorption and velocity in liquefied argon, oxygen, nitrogen, and hydrogen. The primary effort has been placed on obtaining attenuations, since, to the author's knowledge, these have not been measured previously. Velocity measurements have been made with a precision of approximately 1 percent. Measurements have been made at 14.8 and 44.4 Mc/sec., but the attenuations at 14.8 Mc/sec. are so low that quanititative measurements could not be made with satisfactory precision. For this reason no values for attenuation are presented at 14.8 Mc, but indications are that the attenuation varies as frequency squared.

II. EQUIPMENT

The electronic equipment used is essentially the same as that used in previous work on liquids[2] in this laboratory, and no further description of it will be given here.

The tank containing the liquid sample traversed by the ultrasonic vibrations[3] is designed to fit into a helium cryostat of the Collins type.[4] An isometric view of the equipment in place in the the cryostat is shown in Fig. 1. A quartz crystal (A) is used as both the transmitting and receiving transducer. An optically polished fused quartz reflector (B) is used to reflect the transmitted pulse back to the quartz crystal. The reflector surface may be adjusted to be parallel to the quartz by rods (C), which run up above the top of the cryostat. The reflector is connected to a micrometer screw (D) at the top of the equipment by means of a fused quartz rod (E). Fused quartz is used in order to minimize errors caused by the thermal expansion of this rod in reading the position of the reflector. A small stirrer (F) driven by a motor (G) is used to minimize temperature gradients in the liquid sample. The electrical signal is fed in by means of a coaxial cable (H) through the matching network. This equipment has proved quite satisfactory for the present research, but a later model developed by Pellam and Squire[5] is more suitable for very low temperature work.

* This work has been supported in part by the Signal Corps, the Air Materiel Command, and O. N. R.

** Now at H. H. Wills Physical Laboratory, University of Bristol, The Royal Fort, Bristol, England.

[1] M. Cefola, M. E. Droz, S. Frankel, E. M. Jones, G. Maslach, and C. E. Teeter, Jr., M. I. T. Radiation Laboratory Report 963, March 1946.

[2] J. R. Pellam and J. K. Galt, J. Chem. Phys. **14**, 608 (1946).

[3] This equipment was designed in collaboration with J. R. Pellam.

[4] S. C. Collins, Rev. Sci. Inst. **18**, 157 (1947).

[5] J. R. Pellam and C. F. Squire, "Ultrasonic velocity and absorption in liquid helium," M. I. T. Research Laboratory of Electronics Technical Report No. 44, August 1, 1947; Phys. Rev. **72**, 1245 (1947).

III. TEMPERATURE CONTROL, MEASUREMENT

Refrigeration for the argon and some of the oxygen runs was obtained by placing the lower end of the tank (see Fig. 1) in a large Dewar flask and then pouring liquid nitrogen and liquid oxygen into the Dewar. The equilibrium temperature of such an arrangement is determined by the proportions of liquid nitrogen and oxygen used. The level of the liquid in this outer bath was always well above the sample on which measurements were made in order to minimize the temperature gradient over the ultrasonic path. For this same reason the outer bath was continuously stirred.

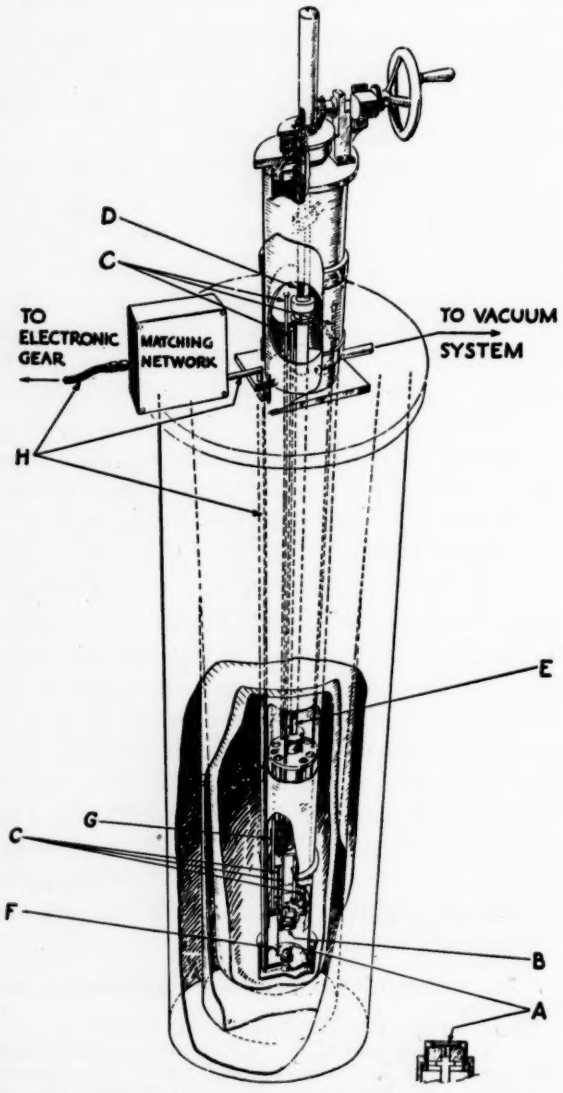

FIG. 1. Low temperature ultrasonic tank.

For the lower temperature measurements on oxygen, and for nitrogen and hydrogen the Collins cryostat was used to obtain refrigeration, as the oxygen-nitrogen mixture would not produce low enough temperatures. Holding the temperature constant is somewhat more of a problem with this equipment, but readings were taken quickly enough so that only on one oxygen run was the variation with time appreciably more than one degree.

Temperatures were measured in two ways. First, the system was closed off and the vapor pressure of the liquid was measured with a mercury manometer. Second, a constant-volume helium thermometer in the cryostat was used. The vapor pressure measurement was satisfactory except in the case of one run on oxygen. Here a small amount of nitrogen impurity raised the vapor pressure above that of oxygen alone. The helium thermometer was quite satisfactory, but it is not a direct measure of the temperature in the liquid sample, of course. No large differences between the two thermometers occurred, fortunately, except in the case of the oxygen run mentioned above. Here there is an uncertainty of about 5°K in the temperature reading.

IV. PURITY OF SAMPLES

The purity of the gases from which the liquid samples used for these measurements were obtained was stated by the supplier (Air Reduction Company) to be as follows: argon 99.8 percent with 0.2 percent nitrogen; oxygen 99.5 percent with 0.5 percent nitrogen; nitrogen 99.5 percent with 0.5 percent oxygen; hydrogen 99.5–99.7 percent with 0.3 to 0.5 percent oxygen. No water was present in any of the gases. As an additional precaution the hydrogen was put through a charcoal trap immersed in liquid nitrogen before it was used.

The impurity in the nitrogen may have caused some change in the velocity of sound, since the value measured here agrees with that of Hirschlaff[6] rather than that of Liepmann[7] (see Table I). It should be mentioned, however, that the freezing point was not appreciably different from that for pure nitrogen.

[6] E. Hirschlaff, Proc. Camb. Phil. Soc. **34**, 296 (1938).
[7] H. W. Liepmann, Helv. Phys. Acta **11**, 381 (1938); **12**, 421 (1939).

V. RESULTS

The results are shown in Table I. Attenuation α is defined by the relation $p = p_0 e^{-\alpha x}$ where x is the distance between the point where the peak pressure due to the sound wave is p_0 and the point where it is p.

The velocity measurements are accurate to within 1 percent. However, as mentioned previously, the value for nitrogen may have been influenced by the impurity of the sample. The value for hydrogen also differs somewhat from the published value,[8] but it is felt that the present value is the more accurate in this case.

On the basis of the reproducibility of the data and the degree to which they fit the assumed exponential dependence on path length, an estimate of the maximum errors in the attenuation may be made. This leads to an estimate of 10 percent or less for argon, hydrogen, and oxygen, and 15 percent or less for nitrogen. Temperature fluctuations in the liquid, which in turn cause fluctuations in the signal, are the most important limitation on accuracy in reading signal amplitude. This effect is minimized by the stirrer, but it is not eliminated.

In theory, the total attenuation which we measure is due to viscosity, heat conductivity, and relaxation phenomena in the liquids.[9] The attenuation to be expected from viscosity (α_{vis}) is presented in Table I. The densities used in these calculations are obtained from Bergmann.[10] The viscosities were obtained from a compilation by Nason.[11] No data on heat conductivity could be found for these liquids, so it has been impossible to take this factor into account. The data would seem to indicate that relaxation processes are not an important mechanism for sound absorption in any of these liquids, possibly with the exception of hydrogen. Here the α_{vis} value is not so good as in the other cases since the viscosity at the boiling point was the only value available, and the measurements were made at a lower temperature.

TABLE I. Ultrasonic absorption and velocities. (All values are measured at 44.4 Mc.)

Liquid	Temp. (°K)	Velocity in units of 10^4 cm/sec.	α_{exp} (cm^{-1})	α_{vis} (cm^{-1}) calculated at 44.4 Mc
Argon	85.2±0.2	8.53	0.20	0.16
Oxygen	87.0±0.2	9.52	0.17	0.11
	70 ±1	10.94	0.17	0.11
	60 ±5	11.19	0.17	0.17 at 60°K 0.12 at 65°K
Nitrogen	73.9±0.2	9.62	0.21	0.13
Hydrogen	17 ±1	11.87	0.11	0.01

In view of the relatively small difference between the measured α and α_{vis} in nitrogen, any impurities present can hardly have caused a large variation in the attenuation.

No appreciable variation of attenuation with temperature was observed. This is especially noticeable in the case of oxygen. Measurements made within a degree or so of the boiling point of any of these liquids indicate an increased attenuation (attenuations of 0.27 cm^{-1} have been measured in nitrogen), but this is attributed to the presence of bubbles and cavitation caused by the ultrasonic wave.

A magnetic field of the order of 1000 gauss was applied to the oxygen sample in our experiment to see whether this would produce a change in attenuation.[12] The experimental arrangement was such that a change of 1 percent in velocity or 20 percent in attenuation could have been observed, but no variations were noted.

VI. ACKNOWLEDGMENTS

The author wishes to thank Dr. J. R. Pellam for his collaboration in building the equipment, Dr. C. F. Squire for discussions and help with the technique of low temperatures, and Messrs. R. P. Cavileer and W. Krag for technical assistance.

[8] A. Pitt and W. J. Jackson, Can. J. Research **12**, 686 (1935).

[9] L. Bergmann, *Der Ultraschall* (Edwards Brothers, Inc., Ann Arbor, Michigan, 1944), p. 191 ff.

[10] Reference 9, p. 171.

[11] W. C. Nason, "Some physical properties of air and its components," compiled for Aero-Medical Laboratory, Wright Field under Contract No. W-33-038. His references for viscosities are: Rudenko and Schubnikow, Phys. Zeits. Sowjetunion **6**, 470 (1934); Rudenko, J. Exper. a. Theoret. Phys. U.S.S.R. **9**, 1078 (1939).

[12] A. Van Itterbeck and L. Thys, Physica Haag **5**, 298 (1938).

THE JOURNAL OF CHEMICAL PHYSICS VOLUME 16, NUMBER 5 MAY, 1948

A Theory of Vapor Pressures of Liquids Based on van der Waals' Equation of State

FREDERICK T. WALL
Noyes Chemical Laboratory, University of Illinois, Urbana, Illinois
(Received February 4, 1948)

An expression is derived for the vapor pressure of a liquid assuming the validity of van der Waals' equation of state. The theory involves the use of an appropriate mathematical expression for the volume of a van der Waals liquid and does not require recourse to any empirical relationships. The vapor pressure equation so obtained can be put into a reduced form, which is of a universal nature. The laws of Guldberg-Guye and of Trouton are shown to be compatible with the theory with constants of the correct order of magnitude.

THE relationships which exist between the liquid and vapor states of matter are of considerable interest and importance, and many attempts have been made to explain them theoretically and to describe them empirically. Numerous equations of state have been considered, but that of van der Waals,

$$[p+(a/V^2)](V-b)=RT \qquad (1)$$

has proved most useful in providing a link between liquid and vapor. Although van der Waals' equation is not quantitatively exact, it can nevertheless be used to predict qualitatively a great many phenomena, such as liquefication, and for that reason it is a most remarkable modification of the ideal gas law expression. It would seem reasonable, therefore, that a vapor pressure relationship ought to be directly derivable from van der Waals' equation by an appropriate thermodynamic analysis. In this paper such a derivation will be given together with some interesting corollaries which account for some of the commonly recognized empirical rules, such as Trouton's law.

A great deal of work has been done on van der Waals' equation, particularly by van der Waals[1] himself and by van Laar.[2] The vapor pressure equation to be derived here closely resembles one obtained by van Laar; in fact, the two relationships can be shown to be equivalent, to a certain degree of approximation, if one uses the appropriate expression for the volume of a liquid in van Laar's result. However, the methods of approach employed by van Laar and the present author are quite different, and the work on vapor pressures here reported is carried further.

Typical isotherms for van der Waals' equation appear in Fig. 1. If the temperature is below the critical temperature (which corresponds to the isotherm passing through the critical point, C), then the pressure as a function of volume exhibits a maximum and a minimum, a behavior not actually observed in nature. Indeed if the temperature is sufficiently low, the calculated pressures might even be negative for a certain range of volumes, as will be observed for the lowest curve in Fig. 1.

Assuming the temperature to be below the critical temperature, the left-hand side (L) of a given van der Waals' isotherm corresponds to the liquid state and the right-hand side (V) represents the vapor. The middle portion provides a hypothetical continuous path by which liquid and vapor can be converted into each other. To make van der Waals' equation correspond more closely to reality—i.e., to make the transition from liquid to vapor discontinuous instead of continuous—the following modification suggested by Maxwell is employed. Horizontal straight lines (L–V) are drawn in the V,p diagrams to connect the liquid and vapor portions of a given isotherm in such a way that the area under the horizontal line is equal to the area under the original curve. Equating areas in this way guarantees that the free energy change will be zero for the evaporation process, assuming that the original equation provides a thermodynamically valid and continuous link

[1] J. D. van der Waals, *Die Continuität des gasförmigen und flüssigen Zustandes* (Johann Ambrosius Barth, Leipzig, 1899).
[2] (a) J. J. van Laar, *Die Zustandsgleichung von Gasen und Flüssigkeiten* (Leopold Voss, Leipzig, 1924). (b) J. J. van Laar, Zeits. anorg. Chemie. 171, 42 (1928).

between the two phases. The pressure corresponding to such a horizontal line is then the vapor pressure of the liquid when it is under an applied pressure equal to its own vapor pressure.

The preceding discussion makes it clear in principle how a vapor pressure can be calculated. To get the mathematical expressions into tractable form, however, it is necessary to adopt some practical expedients or approximations as follows.

Let us assume that the temperature is so low that the vapor in equilibrium with liquid can be considered an ideal gas. This condition will be attained if the corresponding van der Waals isotherm in the V,p diagram exhibits an appreciable negative pressure region, such as for the lowest curve in Fig. 1. Under these circumstances the liquid branch of the isotherm will be practically a straight line of very great slope, indicating that the liquid is nearly incompressible. If the vapor is practically ideal, the vapor pressure will just equal the fugacity of the liquid. Hence if we can find the fugacity of a van der Waals liquid in terms of the temperature and applied pressure, we have in effect solved for the vapor pressure of the liquid. Now it can be readily shown that the fugacity, f, of a van der Waals fluid is given by[3]

$$\ln f=\frac{b}{V-b}-\frac{2a}{VRT}+\ln\left(\frac{RT}{V-b}\right), \qquad (2)$$

where V is the volume, T the absolute temperature, and a and b are van der Waals constants. To get the fugacity (and hence the vapor pressure) of a liquid as a function of temperature and applied pressure, we must find an expression for the volume of the liquid and put the same into Eq. (2). The volume of a van der Waals liquid can be obtained to any desired degree of approximation as follows. van der Waals' equation can readily be written as a cubic equation in V. Solving for the linear term of that cubic, one obtains

$$V=b+\left(\frac{bp+RT-pV}{a}\right)V^2. \qquad (3)$$

If one neglects the cubic and quadratic terms in (3), the solution of the remaining linear equation will be a crude approximation to the lowest root of the original cubic equation, and that root must correspond to the volume of the liquid. This crude approximation, which we shall call the "zeroth" approximation, is simply $V=b$. Substituting the zeroth approximation for V into the right-hand side of Eq. (3), one then obtains a first approximation for V, namely:

$$V=b+(b^2RT/a). \qquad (4)$$

Continuing this process of successive approximations, one finally obtains the following series expression, correct to the third approximation:

$$V=b+\{b^2RT/a\}+\{(2b^3R^2T^2/a^2)-(b^4RTp/a^2)\}+\{(5b^4R^3T^3/a^3)-(6b^5R^2T^2p/a^3)+(b^6RTp^2/a^3)\}+\cdots. \qquad (5)$$

The above series can be expected to converge rapidly if bRT/a and b^2p/a are each small compared to unity. It will be seen later that these conditions are fulfilled if RT is small compared to the heat of vaporization and if p is less than the critical pressure. The condition regarding temperature is the more important one in our treatment, for it also guarantees near ideality of the vapor.

It will be noted that the "zeroth" approxi-

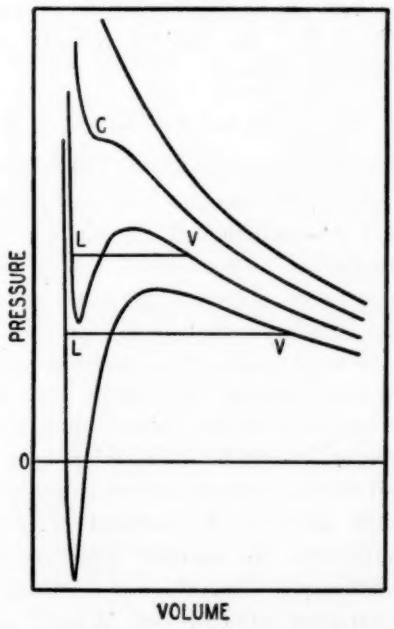

FIG. 1. Isotherms of a van der Waals fluid.

[3] Lewis and Randall, *Thermodynamics* (McGraw-Hill Book Company, Inc., New York, 1923), p. 196.

mation for V implies a liquid of constant volume independent of temperature and applied pressure. The first approximation, however, does involve the temperature although the liquid still appears to be incompressible. Only when one reaches the second and higher approximations does one find the volume dependent upon both temperature and pressure, although the dependence on pressure remains very slight. Numerical calculations show that for a wide range of pressures at a temperature equal to one-half the critical temperature, the zeroth approximation to V is in error by 18 percent, the first by less than six percent, the second by two and one-half percent, and the third by only one percent. It will be seen later that the higher approximations have little effect on the calculated vapor pressures.

The expression for the volume of a liquid can now be substituted into that for the fugacity and the result expanded in simple form. If one neglects the effect of applied pressure on the liquid, it is unnecessary to go beyond the first approximation. Retaining only those terms which are consistent with that approximation, and assuming further that the fugacity of the liquid equals its vapor pressure, p_v, one then obtains

$$\ln p_v = \ln(a/b^2) - (a/bRT). \tag{6}$$

Equation (6) is the desired vapor pressure equation for a van der Waals liquid. It is interesting to note that Eq. (6) has the usually accepted empirical form, namely:

$$\ln p = A - B/T, \tag{7}$$

where A and B are constants. This correspondence is remarkable because the functional form is a direct consequence of the theory and was not assumed as a framework upon which to attach constants obtained in some other way. Equations of state other than van der Waals', which have been proposed as modifications of the ideal gas laws, do not necessarily give a vapor pressure equation of the correct general nature. For example, Berthelot's equation can readily be carried through the above treatment, but the final result involves T^2 instead of T in the denominator of the second term as well as another difference. Thus the extraordinary qualitative character of van der Waals' equation manifests itself again in its relationship to vapor pressure, demonstrating further the essential correctness of van der Waals' assumptions.

The heat of vaporization of a liquid can now readily be calculated. Differentiating Eq. (6) with respect to T, one obtains

$$d\ln p_v/dT = a/bRT^2 = \Delta H_v/RT^2. \tag{8}$$

Hence,

$$\Delta H_v = a/b. \tag{9}$$

The value a/b for the heat of vaporization of a liquid can be obtained more directly as follows. Since $(\partial E/\partial V)_T = a/V^2$ for a van der Waals fluid, it follows that

$$\Delta E_v = \int_{V_1}^{V_2} (a/V^2)dV = a[(1/V_1) - (1/V_2)], \tag{10}$$

where V_1 and V_2 are the volumes of liquid and vapor, respectively. Assuming V_2 to be infinite and V_1 to be given by Eq. (4), it is seen that

$$\Delta E_v = \frac{a}{b[1+(bRT/a)]} \approx \frac{a}{b} - RT, \tag{11}$$

assuming bRT/a is small compared to unity. Therefore,

$$\Delta H_v = \Delta E_v + RT = a/b \tag{12}$$

to a sufficiently good degree of approximation.

REDUCED VAPOR PRESSURE EQUATION

It is well known that by making an appropriate change in variables, van der Waals' equation can be rewritten in a so-called reduced form which is the same for all substances. A similar process can be carried out on the vapor pressure relationship derived above. According to van der Waals' equation, the critical pressure (p_c) and critical temperature (T_c) are given by

$$p_c = a/27b^2$$

and

$$T_c = 8a/27Rb. \tag{13}$$

Substituting into Eq. (6) we find that

$$\ln p_v/p_c = \ln 27 - (27T_c/8T). \tag{14}$$

If we define a reduced vapor pressure $\pi_v = p_v/p_c$ and a reduced temperature $\theta = T/T_c$, it follows that

$$\ln \pi_v = \ln 27 - (27/8\theta). \tag{15}$$

Equation (15) should be a universal vapor pressure equation applicable to all substances providing θ is small. However, like so many other results predicted from van der Waals' equation, it is not quantitatively correct although it has the right functional form. It is known empirically that the logarithm of the reduced pressure of a so-called normal liquid is a universal linear function of the reciprocal of the reduced temperature, although the constants in the equation are not the same as predicted above. In 1881, van der Waals proposed a one-parameter empirical relationship resembling (14) and (15).

NORMAL BOILING POINTS OF LIQUIDS: TROUTON'S RULE[4]

The normal boiling point (T_0) of a liquid can be calculated from Eq. (14) by setting p_v equal to 1 atmos. Then, if p_c is expressed in atmospheres, it follows that

$$T_0/T_c = 27/8 \ln 27 p_c. \tag{16}$$

Examination of a table of critical constants indicates that almost all organic substances have critical pressures in the range 20 to 80 atmospheres. Furthermore, over three-fourths of them have critical pressures in the range 30–55 atmospheres with a clustering about 40 atmospheres, which can be considered a geometric mean value.[5] Many inorganic materials also have critical pressures in the ranges indicated, except such "abnormal" liquids as water, ammonia, hydrogen, and helium.

Since the critical pressure appears only as the argument of a logarithm in Eq. (16), it follows that T_0/T_c is not a very sensitive function of p_c. To illustrate this point quantitatively, suppose the critical pressures in atmospheres do range from 20 to 80 with a geometric mean of 40. Then we can write that

$$\ln p_c = \ln 40 \pm \ln 2 = 3.69 \pm .69.$$

Hence, from Eq. (16),

$$T_0/T_c = 27/[8(6.98 \pm .69)] = 0.48 \pm 10\%.$$

Thus it is seen that the reduced normal boiling points of organic liquids should be roughly constant and equal to about $\frac{1}{2}$ plus or minus ten percent. If we make the corresponding calculation for the critical pressure range 30–55 atmospheres, which was mentioned above, then the fluctuation in T_0/T_c is only about four instead of ten percent. Actually, there is an empirical law, attributed to Guldberg and Guye, which asserts that the reduced normal boiling points of liquids are roughly constant, the empirical constant being about $\frac{2}{3}$ instead of $\frac{1}{2}$ as predicted by the theory.

We are now in a position to calculate Trouton's constant using arguments similar to those employed above. If the theory developed is correct, then the entropy of vaporization at the normal boiling point will be given by

$$\Delta H_v/T_0 = a/bT_0 = 27RT_c/8T_0. \tag{17}$$

But we have just seen that T_c/T_0 should be equal to about 2. Hence,

$$\Delta H_v/T_0 = 13.5 \text{ cal./deg.}$$

The number 13.5 is, of course, considerably smaller than the value usually quoted, namely: 21. Our failure to predict exactly the constants of Guldberg-Guye and of Trouton is not unexpected; the important thing is that correct orders of magnitude are obtained and that the laws are compatible with the theory.

HIGHER APPROXIMATIONS TO THE VAPOR PRESSURE EQUATION

It will be recalled that although the expression for the liquid volume given by Eq. (5) went as far as the third approximation, only terms commensurate with the first approximation were retained in obtaining the vapor pressure relationship (6). The second and third approximations to the fugacity of a liquid can readily be obtained, but the apparent refinements introduced thereby are probably of little quantitative significance.

[4] A discussion similar to that appearing in this section has been carried out in connection with van der Waals' empirical vapor pressure equation. See, for example, Glasstone, *Textbook of Physical Chemistry* (D. Van Nostrand Company, Inc., New York, 1946), second edition, p. 456.

[5] The table used for this purpose was that appearing in the twenty-fifth edition of the *Handbook of Chemistry and Physics* (Chemical Rubber Publishing Company, Cleveland, Ohio), p. 1703. Ninety-four organic compounds (including CO_2, CS_2, etc.) were listed and of them only one (methyl oxalate) had a critical pressure outside the range 20–80 atmos. Assuming that these 94 compounds constitute a fair sample, the statement in the above text and the arguments resulting therefrom appear fully justified.

Nevertheless, the result will be quoted here with brief comments. To the third approximation, we find that

$$RT\ln f=\left\{RT\ln\frac{a}{b^2}-\frac{a}{b}\right\}+\{bp_L\}+\left\{\frac{b^2RT}{a}p_L-\frac{bR^2T^2}{a}\right\}+\cdots, \quad (18)$$

where p_L is the applied pressure on the liquid. In the above equation, the successive contributions of higher approximations are grouped together to indicate precisely what the first, second, and third approximations are. It will be noted that, except for the very small effect of applied pressure, the first and second approximations are the same.

From thermodynamics it is known that

$$V=RT(\partial\ln f/\partial p)_T. \quad (19)$$

Upon substituting (18) into (19), one obtains the first approximation to V from the third approximation for $\ln f$. Likewise, the second approximation to $\ln f$ gives back the zeroth approximation for V. If one utilizes only the first approximation, then the liquid volume would appear to be zero. Thus, in going through the cycle of putting the volume into (2) and getting it out again by differentiating (18), two approximations are lost.

It is worth noting that a $\ln T$ term does not appear in the higher approximations for $\ln f$ although such a term is generally introduced into the more refined empirical expressions for vapor pressures. Van Laar[2a] obtained such a term in his theory but it was necessary for him to assume that b was a particular function of V involving additional parameters. Certain of his equations can be shown to be equivalent to Eq. (6) by making the appropriate identification of parameters and some approximations.

The theory outlined in this paper can be extended to binary solutions by the introduction of appropriate a's and b's into van der Waals' equation. From such a theory it is possible to predict when Raoult's law should apply, when there is partial miscibility, etc. These results will be published shortly.

Nuclear Chemistry of Tellurium: Chemical Effects of Isomeric Transition*

RUSSELL R. WILLIAMS, JR.
University of Notre Dame, Notre Dame, Indiana

(Received February 4, 1948)

The chemical consequences of isomeric transitions in the nuclei Te^{127}, Te^{129}, and Te^{131} have been investigated in aqueous solutions of varying composition. The nuclear reaction gives rise to chemical reduction or oxidation, and a mechanism has been proposed to account for the observed effects. Evidence has been advanced which indicates that the maximum efficiency of the chemical separation of the nuclear isomers can be taken as a measure of the degree of internal conversion.

INTRODUCTION

CHANGE in chemical state as a result of isomeric transition has been demonstrated with several isotopes.[1-3] With tellurium, it has been shown that the nuclear decay is accompanied by a reduction of the tellurium atom from 6+ to 4+. It is the purpose of this investigation to examine this chemical phenomenon quantitatively and to relate it to the characteristics of the nuclear process.

The mechanism by which such a chemical change results from isomeric transition was first suggested by Segrè, Halford, and Seaborg[2] and soon supported by further experimental work.[4] These investigators point out that the recoil from isomeric transition gammas is far from sufficient to break ordinary chemical bonds. However, these weak gammas are often highly internally converted, i.e., the decay energy is carried off by an extra-nuclear electron of the K or L shells. In filling the hole thus created, great disturbances may result in the valence shells with subsequent loss of peripheral electrons.[5] It is therefore postulated that chemical change can occur only when the gamma is internally converted, and that these two phenomena should be quantitatively related.

ACTIVE SPECIES

Three isotopes of tellurium undergo isomeric transition as follows:[6]

Tellurium activities

Te^{127*} (90 d.)
I.T. ↓ 86 kev
Te^{127} (9.3 hr.) $\xrightarrow[\text{no } \gamma]{\beta^-,\ 0.8 \text{ Mev}}$ I^{127} (stable)

Te^{129*} (32 d.)
I.T. ↓ 102 kev
Te^{129} (70 min.) $\xrightarrow[\gamma,\ 0.3,\ 0.8 \text{ Mev}]{\beta^-,\ 0.2,\ 1.8 \text{ Mev}}$ I^{129} (stable or long lived)

Te^{131*} (30 hr.)
I.T. ↓ 177 kev
Te^{131} (25 min.) $\xrightarrow{\beta^-,\ 1.8 \text{ Mev}}$ I^{131} (8d.).

Note: Isomeric transition (I.T.) is the loss of energy by a nucleus without change in atomic or mass number. It may take place by emission of one or more quanta of gamma-radiation, or by interaction with an extra-nuclear electron (internal conversion).

The extent of internal conversion of the isomeric transitions in Te^{127*} and Te^{129*} has been presumed to be nearly 100 percent, since no unconverted gamma-rays have been observed in either case.[7] Samples of Te^{127*} and Te^{129*} were isolated from fission product mixtures furnished by the Tracer Supply Section of Clinton Laboratories. Maximum yields of 32d Te^{129*} are obtained from bombarded uranium metal which has decayed for a period of two weeks to several months. The 90-day Te^{127*} must be obtained from metal decayed at least eighteen months to insure only slight contamination by 32-day

* Originally reported in Report No. CN-3393, March 4, 1946, Clinton Laboratories, Oak Ridge, Tennessee, and is based on work performed under Contract No. W-7401-eng-37 for the Atomic Energy Project and the information covered therein will appear in Division IV, Volume IX-B of the *National Nuclear Energy Series* (Manhattan Project Technical Section) as part of the contribution of the Argonne National Laboratory.

[1] D. DeVault and W. F. Libby, J. Am. Chem. Soc. **63**, 3216 (1941).
[2] E. Segrè, R. S. Halford, and G. T. Seaborg, Phys. Rev. **55**, 321 (1939).
[3] G. T. Seaborg, J. J. Livingood, and J. W. Kennedy, Phys. Rev. **57**, 363 (1940).
[4] G. T. Seaborg, G. Friedlander, and J. W. Kennedy, J. Am. Chem. Soc. **62**, 1309 (1940).
[5] E. P. Cooper, Phys. Rev. **61**, 1 (1942).
[6] Plutonium Project Fission Product Survey, J. Am. Chem. Soc. **68**, 2411 (1946).
[7] A. C. Helmholz, Phys. Rev. **60**, 415 (1941).

Te^{129*}. Carrier-free samples of these two activities were prepared by carrying the tellurium activity on selenium metal. The selenium carrier can be be removed later by volatilization of selenium bromide.

30-hr. Te^{131*} was prepared by neutron bombardment of tellurium metal. 32-day Te^{129*} is also obtained, making the study of the isotope of interest difficult. Absorption and decay curves indicate that Te^{131} has a somewhat harder beta than Te^{129}, but the actual range could not be estimated.

CHEMICAL PREPARATIONS AND SEPARATIONS

Tellurium metal dissolves in nitric and hydrochloric acids principally as tellurous acid. If the nitric acid is removed by evaporation with HCl, the tellurium will be completely tellurous.

The present experiments have demonstrated that carrier-free tellurium tracer is not readily oxidized to tellurate, but macro amounts are easily treated by the method described by Seaborg, Livingood, and Kennedy.[3] This consists in the oxidation of solid silver tellurite by bromine. A solution of telluric acid is formed from which the solid silver bromide and excess bromine may be removed.

Reduction of macro amounts of telluric acid to tellurous acid is rapid in the presence of boiling hydrobromic acid. Further reduction to tellurium metal can be accomplished in hot hydrochloric acid solutions by gassing with sulfur dioxide. This agent reduces tellurous acid rapidly, but telluric acid only slowly, and was used by previous investigators[3] to separate the two valence states. In this work, the separation was made by the precipitation of tellurium sulfide in cold hydrochloric acid. Hydrogen sulfide is even less reactive than sulfur dioxide towards the oxidized state, Te^{6+}.

Gaseous tellurium hexafluoride was prepared by direct action of fluorine gas on tellurium metal at room temperature.[8] The compound is by far the most volatile of all the tellurium fluorides, having a vapor pressure of 29.4-mm Hg. at −79°C.[9] This property was used to effect purification by distillation and to aid in the isomer separations which will be described later.

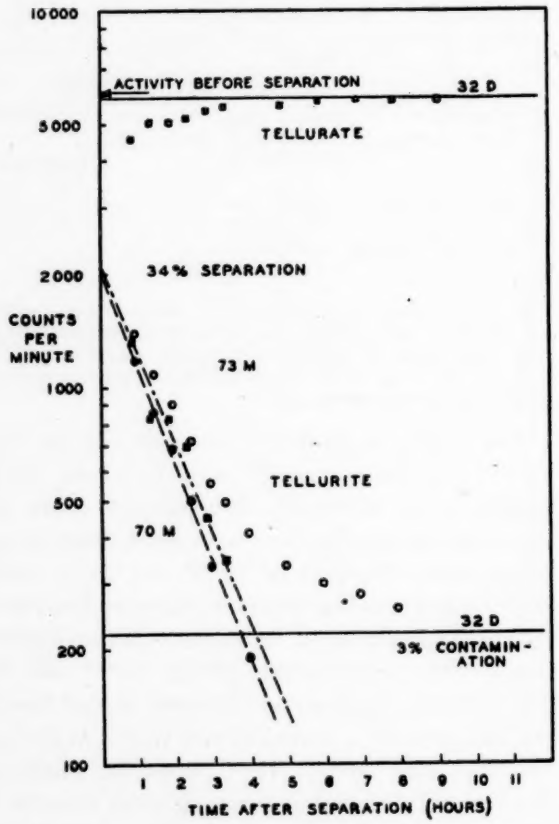

FIG. 1. Daughter separation of Te^{129} in 3M NaOH.

□ Growth of tellurate fraction.
■ — · — Decay of tellurite fraction by subtraction of growth from maximum.
○ Decay of tellurite fraction.
● — — — Decay of 70-min. daughter.

EXPERIMENTAL RESULTS

Te^{129}, Daughter Reduction

The 32-day, 70-minute isomer pair was the subject of the most detailed study because of its availability. The procedure for most of the experiments was as follows:

Tellurium tracer with carrier was oxidized to tellurate. This solution, with various concentrations of acid and base, was allowed to stand at least five hours, in order that new 70-minute daughter atoms might be formed under the desired conditions. After this growth period, tellurite carrier was added, and the previously described separation of valence states made.

As previously reported,[3] a considerable amount

[8] D. M. Yost and J. H. Simon, *Inorganic Synthesis* (McGraw-Hill Book Company, Inc., New York, 1939), Volume I, Prep. No. 44.

[9] D. M. Yost and W. H. Claussen, J. Am. Chem. Soc. **55**, 885 (1933).

of the 70-minute daughter activity is associated with the 4+ valence state, while the parent atoms remain 6+. Experimentally, this is revealed by a growth of beta-activity in the tellurate fraction, and a 70-minute decay of beta-activity in the tellurite fraction (see Fig. 1). Either growth or decay may be taken as a measure of the separation achieved. Some slight contamination by a 32-day parent is usually noted in the decaying tellurite fraction which may be attributed to incomplete separation.

Calculations based on the growth of the tellurite fraction are the most reliable since they involve counting only one sample. The activity extrapolated to separation time is compared with the activity at maximum growth. The decay of the parent is so slow that it is not usually necessary to correct this figure to separation time. However, if the separation is inefficient, the small amount of growth makes this approach inaccurate.

Calculations based on the decay of the tellurite fraction necessitate counting two samples, with the attendent difficulties of mounting and absorption variations. The 70-minute beta-activity, extrapolated to separation time, is compared with the beta-activity of a sample taken before the valence separation was made or with the beta-activity of the tellurate fraction at maximum growth. Both methods of measurement are illustrated in Fig. 1.

If tellurium activity is a mixture of 32-day and 90-day isotopes, the latter may be removed from consideration by the use of a 300 mg/cm^2 aluminum absorber.

The fraction of 70-minute tellurium activity reduced from tellurate to tellurite ("daughter reduction") was found to vary considerably with the acidity or basicity of the solution in which growth took place. The values obtained are summarized in column 1 of Table I. Buffer solutions were used to maintain the desired *p*H in nearly neutral solutions, and there is no reason to doubt the validity of the point at the *p*H value 8.8. This buffer is the only one which employed considerable concentrations of chloride ion, and the apparent inconsistency may be attributable to its reducing properties.

No variation in the yields was observed which could be attributed to presence or absence of tellurous carrier during the growth period or to variation of the temperature from 25 to 75°C.

TABLE I. Daughter separation in Te^{129}.

Growth conditions	Column 1 daughter reduction (%)	Column 2 daughter oxidation (%)	Column 3 chemical oxidation of tellurium ion (%)
6M HCl	57±2		
6M $HClO_4$	53±2		
2M HCl	57±4	0	
0.1M HCl	56±2		
Buffer *p*H 3.4	54±2	<2	
Buffer *p*H 5.0	49±4	5±1	
Buffer *p*H 5.9	50±2		
Buffer *p*H 6.6	45±5		
Buffer *p*H 6.8	39±3	14±1	
Buffer *p*H 8.7	39±2		
Buffer *p*H 8.8*	48±2	6±1	
Buffer *p*H 9.6	40±2		
0.1 M NaOH	41±2	11±1	
0.5M NaOH	40±2	11±1	
1.2M NaOH	37±1	14±1	<3
3M NaOH	33±2	13±1	~4
6M NaOH	25±2	14±1	~15
9M NaOH	32±2		
12M NaOH	36±2	0	~30
16M NaOH	35±2		

* Only buffer containing chloride ion. See text.

Any oxidation of tellurous ion to telluric ion during the course of these experiments would lower the observed yields of tellurite daughter activity. The lowered yields in alkaline solutions especially must be shown to be independent of this ordinary chemical oxidation. Information on this point can be obtained from tellurium tracer experiments starting in the tellurite form. The experiments described in the following section were undertaken for a different purpose, but answer this question as well.

Te^{129}, Daughter Oxidation

The oxidation of tellurium daughter atoms as a result of isomeric transition has not been previously reported. It was observed in these experiments by placing tellurous tracer (with or without tellurous carrier) in alkaline solutions or the growth period previously described. At the end of this period, tellurate carrier was added and the usual separation of the oxidation states by sulfide precipitation made. The beta-activity of the tellurate fraction showed a 70-minute decay period, and the tellurite fraction a corresponding growth (see Fig. 2). The yield of this "daughter oxidation" was computed in exactly

the same manner as that used with the previously described experiments. Values obtained in solutions of different acidity and basicity are indicated in column 2 of Table I. Buffer solutions were again used for *p*H values of around 7. Note again the apparent inconsistency of the point at *p*H value 8.8.

Oxidation of tellurite ion not connected with the nuclear process can be observed after both fractions from the above experiments have returned to a 32-day half-life (see Fig. 2). This type of oxidation was observed in increasing degrees at hydroxide ion concentrations greater than one molar. At these concentrations appreciable amounts of the 70-minute tellurous activity formed in the "daughter reduction" experiments were re-oxidized to the telluric state, thus falsely lowering the yields. The estimated extent of oxidation in strongly basic solution was used to correct the observed values to the probable true "daughter reduction" values. The observed values of daughter reduction and oxidation in solutions of varying acidity and basicity are plotted in Fig. 3. The broken line for "daughter reduction" in basic solutions represents the estimated true values obtained by a consideration of the amount of ordinary chemical oxidation of the daughter tellurite in these solutions.

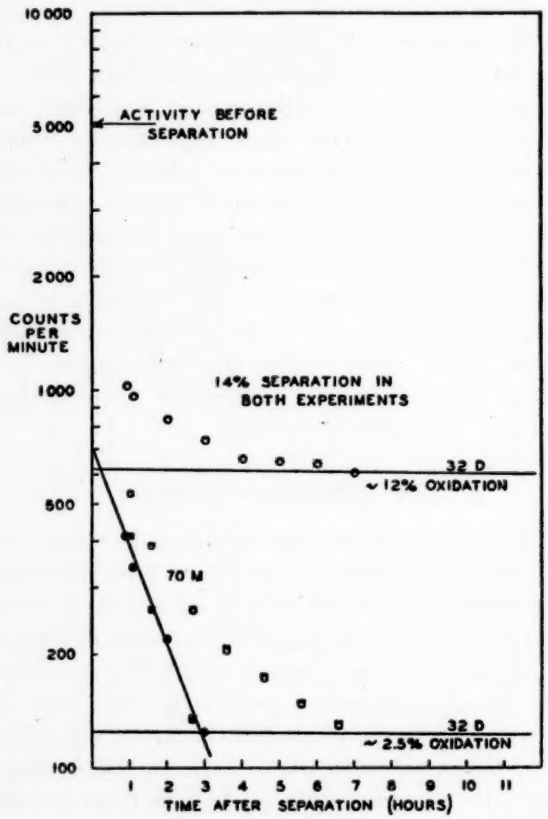

FIG. 2. Decay of tellurate fraction after daughter oxidation of Te^{129}.

○ Grown in 6M NaOH.
● Decay of 70-min. daughter.
□ Grown in 1M NaOH.
■ Decay of 70-min. daughter.

Te^{129}, Daughter Separations with Gaseous Tellurium Hexaflouride

In order to examine the phenomenon in a non-aqueous system, daughter separation experiments were performed starting with Te^{129} activity and carrier as tellurium hexafluoride gas. It is reasonable to assume that no other stable tellurium compound would be sufficiently volatile to have an appreciable vapor pressure at solid carbon dioxide temperatures. After a five-hour growth period at room temperature, separation of the active tellurium hexafluoride from any decomposition or reaction products due to the isomeric transition was accomplished by passing the gas through a trap cooled in a solid carbon dioxide-Cellosolve slurry. The undecomposed gas was then condensed in a two-cubic-centimeter bulb and sealed off. The growth of beta-activity in this bulb was followed at a low counter geometry to minimize any effects due to deposition of activity on the walls.

Pressures of tellurium hexfluoride were five to ten millimeters of mercury during the growth period. In some experiments there were also present about 100 millimeters pressure of some other gas. This should make it very likely that the fragments or activated molecules resulting from isomeric transition will suffer their first collision with some molecule other than tellurium hexfluoride, thus lowering the possibility of back reactions. The degree of daughter separation was computed from the growth of beta-activity in the undecomposed compound. Table II summarizes the conditions and results of these experiments. The observed values are undoubtedly indistinguishable within the precision of the measurements.

Te^{127}, Daughter Separations

A few experiments, similar in every respect to those in aqueous systems with Te^{129}, were con-

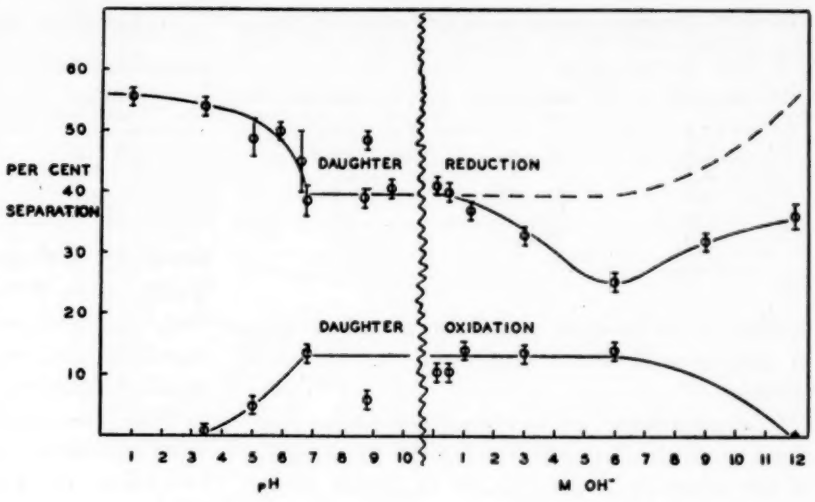

FIG. 3. Daughter separation in Te^{129}.

ducted using the 90-day, 9.3-hour isomer pair. Both "daughter reduction" and "daughter oxidation" were investigated, and the results reported in Table III.

Te^{131}, Daughter Separations

A few experiments were performed to determine the extent of "daughter reduction" with the 30-hour, 25-minute isomer pair. These were made difficult by the presence of other activities and should be regarded as only semiquantitative. Three experiments indicate a "daughter reduction" yield of 34±4 percent in 1M HCl.

DISCUSSION

Daughter Separation in Aqueous Systems

The numerous experiments carried out with Te^{129} in solutions of different acidity and basicity show some interesting relations. From Fig. 3 it is apparent that the yield of both "daughter oxidation" and "daughter reduction" changes abruptly at *p*H values near 6. In more acid solutions oxidation due to nuclear transformation is absent, and the reduction reaction has a yield of about 55 percent. In basic solutions the oxidation reaction shows a yield of about 15 percent and the reduction has dropped to about 40 percent. The situation in solutions above 6M in sodium hydroxide is again like that in acid solutions.

The two reactions are of course studied in separate experiments, but they apparently have some mechanistic relation, since the sum of their yields remains essentially constant. Conditions under which the reduction process is partially ineffective are those under which the oxidation process becomes possible. Leaving out of consideration, for the moment, the 45 percent of nuclear decays which apparently have no chemical effect, the additivity of oxidation and reduction yields suggests a common reaction intermediate in the following sense: Starting with either tellurate or tellurite activity, the process of isomeric transition results in a common activated ion (probably highly oxidized). It is also postulated that the subsequent reactions of the intermediate state are independent of its ancestry, depending only on environment. (See diagram below.)

The constitution of the intermediate is difficult to predict. The opinion that it is highly ionized comes from the knowledge that con-

Proposed Mechanism

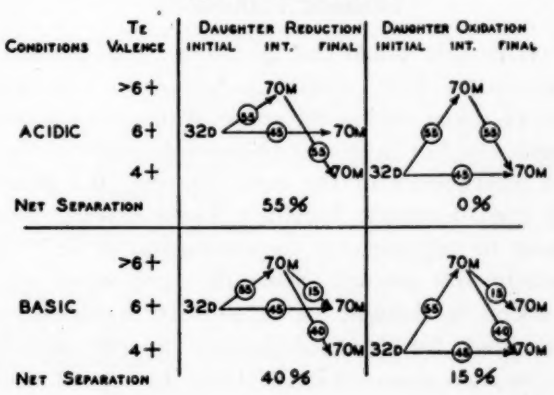

TABLE II. Daughter separation of Te^{129} with TeF_6 gas.

Conditions		
mm TeF_6	mm 2nd gas	% separation
12.5	—	45
5.5	—	55
9.5	—	45
4.5	105 (O_2)	47
5.0	85 (O_2)	49
5.0	150 (H_2)	51

version in an isomeric transition usually results in the loss of more than one extra-nuclear electron.

Configurations can be visualized whose reactions would be dependent upon the constitution of the solution in the manner observed, or the "intermediate" might be two configurations always formed in the same proportions. The reactions of one of these might be independent of conditions, and the reactions of the other dependent on the acidity or basicity of the solution.

The fate of those isomeric transitions which do not seem to result in chemical change is indicated by a consideration of the conversion coefficient of this decay. In the next section evidence will be advanced to show that the conversion is probably 55 percent rather than 100 percent, as previously estimated.[7] If the revised value is accepted, it becomes clear that 45 percent of the isomeric transitions are incapable of producing any chemical change (see Introduction).

Note that the values of "daughter reduction" and "daughter oxidation" obtained with Te^{127*} conform to the remarks made above for the more detailed case of Te^{129*}. Similar observations could not be made on Te^{131*}.

The Conversion Coefficients of the Tellurium Isomeric Transitions

Helmholz[7] could find no unconverted gamma-rays in the Te^{129*} spectrum. A copper absorption curve taken during the couse of this work failed similarly, but these negative results might be due to interference of the weak gamma (0.3 Mev) of the 70-minute daughter. These observations seem to indicate that the conversion of Te^{129*} is nearly 100 percent. Since the process of conversion is thought to be at least a necessary condition for chemical change, the 100 percent separation reported by Seaborg, Livingood, and

TABLE III. Daughter separations of Te^{127} in aqueous systems.

Growth conditions	% daughter reduction	% daughter oxidation
1M HCl	85±2	0
1M NaOH	51±3	25±5

Kennedy[3] did not seem unreasonable. These findings made it difficult to understand the 55 percent maximum separation obtained in this work, especially since experiments were also performed which duplicated the technique of Seaborg *et al.* as closely as possible, and these also gave 55 percent separation. It should be pointed out, however, that the 100 percent figure was obtained from experiments in which all three isomer pairs were considered. This involved the subtraction of several components in the decay curves, a method not used in this work because of its inaccuracy.

It was considered possible that the 55 percent separations observed with Te^{129*} did not measure up to the conversion due to some back reaction of activated ions which gave the initial valence state. This might be due, in aqueous solutions, to the "cage effect," which would make recombination of fragments quite possible. The experiments with gaseous tellurium hexafluoride were undertaken to observe daughter separation in a system where this possibility could be minimized. In a gaseous system, any molecular fragments formed by the isomeric transition are not likely to collide with each other before having an opportunity to react in other ways. Collision of a fragment or activated molecule with other tellurium hexafluoride molecules could also conceivably lead to a reaction which would return the daughter activity to the original chemical state. Large excesses of oxygen or hydrogen in the gaseous mixture made these molecules the most likely collision partner for activated or fragmentary tellurium hexafluoride molecules. The daughter separation values obtained in these gas phase experiments (see Table II) seemed to be constant and not significantly different from those obtained in the aqueous experiments. This indicates that the full value of the conversion is being realized in the separation experiments, and that the isomeric transition may be considerably less than 100 percent converted.

Consideration of the daughter separation experiments with Te^{127*} shows still more convincing evidence that the chemical method of isomer separation is highly efficient. Maximum separation in this case was 85 percent. The possible conversion of 100 percent sets the lower limit for the efficiency of the chemical reactions at 85 percent. Returning to the case of Te^{129*}, and making the very reasonable assumption that the reactions are exactly the same, we see that the conversion cannot be higher than 65 percent. The daughter separation of 34 percent obtained with Te^{131*} predicts a conversion in this isomeric transition no greater than 40 percent. The lower limit of conversion in all cases is assumed to be the maximum separation value achieved.

THE JOURNAL OF CHEMICAL PHYSICS VOLUME 16, NUMBER 5 MAY, 1948

On the Order-Disorder Transition in Solids. Part I

Yosio Mutō
Maebashi Medical College, Maebashi, Japan

(Received February 5, 1948)

Although the phenomena of order-disorder transition and the phenomena of condensation have a marked difference, there is a great similarity in their statistical mechanical treatment. Considering a hypothetical gas in which the molecules can occupy only lattice points of a crystal, and treating the "wrong" molecules as the gas molecules and the "right" molecules as the empty points, the partition function of a binary mixture is easily computed by applying Mayer's method. It is then pointed out that the ordered state is the analog of a condensing system.

SEVERAL years ago the author applied with slight modification Mayer's excellent method which he used in studying phase transition phenomena,[1] and studied the properties of regular solutions.[2] A formula that is more exact than Rushbrooke's was obtained.

The theory of imperfect gas with two components was also applied by the present author to the study of order-disorder phenomena in alloys.[3] The paper issued at that time contained some mistakes although the final result, the expression of the critical temperature as a series, is correct, agreeing with that found by Chang.

In the present paper the method was thoroughly modified and the analogy of condensation and the appearance of order is discussed.

THE PARTITION FUNCTION

As is always done, we assume that we can separate the configurational part from the entire partition function. The two equivalent sublattices are named α and β. In the completely ordered state, A molecules are at α and B's at β. We use the following notarions:

$[A]$: number of A molecules,
$[B]$: number of B molecules,
$[A_\alpha]$: number of A molecules at α,
$[B_\alpha]$: number of B molecules at α,
$[A_\beta]$: number of A molecules at β,
$[B_\beta]$: number of B molecules at β,
$N=2n$: number of total lattice points,
n: number of α and β lattice points each,
X: number of pairs of adjacent wrong atoms (nearest neighbors),
E_0: potential energy at the completely ordered state (with no wrong molecule),
v_{AA}, v_{AB}, v_{BB}: potential energy of pairs of nearest neighbors,
z: number of nearest $\alpha(\beta)$ lattice points surrounding a $\beta(\alpha)$ lattice point,

$$w=2v_{AB}-v_{AA}-v_{BB},$$

ϕ_A, ϕ_B: the part of partition function per molecule independent of configuration.

[1] J. E. Mayer, *Statistical Mechanics* (1940). This book is cited as "S.M."
[2] Y. Mutō, Journal of Physico-Mathematical Society of Japan (in Japanese) **17**, 86 (1943).
[3] See reference 2, p. 445.

Then the partition function for given $[A]$, $[B]$, $[A_\beta]$, and $[B_\alpha]$ is

$$f=\phi_A^{[A]}\phi_B^{[B]}Q([A_\beta],[B_\alpha],T], \tag{1}$$

where

$$\begin{aligned}Q([A_\beta],[B_\alpha],T)&=\exp(-E_0/kT)\exp\{[A_\beta]z(v_{AB}-v_{AA})/kT\}\\&\quad\times\exp\{[B_\alpha]z(v_{AB}-v_{BB})/kT\}\\&\quad\times\Omega([A_\beta],[B_\alpha],N,T),\end{aligned} \tag{2}$$

with

$$\Omega([A_\beta],[B_\alpha],N,T)=\frac{1}{[A_\beta]![B_\alpha]!}\Sigma'\exp\left(-\frac{Xw}{kT}\right). \tag{3}$$

Especially when

$$[A]=[B]=n=N/2$$

and

$$[A_\beta]=[B_\alpha]=N_w/2,$$

we get

$$\begin{aligned}f&=(\phi_A\phi_B)^n\exp(-E_0/kT)\exp(N_wzw/2kT)\\&\quad\times\Omega(N_w/2,N_w/2,N,T).\end{aligned} \tag{4}$$

Now let us consider that we distribute $N_w=a+b$ molecules on N lattice points. The configurational partition function of such a hypothetical gas is given by

$$\Omega(N_w,N,T)=\frac{1}{N_w!}\sum_G\exp\left(-\frac{1}{kT}\sum_{i>j}v_{ij}\right), \tag{5}$$

where v_{ij} should take the value $+\infty$ when ith and jth molecules are on the same lattice point, w when they occupy nearest neighbors, and 0 otherwise. Then consider that a of molecules are put on α sites and b on β sites. Summing for all a and b satisfying the condition $N_w=a+b$, we get

$$\Omega(N_w,N,T)=\sum_{N_w=a+b}\Omega(a,b,N,T),$$

and as we can take the maximum term instead of the sum we may write $\Omega(N_w,N,T)$ instead of $\Omega(N_w/2,N_w/2,N,T)$ in (4). Now (5) is just the formula for $Q_T/N!$ in Chapter 13 of "S.M." The only difference is that summation over the lattice points appears instead of integration. Besides, V, v^{-1}, N are replaced with N, θ, N_w, where

$$\theta=N_w/N,$$

and we use the symbol $\beta(k)$ instead of the irreducible integral β_k:

$$\begin{aligned}\beta(k)&=\frac{1}{Nk!}\sum_G\sum_{k\geq i>j\geq 1}^{\text{irred.}}\prod f_{ij}=\frac{1}{k}\beta_{k-1},\\f_{ij}&=[\exp(-v_{ij}/kT)]-1.\end{aligned} \tag{6}$$

Using the functions G, G', etc., defined by

$$G(\theta)=\sum_{i=2}^{\infty}\beta(i)\theta^i,\quad G'(\theta)=\partial G/\partial\theta,\ \cdots, \tag{7}$$

if θ is not a singular point of G and

$$1-\theta G''>0 \tag{8}$$

is satisfied, we get instead of (13.43) of "S.M."

$$\ln\Omega(N_w,N,T)=N(\theta-\theta\ln\theta+G). \tag{9}$$

This state is the analog of gaseous state, and from (4) we get

$$\ln f=[*]+N\theta zw/2kT+N(\theta-\theta\ln\theta+G), \tag{10}$$

where $[*]$ means the term irrelevant to θ.

The work function is

$$\begin{aligned}A&=-kT\ln f\\&=[*]-N\theta zw/2-NkT(\theta-\theta\ln\theta+G).\end{aligned} \tag{11}$$

THE FIRST ORDERED STATE

Hitherto we took θ as arbitrary. In fact, this should take the value that minimizes A, hence we get

$$zw/2kT=\ln\theta-G'. \tag{12}$$

Now we consider at any given temperature three values of θ that satisfy one of the following conditions:

(α) $\quad zw/2kT=\ln\theta-G'$,

(β) $\quad 1-\theta G''=0$,

(γ) $\quad G$ is singular.

(11) and (12) can be used only when the value for (α) is the smallest and this should not be the case at $T<T_C$. For if the ordered state appears with more A molecules at α sites, then the similar state with α and β exchanged is also possible as well, and hence the mixture, so to say, of them, too. Accordingly, θ must be able to take any arbitrary value between two limits.

Hence the ordered state is the analog of a condensing system, and we consider the case where the value for (β) is the smallest. This corresponds to the temperature $T_m \leq T \leq T_C$.

The least positive root of

$$1-\theta G''=0 \tag{13}$$

being ρ, we get, using the formula (A-XI, 30) of "S.M.,"

$$A=[*]-N\theta zw/2-NkT(\rho-\rho G'+G) +NkT\theta(\ln\rho-G'). \tag{14}$$

The argument of G is ρ.

As considered above, θ should be able to take any value between ρ and $1-\rho$, therefore, we get $\partial A/\partial\theta=0$, that is,

$$zw/2kT=\ln\rho-G'. \tag{15}$$

This equation is to be compatible with $1-\rho G''=0$.[4]

Substituting (15) and (14), we obtain

$$A=[*]-NkT(\rho-\rho G'+G), \tag{16}$$

and

$$E=A-A_T=[*]+NkT(-\rho G_T'+G_T), \tag{17}$$

$$C_V=[*]+Nk(-\rho G_T'+G_T-\rho G_{TT}' +G_{TT}-\rho G_T''\rho_T), \tag{18}$$

where

$$G_T=\partial G/\partial \ln T, \quad G_{TT}=\partial G_T/\partial \ln G.$$

On the other hand, from (15) we get

$$G_T'=zw/2kT, \quad G_{TT}'=-zw/2kT,$$

hence (18) becomes

$$C_V=[*]+Nk(G_T+G_{TT}). \tag{19}$$

T_C is the temperature where (13) has a double root. Exchanging α and β, we soon find that this root must be $\rho_C=\frac{1}{2}$, hence T_C is given by

$$[\theta G''-1]_{\theta=\frac{1}{2}}=0. \tag{20}$$

THE SECOND ORDERED STATE

If (γ) is attained with smaller value of θ than (β), the relations (14), (15), and (16) are still valid, ρ being the singular point. (13) does not hold and we obtain

$$E=[*]+NkT[(1-\rho G'')\rho_T-\rho G_T'+G_T]. \tag{21}$$

On the other hand, from (15)

$$(1/\rho-G'')\rho_T-G_T'=-zw/2kT, \tag{22}$$

hence

$$E=[*]-N\rho zw/2+NkTG_T, \tag{23}$$

and

$$TC_V=[*]-Nzw\rho_T/2+NkT(G_T+G_{TT}+G_T'\rho_T) =[*]+NkT(G_T+G_{TT}) +NkT(G_T'-zw/2kT)^2/(1/\rho-G''). \tag{24}$$

If the range $T_m<T<T_C$ does not exist, T_C cannot be defined as above. When $T>T_C$, $G(\theta)$ is regular for $0\leq\theta\leq\frac{1}{2}$ and (8) holds, hence (11) and (12), too. Exchanging α and β we find that (12) must be satisfied with $\theta=\frac{1}{2}$. T_C is the temperature where this statement just fails. It is conceivable that this is the point where $\theta=\frac{1}{2}$ becomes the double root, and we obtain (20) again.

APPENDIX

For $T>T_C$ we obtain from (11), putting $\theta=\frac{1}{2}$,

$$\left.\begin{aligned} E&=[*]-N\theta zw/2+NkTG_T,\\ C_V&=[*]+Nk(G_T+G_{TT}). \end{aligned}\right\} \tag{A1}$$

The formulae (23) and (24) are valid only when the infinite series have definite values for $\lim\theta\to\rho\to 0$. To decide whether this is the case or not for any given lattice structure may be a matter of considerable difficulty.

From (24) and (A1) it seems as if C_V becomes infinite at T_C when T_m does not exist, and continuous when T_m exists. But as the continuity of G_T+G_{TT} and G_T' itself depends upon the lattice type, we cannot decide as yet.

A. The Approximate Value of $\beta(k)$ for a Large Value of k at Low Temperature

In the formula (6) f_{ij} can take the values -1, ϵ, or 0 according to whether the two molecules i and j occupy the same point, the nearest neighbors, or otherwise, where

$$\epsilon=e^{-w/kT}-1. \tag{A2}$$

Hence we can make a one-to-one correspondence between the terms of $\beta(k)$ and the figures which

[4] As yet the author has not proved this mathematically, but the physical consideration as stated above would be sufficient.

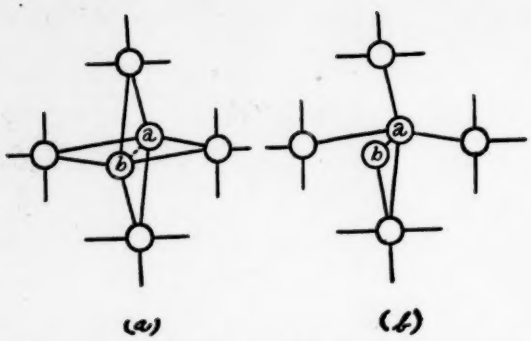

FIG. 1. Terms with two molecules per lattice point: (a) terms which do not contribute, (b) terms which do contribute.

are made by distributing k molecules on lattice points and connecting them so that they become irreducible. To a bond between two molecules on the same point corresponds the factor -1, to a bond between molecules on the nearest neighbors corresponds the factor ϵ, and to a bond between other molecules the factor 0, in each of such terms. Accordingly, in computing $\beta(k)$ we need not consider the figure where molecules situated farther are bonded together. At low temperature ϵ becomes large and we can obtain the approximate value of $\lim\{\ln\beta(k)\}/k$ and hence the radius of convergence Θ of $G(\theta)$.

As the roughest approximation we consider only the figures in which there is at most one molecule on each lattice point. ϵ being large, the figure whose contribution to the value of $\beta(k)$ is the largest has the greatest number of ϵ-bonds, and this number is approximately $zk/2$. Hence we get

$$\lim_{k\to\infty}\{\ln\beta(k)\}/k=(Z/2)\ln\epsilon. \tag{A3}$$

A better approximation will be obtained by considering the figures where some of the ϵ-bonds are removed. If p-bonds are removed we get

$$\frac{(Zk/2)!}{(Zk/2-p)!p!}\epsilon^{Zk/2-p}. \tag{A4}$$

This formula is not exact, for by removing bonds at random a reducible configuration may appear, but for large ϵ and small p/k this is sufficiently correct, and we get by summation

$$\lim_{k\to\infty}\{\ln\beta(k)\}/k=\frac{Z}{2}\ln(\epsilon+1). \tag{A5}$$

A further improvement is gained by taking into account the figures where several lattice points contain pairs of molecules and several points have no molecule—Schottky defect.

Let us consider at first the surroundings of a point with two molecules. Drawing ϵ-bonds maximally we get Fig. 1a. But in this figure the removal of the -1 bond between a and b has no effect upon the irreducibility, and hence the terms with this bond and the terms without this bond appear in pairs in $\beta(k)$ giving no contribution in the end. The terms that contribute to $\beta(k)$ are represented by Fig. 1b.

Then considering the figure with p-points containing pairs of molecules and q empty points we get the term

$$\frac{(k-p+q)!}{p!q!(k-2p)!}Z^p(-1)^p\epsilon^p\epsilon^{Z(k+q-p)/2}\epsilon^{-Zq}\times(1+\epsilon^{-1})^{Z(k-p)/2}. \tag{A6}$$

In this formula we assume again that ϵ is large and p/k and q/k are small enough so that the probability of finding two abnormal points in the nearest neighbors is negligible. The last factor is necessary in order to take into account the configuration where some of the ϵ-bonds are removed.

Now summing up for p and q and using the relations

$$\sum_q\frac{(h+q)!}{h!q!}x^q=\frac{1}{(1-x)^{h+1}}$$

and

$$\sum_p\frac{(k-p)!}{p!(k-2p)!}y^p=\frac{1}{2\pi i}\oint\sum\frac{(1+\zeta)^{k-p}}{\zeta^{p+1}}y^p d\zeta$$

$$=\frac{1}{2\pi i}\oint\frac{(1+\zeta)^{k+1}}{\zeta^2+\zeta-y}d\zeta$$

$$=(\tfrac{1}{2}+(\tfrac{1}{4}+y)^{\frac{1}{2}})^{k+1}/2(\tfrac{1}{4}+y)^{\frac{1}{2}},$$

(A6) becomes

$$\{\tfrac{1}{2}+(\tfrac{1}{4}+y)^{\frac{1}{2}}\}^{k+1}(1+4y)^{-\frac{1}{2}}(1+\epsilon)^{Zk/2}(1-\epsilon^{-Z/2})^{-k-1},$$

where

$$y=-Z\epsilon(1+\epsilon)^{-Z/2}(1-\epsilon^{-Z/2}).$$

Hence we get

$$\lim_{k\to\infty}(\ln\beta(k))/k=-\ln\Theta=\ln(1+y-y^2+\cdots)+\frac{Z}{2}\ln(\epsilon+1)-\ln(1-\epsilon^{-Z/2}),$$

or

$$\left.\begin{aligned}\ln\Theta&=Z\epsilon(1+\epsilon)^{-Z/2}\\&\quad-\frac{Z}{2}\ln(\epsilon+1)-\epsilon^{-Z/2}+O(\epsilon^{-Z+2}),\\\Theta&=(1+\epsilon)^{-Z/2}+O(\epsilon^{-Z+1}).\end{aligned}\right\}\quad(A7)$$

Now it is interesting to examine to what extent these formulae are valid by substituting these into (15), which is equivalent to

$$\ln\Theta-\ln(1-\Theta)-Z\epsilon\Theta+\tfrac{3}{2}Z\epsilon^2\Theta^2+\cdots+(Z/2)\ln(\epsilon+1)=0.\quad(A8)$$

The last formula is obtained by calculating $\beta(k)$ for small values of k and for $w=0$, which gives

$$[\beta(k)]_{w=0}=-\frac{1}{(k-1)k}.$$

From (A8) and (A7) we see that discrepancy begins with the term of

$$-\frac{Z}{2}\epsilon^{-Z/2-1}.$$

Concluding the paper, the author wishes to express his hearty thanks to Professor J. E. Mayer who read the paper and gave kind advice concerning publication, and also to Professor Kotani and Mr. Takahashi for their kind suggestions.

On the Order-Disorder Transition in Solids. Part II

Yosio Mutō
Maebashi Medical College, Maebashi, Japan
(Received February 4, 1948)

In a recent paper with the same title the author studied the phenomena of order-disorder transition in crystals with equivalent sublattices when there are just the same numbers of A and B molecules. In the present paper the case with variable numbers of molecules is considered. As a paper issued some years ago in Japanese contained some mistakes, a complete revision is made and the analogy with the condensation phenomena in two component systems is considered.

INTRODUCTION

We use the same symbols as before[1] and put

$$v_A=v_{AB}-v_{AA},\quad v_B=v_{AB}-v_{BB}. \tag{1}$$

When N, $[A_\beta]$, and $[B_\alpha]$ are given, the partition function f takes the form

$$f=(\phi_A\phi_B)^n(\phi_A/\phi_B)^{[A_\beta]}(\phi_B/\phi_A)^{[B_\alpha]}\times\exp(-E_0/kT)\left(\exp\frac{zv_A}{kT}\right)^{[A_\beta]}\times\left(\exp\frac{zv_B}{kT}\right)^{[B_\alpha]}\Omega([A_\beta],[B_\alpha],N,T), \tag{2}$$

with

$$\Omega([A_\beta],[B_\alpha],N,T)=\frac{1}{[A_\beta]![B_\alpha]!}\Sigma'\exp\left(-\frac{Xw}{kT}\right). \tag{3}$$

Now the configurational partition function $\Omega(N_A, N_B, V)$ of a binary mixture is given by

$$\ln\Omega(N_A,N_B,V)=-N_A(\ln\zeta_A-G_A)-N_B(\ln\zeta_B-G_B)+V(\zeta_A+\zeta_B-\zeta_AG_A-\zeta_BG_B+G), \tag{4}*$$

where N_A and N_B are the numbers of molecules and G's are defined by

$$G=\sum_{j,k}\beta(j,k)\zeta_A{}^j\zeta_B{}^k,\quad G_A=\partial G/\partial\zeta_A,\ \cdots, \tag{5}$$

$\beta(j, k)$ being the irreducible integral containing j of A molecules and k of B molecules.[2] For sufficiently small N_A/V and N_B/V, ζ_A and ζ_B should take the value

$$(\alpha)\qquad \zeta_A=N_A/V,\quad \zeta_B=N_B/V, \tag{6}$$

while for smaller V either of the following conditions must be satisfied:

$$(\beta)\quad D\equiv(1-\zeta_AG_{AA})(1-\zeta_BG_{BB})-\zeta_A\zeta_B(G_{AB})^2=0, \tag{7}$$

or

$$(\gamma)\qquad G \text{ is singular.}$$

DISORDERED STATE

Treating the wrong molecules as gas molecules, we can use these relations after replacing N_A, N_B, and V with $[A_\beta]$, $[B_\alpha]$, and n. Care should be taken in making the irreducible integral or sum, for wrong molecules of the kind A can occupy only β sites and so on. Hence substituting (4) into (2), we get, for sufficiently small $[A_\beta]$ and $[B_\alpha]$,

$$\frac{1}{n}\ln f=\ln\phi_A\phi_B+\zeta_A\ln(\phi_A/\phi_B)+\zeta_B\ln(\phi_B/\phi_A)-E_0/nkT+\zeta_Azv_A/kT+\zeta_Bzv_B/kT-\zeta_A\ln\zeta_A-\zeta_B\ln\zeta_B+\zeta_A+\zeta_B+G, \tag{8}$$

where ζ_A and ζ_B are determined by

$$\zeta_A=[A_\beta]/n,\quad \zeta_B=[B_\alpha]/n. \tag{9}$$

Now when the composition is given,

$$([A]-[B])/N=\zeta_A-\zeta_B=S \tag{10}$$

is fixed, and ζ_A and ζ_B should take the value that minimize the work function. Hence differen-

[1] Y. Mutō, J. Chem. Phys. 16, 519 (1948).

* Formula (4) is the formula (31′) of Mayer's paper (reference 2) multiplied by N_A+N_B. For ordered state Lemaire's theorem was not used explicitely, for a relation between ζ_A and ζ_B is given by the condition (β) or (γ). But by making the total differential from (16) for fixed T we soon find that the condition $df=0$ in the paper cited is just fulfilled.

[2] J. E. Mayer, J. Phys. Chem. 43, 71 (1939)

tiating (8) we get

$$zw/kT-\ln\zeta_A-\ln\zeta_B+G_A+G_B=0. \quad (11)$$

(10) and (11) determine the value of ζ_A and ζ_B at any given temperature and composition.

As α and β are equivalent, we can replace, in (10) and (11), ζ_A and ζ_B with $1-\zeta_B$ and $1-\zeta_A$, respectively, and by the reasoning as stated in the previous paper it will be found that the disordered state that really appear is represented by

$$\zeta_A=\tfrac{1}{2}+\tfrac{1}{2}S, \quad \zeta_B=\tfrac{1}{2}-\tfrac{1}{2}S. \quad (12)$$

ORDERED STATE

The ordered state appears when the root of the simultaneous equations (10) and (11) is not found in the region where D does not vanish and G is regular. In this case the root of (7) or the singular point of G is denoted by

$$\zeta_A=\rho_A, \quad \zeta_B=\rho_B. \quad (13)$$

We consider that the crystal is composed of domains, or, in other words, the whole crystal is divided into two parts, in one of which right A molecules are found in α sites, whereas in the other they are found in β sites, that is, α and β are exchanged. If we regard the A molecules at β sites and B molecules at α sites as the A and B molecules, respectively, of a hypothetical binary mixture, the domain where right A molecules are at α sites in the gas phase, and the domain where right A molecules are at β sites is the condensed phase, hence the ordered state is analogous to the condensing system.

We can use the formula of the partition function for the condensing binary mixture after slight modification and get

$$\begin{aligned}\frac{1}{n}\ln f=&\ln\phi_A\phi_B+(\rho_A-\rho_B)\ln(\phi_A/\phi_B)-E_0/nkT\\&+(\rho_A+\rho_B-\rho_AG_A-\rho_BG_B+G)\\&+\frac{n_1}{n}\Big[\frac{zv_A}{kT}\rho_A+\frac{zv_B}{kT}\rho_B\\&\quad-\rho_A(\ln\rho_A-G_A)\\&\quad-\rho_B(\ln\rho_B-G_B)\Big]\\&+\frac{n_2}{n}\Big[\frac{zv_A}{kT}(1-\rho_B)+\frac{zv_B}{kT}(1-\rho_A)\\&\quad-(1-\rho_B)(\ln\rho_A-G_A)\\&\quad-(1-\rho_A)(\ln\rho_B-G_B)\Big], \quad (14)^{**}\end{aligned}$$

for by the statement mentioned above we have

$$\left.\begin{aligned}n&=n_1+n_2,\\[A_\beta]&=n_1\rho_A+n_2(1-\rho_B),\\[B_\alpha]&=n_1\rho_B+n_2(1-\rho_A).\end{aligned}\right\} \quad (15)$$

As the value of (14) should not change with n_1 and n_2, the relation

$$zw/kT=\ln\rho_A+\ln\rho_B-G_A-G_B \quad (16)$$

also follows.

Now the composition is determined by giving S. At a temperature higher than T_C a disordered state always appears for any S. At a temperature lower than T_C ordered state appears for sufficiently small S. The value of S where the order is just destroyed will be denoted by S_C. This is the point where (16), in which ρ_B is replaced with ρ_A-S, has a double root. On account of symmetry this root should be given by

$$\rho_A=\tfrac{1}{2}(1+S_C), \quad \rho_B=\tfrac{1}{2}(1-S_C),$$

and from (16) we get

$$\left.\begin{aligned}&\frac{1}{\rho_A}+\frac{1}{\rho_B}-G_{AA}-2G_{AB}-G_{BB}=0,\\&\rho_A=\tfrac{1}{2}(1+S_C), \quad \rho_B=\tfrac{1}{2}(1-S_C).\end{aligned}\right\} (17)$$

These determine S_C as a function of T, but its calculation would be quite difficult.

$\beta(j,k)$ and $\beta(k)$ of the previous paper are related by

$$\sum_{j+k=l}\beta(j,k)=2\beta(l). \quad (18)$$

This formula is obtained by dividing unsorted l molecules into A and B. On account of (18), (11) and (16) coalesce with (12) and (15) of the previous paper in the special case of $S=0$.

** (14) is the result of substituting (15) and (13) into the formula obtained by replacing N_A, N_B, and V with $[A_\beta]$, $[B_\alpha]$, and n in (4).

Molecular Orbital Calculations of Vibrational Force Constants. I. Ethylene*, **

ROBERT G. PARR AND BRYCE L. CRAWFORD, JR.
School of Chemistry, University of Minnesota, Minneapolis, Minnesota

(Received February 5, 1948)

As a preliminary to the theoretical evaluation of certain out-of-plane vibrational force constants of benzene, the energy levels and twisting frequency of ethylene are calculated by the method of antisymmetric molecular orbitals, no empirical data being used other than molecular dimensions. The problem is oversimplified to a two-electron one, and yet encouraging results are obtained.

BECAUSE electronic velocities on the average far surpass nuclear velocities, it is permissible in the calculation of vibrational energy levels of molecules to picture the nuclei vibrating in the time-average potential field of the electrons. The force constant associated with the nth normal mode of vibration then turns out to be equal to the curvature at the equilibrium position of the plot of electronic energy *versus* the nth normal coordinate. It is therefore possible, in principle at least, to find the vibrational force constants of a molecule from its electronic energy as a function of nuclear configuration.

The problem of determining the electronic energy of a polyatomic molecule is, in general, extremely difficult, because exact solution of the many-body wave equation is out of the question —very crude approximation methods must be used. Nevertheless, considerable success has been attained in the semiquantitative calculation of electronic energy levels. Up to now very few attempts have been made to calculate electronic energies as functions of configuration, however. The present papers are a try at this: in I the twisting force constant of ethylene is computed from the electronic energy as a function of the twisting angle; in II two analogous force constants of benzene are computed in similar manner.

Of the various approximate methods available for the calculation of electronic energies, the so-called method of molecular orbitals, in the form employed by Goeppert-Mayer and Sklar,[1] appears the most suitable for quantitative calculation on ethylene and benzene. Goeppert-Mayer and Sklar have calculated the energy levels of the equilibrium configuration of benzene, Hartmann,[2] the levels of the equilibrium (planar) form of ethylene; straightforward extension of these calculations should yield the energies for small distortions from equilibrium (and hence the force constants).

In the Goeppert-Mayer-Sklar modification of the molecular orbital method, the wave functions for the various states of an n-electron system are written as products of n one-electron wave functions (called molecular orbitals). The latter are found by the method of variation of parameters as best linear combinations of orbitals on individual atoms (called atomic orbitals); the energies are calculated on the assumption that each electron moves independently in the potential field of the nuclear framework. The wave function for the ground state of the n-electron system is constructed by the placing of electrons in the molecular orbitals of lowest energy, two at a time until all n electrons are used up. The energy of the ground state is then calculated from this wave function, with an n-electron Hamiltonian which includes electronic repulsion terms. Excited states are similarly treated, care always being taken to multiply the wave functions by suitable spin factors and to make them completely antisymmetric as regards electron interchange.

THE ENERGY LEVELS OF ETHYLENE[3]

Anticipating enough trouble with benzene treated as a six-electron problem, one starts by

* This research was supported by the Office of Naval Research, U. S. Navy, through Contract N5ori-147.

** Presented at the Symposium on Molecular Structure and Spectroscopy, Ohio State University, June 10, 1947.

[1] M. Goeppert-Mayer and A. L. Sklar, J. Chem. Phys. 6, 645 (1938).

[2] H. Hartmann, Zeits. f. physik. Chemie **B53**, 96 (1943).

[3] The treatment given in this and the following sections is, like Hartmann's (see reference 2), in the classification

considering ethylene as a two-electron problem, knowing full well that this is not strictly justified.[4] The electrons considered are the "unsaturation" electrons which pair to form the second "double" or "$\pi\pi$" carbon-carbon bond. If the carbon atoms are labeled A_1 and A_2 [in general A_n] and the $2p\pi$-wave functions for electron ν on A_1 and A_2 are denoted by $\alpha_1(\nu)$ and $\alpha_2(\nu)$ [in general $\alpha_n(\nu)$], the problem is to calculate the energy levels of the two electrons which occupy the molecular orbitals which are linear combinations of α_1 and α_2, as a function of the angle φ between the major axes of α_1 and α_2. The position $\varphi=0$ corresponds to the equilibrium, planar configuration of ethylene; the second derivative of the energy with respect to φ, evaluated at $\varphi=0$, is the force constant for twisting about the double bond.

The atomic orbitals α_1 and α_2 are taken to be real, normalized, Zener-type, hydrogen-like functions.[5] They therefore depend upon an effective nuclear charge Z of a carbon nucleus towards a $2p\pi$-electron. Also, by the vector property of p orbitals,[6]

$$\alpha_1=a_1, \quad \alpha_2=a_2\cos\varphi+a_{2s}\sin\varphi, \tag{1}$$

where a_2 is a p orbital parallel to (but not coaxial with) a_1, and a_{2s} is a p orbital perpendicular both to a_1 and the carbon-carbon internuclear axis.

From analogy with the hydrogen molecule,[6] the linear combinations of the α_n which are proper molecular orbitals for the distorted molecule are

$$\begin{aligned}\phi_+(\nu)&=(2\sigma_+)^{-\frac{1}{2}}[\alpha_1(\nu)+\alpha_2(\nu)],\\ \phi_-(\nu)&=(2\sigma_-)^{-\frac{1}{2}}[\alpha_1(\nu)-\alpha_2(\nu)].\end{aligned} \tag{2}$$

Here

$$\sigma_+=1+S_{\alpha_1\alpha_2} \quad \sigma_-=1-S_{\alpha_1\alpha_2}, \tag{3}$$

where

$$S_{\alpha_1\alpha_2}=\int\alpha_1(1)\alpha_2(1)dv_1 \tag{4}$$

is the overlap integral between α_1 and α_2.

The various states of the two electrons result from putting two electrons into ϕ_+ and ϕ_- in all possible ways. This yields the following four wave functions:

$$\begin{aligned}\psi_1&=\phi_+(1)\phi_+(2),\\ \psi_V&=2^{-\frac{1}{2}}[\phi_+(1)\phi_-(2)+\phi_+(2)\phi_-(1)],\\ \psi_T&=2^{-\frac{1}{2}}[\phi_+(1)\phi_-(2)-\phi_+(2)\phi_-(1)],\\ \psi_2&=\phi_-(1)\phi_-(2).\end{aligned} \tag{5}$$

All but the third of these are symmetric in the electrons and therefore require antisymmetric spin factors of the form

$$X_s=2^{-\frac{1}{2}}[\delta_+(1)\delta_-(2)-\delta_+(2)\delta_-(1)], \tag{6}$$

where $\delta_+(\nu)$ and $\delta_-(\nu)$ are possible orthonomal spin functions for the νth electron. The third is antisymmetric in the electrons and so must be combined with a symmetric spin factor

$$X_t=\begin{cases}2^{-\frac{1}{2}}[\delta_+(1)\delta_-(2)+\delta_+(2)\delta_-(1)],\\ \text{or}\quad \delta_+(1)\delta_+(2),\\ \text{or}\quad \delta_-(1)\delta_-(2).\end{cases} \tag{7}$$

Completely antisymmetric wave functions for the four states thus are[7]

$$\begin{aligned}\Psi_1&=\psi_1X_s \text{ (singlet, energy } E_1),\\ \Psi_V&=\psi_VX_s \text{ (singlet, energy } E_V),\\ \Psi_T&=\psi_TX_t \text{ (triplet, energy } E_T),\\ \Psi_2&=\psi_2X_s \text{ (singlet, energy } E_2).\end{aligned} \tag{8}$$

Now Ψ_1 and Ψ_2 are both totally symmetric in the nuclei. They therefore interact to give the two states

$$\Psi_N=C_1\Psi_1+C_2\Psi_2 \quad (\text{singlet, energy } E_N\leqslant\min\{E_1, E_2\}) \tag{9}$$

and

$$\Psi_Z=D_1\Psi_1+D_2\Psi_2 \quad (\text{singlet, energy } E_Z\geqslant\max\{E_1, E_2\}). \tag{10}$$

Ψ_N turns out to be the best wave function for the ground state of planar ethylene obtainable from this approach.

---

of Mulliken [R. S. Mulliken, Chem. Rev. **41**, 203 (1947)] an "approximate theoretical" one; Mulliken's "semiempirical" treatment of ethylene [R. S. Mulliken and C. C. J. Roothaan, Chem. Rev. **41**, 219 (1947)] is formally similar, but appeals to experiment rather than calculation for values of certain integrals.

[4] Thus the neglect of non-unsaturation electrons makes the calculations immediately subject to the "nightmare of inner shells"—the error resulting from the failure to construct wave functions for the unsaturation electrons which are orthogonal to the wave functions for the other electrons (in stabler orbitals).

[5] Cf., for example, Eyring, Walter, and Kimball, *Quantum Chemistry* (John Wiley and Sons, Inc., New York, 1944), pp. 89–90.

[6] Eyring, Walter, and Kimball, *Quantum Chemistry* (John Wiley and Sons, Inc., New York, 1944), Chapter XII.

[7] At this point Hartmann (reference 2) is in error—his (12b) is not a singlet but a mixed singlet and triplet wave function.

The Hamiltonian for the system may be written

$$\mathbf{H}=\mathbf{T}(1)+\mathbf{T}(2)+\mathbf{H}_0(1)+\mathbf{H}_0(2)+(e^2/r_{12}), \quad (11)$$

where $\mathbf{T}(\nu)$ is the kinetic energy of electron ν, $\mathbf{H}_0(\nu)$ is the mutual potential energy of electron ν and the single-bonded H_2C-CH_2 framework, and e^2/r_{12} is the repulsive potential between electrons 1 and 2. Consequently,

$$\begin{aligned} E_1 &= \int \Psi_1 \mathbf{H} \Psi_1 d\nu = \int \psi_1 \mathbf{H} \psi_1 d\nu \\ &= \int \phi_+(1)\phi_+(2)\mathbf{H}\phi_+(1)\phi_+(2)d\nu \\ &= 2\epsilon_+ + \gamma_{++}, \end{aligned} \quad (12)$$

where

$$\begin{aligned} \epsilon_+ &= \int \phi_+(1)\phi_+(2)[\mathbf{T}(1)+\mathbf{H}_0(1)]\phi_+(1)\phi_+(2)d\nu \\ &= \int \phi_+(1)[\mathbf{T}(1)+\mathbf{H}_0(1)]\phi_+(1)d\nu, \end{aligned} \quad (13)$$

and

$$\gamma_{++} = \int \phi_+(1)\phi_+(2)(e^2/r_{12})\phi_+(1)\phi_+(2)d\nu. \quad (14)$$

Similarly,

$$E_2 = 2\epsilon_- + \gamma_-, \quad (15)$$

$$E_V = \epsilon_+ + \epsilon_- + \gamma_{+-} + \delta_{+-}, \quad (16)$$

$$E_T = \epsilon_+ + \epsilon_- + \gamma_{+-} - \delta_{+-}, \quad (17)$$

where

$$\epsilon_- = \int \phi_-(1)[\mathbf{T}(1)+\mathbf{H}_0(1)]\phi_-(1)d\nu, \quad (18)$$

$$\gamma_{\pm-} = \int \phi_\pm(1)\phi_-(2)(e^2/r_{12})\phi_\pm(1)\phi_+(2)d\nu, \quad (19)$$

$$\delta_{+-} = \int \phi_+(1)\phi_-(2)(e^2/r_{12})\phi_-(1)\phi_+(2)d\nu. \quad (20)$$

E_N and E_Z are the two roots of the secular equation

$$\begin{vmatrix} E_1-E & \int \Psi_1 \mathbf{H} \Psi_2 d\nu \\ \int \Psi_1 \mathbf{H} \Psi_2 d\nu & E_2-E \end{vmatrix} = 0. \quad (21)$$

But

$$\begin{aligned} &\int \Psi_1 \mathbf{H} \Psi_2 d\nu \\ &= \int \psi_1 \mathbf{H} \psi_2 d\nu = \int \phi_+(1)\phi_+(2)\mathbf{H}\phi_-(1)\phi_-(2)d\nu \\ &= \int \phi_+(1)\phi_+(2)[\mathbf{T}(1)+\mathbf{T}(2)+\mathbf{H}_0(1) \\ &\qquad +\mathbf{H}_0(2)+(e^2/r_{12})]\phi_-(1)\phi_-(2)d\nu \\ &= \int \phi_+(1)\phi_+(2)(e^2/r_{12})\phi_-(1)\phi_-(2)d\nu \\ &= \delta_{+-} = (1/2)(E_V - E_T). \end{aligned} \quad (22)$$

Hence

$$\begin{aligned} E_N = (1/2)(E_2+E_1) - (1/2)(E_2-E_1) \\ \times[1+(E_V-E_T)^2(E_2-E_1)^{-2}]^{\frac{1}{2}} \end{aligned} \quad (23)$$

and

$$\begin{aligned} E_Z = (1/2)(E_2+E_1) + (1/2)(E_2-E_1) \\ \times[1+(E_V-E_T)^2(E_2-E_1)^{-2}]^{\frac{1}{2}}. \end{aligned} \quad (24)$$

For $\varphi=\pi/2$, E_1 and E_2 coalesce and the perturbation is at a maximum. In this case (23) and (24) give

$$E_N^{\perp} = E_1^{\perp} - (1/2)(E_V^{\perp} - E_T^{\perp}) \quad (25)$$

and

$$E_Z^{\perp} = E_1^{\perp} + (1/2)(E_V^{\perp} - E_T^{\perp}), \quad (26)$$

where the superscript $^{\perp}$ denotes the position $\varphi=\pi/2$.

The above formulas give the energies in terms of integrals over molecular orbitals. The next step is to express these in terms of integrals over atomic orbitals through the use of (2). One finds, after the use of a little algebra,

$$\begin{aligned} \gamma_{++} = 2(2\sigma_+)^{-2}[&(\alpha_1\alpha_1;\alpha_1\alpha_1)+(\alpha_1\alpha_1;\alpha_2\alpha_2) \\ &+2(\alpha_1\alpha_2;\alpha_1\alpha_2)+4(\alpha_1\alpha_1;\alpha_1\alpha_2)], \end{aligned}$$

$$\begin{aligned} \gamma_{--} = 2(2\sigma_-)^{-2}[&(\alpha_1\alpha_1;\alpha_1\alpha_1)+(\alpha_1\alpha_1;\alpha_2\alpha_2) \\ &+2(\alpha_1\alpha_2;\alpha_1\alpha_2)-4(\alpha_1\alpha_1;\alpha_1\alpha_2)], \end{aligned}$$

$$\begin{aligned} \gamma_{+-} = (2\sigma_+\sigma_-)^{-1}[&(\alpha_1\alpha_1;\alpha_1\alpha_1) \\ &+(\alpha_1\alpha_1;\alpha_2\alpha_2)-2(\alpha_1\alpha_2;\alpha_1\alpha_2)], \end{aligned}$$

and

$$\delta_{+-} = (2\sigma_+\sigma_-)^{-1}[(\alpha_1\alpha_1;\alpha_1\alpha_1)-(\alpha_1\alpha_1;\alpha_2\alpha_2)], \quad (28)$$

where, in c.g.s. units,[8]

$$\begin{aligned} (\alpha_i\alpha_j;\alpha_k\alpha_l) &= \int \alpha_i(1)\alpha_k(2)(e^2/r_{12})\alpha_j(1)\alpha_l(2)d\nu \\ &= (\alpha_k\alpha_l;\alpha_i\alpha_j). \end{aligned} \quad (29)$$

The evaluation of the $\epsilon_\pm$ is not so easy.[9] Neglecting the hydrogen atoms, one first assumes that

$$\mathbf{H}_0(\nu) = \mathbf{H}_{A_1}(\nu) + \mathbf{H}_{A_2}(\nu), \quad (30)$$

where $\mathbf{H}_{A_n}(\nu)$ is the potential representing attraction of electron ν by the nth carbon nucleus plus repulsion of electron ν by the other five electrons of that nucleus. Then

$$[\mathbf{T}(\nu)+\mathbf{H}_{A_n}(\nu)]\alpha_n(\nu) = W_{2p}\alpha_n(\nu), \quad (31)$$

where W_{2p} is the energy of a $2p$ electron in a

[8] Note that in atomic units (distances in units of the first Bohr radius $a_0=0.5292$A, energies in units of $e^2/2a_0=13.602$ ev)

$$(\alpha_i\alpha_j;\alpha_k\alpha_l) = \int \alpha_i(1)\alpha_k(2)(2/r_{12})\alpha_j(1)\alpha_l(2)d\nu.$$

[9] The procedure adopted here is due to Goeppert-Mayer and Sklar (reference 1).

TABLE I. Values of integrals over atomic orbitals (atomic units).

Integral	ρ	6	8.13	8.37	10
$S_{a_1a_2}$		0.46800	0.27723	0.25995	0.16396
$Z^{-1}(A_1:a_2a_2)$		0.0773	0.02287	0.01976	0.00703
$Z^{-1}(A_1:a_1a_2)$		0.1200	0.04768	0.04364	0.02090
$Z^{-1}(a_1a_1;a_1a_1)$		0.3914	0.3914	0.3914	0.3914
$Z^{-1}(a_1a_1;a_2a_2)$		0.2616	0.2140	0.2086	0.1806
$Z^{-1}(a_1a_1;a_{2s}a_{2s})$		0.2484	0.2080	0.2036	0.1774
$Z^{-1}(a_1a_2;a_1a_2)$		0.0730	0.0250	0.0220	0.0082
$Z^{-1}(a_1a_{2s};a_1a_{2s})$		0.0035	0.0015	0.0012	0.0004
$Z^{-1}(a_1a_1;a_1a_2)$		0.1538	0.0827	0.0766	0.0448

TABLE II. Values of integrals over molecular orbitals (atomic units).

Integral	ρ	6	8.13	8.37	10
$\varphi=0$: $Z^{-1}(\epsilon_+-W_{2p})$		−0.4174	−0.2876	−0.2767	−0.2176
$Z^{-1}(\epsilon_--W_{2p})$		−0.1224	−0.1474	−0.1462	−0.1458
$Z^{-1}\gamma_{++}$		0.3281	0.3023	0.2993	0.2833
$Z^{-1}\gamma_{--}$		0.3247	0.3107	0.3082	0.2927
$Z^{-1}\gamma_{+-}$		0.3246	0.3008	0.2981	0.2855
$Z^{-1}\delta_{+-}$		0.0831	0.0961	0.0980	0.1083
$\varphi=\pi/2$: $Z^{-1}(\epsilon_++W_{2p})$		−0.3257	−0.2309	−0.2234	−0.1844
$Z^{-1}(\epsilon_--W_{2p})$		−0.3257	−0.2309	−0.2234	−0.1844
$Z^{-1}\gamma_{++}$		0.3234	0.3012	0.2987	0.2848
$Z^{-1}\gamma_{--}$		0.3234	0.3012	0.2987	0.2848
$Z^{-1}\gamma_{+-}$		0.3164	0.2982	0.2963	0.2840
$Z^{-1}\delta_{+-}$		0.0715	0.0917	0.0939	0.1070

carbon atom in its valence state; and Eqs. (2), (13), and (18) give

$$\epsilon_\pm=(2\sigma_\pm)^{-1}\int[\alpha_1(\nu)\pm\alpha_2(\nu)][\mathbf{T}(\nu)+\mathbf{H}_{A_1}(\nu)+\mathbf{H}_{A_2}(\nu)][\alpha_1(\nu)\pm\alpha_2(\nu)]d\nu,$$
$$=W_{2p}+(2\sigma_\pm)^{-1}\int[\alpha_1(1)+\alpha_2(1)]\times[\mathbf{H}_{A_1}(1)\alpha_2(1)+\mathbf{H}_{A_2}(1)\alpha_1(1)]d\nu_1. \quad (32)$$

Now $\mathbf{H}_{A_n}(1)$ is the potential on electron 1 due to the *neutral* carbon atom A_n minus one $2p$ electron in the orbital $\alpha_n(\nu)$:

$$\mathbf{H}_{A_n}(1)=\mathbf{H}_{A_n}{}^*(1)-\int(e^2/r_{12})\alpha_n{}^2(2)d\nu_2. \quad (33)$$

Here $\mathbf{H}_{A_n}{}^*(1)$ is the (assumed) spherically symmetric potential of a neutral carbon atom A_n. Substituting this in (32), one finds

$$\epsilon_\pm=W_{2p}-(\sigma_\pm)^{-1}[(A_1:\alpha_2\alpha_2)\pm(A_1:\alpha_1\alpha_2)+(\alpha_1\alpha_1;\alpha_2\alpha_2)\pm(\alpha_1\alpha_1;\alpha_1\alpha_2)], \quad (34)$$

where

$$(A_1:a_p\alpha_{p'})=-\int\mathbf{H}_{A_1}{}^*(\nu)\alpha_p(\nu)\alpha_{p'}(\nu)d\nu,$$
$$=(A_1:\alpha_{p'}\alpha_p). \quad (35)$$

There remains to make explicit the dependence of the various integrals on the angle φ. To do this, one may note from (1) that

$$\begin{aligned}
S_{\alpha_1\alpha_2}&=\cos\varphi S_{a_1a_2},\\
(A_1:\alpha_2\alpha_2)&=(A_1:a_2a_2),\\
(A_1:\alpha_1\alpha_2)&=\cos\varphi(A_1:a_1a_2),\\
(\alpha_1\alpha_1;\alpha_1\alpha_1)&=(a_1a_1;a_1a_1),\\
(\alpha_1\alpha_1;\alpha_2\alpha_2)&=\cos^2\varphi(a_1a_1;a_2a_2)+\sin^2\varphi(a_1a_1;a_{2s}a_{2s}),\\
(\alpha_1\alpha_2;\alpha_1\alpha_2)&=\cos^2\varphi(a_1a_2;a_1a_2)+\sin^2\varphi(a_1a_{2s};a_1a_{2s}),\\
(\alpha_1\alpha_1;\alpha_1\alpha_2)&=\cos\varphi(a_1a_1;a_1a_2).
\end{aligned} \quad (36)$$

[Integrals such as $S_{a_1a_{2s}}$, $(a_1a_1;a_2a_{2s})$, and $(A_1:a_1a_{2s})$ are zero by symmetry.] Hence

$$\epsilon_\pm=W_{2p}-(1\pm\cos\varphi S_{a_1a_2})^{-1}\times\{(A_1:a_2a_2)\pm\cos\varphi[(A_1:a_1a_2)+(a_1a_1;a_1a_2)]+\cos^2\varphi(a_1a_1;a_2a_2)+\sin^2\varphi(a_1a_1;a_{2s}a_{2s})\}, \quad (37)$$

$$\gamma_{\pm\pm}=(1/2)(1\pm\cos\varphi S_{a_1a_2})^{-2}\times\{(a_1a_1;a_1a_1)\pm4\cos\varphi(a_1a_1;a_1a_2)+\cos^2\varphi[(a_1a_1;a_2a_2)+2(a_1a_2;a_1a_2)]+\sin^2\varphi[(a_1a_1;a_{2s}a_{2s})+2(a_1a_{2s};a_1a_{2s})]\}, \quad (38)$$

$$\gamma_{+-}=(1/2)(1-\cos^2\varphi S_{a_1a_2}{}^2)^{-1}\times\{(a_1a_1;a_1a_1)+\cos^2\varphi[(a_1a_1;a_2a_2)-2(a_1a_2;a_1a_2)]+\sin^2\varphi[(a_1a_1;a_{2s}a_{2s})-2(a_1a_{2s};a_1a_{2s})]\}, \quad (39)$$

$$\delta_{+-}=(1/2)(1-\cos^2\varphi S_{a_1a_2}{}^2)^{-1}\times\{(a_1a_1;a_1a_1)-\cos^2\varphi(a_1a_1;a_2a_2)-\sin^2\varphi(a_1a_1;a_{2s}a_{2s})\}. \quad (40)$$

Combination of these expressions as required by (12), (15)–(17), and (23)–(24) gives the energy levels as function of φ.

As atomic wave functions one may take[5]

$$\begin{aligned}
a_1(\nu)&=(Z^5/32\pi)^{\frac{1}{2}}a_{1\nu}\times\exp(-Za_{1\nu}/2)\sin\theta_{a_{1\nu}}\cos\phi_\nu,\\
a_2(\nu)&=(Z^5/32\pi)^{\frac{1}{2}}a_{2\nu}\times\exp(-Za_{2\nu}/2)\sin\theta_{a_{2\nu}}\cos\phi_\nu,\\
a_{2s}(\nu)&=(Z^5/32\pi)^{\frac{1}{2}}a_{2\nu}\times\exp(-Za_{2\nu}/2)\sin\theta_{a_{2\nu}}\sin\phi_\nu,
\end{aligned} \quad (41)$$

where $a_{n\nu}$, $\theta_{a_{n\nu}}$, ϕ_ν are polar coordinates of electron ν with respect to a coordinate system fixed at nucleus A_n. One then finds that all of the integrals which appear in (37)–(40) are to be found in the literature or can be calculated by methods given in the literature. These integrals will be discussed in detail elsewhere; suffice it here to tabulate the ones needed as functions of the screening constant Z and the

TABLE III. Energy levels of planar and perpendicular ethylene (electron volts) for $R=1.353$A.

Level		Z	Energy-energy of planar N level (electron volts) 2.35	3.18	3.27	3.91
Planar	1		0.3	1.3	1.4	3.0
	2		19.1	13.8	13.4	11.2
	N		0	0	0	0
	T		7.0	3.1	2.8	2.2
	V		12.3	11.5	11.5	12.7
	Z		19.4	15.0	14.8	14.1
Perpendicular	1		6.0	6.2	6.1	6.6
	2		6.0	6.2	6.1	6.6
	N		3.7	2.2	1.9	0.9
	T		3.5	2.1	1.8	0.9
	V		8.1	10.0	10.2	12.3
	Z		8.3	10.1	10.3	12.3

parameter

$$\rho=ZR, \tag{42}$$

where R is the carbon-carbon distance. This is done in Table I.

In Table II the integrals (37)–(40) over molecular orbitals are tabulated as functions of ρ and Z both for planar ($\varphi=0$) and perpendicular ($\varphi=\pi/2$) ethylene. Energies of the various states of the molecule relative to the ground state N of the planar configuration calculated for $R=1.353$A (the experimental value for the internuclear distance in the ground state[10]) from the integrals in Table II, are given in Table III, and plotted in Fig. 1 for $Z=3.18$. The value of Z is quite arbitrary; 3.18 was found by Zener[11] to be the best value in an isolated carbon atom, but may not be the best value for carbon in a molecule. Moreover, both R and Z probably change[12,13] between normal and excited states. Lacking further information one may as well assume constant values for both.

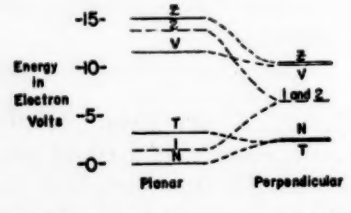

FIG. 1. Energy levels of ethylene: $R=1.353$A, $Z=3.18$.

[10] W. S. Gallaway and E. F. Barker, J. Chem. Phys. **10**, 88 (1942).
[11] C. Zener, Phys. Rev. **36**, 51 (1930).
[12] R. S. Mulliken and C. A. Rieke, Rev. Mod. Phys. **14**, 259 (1942).
[13] R. S. Mulliken, J. Chem. Phys. **3**, 517 (1935).

Table III and Fig. 1 indicate that the planar configuration is more stable than the perpendicular one, as is generally accepted. Qualitatively, Fig. 1 agrees very well with the energy level scheme found by Mulliken,[3] but quantitatively it leaves something to be desired. Experimentally,[3]

$$[E_V-E_N]_{\varphi=0}=7.6 \text{ ev}.$$

The calculated value for $Z=3.18$ is 11.5 volts.[14] Also the calculated $T-V$ splitting is too large. This result is typical of molecular orbital calculations.[1] The dotted lines in the figure indicate how the $\varphi=0$ levels pass continuously into the $\varphi=\pi/2$ ones. (Actual values of the energies for any given value of φ could be calculated from the formulas given above.)

THE TWISTING FORCE CONSTANT AND TWISTING FREQUENCY OF ETHYLENE

Twisting force constants for the various states of the ethylene molecule may be defined as second derivatives of the energy:

$$k_N=(\partial^2E_N/\partial\varphi^2)_{\varphi=0}, \tag{43}$$

$$k_1=(\partial^2E_1/\partial\varphi^2)_{\varphi=0}, \tag{44}$$

etc. From (23), the relation between k_N and the other force constants is found to be

$$2k_N=(k_1+k_2)+(1+\kappa^2)^{-\frac{1}{2}}(k_1-k_2) -\kappa(1+\kappa^2)^{-\frac{1}{2}}(k_V-k_T) \tag{45}$$

where

$$\kappa=[(E_V-E_T)(E_2-E_1)^{-1}]_{\varphi=0}. \tag{46}$$

If κ were zero, k_N would be equal to k_1.

k_1, k_2, k_V, and k_T may be obtained from (12) and (15)–(17). Indeed,

$$\begin{aligned} k_1&=2k_{\epsilon+}+k_{\gamma++},\\ k_2&=2k_{\epsilon-}+k_{\gamma--},\\ k_V&=k_{\epsilon+}+k_{\epsilon-}+k_{\gamma+-}+k_{\delta+-},\\ k_T&=k_{\epsilon+}+k_{\epsilon-}+\gamma_{+-}-k_{\delta+-}; \end{aligned} \tag{47}$$

where, by (37)–(40),

$$\begin{aligned} k_{\epsilon\pm}&=(\partial^2\epsilon_\pm/\partial\varphi^2)_{\varphi=0}\\ &=(1\pm S_{a_1a_2})^{-2}\{[\pm(A_1:a_1a_2)\\ &\quad+2(a_1a_1;a_2a_2)-2(a_1a_1;a_{2s}a_{2s})\\ &\quad\pm(a_1a_1;a_1a_2)]\pm S_{a_1a_2}[-(A_1:a_1a_2)\\ &\quad+(a_1a_1;a_2a_2)-2(a_1a_1;a_{2s}a_{2s})]\}, \end{aligned}$$

[14] Hartmann's value (corrected as required by reference 7) is 8.54 ev, but he used values for certain integrals different from those given in Table I.

$$k_{\gamma\pm\pm}=(\partial^2\gamma_{\pm\pm}/\partial\varphi^2)_{\varphi=0}$$
$$=(1\pm S_{a_1a_2})^{-3}\{[\mp 2(a_1a_1;\,a_1a_2)$$
$$-(a_1a_1;\,a_2a_2)-2(a_1a_2;\,a_1a_2)$$
$$+(a_1a_1;\,a_{2s}a_{2s})+2(a_1a_{2s};\,a_1a_{2s})]$$
$$\pm S_{a_1a_2}[(a_1a_1;\,a_1a_1)\pm 2(a_1a_1;\,a_1a_2)$$
$$+(a_1a_1;\,a_{2s}a_{2s})+2(a_1a_{2s};\,a_1a_{2s})]\},\quad(48)$$

$$k_{\gamma+-}=(\partial^2\gamma_{+-}/\partial\varphi^2)_{\varphi=0}$$
$$=(1-S_{a_1a_2}{}^2)^{-2}\{[-(a_1a_1;\,a_2a_2)$$
$$+2(a_1a_2;\,a_1a_2)+(a_1a_1;\,a_{2s}a_{2s})$$
$$-2(a_1a_{2s};\,a_1a_{2s})]+S_{a_1a_2}{}^2[-(a_1a_1;\,a_1a_1)$$
$$-(a_1a_1;\,a_{2s}a_{2s})+2(a_1a_{2s};\,a_1a_{2s})]\},$$

$$k_{\delta+-}=(\partial^2\delta_{+-}/\partial\varphi^2)_{\varphi=0}$$
$$=(1-S_{a_1a_2}{}^2)^{-2}\{[(a_1a_1;\,a_2a_2)$$
$$-(a_1a_1;\,a_{2s}a_{2s})]+S_{a_1a_2}{}^2[(a_1a_1;\,a_{2s}a_{2s})$$
$$-(a_1a_1;\,a_1a_1)]\}.$$

The force constants are thus all expressible in terms of the quantities in Tables I and II; Table IV gives them as functions of ρ and Z.

The formula relating twisting frequencies ω and force constants k is[15]

$$\omega=(1/\pi c)(k/I)^{\frac{1}{2}},\quad(49)$$

where c is the velocity of light, I is the total moment of inertia about the carbon-carbon axis, and ω is in wave numbers (cm^{-1}). With $R=1.353$A, HCH angle $=119°\,55'$ and CH distance $=1.071$A,[10] one finds $I=5.7535\times10^{-40}$ g/cm^2, and then obtains from (49)[16]

$$\omega=2066k^{\frac{1}{2}},\quad(50)$$

where k is in atomic units and ω in wave numbers (cm^{-1}). Values of ω for the pseudo-ground state Ψ_1 and the ground state Ψ_N calculated by (50) from the force constants in Table IV, with $R=1.353$A, are given in Table V and plotted in Fig. 2.

The actual (experimental) value of ω is in doubt. The value usually accepted[17] is *ca.* 825 cm^{-1}, but Rasmussen and Brattain have pointed out that 950 cm^{-1} is also possible.[18] The present results are too approximate to aid in settling the assignment.

[15] W. G. Penney, Proc. Phys. Soc. **46**, 333 (1934).
[16] One atomic unit $=2.1792\times10^{-11}$ ergs, $c=2.9977\times10^{10}$ cm/sec.
[17] G. Herzberg, *Infrared and Raman Spectra of Polyatomic Molecules* (D. Van Nostrand Company, Inc., New York, 1945), p. 328.
[18] R. S. Rasmussen and R. R. Brattain, J. Chem. Phys. **15**, 120 (1947).

TABLE IV. Force constants of planar ethylene (atomic units).

Force constant	ρ	6	8.13	8.37	10
$Z^{-1}k_{\epsilon_+}$		+0.07143	+0.04907	+0.04625	+0.03129
$Z^{-1}k_{\epsilon_-}$		−0.35739	−0.10730	−0.09755	−0.04233
$Z^{-1}k_{\gamma_{++}}$		−0.00415	−0.00266	−0.00234	−0.00020
$Z^{-1}k_{\gamma_{--}}$		−0.02222	−0.02317	−0.02188	−0.01352
$Z^{-1}k_{\gamma_{+-}}$		−0.02098	−0.00568	−0.03396	−0.00303
$Z^{-1}k_{\delta_{+-}}$		−0.02971	−0.00950	−0.00884	−0.00270
$Z^{-1}k_1$		+0.13871	+0.09548	+0.09016	+0.06238
$Z^{-1}k_2$		−0.73700	−0.23777	−0.21698	−0.09818
$Z^{-1}(k_V-k_T)$		−0.05942	−0.01900	−0.01768	−0.00540
$Z^{-1}k_N$		+0.13021	+0.07283	+0.06604	+0.03062

DISCUSSION

Penney[19] discussed the ethylene molecule many years ago in some detail, employing both the HLSP method and a molecular orbital procedure. Considering the problem as a twelve-electron one, he showed by both methods that the stable configuration of the molecule is the planar structure involving sp^2 hybridization and $\pi\pi$-bonding (as assumed above). From his HLSP treatment, Penney obtained the dependence of the energy on the angle φ, finding approximately that

$$E_\varphi-E_0=(3/2)J\sin^2\varphi,\quad(51)$$

where J is a certain exchange integral that had been previously evaluated by Bartlett.[20] To the simple harmonic approximation,. (51) gives for the twisting force constant

$$k=3J,\quad(52)$$

so that by (50)

$$\omega=3578J^{\frac{1}{2}}.\quad(53)$$

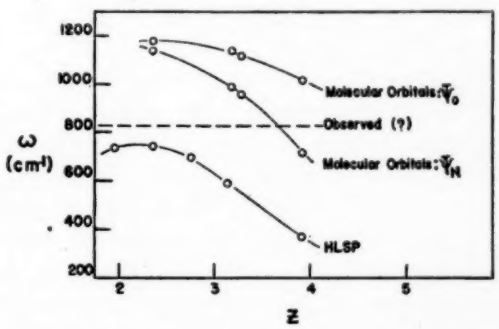

FIG. 2. Calculated twisting frequency of ethylene. Upper curve should be labeled Ψ_1.

[19] W. G. Penney, Proc. Roy. Soc. **A144**, 166 (1934); also reference 15.
[20] J. H. Bartlett, Phys. Rev. **37**, 507 (1931). In Bartlett's notation $J=I_2$.

TABLE V. Twisting frequency of ethylene (cm^{-1}) calculated by the method of molecular orbitals for $R=1.353A$.

State	Z 2.35	3.18	3.27	3.91
Ψ_1	1180	1140	1120	1020
Ψ_N	1140	995	960	715

Penney used this formula to determine J. Alternatively, one can employ it to compute theoretical values of ω from calculated values of J. Results of some calculations using this approach are given in Table VI and plotted in Fig. 2.

It is interesting, but probably not significant, that the molecular orbital and HLSP results bracket the observed value of ω. Decrease of ω with increase in Z for large Z might have been expected in both methods because an increase in Z causes a shrinkage of the $2p\pi$-orbitals and consequently a decrease in the overlap between them and the strength of the $\pi\pi$-bond.

The molecular orbital results are definitely encouraging, especially in view of the following considerations:

(1) One might expect Z in ethylene to be slightly larger than the optimum value 3.18 for an isolated carbon atom. For the electrons in the trigonal bonds in the planes of the CH_2 group should have relatively little screening effect on the $2p\pi$-electrons in orbital perpendicular to those planes.

(2) The amount of perturbation of the state Ψ_1 by the state Ψ_N is largely determined by the quantity κ, which is directly proportional to the T-V splitting. Because the latter comes out too large, κ is too large, and the calculated decrease in force constant too great. The best molecular orbital curve therefore probably lies between the two curves in Fig. 2.

(3) For the distorted ethylene molecule the true $\pi\pi$-bond is not a simple combination of $2p$ orbitals perpendicular to the CH_2 groups (as assumed in the calculation above) but a mixed bond which involves p orbitals in the planes of these groups. This gives rise to an increased stability of the distorted molecule, as has indeed been shown by Mulliken.[3] Since this has not been included in the above calculation, the computed frequency would on this account be expected to be high.

TABLE VI. Twisting frequency of ethylene (cm^{-1}), calculated by HLSP method for $R=1.353A$.

Z	J[a]	ω
1.17	−0.096	imaginary
1.96	0.0425	738
2.35	0.0430	742
2.74	0.0381	698
3.13	0.0269	587
3.91	0.0109	374

[a] J values are from Bartlett, reference 20, and are in atomic units.

For immediate results on ethylene, the semi-empirical approach of Mulliken[3] should be preferred to the present approach. The latter uses fewer extra-geometrical empirical results, however, and so is a step towards the ideal "first principle" treatment.

ACKNOWLEDGMENT

The authors are grateful to Professor R. S. Mulliken for several helpful suggestions.

THE JOURNAL OF CHEMICAL PHYSICS VOLUME 16, NUMBER 5 MAY, 1948

A Search for Spectral Absorption in Active Nitrogen

R. EDWIN WORLEY*
University of California, Berkeley, California

(Received February 6, 1948)

The problem of absorption through active nitrogen has been re-attacked, using a 13-meter path, at pressures of a few millimeters. A supplementary observation of the O_2 "atmospheric" bands indicated that an *allowed* transition would have been detected at a concentration of 10^{10} molecules/cm^3 in the initial vibrational level. Absence of the $0-0$ band of N_2^+ implies that the (unexcited) ion is not a primary carrier of the energy, as was proposed by Mitra. Failure to observe first positive bands (N_2, $B\,^3\Pi \leftarrow A\,^3\Sigma$) is discussed. A speculation is advanced concerning the activated molecules.

INTRODUCTION

SEVERAL unsuccessful attempts have been made to detect metastable atoms or molecules in active nitrogen by observing the absorption spectrum.[1,2] Theories of active nitrogen have usually postulated such particles as the active centers or energy carriers, although a recent suggestion proposes the molecular ion.[3] Inasmuch as a positive result in absorption should provide some direct evidence concerning the mechanism of excitation and afterglow, it was felt that a reinvestigation, using a substantially longer optical path than has been previously reported, would be worth while. Specifically, the experiments were designed to test for: (1) absorption by the small fraction of metastable molecules known to arrive in the $A\,^3\Sigma$ state as a result of the afterglow; (2) absorption by ions in the $X\,^2\Sigma$ state (Mitra's ion theory); (3) unsuspected absorption in the ranges studied, *viz.* λλ3600–4200; λλ4550–10950.

The negative result obtained in every case is believed to emphasize again a view made plausible by the more recent studies of Rayleigh,[4] *viz.* that ions, and *low lying* metastable molecules (or atoms) play only a secondary or indicative role in the phenomena of active nitrogen. These matters will be reviewed after describing the experiment.

EXPERIMENTAL ARRANGEMENT

The absorption tube, diagrammed in Fig. 1, utilizes the mirror system of Smith and Marshall.[5] M_0 is a concave mirror of 130-cm focus; M_1, M_2 are plane mirrors. All three were of glass, coated with an aluminum alloy (95 percent Al, 5 percent Mg), and held in adjustable mounts of nickel-plated brass.[6] The optical path was 13 meters (ten traversals, 14 reflections).

A vertical-ribbon tungsten projection lamp, operated at 20 percent current overload, provided the continuum in the visible and near infra-red. Jena filters (GG-2 or OG-2) passed only the first order in the region photographed. A hydrogen arc continuum was used in the second order of the grating to test for the $0-0$ band of N_2^+ at λ3914. The spectrograms were made with a red-concentrating Wood's grating of 3-meter radius and theoretical resolving power 80,000; (1st-order dispersion, ~5.5 A/mm). Care was taken to assure an accurate focus over the central portion of 18″ plates.

Nitrogen was drawn from a cylinder of water-pumped gas (Linde) and passed over moist red phosphorus to remove residual oxygen; it was dried by passage through tubes of $CaCl_2$ and

* Currently, Research Associate, University of Southern California, Los Angeles, California.

[1] Molecular absorption: K. F. Bonhoeffer and G. Kaminsky, Zeits. f. phys. Chemie **127**, 385 (1927); A. E. Ruark, P. D. Foote, P. Rudnick, and R. L. Chenault, J. Opt. Soc. Am. **14**, 17 (1927); see also A. A. Frost and O. Oldenberg, Phys. Rev. **48**, 66 (1935).

[2] Atomic absorption: W. S. Herbert, G. Herzberg, and G. A. Mills, Can. J. Research **15**, 35 (1937); B. M. Anand, P. N. Kalia, and Mela Ram, Indian J. Phys. **17**, II, 69 (1943).

[3] S. K. Mitra, *Active Nitrogen—A New Theory* (Indian Press, Calcutta, 1945). It was a reading of this review that stimulated my interest in the absorption problem.

[4] Lord Rayleigh, Proc. Roy. Soc. **151**, 567 (1935); **176**, 1, 16 (1940); **180**, 123, 140 (1942).

[5] H. D. Smith and J. K. Marshall, J. Opt. Soc. Am. **30**, 338 (1940). The mirror assembly used was kindly loaned by Professor Harvey White.

[6] Preliminary tests had shown that these surfaces did not noticeably impair the afterglow.

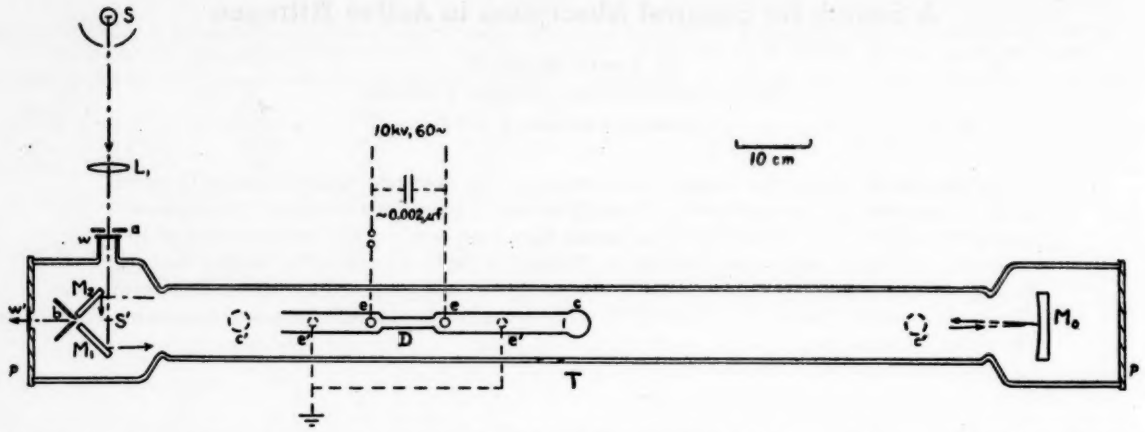

FIG. 1. Absorption tube and optical system (viewed from above). The tube T was of heavy-walled Pyrex, closed by nickel-plated brass end plates p, p fitted with Neoprene gaskets. Purified nitrogen was activated by a condensed discharge in side tube D, mounted just above T. e, e are the high tension electrodes of tungsten rod, with tantalum skirts; e', e' are grounded electrodes used to confine the discharge. The activated gas entered T through a right-angle bend at c (~30-cm path), and was withdrawn at c', c'; it was deactivated before reaching the pumps by a plug of oxidized copper screen.

Light from S, focused to S' by lens L_1, traversed the tube ten times by reflections at mirrors M_1, M_0, M_2, and was imaged at the exit aperture b. It then passed through a filter, and a lens L_2 (not shown), to the spectrograph slit ~80 cm from b. w, w' were quartz windows. External shields and apertures a, b, served to reduce stray light.

P_2O_5. A fritted-glass filter, preceding the drying tubes, cushioned the flow and removed a fine yellow dust evidently carried over from the phosphorus. A slant-arm mercury manometer in the inlet, calibrated *in situ*, gave the pressure. Although a mercury circulating pump was used in preliminary work, it was found convenient simply to draw the nitrogen out by means of a Megavac mechanical pump. Usually the gas passed through a single trap in liquid nitrogen just before entering the (continuously operated) activating discharge shown at D, Fig. 1. The precautions for purification were *not* sufficient to eliminate spectroscopic traces of mercury vapor, nor of oxygen, during the work at large dispersion.[7]

Success in filling the absorption tube with glowing gas depended, in order of importance, on the pressure, the wall coating, and the rate of pumping. A metaphosphoric acid coating was applied for most of the work, and a good filling was usually obtained at pressures from 2 to 6 mm.[8] Within reasonable limits, the pumping rate was not critical.

A striking phenomena was observed when the inlet cock was opened suddenly, with the pressure in D and T comparatively low. With the momentary pressure blast, the characteristic orange glow was displaced downstream, and was first visible some 20 cm beyond the discharge (near c, Fig. 1), corresponding to a time lag of about 10^{-2} sec.[9] The glow quickly returned to the discharge (e–e, Fig. 1) as the velocity of the gas fell off. This phenomenon clearly supports a secondary-reaction theory, for the afterglow.

RESULTS

Table I shows the four spectral ranges studied, and lists the experimental details for each. It will be seen that exposures in the visible and red were short. The slowness of Z plates made longer exposures necessary in the infra-red. In the ultraviolet, weakness of the 2nd-order hydrogen continuum, and diminished reflectance of the mirrors,[10] made for long exposures, even on sensitive IIa-O plates. A sensibly constant pressure was maintained during these long exposures.

[7] Initial low dispersion spectrograms showed only CN bands in the ultraviolet, with weak Hg 2536, but at the conclusion of the experiments, NO β bands were prominent.

[8] The intensity in the exhaust tubes was, however, much less than at the inlet. It is believed that the acid wall coating passed partially to ordinary phosphoric acid, as it yielded only a moderate improvement of the afterglow.

[9] The gas velocity was taken as 10 times the final, steady value of 1 or 2 meters/sec.

[10] The ultraviolet limit of 3600A was presumably set by the decrease in reflectance. In preliminary low dispersion work, the range extended to 2900A, but no absorption, such as might occur at the heads of strong bands, was found. Further work in the Schumann region is desirable in order to test for molecules in the metastable $a\ ^1\Pi_g$ state (G. Herzberg, Phys. Rev. **69**, 362 (1946)).

The last column refers to positive tests for absorption in the visible, near infra-red, and red. These were: (1) the *D*-lines, from a small sodium flame placed just before either L_1 or L_2 (Fig. 1); (2) faint rotation-vibration lines of water vapor, near λλ9400, 8200, and 7200, due to the external 7-meter air path;[11] (3) the forbidden *A* band of O_2 at λ7600, due also to the air path. A similar check was not made in the ultraviolet, but there seems no reason to question the results for the range indicated. An over-all test of the absorption system was made at the end of the series by filling the tube first with dry air, then with dry oxygen at atmospheric pressure. Enhancement of the *A* band, above, was pronounced, and in the latter case the *B* band at λ6880 appeared faintly.

Absorption due to active nitrogen was not observed in any of the regions photographed. The visible range is significant because it includes the (stronger) predicted first positive bands ($B\,^3\Pi \leftarrow A\,^3\Sigma$) that would originate on levels 6, 7, 8 of $A\,^3\Sigma$; these are the vibrational levels most favored by the afterglow transitions. It is shown that observable absorption would have implied a minimum (actual) life for state *A* of the order 10^{-3} sec.

If a molecule in $A\,^3\Sigma$ were to survive 10^{-3} sec., it would experience some 10^4 or 10^5 collisions at the pressures used. Hence, a vibrational redistribution, with lower energies favored, might occur. A test was accordingly made for the *0−0* and *1−0* first positive bands (heads at λλ10491, 8912)[12] but no clear indication of absorption was found.

The instrument focus for the 2nd-order ultraviolet was the same as for the first-order red (below). The best plate was a four-hour exposure at a nitrogen pressure of 6 mm, slit ∼0.015 mm. The continuum was of only moderate intensity, but there was no confusion from emission bands near λ3900. Hence there is believed to be no doubt as to the absence of the *0−0* absorption band of N_2^+ at λ3914.

No nitrogen absorption was found in the red region, but oxygen absorption due to the external air path provided a reference for evaluating the sensitiveness of the tests. About one-fourth the actual concentration in the 7-meter air path would have sufficed for detecting the *A* band; this corresponds to $\sim 10^{18}$ molecules/cm³ for the 13-meter instrument path. The measurements of Childs and Mecke,[13] and their interpretation by Van Vleck,[14] show that the intercombination, magnetic dipole transition in O_2 ($^1\Sigma_g^+ \leftarrow {}^3\Sigma_g^-$) is some 10^{-8} as probable as an allowed dipole transition. Hence, one would expect to detect *allowed dipole* absorption from a given initial vibrational level, at a concentration in that level of $c_0 \sim 10^{10}$ molecules/cm³.[15] Thus, the experimental method is seen to be quite sensitive.

Account must now be taken of the fact that only a small fraction of the N_2 molecules pass through the afterglow transition. In an arrangement rather similar to mine (internal electrodes, 6-mm pressure), Herbert, Herzberg, and Mills[2] measured about 5×10^{14} quanta/cm³/sec. from the visible afterglow. If this represented a region near the discharge tube, the *average* intensity for my absorption tube was considerably less. It may be assumed, however, that a mean of at least 10^{13} molecules/cm³/sec. reached state *A*.[16] If now *t* is an effective mean life of state *A* for the prevailing experimental conditions, the concentration would be $10^{13}t$. To obtain the life *needed* for detectable absorption, this is equated

TABLE I.

Wave-length Range	Slit width	Plate type	Exposures required	Nitrogen pressures	Check test
Visible 4550–6800	0.01 mm	panchro. (18″) 103-F (10″)	10 min. 1 min.	2–6 mm	sodium flame
Near i. r. 8600–10950	0.02 mm	Z (18″) (hypersens.)	2–3 hrs.	3–6 mm	water vapor
Red 6500–8900	0.01 mm	I-N (18″)	2 min.	3–4 mm	O_2 band; water vapor
Near u. v. 3600–4200 (2nd order)	0.015 mm	IIa-O (10″)	3–4 hrs.	4–6 mm	—

[11] The equivalent path for water vapor was ∼100 mm-atmos. (hygrometric data kindly supplied by Professor John Leighly).

[12] A. H. Poetker, Phys. Rev. **30**, 812 (1930).

[13] W. H. J. Childs and R. Mecke, Zeits. f. Physik **68**, 344 (1931).

[14] J. H. Van Vleck, Astrophys. J. **80**, 161 (1934).

[15] The single-level restriction relates to the fact that in O_2 ∼90 percent of the absorption occurs in one band.

[16] A figure of 10^{13} is given also by Rayleigh's measurements at lower pressures, if the *ratios* of active to inert particles are assumed independent of pressure. (The molecules remained in the absorption tube several seconds, long enough for most to undergo transition.)

to the required concentration c. Here $c=c_0$ (above), or $c\sim 10c_0$, according as the molecules are distributed chiefly in a single, or in several vibrational levels. One thus finds for t, 10^{-3} or 10^{-2} sec., respectively. A rough estimate of the *spectroscopic* life of state A (effect of collisions, neglected) gives 10^{-4} to 10^{-3} sec.[17] Hence it appears that a 10-fold increase in optical path should yield detectable absorption.[18] Shortening of the inlet tube between e and c (Fig. 1) might be nearly as effective. At the same time, attention should be given to the elimination of mercury vapor, as even small traces may reduce the effective mean life below the spectroscopic value.[19]

DISCUSSION

The studies by Rayleigh, referred to in the Introduction, reveal a phenomenally long life for the afterglow, and a much higher energy content for the gas as a whole than had previously been suspected. In fact, the average energy of $\sim$10 ev per molecule of N_2 admitted[20] is evidently a lower limit to the energy of active centers, if the ionization associated with the afterglow is actually produced in the gas by single processes. However, the ionization and afterglow phenomena together accounted for only a small fraction of the molecules; hence the chief modes by which the active centers dissipate their energy, when wall reactions are avoided, still appear to be unknown.

It is, of course, just the small concentration of molecules in $A\ ^3\Sigma$, inherent in the afterglow process, that has prevented detection of this state by absorption. Even if a positive result were obtained by refinements in technique such as those suggested above, the absorption would be intrinsically weak. Strong absorption from the populous active centers presumably occurs in some unexplored region of the spectrum.

The situation in respect to the N_2^+ ion is different. If one *assumes* these ions to be in fact the active centers, then one must expect them to be present in large concentration. Inasmuch as previous tests, and particularly the one reported here at high resolution, give no indication of the predicted absorption, it seems safe to assume that the ion in $X\ ^2\Sigma$ is *not* the carrier of the energy.[21]

In conclusion, I wish to mention a speculation concerning the mechanism of active nitrogen, which may lend itself to a test. In order to explain the recent evidence for a high concentration of active centers, apparently capable of producing volume ionization, one is led to think of stable, neutral molecules in states above the first ionization limit. The absorption spectrum does, in fact, reveal the existence of such states, for in addition to continuous absorption beyond the ionization limit, a number of narrow bands are found.[22] These levels shown by absorption would hardly be long-lived, but others in the same range might be metastable. In particular, the upper levels of the Rydberg *emission* bands reported by Hopfield[23] and by Takamine, Suga, and Tanaka[24] were attributed by me to "hybrid" and presumably metastable states. An attempt to observe weak emission from these levels by means of a vacuum spectrograph, used with an active nitrogen source, is planned.

I appreciate the courtesy extended by Professor Birge, and the encouragement of Professor Jenkins to work on this problem in the physics department at Berkeley during parts of two summers. I wish to thank Dr. Kasha and Miss Gundelfinger at the chemistry department for the loan of equipment needed on short notice.

[17] I have used simply $\tau\sim(\nu/\Delta\nu)10^{-8}$ sec. For $\Delta\nu$ of $A\ ^3\Sigma$, see S. M. Naudé, Proc. Roy. Soc. **136**, 114 (1932).

[18] In correspondence, Professor Herzberg has called my attention to the feasibility of such an increase in path, by use of the mirror system of J. U. White, J. Opt. Soc. Am. **32**, 285 (1942).

[19] Compare J. Janin, Ann. de physique (Ser. 12) **1**, 570 (1946).

[20] In a more recent paper (Proc. Roy. Soc. **189**, 296 (1947)), Rayleigh reports energies as high as 230 ev/molecule. The new experimental arrangement was designed to avoid loss of energy between exciter and detector, but it seems probable that kinetic energy given electrons (and ions) by the ring discharge may have been passed on to the detector foil. The inverse dependence on pressure favors this explanation. There seems no reason however to question the previous results.

[21] It may also be noted that Mitra's argument for the metastability of $X\ ^2\Sigma_g$, *viz.* that it combines but weakly with the ground state of N_2, is not substantiated here. Thus the A band of O_2 whose upper state has a life of $\sim$10 sec. appeared clearly at $\sim 10^4$ mm-atmos., while with comparable resolution the Rydberg absorption bands of N_2 that converge to $X\ ^2\Sigma_g$ were well developed at 0.2 mm-atmos. (reference 22).

[22] R. E. Worley, Phys. Rev. **64**, 207 (1943).

[23] J. J. Hopfield, Phys. Rev. **36**, 789 (1930).

[24] T. Takamine, T. Suga, and Y. Tanaka, Sci. Pap. Inst. Phys. Chem. Research Tokyo **34**, 854 (1938).

The Solubility of Water in Hydrocarbons

CLINE BLACK,* GEORGE G. JORIS,** AND HUGH S. TAYLOR
Frick Chemical Laboratory, Princeton University, Princeton, New Jersey

(Received February 12, 1948)

The method in which tritium oxide acts as a tracer in the determination of water solubility in hydrocarbons has been used for the measurement of the solubility of water in a number of paraffinic, olefinic, and diolefinic hydrocarbons. The effect of temperature, pressure, size of hydrocarbon molecule, and the constitutive factors have been studied. Solubilities were determined in the temperature range from 5° to 30°C at pressures from 1 to 6 atmospheres.

THE method which is based upon the use of tritium oxide as a tracer in the determination of minute amounts of water has previously been tested in the measurement of the solubility of water in benzene.[1] The same method has now been further applied to the determination of the solubility of water in a series of paraffinic, olefinic, and diolefinic hydrocarbons.

EXPERIMENTAL PROCEDURE

1. Radioactive Water

The radioactive water was from the same sample used in the preceding study:[1] it was deuterium oxide containing about 10^{-12} mole per mole of tritium oxide.

2. Hydrocarbons

The hydrocarbons were of the highest purity available. The liquid hydrocarbons were, for the most part, samples of pure compounds produced at The Ohio State University under an American Petroleum Institute project. The samples of heptene-1 and hexadiene-1,5 were kindly provided by Professor G. B. Kistiakowsky of Harvard University. The butanes, butenes, and the butadiene-1,3 were hydrocarbons from the Phillips Petroleum Company, available in cylinders, and shown by mass-spectrometer analysis to be better than 98 percent pure as used.

3. Apparatus and Technique

For the liquid hydrocarbons the apparatus described in the previous paper[1] was again used. For the lower hydrocarbons, a brass apparatus and a slightly different experimental technique were utilized. The all-metal system is shown in Fig. 1.

The saturator *C* was charged by cooling it with liquid air while the chamber was connected to the hydrocarbon supply cylinder, *H*. Since the sample could not be observed during saturation, it was necessary to follow carefully the proved technique employed in the glass system. The sampling device in Fig. 1 consisted of a small brass cylinder (approximately 2.5 cc in volume) connected at each end through $\frac{1}{8}$-in. copper tubes to "Baby Hoke Valves." It was connected to chamber *C* by means of the flanged pressure connector *b*. The upper end of the sample tube was connected through a Kovar tube to the male section of a ground glass joint which provided a connection to the vacuum system. The sampling device could withstand high pressure or high vacuum without leakage.

The circulation rate of the vapors in this system was of the order of 500 cc per minute, and approximately three hours of continuous circulation was required to saturate a hydrocarbon sample with water.

The vacuum system was utilized to draw a fraction of the saturated hydrocarbon liquid from chamber *C* into the sample tube, *T*. After closing valves 4, 3, and 2, the fully charged sample tube was disconnected at *Y* and at *b* and was transferred to the analytical apparatus.

The analytical procedure was similar to that used with liquid hydrocarbons.[1] The amount of hydrocarbon was measured by vaporizing and expanding into a large evacuated system of known volume after it had been freed in the U-tube, *E*, from its water content. From pressure and tem-

* Present address: Shell Development Company, San Francisco, California.
** Present address: Allied Chemical and Dye Central Research Laboratory, Morristown, New Jersey.

[1] G. G. Joris and H. S. Taylor, J. Chem. Phys. 16, 45 (1948).

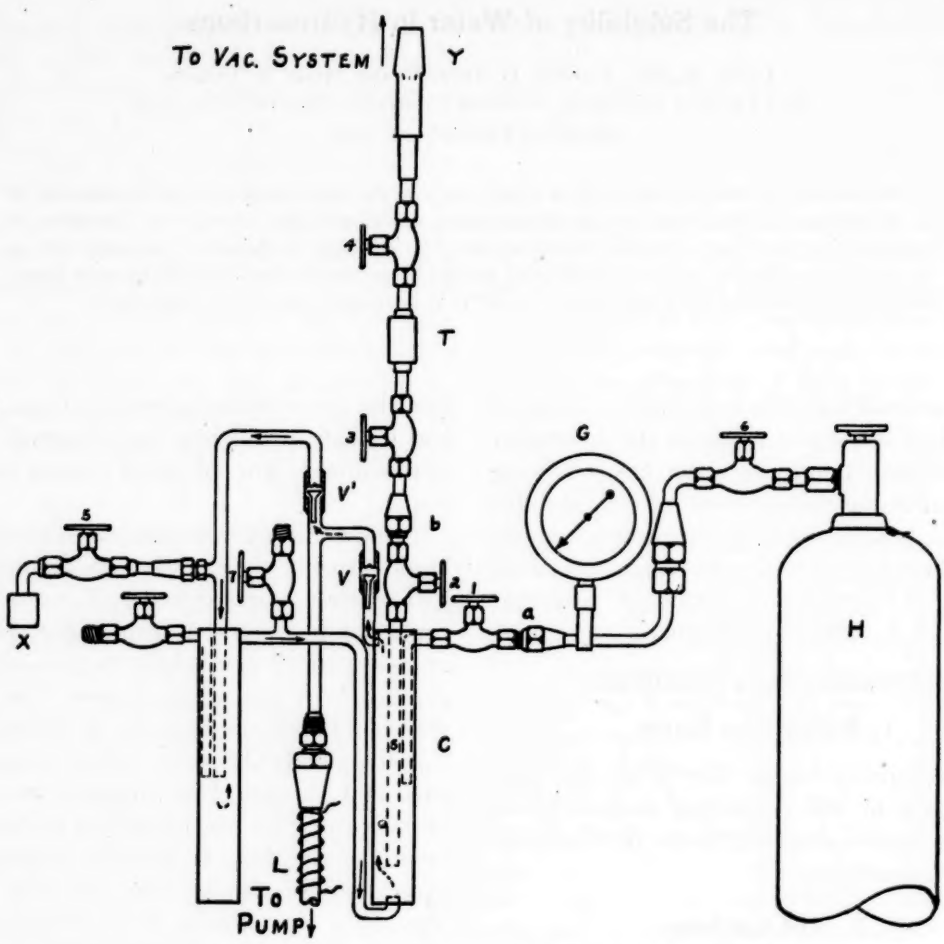

FIG. 1. Apparatus for saturating hydrocarbons with water (all-metal).

perature readings the weight of the hydrocarbon could be calculated. This indirect procedure was necessary because exact quantitative reproducibility could not always be obtained with the sampling device of the all-metal system.

The same technique of radioactivity measurement and of estimation of corrections, as described in the earlier paper, was used.

EXPERIMENTAL RESULTS

The solubility data obtained are recorded in Table I. These data are plotted in the following manner. In Fig. 2† the solubilities in mole percent are plotted as a function of temperature. Figure 3† gives the solubility in grams water per 100 grams of hydrocarbon *versus* the temperature in degrees centigrade. The relationships in Fig. 4† are the result of plotting the logarithm of the solubility (expressed in mole percent) against the reciprocal of the absolute temperature.

The data and their plots emphasize the regularities which exist in the water solubilities of these hydrocarbons. With the normal paraffin hydrocarbons at a given temperature there is a progressive increase in the water solubility in passing from *n*-butane to *n*-octane.

The solubility of water in cyclohexane at 20°C (0.047) is of the same order of magnitude as in *n*-hexane and is in good agreement with results published by Tarassenkow and Poloshinzewa[2] for

† Index of solvents given in Figs. 2, 3 and 4:
⊖ Butadiene-1,3 ◑ N-Butane ⊘ Benzene
⊖ Butene-1 ○ Isobutane ◒ N-Heptane
⊗ Butene-2 ⊙ N-Pentane ◐ Heptene-1
⊘ Isobutylene ●◫ Isopentane ⊜ Hexadiene-1,5
△ Cyclohexane (Data for Tarassenkow and Poloshinzewa (see reference 2.))
— Interpolated for N-Hexane

[2] N. D. Tarassenkow and E. N. Poloshinzewa, Zhur. Obshchei Khim. Khim. Ser. **I**, 71–9 (1931); Chem. Abs. **25**, 4762 (1931); Ber. **65B**, 184–6 (1932); C.A. **26**, 2363 (1932).

TABLE I.

Hydrocarbon (*HC*)	Saturation temp. C	Total sat. press. atmos.	Sat. time hrs.	Solubility mole water per 100 moles *HC*.	Solubility g water per 100 g *HC*.
Butadiene-1,3	7.0	3.7	4.0	0.1466	0.0488
	7.5	3.7	3.0	0.1430	0.0476
	14.0	4.0	4.0	0.1706	0.0568
	15.0	3.7	3.5	0.1700	0.0566
	21.0	4.0	4.5	0.1988	0.0662
	21.0	3.7	3.5	0.1940	0.0646
Butene-1	6.0	3.0	3.0	0.0633	0.0203
	7.5	2.9	3.5	0.0764	0.0245
	14.0	3.3	3.0	0.0957	0.0307
	20.0	3.0	4.0	0.1237	0.0397
	21.5	2.9	4.0	0.1253	0.0402
Butene-2	7.0	2.8	3.0	0.0867	0.0278
	7.5	2.4	3.5	0.0876	0.0281
	14.0	2.8	3.5	0.1123	0.0360
	20.8	2.4	5.5	0.1416	0.0454
	21.0	2.8	4.5	0.1343	0.0431
Isobutylene	6.0	4.0	3.0	0.0717	0.0230
	7.0	4.4	4.0	0.0711	0.0228
	7.0	4.2	3.0	0.0671	0.0215
	14.0	4.0	3.5	0.0998	0.0320
	16.0	4.0	4.0	0.1141	0.0366
	21.0	4.4	6.0	0.1209	0.0388
	21.0	5.0	6.0	0.1200	0.0385
n-butane	5.0	2.7	4.0	0.00775	0.00240
	5.0	2.7	4.0	0.00775	0.00240
	5.5	2.8	2.5	0.00985	0.00305
	14.5	3.1	6.0	0.01227	0.00389
	15.0	3.4	3.8	0.01453	0.00459
	20.0	6.4	4.0	0.02002	0.00620
	20.0	3.4	2.5	0.02220	0.00688
	21.0	3.4	3.5	0.02430	0.00753

TABLE I.—*Continued.*

Hydrocarbon (*HC*)	Saturation temp. C	Total sat. press. atmos.	Sat. time hrs.	Solubility mole water per 100 moles *HC*.	Solubility g water per 100 g *HC*.
Isobutane	7.0	3.4	3.3	0.00898	0.00278
	18.0	3.9	4.3	0.02060	0.00638
	19.0	4.0	3.5	0.02220	0.00688
	21.8	4.0	5.0	0.02695	0.00835
n-pentane*	5.5	1.0		0.0144	0.0036
	15.0	1.0		0.0245	0.0061
	24.8	1.0		0.0477	0.0119
	24.8	1.0		0.0481	0.0120
Isopentane*	15.3	1.0		0.0263	0.0066
	21.3	1.0		0.0383	0.0096
	21.8	1.0		0.0390	0.0097
Isopentane	6.0	1.0	3.5	0.01777	0.00443
	6.0	1.0	4.0	0.01735	0.00433
	6.0	1.0	4.5	0.01762	0.00440
	20.0	1.0	8.0	0.03764	0.00940
	20.0	1.0	4.0	0.03613	0.00902
	20.0	1.0	4.5	0.03770	0.00942
	20.5	1.0	4.0	0.04020	0.01001
Benzene*	10	1.0		0.1305	0.030
	20	1.0		0.1846	0.0425
	20	1.0		0.1932	0.0445
	26	1.0		0.2344	0.0540
n-hexane*	20	1.0		0.053	0.0111
Cyclohexane*	20	1.0		0.047	0.010
n-heptane*	10	1.0		0.0429	0.0077
	20	1.0		0.0757	0.0136
	20	1.0		0.0701	0.0126
	25	1.0		0.0840	0.0151
Heptene-1*	10.0	1.0	6.0	0.3774	0.0692
	20.1	1.0	6.5	0.6139	0.1126
	20.5	1.0	4.5	0.5710	0.1047
	21.2	1.0	6.3	0.6310	0.1158
Hexadiene-1,5*	13.5	1.0	6.0	0.2820	0.0618
	20.2	1.0	7.5	0.4417	0.0969
n-octane*	20	1.0		0.090	0.0142

* Determinations made in glass apparatus.

the solubility of water in cyclohexane. Two points of the Russian data are shown on the graph in Fig. 4.

There is but small variation in solubility with isomerism in the paraffin series, as evidenced by the result of the water solubilities in *n*-butane and isobutane and in *n*-pentane and isopentane. A similar conclusion can be reached for the olefin series as far as it has been investigated, butene-1, butene-2, and isobutylene having water solubilities of about the same magnitude.

The very large increase in water solubility as one passes from the paraffin to the olefin hydrocarbons is illustrated in the water solubilities of the butanes and butenes. A similar increase is noted in passing from *n*-heptane to heptene-1. This effect recalls the increased solubility of oleic acid over stearic acid in water. The attraction of the double bond to the surface with oleic acid films on water is evidence[3] of the affinity of the double bond for water.

Again, as in the paraffin series, the solubility of water in the olefins increases with increasing chain length, as evidenced from the data for the butenes and for heptene-1. It will be noted that the solubilities of water are not additive in the sense of there being a solubility in the hydrocarbon portion of the molecule plus one to be attributed to the attraction of the double bond for the water. Instead, the double bond acts more nearly

[3] I. Langmuir, Met. Chem. Eng. **15**, 469 (1916); J. Am. Chem. Soc. 1848 (1917).

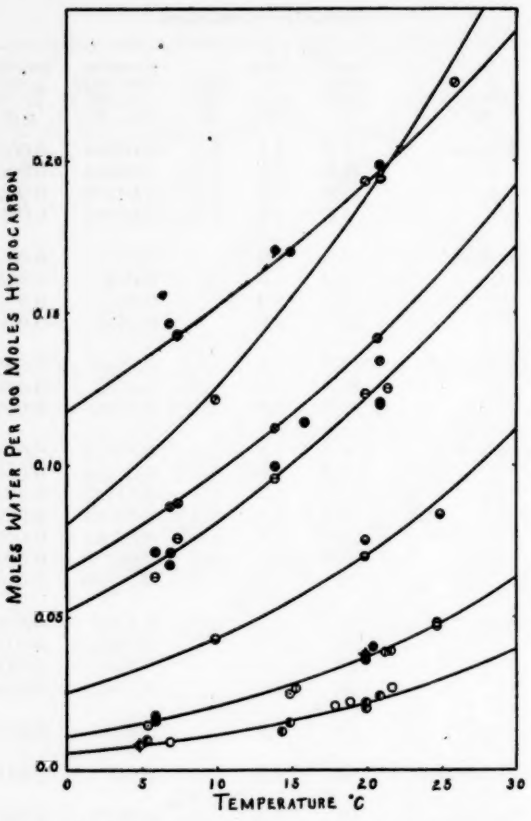

FIG. 2. Solubility of water in hydrocarbons as a function of temperature.

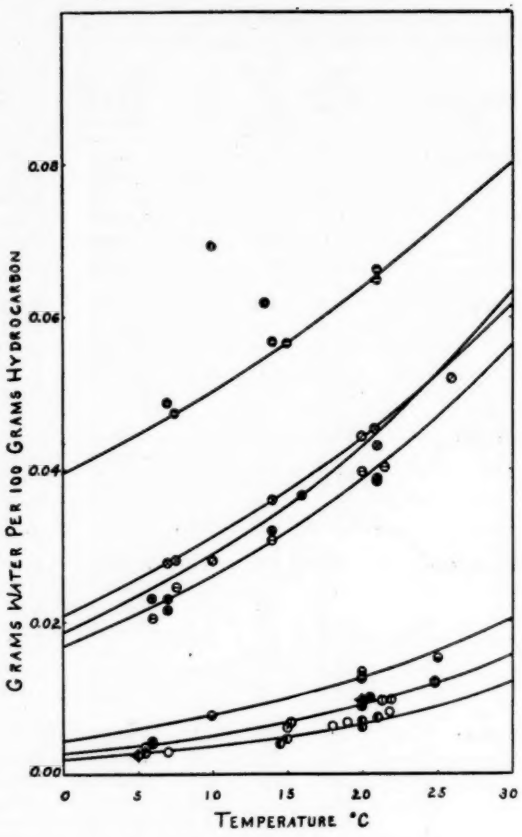

FIG. 3. Solubility of water in hydrocarbons as a function of temperature.

as though it multiplied the solubility of water in the hydrocarbon by some factor.

Butadiene, with two double bonds, shows a further increase of water solubility above that in the butenes, although the effect is not as great as that observed in going from butane to the butene solvents. This might suggest the effect of conjugation of the double bonds in butadiene-1,3. However, hexadiene-1,5 gave analogous results, indicating that conjugation was probably not responsible for this effect.

Near 20°C the molar solubilities of water in benzene and in butadiene-1,3 are of about the same order; with the benzene solvent, however, the solubility shows a steeper temperature coefficient. Qualitative measurements at 20°C indicate that cyclohexene with the single ethylenic linkage shows slightly greater water solubility than benzene with its three conjugated double bonds. Similarly, values for the solubility of water in hexene-1 (as determined by interpolating between values obtained for butene-1 and heptene-1 in Fig. 4) indicate slightly higher solubilities than for the solvent benzene.

DISCUSSION

The variations in the solubility of water from one hydrocarbon to another are well outside the limits of experimental error which are estimated to be of the order of a few percent. The highest molar concentration of water recorded is that in heptene-1 at 20°C; it corresponds to only one molecule of water in 160 molecules of the heptene. It is therefore apparent that, in all the examples studied, the water molecules should be exclusively surrounded by hydrocarbon molecules and should be in a constant environment in a particular hydrocarbon. The tendency of the water molecules to escape into the gaseous phase should, as a consequence, be proportional to their concentration in the hydrocarbon solvent; it will also depend on the interaction between a water molecule and the neighboring hydrocarbon mole-

cules. Since the experimental conditions were such as to maintain constant the vapor pressure of water in the gaseous phase, the variations in solubility with the different hydrocarbons reflect differences of interaction between water and the various hydrocarbon molecules. The assumption implicit in the calculation of solubilities that the Henry's law constants were identical for TDO and for H_2O, thus neglecting the isotope effect, undoubtedly introduces a systematic error into the results. Such an error is, however, obviously too small to vitiate any comparison between the calculated solubilities of water in the various hydrocarbons.

The increase with temperature of the solubilities of water in all the hydrocarbons studied indicates a positive deviation from Raoult's law. Such a deviation is, in general, observed when (a) there is a large difference in the internal pressures of the two substances, (b) the polarity is different, (c) the molecules are dissimilar, and (d) one or both of the substances are associated in the liquid state. Hildebrand, examining the case of components of unequal volumes with differences in internal pressures, obtains[4] the following expression:

$$RT \ln \frac{\alpha_1}{N_1} = V_1 \left(\frac{N_2 V_2}{N_1 V_1 + N_2 V_2} \right)^2 \times \left[\left(\frac{\Delta E_1}{V_1} \right)^{\frac{1}{2}} - \left(\frac{\Delta E_2}{V_2} \right)^{\frac{1}{2}} \right]^2, \quad (1)$$

where $\alpha_1 = f/f_0$, f being the fugacity of the solute in the solution and f_0 the fugacity of the pure solute. N_1 and N_2, V_1 and V_2 are, respectively, the molar concentrations and volumes of solute and solvent, ΔE_1 and ΔE_2 their heats of vaporization. Several assumptions are involved in the derivation of this relation. The repulsion potentials are neglected; the different molecular species are assumed to possess spherical symmetry and to follow the same general type of arrangement; the attraction constants are assumed to be the geometric mean of the constants of like molecules. If this equation were applicable to the present measurements a further simplification could be made since, because of the small solubilities of water in these hydrocarbon systems, $N_1 V_1$ is small compared with $N_2 V_2$, so that

$$RT \ln \frac{\alpha_1}{N_1} = V_1 \left[\left(\frac{\Delta E_1}{V_1} \right)^{\frac{1}{2}} - \left(\frac{\Delta E_2}{V_2} \right)^{\frac{1}{2}} \right]^2. \quad (2)$$

If one makes the further assumption that α_1 is

[4] J. H. Hildebrand, *Solubility* (Reinhold Publishing Corporation, Inc., New York, 1936), Chapter 3, p. 73.

TABLE II.

Hydrocarbon	$(\Delta E/V)^{\frac{1}{2}}$	N_1 10^{-2} mole % calc.	N_1 10^{-2} mole % obs.	$\frac{N_1 \text{ obs.}}{N_1 \text{ calc.}}$
n-butane	6.6	1.66	2.1	1.26
n-pentane	7.0	2.41	3.6	1.49
n-hexane	7.2	2.94	5.3	1.80
n-heptane	7.4	3.70	7.3	1.97
n-octane	7.6	4.46	9.0	2.02
iso-butane	6.15	1.04	2.4	2.3
iso-pentane	6.75	1.95	3.6	1.85
cyclohexane	7.8	5.56	4.65	0.88
toluene	8.9	15.3	22.0	1.44
benzene	9.15	19.0	19.0	1.0
1-butene	7.0	2.41	12.4	5.15
2-butene	6.9	2.29	14.0	6.10
1-heptane	7.7	6.14	57.0	9.3
butadiene	7.6	4.52	19.0	4.2
1–5 hexadiene	8.2	8.4	46.0	5.48

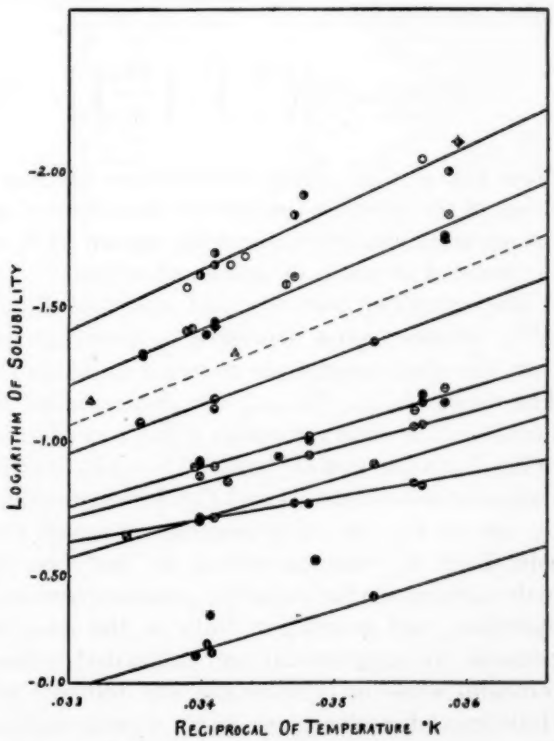

FIG. 4. Logarithm of solubility in mole percent asa function of the reciprocal temperature in degrees Kelvin.

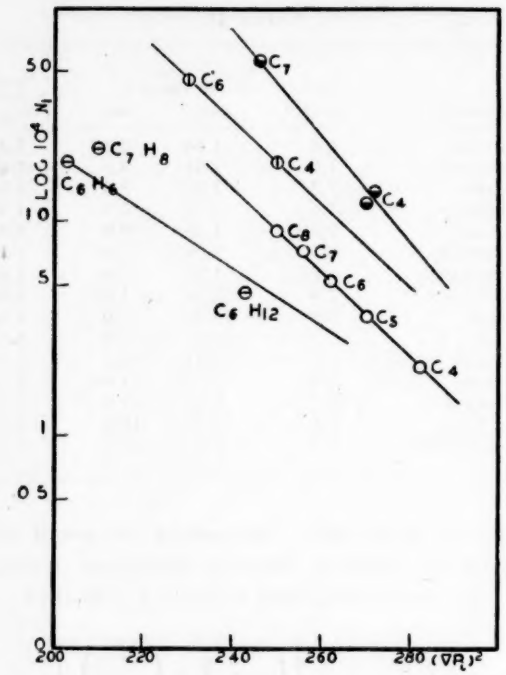

FIG. 5. Logarithm of molar solubilities (10^4) plotted against $[(\Delta E_1/V_1)^{\frac{1}{2}}-(\Delta E_2/V_2)^{\frac{1}{2}}]^2$. ○: *n*-paraffinic hydrocarbons; ◒: olefins; ⊕: diolefins; ⊖: aromatics.

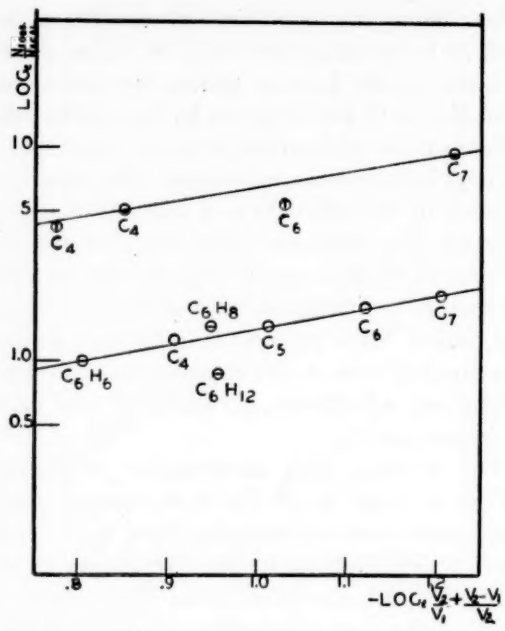

FIG. 6. Logarithm of ratio $N_{1\ \text{obs.}}/N_{1\ \text{calc.}}$ plotted against $-\ln(V_2/V_1)+(V_2-V_1)/V_2$. ○: *n*-paraffinic hydrocarbons; ◒: olefins; ⊕: diolefins; ⊖: aromatics.

unity, one obtains

$$-RT\ln N_1 = V_1\left[\left(\frac{\Delta E_1}{V_1}\right)^{\frac{1}{2}}-\left(\frac{\Delta E_2}{V_2}\right)^{\frac{1}{2}}\right]^2. \quad (3)$$

From Eq. (3), at a given temperature, the logarithm of the solubility should be proportional to the square of the difference of the square roots of the internal pressures of solute and solvent.

The calculated and observed values of N_1 at 20°C, obtained when necessary by interpolation from the observations, are recorded in Table II. The ratios, $N_{1\ \text{obs.}}/N_{1\ \text{calc.}}$, are also recorded in the table. The observed values of $\ln N_1$ are plotted in Fig. 5 as a function of $[(\Delta E_1/V_1)^{\frac{1}{2}}-(\Delta E_2/V_2)^{\frac{1}{2}}]^2$. Examination of Table II and Fig. 5 indicates that by use of Eq. (3) it is possible to group the solubilities of water according to the class of hydrocarbons studied, whether paraffins, olefines, diolefines, and aromatics. Only in the case of benzene do experimental and calculated values coincide, while in cyclohexane and toluene the Hildebrand function gives a fair approximation. The solubilities of water in the paraffin hydrocarbons increase linearly as the internal pressure of the hydrocarbon increases, but the curve falls markedly above the theoretical curve, with the deviations increasing with increasing molecular weight of the solvent. The solubility in the olefines and the diolefines is considerably higher than that calculated from the Hildebrand equation. What is more surprising is that the data for the diolefines lie on a plot intermediate to those of the paraffin and olefine solubilities.

In a recent communication[5] on the entropy of solution of molecules of different size, Hildebrand has related the entropy of mixing and hence the activity to the molal volumes of the two constituents. Hildebrand's expression takes the form

$$\frac{\bar{S}_1}{R}=\ln\frac{N_1(V_1-b_1)+N_2(V_2-b_2)}{N_1(V_1-b_1)} + \frac{N_2[(V_1-b_1)-(V_2-b_2)]}{N_1(V_1-b_1)+N_2(V_2-b_2)}. \quad (4)$$

If the free volumes are proportional to the molal volumes and if we can neglect N_1V_1 in comparison with N_2V_2 by reason of the low solubility, the expression for the activity a_1 becomes, since

[5] J. H. Hildebrand, J. Chem. Phys. **15**, 225 (1947).

$\bar{S}_1 = -R \ln a_1$,

$$\ln a_1 = -\ln \frac{N_2 V_2}{N_1 V_1} + \frac{V_2 - V_1}{V_2}, \quad (5)$$

and the solubility N_1 per mole of solvent with unit activity becomes

$$\ln N_1 = -\ln \frac{V_2}{V_1} + \frac{V_2 - V_1}{V_2}. \quad (6)$$

In Fig. 6 we have plotted the value of the logarithm of the ratio $\ln(N_{1\ \text{obs.}}/N_{1\ \text{calc.}})$ against the function on the right of Eq. (6). It is evident that the hydrocarbons now fall into two classes, the paraffinic and aromatic in one class and the olefinic and diolefinic in the other. The linear relationship is quite satisfactory if one considers the sensitivity of $N_{1\ \text{obs.}}/N_{1\ \text{calc.}}$ to small errors in $N_{1\ \text{calc.}}$ caused by uncertainties in the heats of vaporization used in certain of the calculations, and to the experimental errors in $N_{1\ \text{obs.}}$. The slopes of the two curves are practically the same for the two classes. The net effect of the double bond is constant for the whole range of internal pressures and molar volumes. The presence of the double bonds in the hydrocarbon chain appears to cause a fivefold increase in solubility of water over that obtained with the saturated hydrocarbon.

The data indicate that the deviation from theory becomes progressively greater with both olefinic and non-olefinic hydrocarbons the greater the length of the hydrocarbon chain, even when the Hildebrand expression in terms of the molal volumes has been applied. It must, however, be observed that in the calculations we have made use of the oversimplified assumption that the covolumes of the liquids are proportional to the molal volumes which we have used. Data which would enable us to test the effect of such a simplification are not sufficiently reliable to justify further examination of this point.

ACKNOWLEDGMENT

We again wish to express our indebtedness to the Texaco Company for the grant-in-aid and fellowship which made this work possible, and also to Professor Ernest O. Lawrence who made available to us the supply of tritium water.

THE JOURNAL OF CHEMICAL PHYSICS VOLUME 16, NUMBER 5 MAY, 1948

The Average Boundaries of Statistical Chains

C. A. HOLLINGSWORTH
E. I. du Pont de Nemours and Company, Waynesboro, Virginia
(Received February 20, 1948)

A general problem of determining what might be called the "average boundaries" of statistical chains is solved formally. As a specific example, the average distance between the first link and the link (or links) which is farthest from the first link is calculated approximately for the case of a random chain. This value is only a small fraction greater than the average distance between the end links.

1. INTRODUCTION

CERTAIN problems dealing with the dimensions of statistical chains can be solved by determining what might be called an "average boundary" of the chain. The exact meaning of this term will be made clear by the examples given in the next paragraphs and by the development in Section 2.

The type of "boundary" involved in any specific instance will depend upon the particular problem to be solved. For example, one might be interested in the average (over a large number of chains) of the component in the x direction of the distance between the first link of the chain and that link (or links) which has the greatest x component of distance from the first link (Fig. 1). In this case the boundary involved will be a plane normal to the x axis. Similarly, the corresponding y and z components may be desired. Such a problem could arise in a treatment of chains which are deformed by a vector field.

Or, one might wish to calculate the average distance from the line passing through the ends of the chain to that link (or links) which is most distant from this line (Fig. 1). In this case the boundary to be determined will be a cylinder having its axis along the line through the ends of the chain. This problem is related to one solved by Kuhn[1,2] in which the average distance of a given link from the line joining the ends of a random chain is calculated.

As a third example, it might in some cases be useful to calculate the average distance from the first link to the link (or links) which is most distant from the first link (Fig. 1). This will involve the determination of the radius of a sphere with its center at the first link. One would think that in the case of flexible chains this distance, rather than an average of the distance between the end links, should approach that dimension which one might call the "length" of the chain. However, even this value would be smaller than the "length," if by "length" one means the maximum dimension of the chain (Fig. 1).

The third example given above is solved approximately for a random chain (a chain with links of constant length, but random in direction) in Section 3 as an illustration of the use of the formal solution to the more general problem treated in Section 2.

2. THE GENERAL PROBLEM

Let $W(\mathbf{R}, N)dV$ be the probability that a statistical chain (of the most general type) of N links, starting at the origin, ends in the volume element dV which has the position vector $\mathbf{R}$. Further, $W(\mathbf{R}, N; S)dV$ will be used to designate this probability with the added condition that there be an absorbing barrier at the surface S, where the equation of the surface is given by

$$S(x, y, z)=0.$$

In other words, $W(\mathbf{R}, N; S)dV$ is proportional to the ratio of the number of chains which start at the origin and end in dV, without having at any point gone beyond S, to the total number of chains starting at the origin.

Suppose that the surface is given a uniform, infinitesimal expansion from S to $S+\delta S$, and we define

$$\delta W(\mathbf{R}, N; S)dV=[W(\mathbf{R}, N; S+\delta S) - W(\mathbf{R}, N; S)]dV. \quad (1)$$

[1] W. Kuhn, Kolloid. Zeits. 68, 2 (1934).
[2] W. Kuhn, J. Polymer Sci. 1, 380 (1946).

This quantity is then proportional to the fraction of the total chains which end in dV, having at one point, at least, extended beyond S, but having at no point extended beyond $S+\delta S$. In case distinction can be made by means of a single parameter ζ between the various surfaces of the family produced by the uniform expansion or contraction of S, then

$$\delta W(\mathbf{R}, N; S) = \frac{\partial W(\mathbf{R}, N; S)}{\partial \zeta} d\zeta. \quad (2)$$

Integrating over that part of the volume enclosed by S which is accessible to the last link gives

$$\int_V \frac{\partial W(\mathbf{R}, N; S)}{\partial \zeta} dV = F(N; S), \quad (3)$$

where $F(N; S)$ is proportional to the fraction of the total chains which extend to (but not beyond) S at least at one point and end anywhere within that part of the volume enclosed by S which, under the conditions of the problem, is accessible to the last link.

The average "boundary" of type S can now be obtained from

$$\langle \zeta \rangle_{Av} = \frac{\int \zeta F(N; S) d\zeta}{\int F(N; S) d\zeta}, \quad (4)$$

where the integration is taken over all possible values of ζ.

For large values of N it is possible[3] to obtain $W(\mathbf{R}, N; S)$ from the differential equation for $W(\mathbf{R}, N)$, with the boundary condition that

$$W(\mathbf{R}, N; S) = 0$$

on the surface S, i.e., for $\mathbf{R}$ ending on S. Perhaps it should be pointed out that, formally, this method is applicable to all types of statistical chains.[3] However, the partial differential equation involved may be quite difficult for some chains.

3. EXAMPLE

As an illustration of the use of the method outlined above a relatively simple problem is chosen. This problem is to determine the average distance between the first link of a random chain and the link (or links) which is most distant from the first link. Here, by random chain is meant a chain with links of constant length but random in direction.

In this case the absorbing barrier is the sphere $r=c$, and the parameter ζ is c.

For the random chain the differential equation is the diffusion equation[3] (or the heat equation) in which the time variable has been replaced by N,

$$[\partial W(\mathbf{R}, N; c)]/\partial N = (l^2/6)\nabla^2 W(\mathbf{R}, N; c), \quad (5)$$

where l is the length of each link, and we have written $W(\mathbf{R}, N; c)$ to correspond to $W(\mathbf{R}, N; S)$ defined in the previous section.

The boundary conditions are:

$$W(\mathbf{R}, N; c) = W(R, N), \quad \text{when} \quad Nl = c, \quad (6)$$

and,

$$W(\mathbf{R}, N; c) = 0, \quad \text{when} \quad |\mathbf{R}| = c. \quad (7)$$

For $W(\mathbf{R}, N)$ we will use the asymptotic solution for large values of N,

$$W(\mathbf{R}, N) = 1/(2\pi N l^2/3)^{\frac{3}{2}} \exp[-3|\mathbf{R}|^2/2Nl^2]. \quad (8)$$

The problem corresponds to that of determining the variable temperature of a solid sphere the surface of which is kept at zero temperature. The

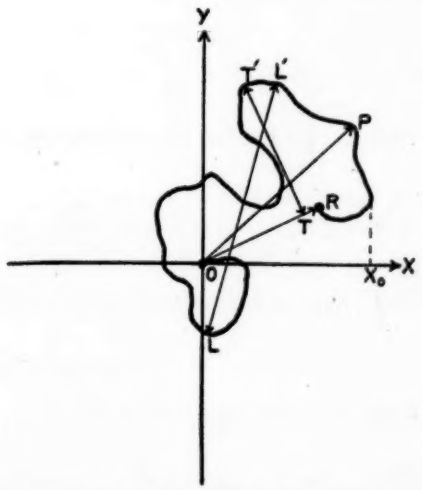

FIG. 1. Dimensions of a statistical chain—OR, distance between end links. OP, maximum distance from first link. TT', maximum distance from OR. LL', maximum dimension, or length, of the chain. OX_0, maximum x component from the first link.

[3] S. Chandrasekhar, Rev. Mod. Phys. 15, 1 (1943).

formal solution is, therefore,[4]

$$W(\mathbf{R}, N; c) = \frac{2}{cr(2\pi cl/3)^{\frac{1}{2}}} \times \sum_{n=1}^{\infty} \exp\left[\frac{-n^2\pi^2 l^2(N-c/l)}{6c^2}\right] \sin(n\pi r/c) \times \int_0^c t \exp[-3t^2/2cl] \sin(n\pi t/c)dt. \quad (9)$$

The next step will be to obtain an approximate evaluation of the integral in the above expression. This can be done by replacing c in the upper limit of the integral by ∞. An idea of the accuracy of this approximation can be obtained from the following treatment:

We have, letting the integral be represented by A_n and integrating by parts,

$$A_n = (n\pi l/3) \int_0^c \exp[-3t^2/2cl] \cos(n\pi t/c)dt$$
$$= (n\pi l/3) \int_0^\infty \exp[-3t^2/2cl] \cos(n\pi t/c)dt$$
$$- (n\pi l/3) \sum_{k=1}^{\infty} \int_{kc}^{(k+1)c} \exp[-3t^2/2cl] \times \cos(n\pi t/c)dt. \quad (10)$$

In the summation let

$$x = t - kc.$$

Then

$$A_n = (n\pi l/3) \int_0^\infty \exp[-3t^2/2cl] \cos(n\pi t/c)dt$$
$$- (n\pi l/3) \sum_{k=1}^{\infty} (-1)^{nk} \exp[-3k^2c/2l] \times \int_0^c \exp[-3x(x+2kc)/2cl] \times \cos(n\pi x/c)dx$$
$$= n(\pi l/3)^{\frac{1}{2}}(c/2)^{\frac{1}{2}} \exp[-n^2\pi^2 l/6c] - (n\pi l/3) \sum_{k=1}^{\infty} (-1)^{nk} T(k), \quad (11)$$

where the symbol $T(k)$ is used for simplification. The terms of the summation approach zero for higher values of k. In fact, even $T(1)$ is quite small, for

$$|T(1)| < \exp[-3c/2l] \int_0^c \exp[-3x/l]dx < (l/3) \exp[-3c/2l].$$

Since we are dealing with large values of N it is obvious that $W(\mathbf{R}, N; c)$, and its derivative with respect to c, are very small when c is not appreciably greater than l. It follows that $T(1)$ is small compared to the first term on the right. Not only is $T(1)$ small, but the series in Eq. (11) converges rapidly. Therefore, as a first approximation the entire series of $T(k)$ terms in Eq. (11) can be neglected.

Equation (9) becomes

$$W(\mathbf{R}, N; c) \sim (1/2c^2r) \sum_{n=1}^{\infty} n \times \exp[-n^2\pi^2 l^2 N/6c^2] \sin(n\pi r/c). \quad (12)$$

If $F(N; c)$ corresponds to $F(N; S)$ of Section 2, we have

$$F(N; c) = \begin{cases} 4\pi \int_0^c r^2[\partial W(r, N; c)/\partial c]dr \\ \text{when } c \leq Nl/2 \\ 4\pi \int_{2c-Nl}^c r^2[\partial W(r, N; c)/\partial c]dr \\ \text{when } c \geq Nl/2 \end{cases}. \quad (13)$$

The average value of c is given by

$$\langle c \rangle_{Av} = \frac{\int_l^{Nl} cF(N; c)dc}{\int_l^{Nl} F(N; c)dc}. \quad (14)$$

The work can be greatly simplified by making the approximation that

$$\langle c \rangle_{Av} \sim \frac{\int_l^{Nl/2} cF(N; c)dc}{\int_l^{Nl/2} F(N; c)dc}. \quad (15)$$

[4] See, for example, Churchill, *Fourier Series and Boundary Value Problems* (McGraw-Hill Book Company, Inc., New York, 1941), p. 112.

This gives

$$\langle c\rangle_{Av}\sim\frac{\int_{l}^{Nl/2}(1/c)^2\sum_{n=1}^{\infty}(-1)^n n^2\exp[-n^2\pi^2l^2N/6c^2]dc}{\int_{l}^{Nl/2}(1/c)^3\sum_{n=1}^{\infty}(-1)^n n^2\exp[-n^2\pi^2l^2N/6c^2]dc}.$$

Taking $x=lN^{\frac{1}{2}}/c$ leads to

$$\langle c\rangle_{Av}\sim\frac{N^{\frac{1}{2}}l\int_{2/\sqrt{N}}^{\infty}\sum_{n=1}^{\infty}(-1)^n n^2\exp[-n^2\pi^2x^2/6]dx}{\int_{2/\sqrt{N}}^{\infty}\sum_{n=1}^{\infty}(-1)^n n^2x\exp[-n^2\pi^2x^2/6]dx}.$$

Therefore,

$$\langle c\rangle_{Av}\sim N^{\frac{1}{2}}lK(N), \tag{16}$$

where

$$K(N)=(2/3)^{\frac{1}{2}}\pi\left[\frac{\sum_{n=1}^{\infty}(-1)^n n[1-\Phi(2\pi n/(6N)^{\frac{1}{2}})]}{\sum_{n=1}^{\infty}(-1)^n\Phi_1[2\pi n/(6N)^{\frac{1}{2}}]}\right], \tag{17}$$

and where $\Phi[2\pi n/(6N)^{\frac{1}{2}}]$ is the tabulated "error integral" defined by

$$\Phi(x)=(2/\sqrt{\pi})\int_{0}^{x}\exp-t^2dt, \tag{18}$$

and $\Phi_1(x)$ is the derivative of $\Phi(x)$ given by

$$\Phi_1(x)=(2/\sqrt{\pi})\exp-x^2. \tag{19}$$

As specific numerical examples we have $K(2600)=1.14$ and $K(670)=1.14$. Thus $K(N)$ must be almost independent of N, and we have

$$\langle c\rangle_{Av}\sim 1.14N^{\frac{1}{2}}l. \tag{20}$$

This result is very nearly the same as the average distance between the end links given by

$$\langle r\rangle_{Av}=\frac{4\pi\int_{0}^{Nl}r^3W(r,N)dr}{4\pi\int_{0}^{Nl}r^2W(r,N)dr} \tag{21}$$

$$\sim 2(2/3\pi)^{\frac{1}{2}}N^{\frac{1}{2}}l\sim 0.92N^{\frac{1}{2}}l. \tag{22}$$

In the case of chains which are more extended than the random chain the values of $\langle c\rangle_{Av}$ and $\langle r\rangle_{Av}$ are even closer together. For a completely extended chain the values are, of course, equal.

Letters to the Editor

THIS section will accept reports of new work, provided these are terse and contain few figures, and especially few halftone cuts. The Editorial Board will not hold itself responsible for opinions expressed by the correspondents. Contributions to this section should not exceed 600 words in length and must reach the office of the Managing Editor not later than the first of the month preceding that of the issue in which the letter is to appear. No proof will be sent to the authors. The usual publication charge ($4.00 per page) will not be made and no reprints will be furnished free.

The Infra-Red and Raman Spectra of Heavy Cyclooctatetraene

ELLIS R. LIPPINCOTT, R. C. LORD, JR., AND R. S. MCDONALD
Department of Chemistry and Spectroscopy Laboratory, Massachusetts Institute of Technology, Cambridge 39, Massachusetts
March 15, 1948

WE wish to give a preliminary report of the vibrational spectra of completely deuterated cyclooctatetraene (C_8D_8), which we have prepared by the polymerization of heavy acetylene. The purification of our C_8D_8 has been followed spectroscopically. We feel confident that with respect to light hydrogen and the by-products of the polymerization, such as heavy styrene, its purity is more than adequate for the determination of the molecule's structure from its spectra.

The more prominent frequencies in the infra-red and Raman spectra of both C_8H_8 and C_8D_8 are given in Tables I and II. Further study of the Raman spectrum of C_8H_8 has confirmed our earlier results,[1] with the addition of two rather strong lines found by Hg-5770 and -5791 excitation. Although we have not previously published the infra-red data, we have been using infra-red spectra[2] since the fall of 1946 as a guide in the purification of C_8H_8 and, more recently, of C_8D_8. The spectra of C_8H_8 published by others[3,4] agree almost completely, so far as they go, with those listed here. We have received a private communication from Professor Langseth which indicates that he has prepared C_8D_8 and taken its Raman spectrum.

In the interpretation of the vibrational spectra of C_8H_8 and C_8D_8 certain general features are of importance:

(1) The number of Raman lines and infra-red bands in both compounds strong enough to be called fundamentals is small, as is the number of polarized Raman lines;
(2) There are a number of definite coincidences in both compounds between relatively strong infra-red bands in the vapor and relatively strong Raman lines;
(3) There are several very strong infra-red bands at frequencies where no Raman lines are found, and several very strong Raman lines at frequencies where no infra-red bands occur. In particular the polarized Raman frequencies are not found in the infra-red, with one, presumably accidental, exception in C_8D_8.

For a molecule with 42 vibrational degrees of freedom, (1) bespeaks considerable symmetry. A symmetry center is, however, incompatible with (2). A detailed consideration of possible symmetries for C_8H_8 on the basis of (1) and (2) enables almost all of the plausible structures to be ruled out. It is our belief that (3) enables the remaining structures to be excluded with the exception of the D_4 model* suggested in our earlier discussions of the problem.[1,5,6]

A more detailed interpretation, as well as an account of the preparation and purification of C_8H_8 and C_8D_8, will be published later. At present we wish to point out some

TABLE I. Infra-red absorption spectra of liquid C_8H_8 and C_8D_8.

C_8H_8		C_8D_8	
ν in cm^{-1}	Intensity	ν in cm^{-1}	Intensity
584	W	527	VS
630	VS	551	W
670	VS	592	W
800	VS	720	S
873	W	822	M
890	W	838	W
942	S	879	S
966	M	889	W
988	W	899	S
1202	S	928	M
1221	S	1286	M
1399	M	1554	VW
1439	W	1582	W
1573	W	1614	S
1605	M	2220	S
1635	S	2236	VS
1706	W	2252	VS
1725	W		
1750	M		
1781	W		
1845	W		
1922	W		
2004	W		
2425	W		
2745	W		
2781	W		
2826	W		
2950	M		
3004	VS		

TABLE II. Raman spectra of C_8H_8 and C_8D_8.

C_8H_8			C_8D_8		
$\Delta\nu$ in cm^{-1}	I	Approximate depolarization	$\Delta\nu$ in cm^{-1}	I	Approximate depolarization
194	10	1/2	172	10	1/2
249	9	6/7	238	8	6/7?
292	9	6/7	265	9	6/7?
366	10	6/7	312	10	6/7
655	5		565	1	
728	1		576	8	
758	2		591	3	
873	10	1/10	745	1	
908	3		761	8	6/7
948	9	6/7	812	4	1/3
967	7?		822	10	1/6
976	4?		838	3	6/7
994	6?		872	4	6/7
1202	9	6/7	881	8	6/7
1221	4		890	2	
1399	2		930	2	
1417	2		1287	2	
1439	9	6/7	1297	8	6/7
1461	1		1355	2	
1570	1		1542	3	
1601	7	6/7?	1554	2	
1631	8	6/7?	1579	6	
1651	10	1/5	1597	2	
1743	4		1615	6	
2793	2		1636	9	1/6
2832	2		1653	10	1/10
2853	2		1675	2	
2954	9	6/7	2225	9	6/7?
3003	10	6/7	2250	10	<1/10
3013	10	<6/7	2245 to 2263	8	
3048	4				

specific results for C_8D_8 which appear to confirm the D_4 structure. If C_8H_8 and C_8D_8 have this structure, these molecules have a species of vibration A_2 (see Herzberg, "Infrared and Raman Spectra," D. Van Nostrand Company, New York, 1945, p. 252), which is infra-red active and Raman inactive. There are four vibrations of this species in both C_8H_8 and C_8D_8. We have located unequivocally three strong bands, presumably of this species, at 670, 800, and 3004 cm^{-1} in C_8H_8 and at 527, 720, and 2236 in C_8D_8. The location of a fourth vibration will be discussed when this work is published in detail. Here we wish only to make the point that prolonged exposure of the Raman spectrum has failed to reveal any sign of the 670 and 800 frequencies in C_8H_8 or of 527 and 720 in C_8D_8, although these over-exposed spectra have produced a total of some forty Raman overtones in C_8H_8.

In the symmetry D_{2d}, which has been suggested on the basis of x-ray and electron diffraction studies,[7] all infra-red-active species are Raman-active also. The spectroscopic data accordingly appear to favor strongly the D_4 over the D_{2d} structure.

One of the striking features of the Raman spectra of both C_8H_8 and C_8D_8 is the collection of four strong lines of low frequency. These are presumably to be assigned to ring-puckering vibrations analogous to the non-planar benzene ring vibrations. There should be four such frequencies in both the D_4 and D_{2d} structures. In the D_{2d} structure, however, one of the four is forbidden in both Raman and infra-red spectra, whereas four are Raman-active in D_4. While the assignment of these four lines to the puckering vibrations is not an absolute necessity, the large gap of more than 250 cm^{-1} between the highest of these and the next lowest Raman line in both C_8H_8 and C_8D_8 is convincing support for such assignment and for the D_4 structure.

The authors wish to acknowledge the generous support of the Office of Naval Research (Task Order 10 of Contract N 5ori-78).

[1] Lippincott and Lord, J. Am. Chem. Soc. **68**, 1868 (1946).
[2] Cf. Cope and Overberger, J. Am. Chem. Soc. **69**, 976 (1947).
[3] Flett, Cave, Vago, and Thompson, Nature **159**, 739 (1947).
[4] Bastiansen, Hassel, and Langseth, Nature **160**, 128 (1947).
* The D_4 structure, which has been called the "crown structure" by some, consists of a puckered eight-membered ring with alternate single and double bonds. The puckering occurs in such a way that a four-fold axis (C_4) is present, so that the ring has a saw-toothed appearance when viewed edgewise. Even-numbered carbon atoms lie in the same plane, which is parallel to the plane in which the odd-numbered carbon atoms lie. An analogous statement holds for the hydrogen atoms. By symmetry all carbon atoms are equivalent as are all hydrogen atoms. It should be noted that the D_4 structure implies optical isomerism.
[5] R. C. Lord, Jr., Proceedings of the Colloquium on Molecular Structure, Paris, May 27, 1947 (to be published in J. de Chim. physique).
[6] Lippincott and Lord, Symposium on Molecular Spectra, Ohio State University, June 1947.
[7] Kaufman, Fankuchen, and Mark, Nature **161**, 165 (1947); J. Chem. Phys. **15**, 414 (1947). Personal communication from Professor V. Schomaker.

Hysteresis of the Contact Angle

S. J. GREGG
Department of Chemistry, University College, Exeter, England
March 12, 1948

THE angle of contact θ of a liquid against a solid is profoundly influenced by the presence of an adsorbed film on the unimmersed portion of the solid (and formed by spreading from the liquid, or by adsorption from the vapor phase, or both). This is implicit in Harkins and Dahlstrom's treatment[1] of the subject in 1930, but was first explicitly and quantitatively discussed by Bangham and Razouk[2] in 1937; they arrived at the expression

$$F_L - F_V = \gamma_L \cos\theta, \tag{1}$$

where F_L and F_V are the diminutions in free energy when 1 cm^2 of the *clean* solid (i.e., free from film) is immersed in the liquid and exposed to the vapor, respectively; γ_L is the free surface energy of the liquid. In effect, almost all other workers had taken $F_L = \gamma_L \cos\theta$.

For a mobile film, Bangham[3] has shown that F_V may be equated with π, the surface pressure of the film; consequently, Eq. (1) may be written

$$F_L - \pi = \gamma_L \cos\theta. \tag{2}$$

This form of the Bangham-Razouk relationship possesses the merit of expressing the dependence of θ on the adsorbed film in terms of a simple property of the latter, its surface pressure; and this is calculable, in principle[3,4] and often in practice, from the adsorption isotherm of the vapor on the solid by means of the integrated Gibbs adsorption equation: $\pi = RT\int_0^p \Gamma d \ln p$ (Γ moles = adsorption per unit area of the solid and p = pressure of the vapor). In particular it suggests an immediate connection between hysteresis of the contact angle and hysteresis in adsorption;[4] in this latter phenomenon the pressure P (and with it the surface pressure π) is greater on the "adsorption-increasing" run than on the "adsorption-decreasing" one, for a given adsorption Γ. It should be noted that hysteresis can occur with non-porous adsorbents[5] and is not confined to porous bodies, as is often supposed.

Now in measurements of the advancing contact angle, θ_a, the adsorbed film (surface pressure = π_a) is in the process of formation by spreading or by adsorption from the vapor phase; it corresponds to the "adsorption-increasing" run of a vapor adsorption experiment. But in measurements of the receding angle, θ_r, the film ($\pi = \pi_r$) adjacent to the line of contact has recently been covered with the bulk liquid, and it corresponds to the "adsorption-decreasing" run. If adsorption hysteresis occurs, $\pi_a > \pi_r$, consequently $\theta_a > \theta_r$, i.e., there is hysteresis of the contact angle.

To eliminate any difference between θ_a and θ_r it is necessary that $\pi_a = \pi_r$, and this requires (i) that adsorption hysteresis be eliminated, and (ii) that the pressure p over the film shall be the same during both measurements. To achieve (ii) is difficult in practice unless p be chosen as p_0, the saturated vapor pressure. Attainment of (i) calls for a number of precautions, notably that ample time be allowed for attainment of adsorption equilibrium, and that impurities be absent. Both these points are implicitly, though not explicitly, taken into account in the procedure adopted by Harkins and Fowkes,[6] whereby they have been able to eliminate hysteresis of the contact angle in a large number of cases.

Nevertheless, Harkins' assertion[7] that the "advancing and receding angles obtained by nearly all investigators other than those in this laboratory is due to improper preparation of the surface and poor techniques in making the measurements," is, in view of the known characteristics

of adsorption hysteresis, almost certainly too sweeping. In the first place, adsorption hysteresis is known to be greatly aggravated in some cases by the presence of air[8]—an impurity almost inevitably present during measurements of the contact angle. In the second place, adsorption hysteresis occasionally persists even when scrupulous attention has been paid to removal of impurities;[9] it is also known in films on water.[10] Finally, it is now widely recognized that phase transformations can occur in films on solids;[11] and by analogy with phase changes in bulk matter and also from general considerations, it is only to be expected that such transformations would sometimes occur excessively slowly. Indeed, these delayed phase changes may well be the cause of adsorption hysteresis itself, in many cases;[12] but in any event it is to be expected that the time lag would often be so long that the phase change would not be completed within the time of an experiment.

No doubt the hysteresis of adsorption and, therefore, of the contact angle may, *in principle*, be completely eliminated in all cases where impurities are absent by allowing sufficient time to elapse before taking the measurements of θ; but, judging from common experience with the adsorption of vapors, the time required would occasionally be impracticably long. Consequently, *under conditions attainable in practice*, it seems that in a residue of cases, at least, hysteresis of the contact angle will persist despite the most careful precautions.

[1] W. D. Harkins and R. Dahlstrom, Ind. Eng. Chem. **22**, 897 (1930).
[2] D. H. Bangham and R. I. Razouk, Trans. Faraday Soc. **33**, 1459 (1937).
[3] D. H. Bangham, Trans. Faraday Soc. **33**, 805 (1937).
[4] D. H. Bangham, J. Chem. Phys. **14**, 352 (1946).
[5] J. B. M. Herbert, Trans. Faraday Soc. **26**, 118 (1930). D. H. Bangham and S. Mosallam, Proc. Roy. Soc. **166A**, 559 (1938). F. Durau, Ann. d. Physik **87**, 365 (1928). F. C. Tompkins, Trans. Faraday Soc. **32**, 643 (1936). J. Holmes and P. H. Emmett, J. Phys. Chem. **51**, 1262 (1947). R. T. Davis, T. W. de Witt, and P. H. Emmett, J. Phys. Chem. **51**, 1232 (1947).
[6] W. D. Harkins and F. M. Fowkes, J. Am. Chem. Soc. **62**, 3380 (1940).
[7] W. D. Harkins, *Advances in Colloid Chemistry* (edited by J. Alexander, 1946), Vol. VI, p. 61.
[8] J. W. McBain, "Sorption of gases and vapours by solids." S. Brunauer, "The physical adsorption of gases and vapours."
[9] B. Lambert and A. G. Foster, Proc. Roy. Soc. **136A**, 375 (1932).
[10] N. K. Adam, *Physics and Chemistry of Surfaces*, p. 56.
[11] D. H. Bangham, N. Fakhoury, and A. F. Mohamed, Proc. Roy. Soc. **138A**, 162 (1932); **147A**, 152 (1934). S. J. Gregg, J. Chem. Soc., 696 (1942). W. D. Harkins and G. Jura, J. Chem. Phys. **12**, 112, 114 (1944); J. Am. Chem. Soc. **66**, 1356 (1944); **68**, 1941 (1946).
[12] S. J. Gregg, J. Chem. Soc., 706 (1942); Trans. Faraday Soc., to be published.

Cyclic Acetylenic Compounds

THOMAS J. SWORSKI*
University of Notre Dame, Notre Dame, Indiana
March 24, 1948

CYCLIC conjugated ring systems have been of experimental and theoretical interest in recent years. For example, the work of Prosen, Johnson, and Rossini[1] indicates quite definitely that cyclooctatetraene lacks the stability inherent in the benzene ring. This has been explained on the basis of a non-planar structure which, although permitting maximum overlapping of the σ-orbitals, does not permit maximum overlapping of the π-orbitals.

It is of interest to consider whether the quantum mechanical representation of hybridized carbon atoms may permit the prediction of stable, planar, conjugated ring structures of more than six carbon atoms. It is the purpose here to present a few illustrative examples of such a potential series. These can be shown to be derived from the corresponding benzene derivatives by the insertion of either the linear acetylenic group ($-C\equiv C-$) or the linear cumulene group ($=C=C=$) at appropriate places as follows.

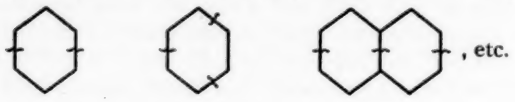

I II III

Operation I leads to the following resonating structure.

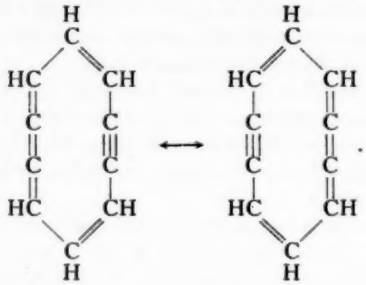

Operation II similarly produces the following interesting resonating structure.

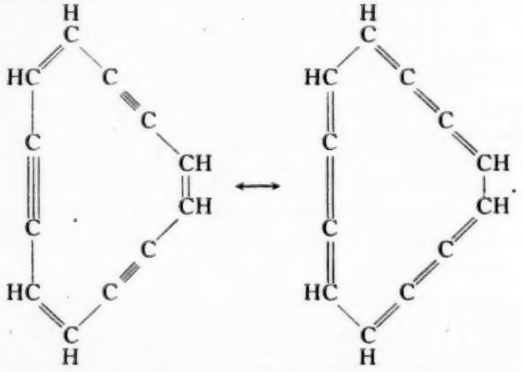

Examination of the bond angles of these compounds readily verifies their planar and strainless nature. It is further evident that each carbon atom will have a p-orbital which may be perpendicular to the ring and thus capable of overlapping the adjacent orbitals on either side to form a continuous molecular π-orbital just as for benzene. In addition, the acetylenic carbons are presumed to have localized π-orbitals in the plane of the ring. The prediction of resonance in these structures implies conjugative properties for the triple bond similar to those for the double bond.

It is of interest to establish experimentally the validity of such a prediction. Synthetic work on the preparation of ring systems of these types is under way in these laboratories through dimerization of phenylpropiopyl chloride and by condensation of glyoxal with acetylene diGrignard.

* Work by the writer at the University of Notre Dame is assisted by the Office of Naval Research of the United States Navy Department under contract N6 ori 165, T.O.II.
[1] Prosen, Johnson, and Rossini, J. Am. Chem. Soc. **69**, 2068 (1947).

Near Infra-Red Absorption of Nylon Films: Dichroism and Rupture of N−H···O Bonds on Melting

LEONARD GLATT AND JOSEPH W. ELLIS
Department of Physics, University of California, Los Angeles, California
March 4, 1948

A RECENT x-ray diffraction investigation[1] gave evidence that a study of the absorption spectra of Nylon with polarized infra-red should prove of considerable interest. A mention of dichroism in the 3- 7μ- wave-length region in Nylon had already been briefly made by Elliott and Ambrose.[2] A Nylon (6.10 polyamide) sheet was kindly furnished by Dupont.

The $>CH_2$ absorption in Nylon was, except for a considerable broadening and slight position shift of the bands, quite similar to that we previously reported for polythene.[3] The interesting band which had its change of electric moment parallel to the molecular chain axes, appeared, considerably diminished, at 4219 cm^{-1} in the parallel *E*-component for stretched (or rolled) Nylon film. It was too weak to appear in unpolarized light spectrograms. If the origin of this band is that postulated in our earlier paper, such a diminution might be expected owing to the presence of the −CO−NH units in the Nylon chains.

The Nylon crystalloids consist of parallel sheets, the backbone planes lying in the sheets with adjacent chains held together by intermolecular N−H···O bonds which extend perpendicularly to the chain axes.[1] The second harmonic of the perturbed N−H stretching vibration is almost certainly responsible for a band which appears at 6523 cm^{-1}, as well as for at least some of the neighboring structure. This band is about three times as intense in the perpendicular as in the parallel vibration component. Its failure to vanish more nearly completely in the latter component might possibly indicate that the H-atoms do not lie strictly on the N−O line, normal to the chain axes, between adjacent molecules. A strong 4883-cm^{-1} band, with weak neighbors, is attributed to a combination N−H bond stretching and deformation vibration. This band is roughly twice as intense in the parallel as in the perpendicular *E*-component, which is convincing evidence that the N−H deformation takes place in, rather than normal to, the backbone planes. The complexity in the above N−H regions might indicate that not all the N−H···O units are equivalent.

The third harmonic of the perturbed C=O vibration is probably responsible for a band, at 4975 cm^{-1}, which strengthened in the perpendicular and *completely* vanished in the parallel *E*-component. A comparison with a published percentage absorption curve[4] (unpolarized light and comparatively low dispersion) indicates that both the mutually perturbing N−H and C=O units show a definite positive rather than the usual negative anharmonicity.

Spectrograms of Nylon strips in which we had attempted to produce the type of "double orientation" described by Bunn and Garner[1] showed little evidence, in the intensity ratios of $>CH_2$ bands, of any appreciable alignment of molecular backbone planes. It is probable that, owing perhaps to inferior rollers and improperly developed technique, the degree of orientation of the backbone planes that we have been able to obtain is highly incomplete. If this is not true, the designations "antisymmetric" and "symmetric" $>CH_2$ valence bond stretching vibrations will have to be re-examined.

Spectrograms made of molten Nylon specimens kept at 300°C gave unmistakable evidence of rupture of the intermolecular N−H···O bonds. A new extremely sharp band appeared at 6757 cm^{-1}, with a broad undefined shoulder which contained perhaps the residue of the 6523-cm^{-1} *perturbed* N−H stretching band. The combination N−H valence stretching and deformation band also altered considerably.

Specimens kept at 200°C, below the 260°C melting point, show the bands characteristic of both the bonded N−H···O (perturbed) and free N−H groups. Evidently some of the intermolecular bonds rupture before melting, thus allowing the rotational movements and realignments inferred from x-ray diffraction data.

A detailed account will be published in the future when observations will have been completed.

[1] C. W. Bunn and E. V. Garner, Proc. Roy. Soc. **A189**, 39 (1947).
[2] A. Elliott and E. J. Ambrose, Nature **159**, 641 (1947).
[3] L. Glatt and J. W. Ellis, J. Chem. Phys. **15**, 884(L) (1947).
[4] H. W. Thompson and P. Torkington, Trans. Faraday Soc. **41**, 256 (1945).

The Ultraviolet Spectra and Ionization Potentials of the Hydrides and Deuterides of Sulfur, Selenium, and Tellurium

W. C. PRICE*
Ryerson Physical Laboratory, University of Chicago, Chicago, Illinois
March 1, 1948

THE absorption spectra of the hydrides and deuterides of sulfur, selenium, and tellurium have been obtained in the vacuum ultraviolet. All these substances have regions of weak continuous absorption between 3000 and 2000A. Below 2000A the spectra consist of a large number of relatively discrete bands. Many of these have sharp *Q* branches and are accompanied by rotational structures of such a nature as to indicate very little change in the molecular dimensions as a result of the excitation. Thus the excitation is clearly that of a non-bonding electron ($2p_y$ of S, Se, or Te) which is also indicated by the almost complete absence of vibrational patterns. Nearly every band is a different electronic transition, a fact which can be clearly demonstrated by comparison of the spectra of the hydrides with those of the corresponding deuterides. The long wavelength bands are strong and on going to shorter wavelengths, the bands gradually get weaker and closer together, and eventually converge into photo-ionization continua. The convergence limits are clearly visible on the original plates. The bands of hydrogen sulfide start around 1590A and converge to an ionization limit corresponding to 10.5 volts, those of hydrogen selenide start at 1693A and converge to 9.7 volts while those of hydrogen telluride start at

1920A and converge to 9.1 volts. The closeness of these ionization potentials to the corresponding values for the atoms (*viz.* S, 10.3 volts; Se, 9.5 volts; Te, not known accurately but close to 9.0 volts) is clearly significant. The ionization potentials of the deuterides are not appreciably different from those of the corresponding hydrides.

There are very many obvious correlations among the spectra of sulfides, the selenides, and the tellurides, and it is quite clear that their analysis is going to be of interest both from the atomic and molecular point of view.

The spectra of methyl mercaptan, dimethyl sulfide and diethyl selenide have also been taken. These show the long wave-length shifts and ionization potential reductions usually associated with alkyl substitution and the interpretation of their spectra is naturally along the lines of those of the parent molecules.

This work was assisted by the Office of Naval Research under Task Order IX of Contract N6-ori 20 with the University of Chicago.

* Present address: Imperial Chemical Industries, Ltd., Billingham, England.

The Infra-Red Spectrum and Structure of Aluminum Trimethyl

KENNETH S. PITZER AND RAYMOND K. SHELINE
Department of Chemistry, University of California, Berkeley, California
March 22, 1948

RECENTLY a general investigation of aluminum alkyls[1] was presented which included an infra-red spectrum of $Al_2(CH_3)_6$ from 700 to 3000 cm^{-1} provided by the Spectroscopic Department of the Shell Development Company. We have now investigated the infra-red absorption of this same preparation of aluminum trimethyl at longer wave-lengths with a Perkin and Elmer spectrometer. The sample was repurified by distillation and its melting point checked at 15.1°C. The results are shown in Fig. 1. The cell was 9 cm long and was filled to 11.5 mm of Hg pressure. No absorption outside of experimental error (which becomes large) was observed from 440 to 530 cm^{-1}.

In the range expected for Al−C vibrations (500 to 800 cm^{-1}) there are four very intense bands: 776, 696, 604, and 563 cm^{-1}. These are all very markedly stronger than C−H bending vibrations which might also be as low as 800 cm^{-1}. Thus their interpretation seems unequivocal. Also the intensity of these bands indicates very considerable polarity (or ionic character) in the Al−C bond.

An ethane-like structure for the Al_2C_6 skeleton would have two infra-red active Al−C stretching frequencies. The present results make this seem most unlikely. Any reasonable bridged model[1,2] of either D_{2h} or C_{2h} symmetry will have four infra-red active Al−C stretching frequencies.[3] This is in perfect agreement with our observations and would seem definitely to establish the correctness of some bridge type structure. Unfortunately, these data do not help distinguish the D_{2h} and C_{2h} models. The aspect of the

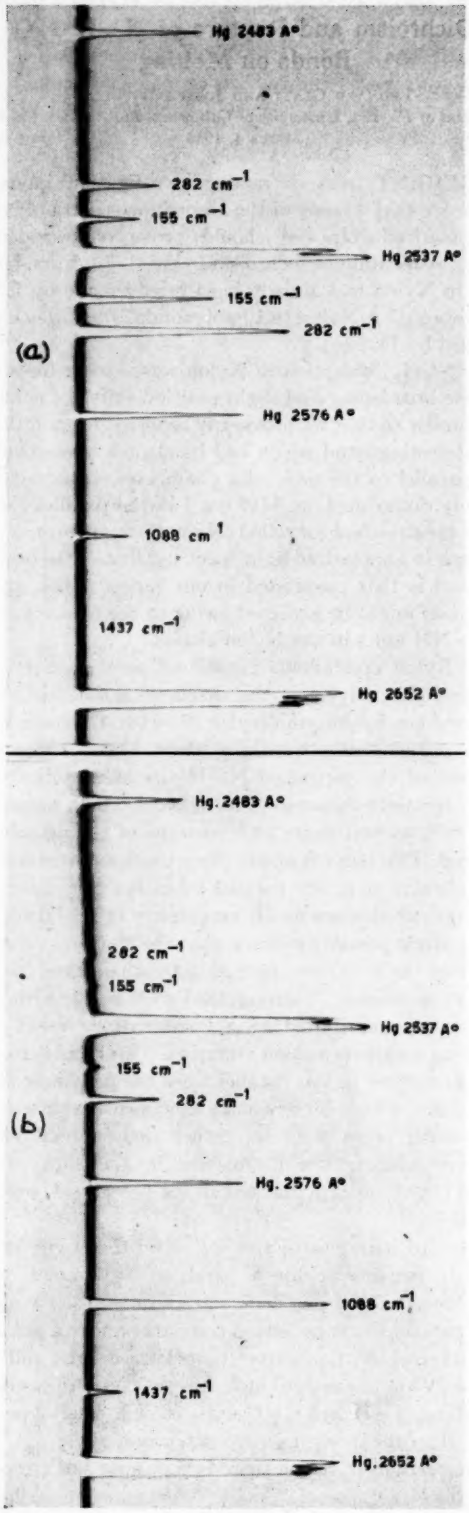

FIG. 1. The infra-red absorption of $Al_2(CH_3)_6$. Cell length, 9 cm. Pressure, 11.5 mm.

Raman spectrum of Kohlrausch and Wagner,[4] which favors a C_{2h} model, has already been discussed.[1]

[1] K. S. Pitzer and H. S. Gutowsky, J. Am. Chem. Soc. **68**, 2204 (1946).
[2] B. Eistert, Zeits. f. physik. Chemie **B52**, 202 (1942); H. A. Skinner and L. E. Sutton, Nature **156**, 601 (1945); R. E. Rundle, J. Am. Chem. Soc. **69**, 1327 (1947); and other references cited in those already given.
[3] For selection rules for ethane-like and bridged models see, for example, G. Herzberg, *Infrared and Raman Spectra of Polyatomic Molecules* (D. Van Nostrand Company, New York, 1945).
[4] K. W. F. Kohlrausch and J. Wagner, Zeits. f. physik. Chemie **B52**, 185 (1942).

Errata: Origin of the Potential Barrier Hindering Rotation in Ethane and Related Substances

[J. Chem. Phys. 16, 151 (1948)]

EDWIN N. LASSETTRE AND LAURENCE B. DEAN, JR.
Department of Chemistry, The Ohio State University, Columbus, Ohio

DURING the course of further calculations a large error has been found in the quadrupole moments calculated from the approximate molecular orbital (column 3, Table I). The revised results are given below. The calculated barrier is now *less* than that observed. Agreement with experiment is somewhat closer, although we do not regard this as significant. The changes result entirely from the change in P. There is no change in Table II of the above letter.

TABLE I.

a/b	$\mu\times10^{18}$ e.s.u.	P atomic units	$D-D$ kcal.	$D-Q$ kcal.	$Q-Q$ kcal.	Barrier kcal.	V(stag.)
1.0	−2.30	1.44	1.58	−1.52	1.17	1.23	95.2
1.5	−1.51	1.58	0.68	−1.09	1.41	1.00	52.4
2.0	−0.98	1.64	0.29	−0.74	1.51	1.06	31.7
4.0	0.03	1.65	0.00	0.03	1.54	1.57	10.6
5.75	0.40	1.63	0.05	0.30	1.50	1.84	9.2

The revised quadrupole moments are now *smaller* than those required to account for the observed barrier. Our previous statement that the actual charge distributions overlap even less than the approximate distributions is therefore unjustified. The remaining conclusions are unchanged.

The Geometry of CH_3X Molecules

H. A. SKINNER
Department of Chemistry, The University of Manchester, Manchester, England

March 12, 1948

THE geometric structures of the molecules CH_3Cl and CH_3Br have been the subject of a discussion by Bak,[1] who concluded that the CH_3 group in these molecules is almost "flat," i.e., HC−Cl∼93° and HC−Br∼90°. Coulson,[2] on theoretical grounds, has pointed out that a widening of the HCH angle may occur in CH_3X as a result of departures from pure sp^3-bonding in the CH and CX bonds. A similar trend might be anticipated if (as Dennison[3] has remarked) there is an appreciable contribution from the ionic structure $\overset{+}{C}H_3\overset{-}{X}$ to the ground state of CH_3X. It is, therefore, a matter of some interest to know the precise details of the geometry in CH_3X molecules.

The values of the large moments of inertia (I_B) in the methyl halides have been redetermined recently by Gordy, Smith, and Simmons[4] (microwave spectra of CH_3Cl, CH_3Br, and CH_3I), and by Yates and Nielsen[5] (infra-red spectrum of CH_3F). The new values (which are probably accurate to 1 percent) differ markedly from those used by Bak in his calculations of the bond angles. Using the recent values for I_B, and electron diffraction values for the C−X bond lengths, we have calculated the *range* in the allowable values for the bond angles in the methyl halides, and conclude that although the CH_3 group in these molecules may be slightly "flat" (relative to CH_3 in CH_4), the extent of "flattening" cannot be large.

Below are summarized the experimental data we have used:

(1) *Methyl Fluoride*

(a) $I_B=32.22\times10^{-40}$ g cm², derived from the line spacing as measured by Yates and Nielsen.[5]

(b) $I_C=5.47\times10^{-40}$ g cm², derived from the sum of the doublet spacings in the ⊥ bands, and the Johnson-Dennison formula.[6]

(c) r(C−F)=1.39±.02A, from the electron diffraction study by Stevenson and Schomaker.[7]

(d) r(C−H)=1.10A (±.05A). This is an assumed value, partially justified by Linnett's estimation r(C−H)=1.103A (from Badger's rule and the C−H force constant in CH_3F).[8] The uncertainties in the above experimental data allow a range in the value of α=HCF from 100°–110°, corresponding to a mean value $\alpha=105°\pm5°$.

(2) *Methyl Chloride*

(a) $I_B=63.1\times10^{-40}$ g cm², as measured by Gordy, Simmons, and Smith.[4a]

(b) $I_C=5.552\times10^{-40}$ g cm², from the doublet spacings.

(c) r(C−Cl)=1.77±.02A, from the electron diffraction studies by Sutton and Brockway[9] and Stevenson and Schomaker.[7]

(d) r(C−H)=1.10±.05A: Linnett[8] calculated r(C−H) =1.095A from the C−H force constant.

These data allow a range in the value of α=HC−Cl from 106° to 117°, with the mean value $\alpha=111°$ (for r(C−Cl) =1.77A and r(C−H)=1.10A). A slightly "flat" CH_3 group would require the correct value of r(C−Cl) to be not less than 1.78A.

(3) *Methyl Bromide*

(a) $I_B=87.5\times10^{-40}$ g cm², as quoted by Gordy, Simmons, and Smith.[4a]

(b) $I_C=5.399\times10^{-40}$ g cm², from the doublet spacings.

(c) r(C−Br)=1.92±.02A. This is an assumed value, slightly larger than the electron diffraction value quoted by Levy and Brockway[10] (1.91±.06A). We have chosen the larger value in view of the observed distance r(C−Br) =1.94A, reported by Hassel[11] in CBr_4 (electron diffraction with rotating sector camera).

(d) $r(C-H)=1.10\pm.05$A: Linnett quotes 1.094A.
The spread in the values of $\alpha=HC-Br$ corresponding to these data is from 107° to 118°. Unless $r(C-Br)$ is greater than 1.93A, there is no "flattening" of the CH_3 group.

(4) *Methyl Iodide*

(a) $I_B=111.4\times10^{-40}$ g cm², as quoted by Gordy, Smith, and Simmons.[4b]

(b) $I_C=5.54\times10^{-40}$ g cm², from the doublet spacings.

(c) $r(C-I)=2.11\pm.03$A. This is an estimated value, based on the electron diffraction values for $r(C-I)$ in CH_2I_2 and CHI_3 reported by Hassel[11] (2.12A in both these compounds).

(d) $r(C-H)=1.10\pm.05$A: Linnett quotes 1.092A.
The values of $\alpha=HC-I$ complying with the range in the values $r(C-H)$ and $r(C-I)$ extend from 104° to 121°, but unless $r(C-I)$ is greater than 2.12A, there can be no "flattening" in the CH_3 group.

While the experimental data do not exclude the possibility that the CH_3 groups in the methyl halides are slightly "flat," it seems unlikely that the extent of their flattening amounts to more than two or three degrees, and is certainly less than suggested by Bak to be the case in CH_3Cl and CH_3Br. Moreover, it would seem that those factors which might be expected to flatten the CH_3 group (mentioned by Coulson) are either small in themselves or are offset in their effect by steric repulsion between the H and X atoms.

[1] B. Bak, J. Chem. Phys. **14**, 698 (1946).
[2] C. A. Coulson, V. Henri Memorial Volume (Liège, in press).
[3] D. M. Dennison, Rev. Mod. Phys. **12**, 175 (1940).
[4] (a) Gordy, Simmons, and Smith, Phys. Rev. **72**, 344 (1947); (b) Gordy, Smith, and Simmons, Phys. Rev. **72**, 249 (1947).
[5] K. P. Yates and H. H. Nielsen, Phys. Rev. **71**, 349 (1947).
[6] D. M. Dennison and M. Johnston, Phys. Rev. **47**, 93 (1935).
[7] Stevenson and Schomaker, J. Am. Chem. Soc. **63**, 37 (1941).
[8] Linnett, Trans. Faraday Soc. **41**, 223 (1945).
[9] Sutton and Brockway, J. Am. Chem. Soc. **57**, 473 (1935).
[10] Levy and Brockway, J. Am. Chem. Soc. **59**, 1662 (1937).
[11] Hassel and Viervoll, Acta chim. Scand. **1**, 149 (1947).

An Equation of State for Gases at High Pressures and Temperatures from the Hydrodynamic Theory of Detonation

MELVIN A. COOK
University of Utah, Salt Lake City, Utah
March 5, 1948

THIS note is in reply to comments by S. Paterson[1] on my recent article.[2] Paterson first challenged the (supposed) claim that method (a) of my article is an "exact" solution. As a matter of fact, no such claim was made. In the summary of the paper I referred to method (a) as ". . . in principle at least, a general solution." However, I hastened to add that, in fact, a general solution was impossible because of the necessity of postulating a particular form of $\alpha(T,v)$ in evaluating the detonation temperature. Paterson merely restated my own arguments in pointing out that ". . . (detonation) velocities alone do not allow us to discriminate between such a solution (i.e., of $\alpha(v)$ from velocity data) and any alternate solution, e.g., Kistiakowsky and Wilson's in which α depends also on T." Thus my article stated that "it is quite evident that the detonation temperature is really the only detonation property which may be used to provide experimental information on the accuracy of the various equations of state . . . all other quantities being relatively insensitive to the particular equation of state employed." Realizing the limitations of the hydrodynamic theory in providing by itself an unambiguous equation of state, I considered it necessary to bring in several external evidences to support the $\alpha(v)$ approximation and discussed the agreement between methods (a) and (b) as supporting evidence. It was required by sufficiently strong implications that the final answer should rest entirely on comparisons between experimental and theoretical detonation temperatures in view of the impossibility of evaluating the heat capacity (Eq. (17)) from detonation velocities and the hydrodynamic theory alone.

Paterson is in error in his statement that ignoring Eq. (9) in method (a) "amounts to discarding the Chapman-Jouguet condition." As a matter of fact, Eq. (11) is nothing more than the Chapman-Jouguet postulate allowing the completely justifiable approximation $p_2\cong p_2-p_1$. That is, the Chapman-Jouguet postulate is expressed in the equation

$$-(dp_2/dv_2)_s=(p_2-p_1)/(v_1-v_2)=p_2\beta/(v_2-\alpha) \qquad (a)$$

which, upon canceling p_2-p_1 with p_2, gives Eq. (11).

Paterson argued that, since Eq. (13) follows from Eqs. (11) and (12), one does not obtain a unique solution by solving Eqs. (11), (12), (13), and (16) for the four independent variables T_2, v_2, α, and β. While it is true that Eq. (11) may be derived from (12) and (13), this is made possible only by virtue of the approximation $p_2\gg p_1$; the four equations are in reality independent. The five independent equations are (1), (2), (3), (4), and (6). Under the approximation $p_2\gg p_1$ and employing the auxiliary Eq. (8), Eq. (11) is equivalent to Eq. (4); Eq. (12) follows from (1) and (6); Eq. (13) may be derived from (1), (2), and (6); Eq. (16) follows from (3). Hence, it is only the very small value of p_1 relative to p_2 that makes it appear that Eqs. (11), (12), (13), and (16) are not independent. Paterson was evidently troubled by the consideration that six independent unknown variables W, T_2, α, β, p_2, v_2 were evaluated from five independent equations, evidently overlooking or ignoring the fact that the condition $p_2\gg p_1$ is, in fact, the sixth condition needed to complete the solution. I fail to see, therefore, why the solution obtained by solving the four Eqs. (11), (12), (13), and (16) for β, α, v_2, T_2 by the method of successive approximations should not be a unique solution.

Paterson suggested that since method (b) preceded (a) in the development of the theory, the results obtained in method (b) would influence those in method (a). Such a suggestion could have been easily evaluated by Paterson himself if he had been willing to carry out a few series of approximations starting with different assumed values of β.

Paterson's argument that a step-by-step integration of the fifth equation of the theory (Eq. (a) above) leads to an entire family of $\alpha(v)$ curves is incorrect because it fails to

recognize that in this problem we are dealing with well-defined thermodynamic functions. Equation (9) derived from the laws of thermodynamics and the assumed equation of state gives β as follows:

$$\beta=(C_v+R)/C_v-(\partial\alpha/\partial v_2)_s+(\partial E/\partial v)_T nR/C_v p_2. \quad \text{(b)}$$

Since no critical points are involved, obviously the two functions α and $(\partial E/\partial v)_T$ are single valued in v, and one should thus expect β to be a single-valued function of v. However, if one needs an additional argument, the integration constant referred to by Paterson may be established as zero from the fact that Eq. (b) must reduce to $\beta=C_p/C_v=\gamma$ for the case where factors for non-ideality become vanishingly small, a condition which applies in the detonation of gaseous explosives. In fact, Paterson's argument should apply equally well to any assumed equation of state but is invalidated for one thing by the experimental verification of the hydrodynamic theory for gaseous explosives.

[1] S. Paterson, J. Chem. Phys. **16**, 159 (1948).
[2] M. A. Cook, J. Chem. Phys. **15**, 518 (1947).

Ignition of Explosive Gas Mixtures by Electric Sparks. Minimum Ignition Energies

R. VIALLARD
Laboratoire de Chimie Physique de la Faculté des Sciences, Paris, France
March 10, 1947

IN a recent paper[1] Lewis, von Elbe, and co-workers conclude that there exist minimum values for the energies of electric sparks which initiate flames in explosive gas mixtures, and that these values may be considered as absolute minimum values. In a second paper[2] Lewis and von Elbe develop a theory showing the existence of an absolute minimum energy in the case of flames propagated from an instantaneous point source of ignition, and they consider that the theory can be applied to capacitance sparks.

Attention must be paid to the fact that other experiments[3] have given results contradictory to the conclusions of the authors. These experiments have shown that for given mixtures effective minimum energy values exist, but that these are not absolute values and depend (1) on the voltage applied to the spark gap and (2) on the shape of the electrodes. For the best inflammable mixtures the relationship between the voltage applied to the gap and the capacity of the system is of the form $CV^x=$constant, with $x=3$ when the two electrodes have sharp points, $x\simeq 6$ if one of them has a sharp point, the other being a large sphere or a plane surface, $x\simeq 9$ if the two are large spheres or plane surfaces.

No theory has been developed to explain these results. But it appears that they may agree with Lewis and von Elbe's theory provided that the following assumptions are made: (1) the maximum amount of energy distributed in the ignition zone depends directly on the energy of the fastest electrons initiating an avalanche process in the first steps of the spark discharge and (2) chain carriers in this zone are, or are generated by, charged particles, which travel through the gap with a mean velocity approximately proportional to that of particles starting from the electrodes. Since the energy of such particles is proportional to V, and because the minimum energy values are inversely proportional to V in the case of sharp electrodes, this suggests that the energy in the ignition zone depends directly on the energy per initiating particle, and that the geometry of the gap need not to be taken into account. If one of the electrodes is a plane surface, the field distribution is different, the lines of force being approximately parallel near the surface. In this case it is necessary to take into account the effect of this non-radial distribution on the density of chain carriers in active zones, such as are formed along current bursts or streamers in the spark gap during the first steps of the discharge. The factor $V^3=(V^1)^2$ is apparently due to this non-radial field distribution. This factor may be introduced on the assumptions (1) that the number of carriers given rise to by an electron of energy eV is proportional to V and (2) that the rate of formation of carriers depends directly on the velocity of such an electron, proportional to $V^{\frac{1}{2}}$. In the case of two spheres or plane surfaces, the proportionality to $1/V\cdot 1/V^3\cdot 1/V^3$ appears also to be due to the geometry of the gap. The double factor $(1/V^3\cdot 1/V^3)$ suggests that both electrodes are effective in the generation of carriers.

[1] M. V. Blanc, P. G. Guest, Guenther von Elbe, and Bernard Lewis, J. Chem. Phys. **15**, 798 (1947).
[2] Bernard Lewis and Guenther von Elbe, J. Chem. Phys. **15**, 803 (1947).
[3] Rodolphe Viallard, Comptes Rendus **207**, 1405 (1938); J. de chim. Phys. **40**, 101 (1943).

Low Frequency Raman Spectrum of Calcite

L. GIULOTTO AND G. OLIVELLI
Istituto di Fisica "A. Volta" dell'Università di Pavia, Pavia, Italy
December 22, 1947

IT has been demonstrated by Raman and Nedungadi[1] that because of their particular polarization characters two low frequency Raman lines in a $NaNO_3$ crystal are attributable to angular oscillations of NO_3 ions. Later Kastler, Rousset, and other authors[2] established that also in organic crystals (benzene, naphthalene, paradichlorobenzene, paradibromobenzene) low frequency lines, which disappear at the liquid state giving place to a continuum at the sides of the exciting line, are to be assigned to oscillations of the same type.

However, for $NaNO_3$ the question has not yet been cleared entirely; in fact, we are not aware that the presence of two low frequency Raman lines, both attributable to angular oscillations, has been explained. Also the calcite, which has a structure analogous to the $NaNO_3$, presents two low frequency Raman lines. We have examined the polarization state of these lines illuminating a calcite crystal parallel to the optic axis, and collecting the diffuse light perpendicular to it.

In Fig. 1 (a) and (b) the microphotometer curves of two spectra relative to the electric vector, and respectively parallel and perpendicular to the optic axis, are repro-

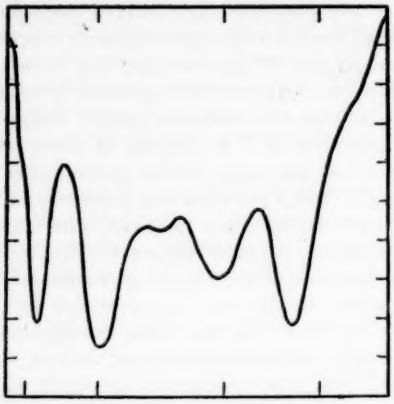

FIG. 1. Microphotometer curves of Raman spectra of calcite relative to the electric vector (a) parallel and (b) perpendicular to the optic axis.

duced. Examination of these shows that, as for $NaNO_3$, while the internal lines (1088 and 1437 cm^{-1}) are polarized with the electric vector perpendicular to the optic axis, both the external lines (155 and 282 cm^{-1}) are polarized with the electric vector parallel to the optic axis. This result shows that in calcite crystal the CO_3 ions can execute angular oscillations around axes perpendicular to the optic axis with two different frequencies. The angular oscillations of the ions appertaining to a certain domain of the crystal shall give a non-zero resultant only if they are incoherent or coherent and in phase. However, since external lattice oscillations are in question, the last seems to be the only possibility.

An explanation of the possibility of two angular oscillating frequencies in phase for all the ions appertaining to a certain domain of the crystal can be derived from the examination of the calcite lattice structure. The calcite lattice is constituted by lattice planes of Ca alternated with planes of CO_3, perpendicular to the optic axis. Figure 2 shows the situation of a CO_3 ion relating to the nearest Ca ions appertaining to the two adjacent planes: each atom O is at equal distance from two atoms Ca. Now if we displace the CO_3 ion in its plane, for instance in the direction indicated in Fig. 2, the atom O aligned with C in this direction maintains itself at equal distance from the two Ca; for the other two atoms O, on the contrary, the equi-

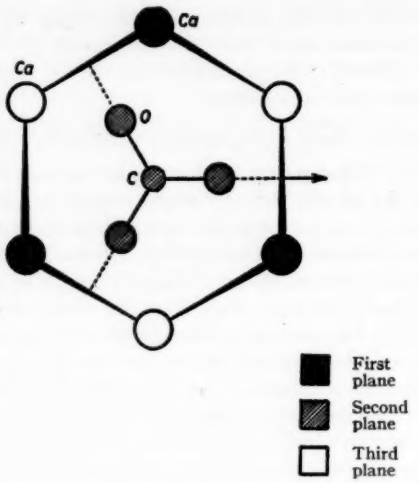

FIG. 2. Situation of a CO_3 ion relating to the nearest Ca ion appertaining to the two adjacent planes.

distance conditions are altered: while for the one the distance from the inferior Ca increases and the distance from the superior Ca decreases, for the other the opposite occurs. Therefore, there will arise a moment which tends to turn the ion around the translation direction.

The situation of CO_3 relating to Ca is always such that a translation of the Ca lattice relating the CO_3 lattice perpendicularly to the optic axis causes, in the CO_3 ions, a moment which tends to turn every one in the same sense. So the angular oscillations of CO_3 ions cannot be independent of the oscillations of the two lattices of Ca and CO_3, the one against the other, but only oscillations are possible which consist in translatory motions perpendicular to the optic axis, accompanied by a periodical variation in the orientation of the CO_3 ions. Then the conditions are similar to the ones of two coupled oscillators, which form a system capable of oscillating with two frequencies. These two external frequencies of calcite should be active in the infra-red. They could correspond to two reflection maxima found by the residual-ray method, considering that by this method the oscillation frequencies of a crystal can be established only approximately.[3]

[1] C. V. Raman and T. M. K. Nedungadi, Nature **143**, 679 (1939).
[2] For the bibliography on this argument see A. Kastler and A. Rousset, Phys. Rev. **71**, 455 (1947).
[3] C. Schaefer and M. Schubert, Ann. d. Physik **50**, 283 (1916).